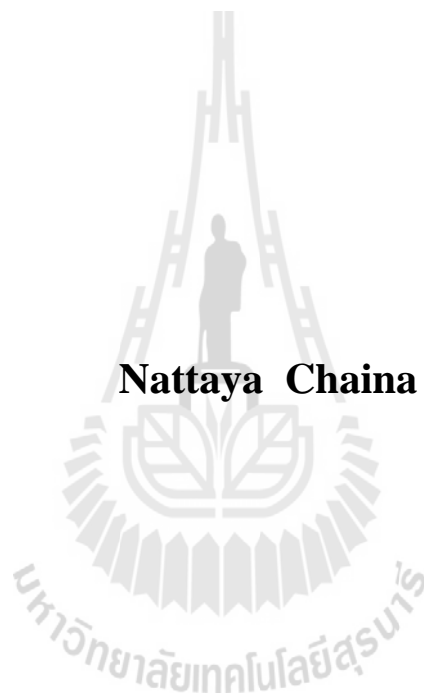


**PETROLEUM SOURCE ROCK STUDY AND MIGRATION
PATHWAY IDENTIFICATION IN THE MERGUI
BASIN, THE ANDAMAN SEA, THAILAND**



**A Thesis Submitted in Partial Fulfillment of the Requirements for the
Degree of Master of Engineering in Geotechnology
Suranaree University of Technology
Academic Year 2011**

การศึกษาหัตถ์กำเนิดและระบุงการเคลื่อนที่ของปีโตรเลียม
ของแองเมอรูกูย ทะเลอันดามัน ประเทศไทย



นางสาวนาฏยา ชัยนา

วิทยานิพนธ์นี้เป็นส่วนหนึ่งของการศึกษาตามหลักสูตรปริญญาวิศวกรรมศาสตรมหาบัณฑิต
สาขาวิชาเทคโนโลยีธรณี
มหาวิทยาลัยเทคโนโลยีสุรนารี
ปีการศึกษา 2554

**PETROLEUM SOURCE ROCK STUDY AND MIGRATION
PATHWAY IDENTIFICATION IN THE MERGUI BASIN,
THE ANDAMAN SEA, THAILAND**

Suranaree University of Technology has approved this thesis submitted in partial fulfillment of the requirements for a Master's Degree.

Thesis Examining Committee

(Assoc. Prof. Kriangkrai Trisarn)

Chairperson

(Dr. Akkhapun Wannakomol)

Member (Thesis Advisor)

(Dr. Chongpan Chonglakmani)

Member

(Prof. Dr. Sukit Limpijumnong)

Vice Rector for Academic Affairs

(Assoc. Prof. Flt. Lt. Dr. Kontom Chamniprasart)

Dean of Institute of Engineering

นาฏยา ชัยนา : การศึกษาหินต้นกำเนิดและกระบวนการเคลื่อนที่ของปิโตรเลียมของแอ่ง
เมอร์กูย ทะเลอันดามัน ประเทศไทย (PETROLEUM SOURCE ROCK STUDY AND
MIGRATION PATHWAY IDENTIFICATION IN THE MERGUI BASIN, THE
ANDAMAN SEA, THAILAND) อาจารย์ที่ปรึกษา : อาจารย์ ดร.อัมพรศักดิ์ วรรณโกมล,
176 หน้า.

แอ่งเมอร์กูยเป็นแอ่งอายุเทอร์เชียรีซึ่งตั้งอยู่ในบริเวณทะเลอันดามันของประเทศไทย การศึกษาที่ผ่านมาทราบว่า แอ่งเมอร์กูยนั้นมีหินต้นกำเนิดปิโตรเลียมที่ดีและโครงสร้างกักเก็บที่เหมาะสมกับการเป็นแหล่งปิโตรเลียมที่ดีได้ อย่างไรก็ตามจากการสำรวจที่ผ่านมาไม่ประสบความสำเร็จเท่าที่ควรและงานวิจัยที่ผ่านมาที่สรุปไว้ว่าเป็นเพราะหินต้นกำเนิดในบริเวณนี้ยังไม่สุกบ่มพอ การวิจัยครั้งนี้มีเป้าหมายเพื่อทำการระบุหินต้นกำเนิดของปิโตรเลียมและความสมบูรณ์ พร้อมทั้งสภาพการสุกบ่ม ประวัติทางด้านสิ่งแวดล้อมและการสะสมตัวของตะกอน และเพื่อทำการระบุทิศทางการเคลื่อนตัวของปิโตรเลียมของแอ่งเมอร์กูยโดยใช้เทคนิคทางธรณีเคมี และโปรแกรม PetroMod ผลที่ได้จากการศึกษาระบุได้ว่า แอ่งเมอร์กูยนั้นมีหินต้นกำเนิดปิโตรเลียมที่เป็นไปได้อยู่ 3 ชุดหิน ได้แก่ ชุดหินยะลา, ชุดหินกันตรัง และชุดหินตรัง อย่างไรก็ตามมีเพียงชุดหินยะลาเท่านั้นที่มีความเหมาะสมในการให้ปิโตรเลียม หินต้นกำเนิดปิโตรเลียมของชุดหินยะลาเป็นหินดินดานที่เกิดในทะเลโดยมีปริมาณสารประกอบคาร์บอนโดยรวมและค่าดัชนีไฮโดรคาร์บอนต่ำ หินต้นกำเนิดปิโตรเลียมหลักนี้เป็นคีโรเจนแบบชนิดที่สามและมีแนวโน้มในการให้ก๊าซ ผลจากการศึกษาสภาพการสุกบ่มของหินต้นกำเนิด ระบุว่าหินต้นกำเนิดปิโตรเลียมหลักนี้ตั้งอยู่ในส่วนทางด้านทิศตะวันตกเฉียงใต้ของแอ่ง ผลการศึกษาทางด้านกระจายตัวของคุณสมบัติทางด้านความพรุนและความซึมซาบ ระบุว่าหินกักเก็บปิโตรเลียมที่เป็นไปได้ในบริเวณนี้ก็คือหินทรายของชุดหินระนอง ผลการศึกษาข้างชี้ให้เห็นอีกว่า ชุดหินระนองตอนบนนั้นมีความเหมาะสมในการเป็นหินกักเก็บปิโตรเลียมที่ดีกว่าตอนกลางและตอนล่าง อันเนื่องมาจากการมีค่าของความซึมซาบและความต่อเนื่องของชุดหินที่ดีกว่าและยังมีชั้นหินทรายที่หนากว่าอีกด้วย การขับปิโตรเลียมออกจากหินต้นกำเนิดและการเคลื่อนตัวของปิโตรเลียมนั้นเชื่อว่าน่าจะเกิดขึ้นส่วนใหญ่ในช่วงปลายของยุคไมโอซีนจนถึงยุคไพลโอซีน ที่ระดับความลึก 3,000-3,500 เมตร การเคลื่อนที่ของปิโตรเลียมหลักจะเดินทางเข้าไปสู่บริเวณ โครงสร้างสันตรงกลางแอ่ง ซึ่งตั้งอยู่บริเวณตอนกลางของแอ่งเมอร์กูย

สาขาวิชาเทคโนโลยีธรณี

ปีการศึกษา 2554

ลายมือชื่อนักศึกษา _____

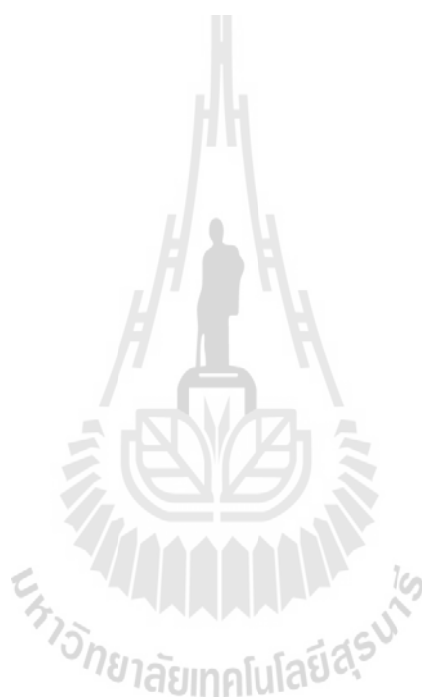
ลายมือชื่ออาจารย์ที่ปรึกษา _____

NATTAYA CHAINA : PETROLEUM SOURCE ROCK STUDY AND
MIGRATION PATHWAY IDENTIFICATION IN THE MERGUI BASIN,
THE ANDAMAN SEA, THAILAND. THESIS ADVISOR : AKKHAPUN
WANNAKOMOL, Ph. D., 176 PP.

SOURCE ROCK/MATURITY/MIGRATION PATHWAY/MERGUI BASIN/THE
ANDAMAN SEA

Mergui basin is a Tertiary basin located in the Andaman Sea, Thailand. Previous studies indicate that Mergui basin has good petroleum source rocks and proper petroleum trapping structures for being a good petroleum field. However, previous explorations are not success and many researchers concluded that source rocks in this region are immature. This research aims to identify petroleum source rocks and their richness and maturity, environment and burial history of deposition, and to identify possible petroleum migration pathway of Mergui basin by using geochemical technique and PetroMod program. Results of the study indicated that Mergui basin has three possible petroleum source rocks formations; Yala, Kantang, and Trang Formation. However, only the Yala Formation is proper to generate petroleum. Petroleum source rock of the Yala formation is marine shale having low total organic carbon and low hydrogen index. This major petroleum source rock is kerogen type III and trends to generate gas prone. Results from source rock maturity study indicated that the main petroleum source rock is located in the southwestern part of the basin. Results from porosity and permeability distribution study revealed that possible reservoir rocks in this region are sandstones of the Ranong Formation. It is also pointed out that the Upper Ranong Formation is more proper to be a good

reservoir than the Middle Ranong and Lower Ranong Formation with having higher permeability, higher continuity, and thicker bed of sandstones. Hydrocarbons expulsion and migration were believed to take place mainly in Late Miocene to Pliocene and at depth more than 3,000-3,500 meter. Main migration pathways are forward to the central high structure located in the central part of Mergui basin.



School of Geotechnology

Academic Year 2011

Student's Signature _____

Advisor's Signature _____

ACKNOWLEDGEMENTS

I wish to acknowledge the Suranaree University of Technology (SUT) for this research funding.

I would like to express my sincere appreciation and gratitude to Dr. Akkhapun Wannakomol, my thesis advisor, who gave a critical review and constant encouragement throughout the course of this research. Further appreciation is extended to Assoc. Prof. Kriangkrai Trisarn: chairman, School of Geotechnology and Dr. Chongpan Chonglakmani who are member of my examination committee. In addition, I am grateful for the Schlumberger, Limited. for academic software loan supporting of PetroMod software, Thirada Kensakoo, Suwisa Koysamran, and other persons for their suggestions and all their help.

Finally, I most gratefully acknowledge my parents and friends for all their supports throughout the period of this research.

Nattaya Chaina

TABLE OF CONTENTS

	Page
ABSTRACT (THAI).....	I
ABSTRACT (ENGLISH).....	II
ACKNOWLEDGEMENTS.....	IV
TABLE OF CONTENTS.....	V
LIST OF TABLES.....	IX
LIST OF FIGURES.....	X
CHAPTER	
I INTRODUCTION.....	1
1.1 Rationale and background.....	1
1.2 Research objectives.....	2
1.3 Research methodology.....	2
1.3.1 Literature review.....	2
1.3.2 Required data collecting and preparing.....	2
1.3.3 Petroleum source rock analysis.....	3
1.3.4 Petroleum migration pathway generating.....	3
1.3.5 Thesis writing and presentation.....	3
1.4 Scope and limitations of the study.....	4
1.5 Thesis contents.....	4
II LITERATURE REVIEW.....	6

TABLE OF CONTENTS (Continued)

	Page
2.1 Mergui basin.....	6
2.1.1 Physiography of the basin.....	6
2.1.2 Geological setting.....	8
2.1.3 Geological structure.....	15
2.1.4 Stratigraphy.....	19
2.2 Petroleum system of the Mergui basin.....	30
2.2.1 Source rocks.....	30
2.2.2 Reservoir rocks.....	30
2.2.3 Migration.....	31
2.2.4 Seals and Traps.....	31
2.3 Exploration history in the Mergui basin, Andaman Sea.....	31
III METHODOLOGY.....	33
3.1 Introduction.....	33
3.2 Petroleum source rock.....	33
3.2.1 Element for petroleum source rock study.....	33
3.2.2 PetroMod 1D modeling workflow.....	48
3.3 Petroleum migration pathway.....	49
3.3.1 Element of migration pathway Reservoir rock properties.....	50

TABLE OF CONTENTS (Continued)

	Page
3.3.2 Oil and gas reservoirs.....	53
3.3.3 Introduction to migration and accumulation of oil and gas.....	55
3.3.4 Migration stages.....	56
3.3.5 Factors that cause migration.....	56
3.3.6 Migration pathways.....	58
3.3.7 Defining migration pathways from Source to Trap.....	58
3.3.8 Reservoir of the Mergui basin.....	59
IV RESULT OF THE STUDY	63
4.1 Petroleum source rock.....	63
4.1.1 Petroleum source rock of the Mergui basin.....	63
4.1.2 Thermal maturation and timing of hydrocarbon generation and migration.....	70
4.1.3 Hydrocarbon indications.....	71
4.1.4 Biomarker.....	74
4.1.5 Modeling of the Mergui basin by using PetroMod 1D.....	75
4.1.6 Hydrocarbon expulsion.....	131
4.1.7 TOC distribution map.....	132

TABLE OF CONTENTS (Continued)

	Page
4.2 Petroleum migration pathway.....	137
4.2.1 Porosity.....	137
4.2.2 Permeability.....	147
V CONCLUSIONS AND RECOMMENDATIONS.....	163
5.1 Conclusions.....	163
5.1.1 Petroleum system in the Mergui basin.....	163
5.1.2 Petroleum source rock of the Mergui basin.....	164
5.1.3 Petroleum migration pathway of the Mergui basin.....	165
5.2 Recommendations for future studies.....	165
REFERENCES.....	166
BIOGRAPHY.....	176

LIST OF TABLES

Table	Page
3.1 Classification of kerogen.....	34
3.2 A cyclic biomarkers as indicators of biological input or depositional environment; assumes high concentration of component	46
3.3 Generalized geochemical properties differ between nonbiodegraded crude oils from marine, terrigenous, or lacustrine source-rock organic matter.....	47
3.4 Generalized correlation of level of maturity.....	47
3.5 The factors primarily cause hydrocarbon migration.....	57
3.6 Procedures for defining migration pathways.....	59
4.1 Geochemical data analysis data of rocks.....	75

LIST OF FIGURES

Figure	Page
1.1 Location of study area in the Mergui basin.....	5
2.1 Physiography of the Andaman Sea	8
2.2 Tectonic map of the Mergui basin and Andaman Sea region	9
2.3 Model for the development of the Mergui basin through the combination of transtensional dextral shears along the NW-SE trending Sumatra Fault System (SFS) and the NNW-SSE trending Mergui Fault Zone (MFZ)	13
2.4 Physiography cross-section across the Mergui basin and the North Sumatra basin.	14
2.5 The seismic profile depicts half graben geometry sub-basin in the southern part of Mergui basin	16
2.6 The seismic profile depicts negative flower structure in the southern part of Mergui basin	18
2.7 Generalized stratigraphy of the Mergui basin and stratigraphic correlation to the North Sumatra basin	28
2.8 Stratigraphy of the Mergui basin.....	29
3.1 Classification of the source rock type by using hydrogen and oxygen indices	35
3.2 Principle of the Rock-Eval pyrolysis	37

LIST OF FIGURES (Continued)

Figure	Page
3.3 Cycle of analysis and example of record obtained by the pyrolysis method of Espitalie et al., 1977	38
3.4 Characterization of source rock maturity by pyrolysis methods	40
3.5 PetroMod 1D modeling workflow	49
3.6 Characteristics of porosity in other rocks	51
3.7 Relationship of porosity and permeability in other rocks	53
3.8 Pores in rock	54
3.9 Connected pores in rock	54
4.1 Results of pyrolysis (Rock-Eval) cutting samples of the Yala Formation	64
4.2 Hydrogen Index (HI) versus Oxygen Index (OI) of the Yala Formation plotted	65
4.3 Results of pyrolysis (Rock-Eval) cutting samples of the Kantang Formation	66
4.4 Hydrogen Index (HI) versus Oxygen Index (OI) of the Kantang Formation plotted	67
4.5 Results of pyrolysis (Rock-Eval) cutting samples of the Trang Formation	68

LIST OF FIGURES (Continued)

Figure	Page
4.6 Hydrogen Index (HI) versus Oxygen Index (OI) of the Trang Formation plotted.....	69
4.7 Burial history of the Payang-1 well.....	77
4.8 Temperature Index (°C) of the Payang-1 well.....	77
4.9 Time Temperature Index (TTI) of the Payang-1 well.....	78
4.10 Maturity overlay R_o compare with temperature and depth of the Payang-1 well.....	79
4.11 Burial history of the Kantang-1 well.....	80
4.12 Temperature Index (°C) of the Kantang-1 well.....	80
4.13 Time Temperature Index (TTI) of the Kantang-1 well.....	81
4.14 Maturity overlay R_o compare with temperature and depth of the Kantang-1 well.....	82
4.15 Burial history of the Kathu-1 well.....	83
4.16 Temperature Index (°C) of the Kathu-1 well.....	83
4.17 Time Temperature Index (TTI) of the Kathu-1 well.....	84
4.18 Maturity overlay R_o compare with temperature and depth of the Kathu-1 well.....	85
4.19 Burial history of the Kra Buri-1 well.....	86
4.20 Temperature Index (°C) of the Kra Buri-1 well.....	86
4.21 Time Temperature Index (TTI) of the Kra Buri-1 well.....	87

LIST OF FIGURES (Continued)

Figure	Page
4.22 Maturity overlay R_o compare with temperature and depth of the Kra Buri-1 well.....	88
4.23 Burial history of the Ranot-1 well.....	89
4.24 Temperature Index ($^{\circ}\text{C}$) of the Ranot-1 well.....	89
4.25 Time Temperature Index (TTI) of the Ranot-1 well.....	90
4.26 Maturity overlay R_o compare with temperature and depth of the Ranot-1 well.....	91
4.27 Burial history of the Sikao-1 well.....	92
4.28 Temperature Index ($^{\circ}\text{C}$) of the Sikao-1 well.....	92
4.29 Time Temperature Index (TTI) of the Sikao-1 well.....	93
4.30 Maturity overlay R_o compare with temperature and depth of the Sikao-1 well.....	94
4.31 Burial history of the Thalang-1 well.....	95
4.32 Temperature Index ($^{\circ}\text{C}$) of the Thalang-1 well.....	95
4.33 Time Temperature Index (TTI) of the Thalang-1 well.....	96
4.34 Maturity overlay R_o compare with temperature and depth of the Thalang-1 well.....	97
4.35 Burial history of the Yala-1 well.....	98
4.36 Temperature Index ($^{\circ}\text{C}$) of the Yala-1 well.....	98
4.37 Time Temperature Index (TTI) of the Yala-1 well.....	99

LIST OF FIGURES (Continued)

Figure	Page
4.38 Maturity overlay R_o compare with temperature and depth of the Yala-1 well.....	100
4.39 Burial history of the W9-A-1 well.....	101
4.40 Temperature Index ($^{\circ}\text{C}$) of the W9-A-1 well.....	101
4.41 Time Temperature Index (TTI) of the W9-A-1 well.....	102
4.42 Maturity overlay R_o compare with temperature and depth of the W9-A-1 well.....	103
4.43 Burial history of the W9-B-1 well.....	104
4.44 Temperature Index ($^{\circ}\text{C}$) of the W9-B-1 well.....	104
4.45 Time Temperature Index (TTI) of the W9-B-1 well.....	105
4.46 Maturity overlay R_o compare with temperature and depth of the W9-B-1 well.....	106
4.47 Burial history of the W9-C-1 well.....	107
4.48 Temperature Index ($^{\circ}\text{C}$) of the W9-C-1 well.....	107
4.49 Time Temperature Index (TTI) of the W9-C-1 well.....	108
4.50 Maturity overlay R_o compare with temperature and depth of the W9-C-1 well.....	109
4.51 Burial history of the W9-E-1 well.....	110
4.52 Temperature Index ($^{\circ}\text{C}$) of the W9-E-1 well.....	110
4.53 Time Temperature Index (TTI) of the W9-E-1 well.....	111

LIST OF FIGURES (Continued)

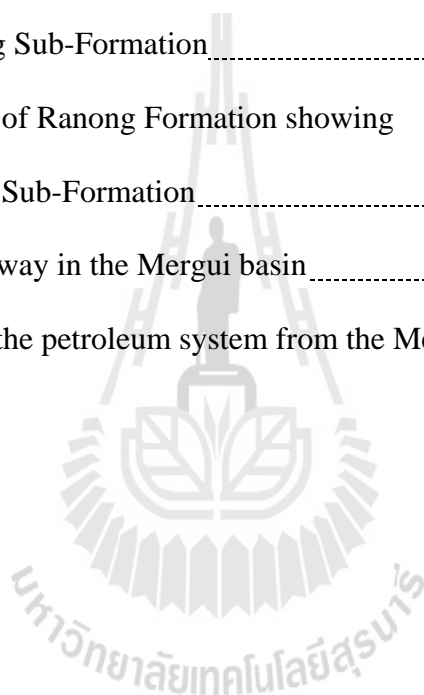
Figure	Page
4.54	depth Maturity overlay R_o compare with temperature and of the W9-E-1 well 112
4.55	Burial history of the Mergui-1 well 113
4.56	Temperature Index ($^{\circ}\text{C}$) of the Mergui-1 well 113
4.57	Time Temperature Index (TTI) of the Mergui-1 well 114
4.58	Maturity overlay R_o compare with temperature and depth of the Mergui-1 well 115
4.59	Burial history of the Phangha-1 well 116
4.60	Temperature Index ($^{\circ}\text{C}$) of the Phangha-1 well 116
4.61	Time Temperature Index (TTI) of the Phangha-1 well 117
4.62	Maturity overlay R_o compare with temperature and depth of the Phangha-1 well 118
4.63	Burial history of the Trang-1 well 119
4.64	Temperature Index ($^{\circ}\text{C}$) of the Trang-1 well 119
4.65	Time Temperature Index (TTI) of the Trang-1 well 120
4.66	Maturity overlay R_o compare with temperature and depth of the Trang-1 well 121
4.67	Burial history of the W9-D-1 well 122
4.68	Temperature Index of the W9-D-1 well ($^{\circ}\text{C}$) 122
4.69	Time Temperature Index (TTI) of the W9-D-1 well 123

LIST OF FIGURES (Continued)

Figure	Page
4.70 Maturity overlay R_o compare with temperature and depth of the W9-D-1 well.....	124
4.71 TOC distribution map of the Yala Formation.....	133
4.72 TOC distribution map of the Kantang Formation.....	134
4.73 TOC distribution map of the Trang Formation.....	135
4.74 Geothermal gradient distribution map of the Mergui basin.....	136
4.75 Lower Ranong Sub-Formation porosity map.....	139
4.76 Middle Ranong Sub-Formation porosity map.....	140
4.77 Upper Ranong Sub-Formation porosity map.....	141
4.78 Lower Ranong porosity vs. depth plot.....	144
4.79 Middle Ranong porosity vs. depth plot.....	145
4.80 Upper Ranong porosity vs. depth plot.....	146
4.81 Relationship between porosity and permeability plot.....	147
4.82 Lower Ranong Sub-Formation permeability map.....	149
4.83 Middle Ranong Sub-Formation permeability map.....	150
4.84 Lower Ranong Sub-Formation permeability map.....	151
4.85 Lower Ranong Sub-Formation permeability vs. porosity plot.....	154
4.86 Middle Ranong Sub-Formation permeability vs. porosity plot.....	155
4.87 Upper Ranong Sub-Formation permeability vs. porosity plot.....	156
4.88 Structural map of Ranong Formation of the Mergui basin.....	158

LIST OF FIGURES (Continued)

Figure	Page
4.89 Structural map of Ranong Formation showing Lower Ranong Sub-Formation.....	159
4.90 Structural map of Ranong Formation showing Middle Ranong Sub-Formation.....	160
4.91 Structural map of Ranong Formation showing Upper Ranong Sub-Formation.....	161
4.92 Migration pathway in the Mergui basin.....	162
5.1 Event chart of the petroleum system from the Mergui basin.....	163



CHAPTER I

INTRODUCTION

1.1 Rationale and background

Tertiary basins are the main target of petroleum exploration and production in Thailand. Mergui basin is one of Tertiary basins which is located in the Andaman Sea, western offshore, Thailand. An exploration in the Mergui basin has so far been unsuccessful. Ten wells had been drilled within block No. W-9 resulting in minor gas show and trace was observed in Trang-1 and Mergui-1 wells. Many researches had been concluded that this area is immature stage with presenting the trace gas/oil show. The possible reasons for this are: (1) the petroleum source rocks were matured to generate and expulsion before petroleum traps were, or (2) There were some activities occurred to the petroleum trap and resulting in petroleum linkage. Therefore, the petroleum source rock identification is an important task in evaluating a petroleum-bearing basin since it is directly related to its petroleum resource potential and exploration directions. Organic geochemistry is commonly used for oil/gas-source correlation.

In this study the identification the generation and expulsion history of petroleum source rocks, and the migration pathway of petroleum were studied and analyzed using geochemical, seismic, electrical wireline logs, sequence deposition and biostratigraphic data. The expected results be described the petroleum resources in the Mergui basin based on the petroleum source rock and also could be depicted the pathway

for petroleum migration into reservoir within the study area. In addition, the result of research could be informatively supported for petroleum resources exploration management plan of the Andaman Sea in the future.

1.2 Research objectives

The objectives of this research are: (1) to identify the petroleum source rock, and (2) to deduce the generation and expulsion history of the source rocks and the migration pathway of petroleum by integrating the geological setting from other previews with kinetic models of petroleum source rock potential, petroleum generation, expulsion and migration pathway.

1.3 Research methodology

1.3.1 Literature review

All information on regional geology of the Mergui basin, the Andaman Sea was reviewed to serve as a background of the present study, including the geological setting of the Mergui basin and other previous reviews in order to give basic understanding about the geological history, tectonic evolution and general stratigraphy. The sources of information are from Social Petroleum Engineering (SPE), Journal of Petroleum Technology (JPT), Department of Mineral Fuels library (Thailand), technical report, and conference papers.

1.3.2 Required data collecting and preparing

Required were collected and prepared to serve the objective of the study, including seismic, electrical wireline logs, sequence deposition, biostratigraphy and geochemical data

1.3.3 Petroleum source rock analysis

The identification of source rocks and the evaluation of their capability to generate hydrocarbons in sufficient quantity to migrate up to the traps are important in the assessment of the region. Modern geochemical analyses are particularly useful to reach an evaluation.

The type of organic matter, burial and local thermal history are particularly important for the understanding of maturity evolution. They have generally played a decisive role in the timing of migration versus trap formation and in the discrimination of oil and gas. Modern tools are available to unravel the various parameters involved.

1.3.4 Petroleum migration pathway generating

Porosity and permeability data are selected were analyzed to draw possible source rocks boundaries of depositional sequence and important geological structures.

Porosity and permeability distribution mapping were assessed on sedimentary studies using all available geological and geophysical data. Then, from porosity and permeability distribution maps, petroleum migration pathway could be identified.

1.3.5 Thesis writing and presentation

Results of the study e.g. identified petroleum source rocks, the generation and expulsion history of the source rocks, and the migration pathway of petroleum in the Mergui basin, the Andaman Sea, Thailand. The final results were summarized and written as a thesis.

1.4 Scope and limitations of the study

The study prospect was covered the Mergui basin, the Andaman Sea only in continental shelf part of Thailand. The area was located at UTM 690000 to 1078786 North and 120000 to 411636 East in zone 47. It is approximately 50,000 square kilometers (Figure 1.1).

This research used the existing and published data provided by Department of Mineral Fuels (DMF), Thailand. The required data were seismic data set, final well reports, sidewall cores analysis reports, mud logs reports, biostratigraphy reports, geophysical log, general geological data and evaluation geochemical reports.

1.5 Thesis contents

Chapter I introduces the study by describing the rationale and background, research objectives, research methodology, scope and limitations. **Chapter II** summarizes the results of the literature review of generalized the Mergui basin. **Chapter III** describes the method of the study; petroleum source rock and petroleum migration pathway. **Chapter IV** present results from petroleum source rock studies; kerogen type, potential source rock, hydrocarbon identification, timing maturation and the results from the PetroMod modeling in terms of petroleum source rock. **Chapter V** present results from petroleum migration pathway studies; porosity, permeability, and structure of the Mergui basin. **Chapter VI** reports the conclusion and discussion on the research results, and recommendation for future research studies.

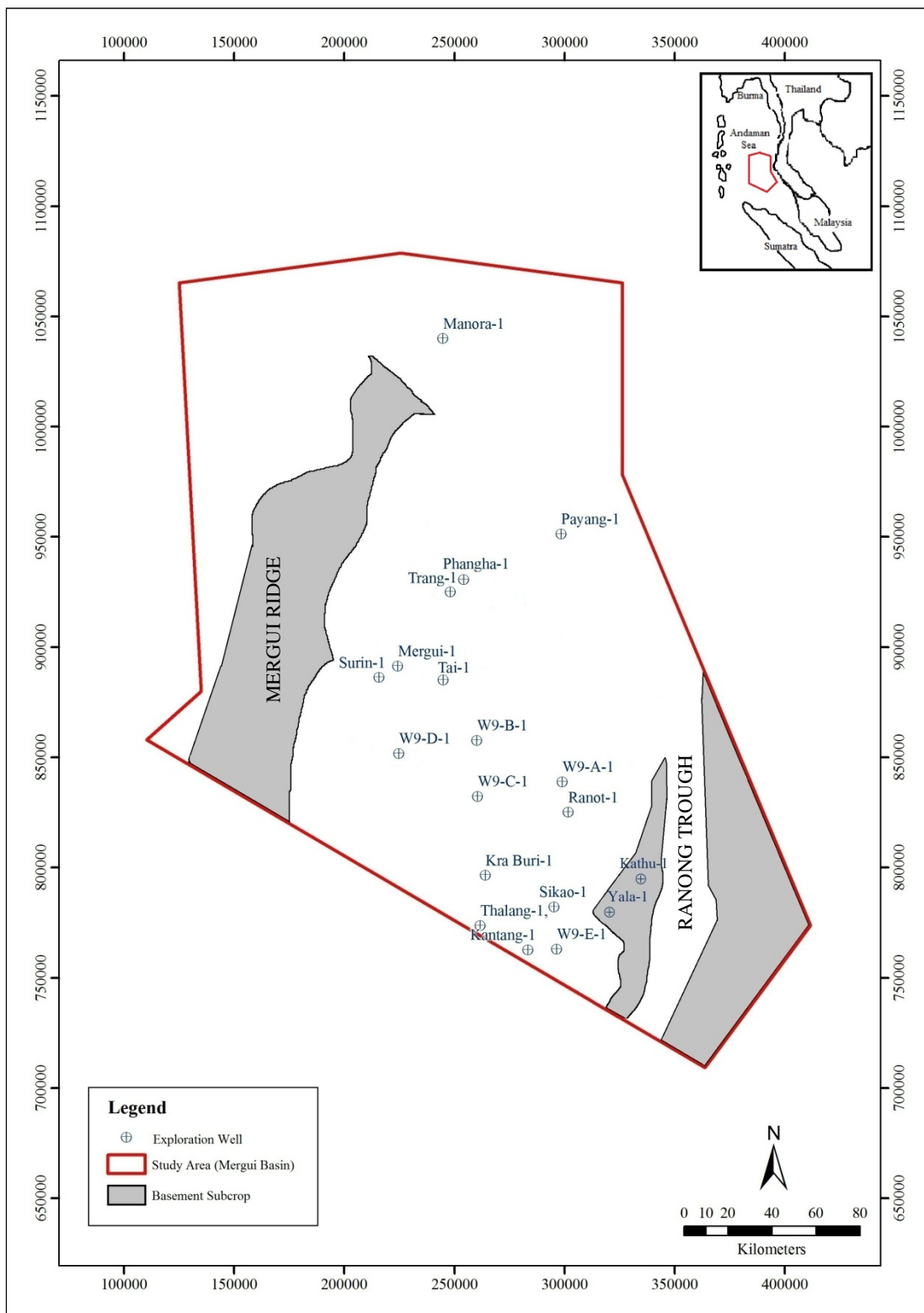


Figure 1.1 Location of study area in the Mergui basin (modified after DMF, 2008)

CHAPTER II

LITERATURE REVIEW

2.1 Mergui basin

2.1.1 Physiography of the basin

The physiography of the Mergui basin description in this study was summarized based on Rodolfo (1969) as follows. The Mergui basin is located in the Thai part of the Andaman Sea, which is bordered to the east by western coastal line of Thai–Malay Peninsula. It is limited to the west by the Indian area, to the North by the Myanmar and to the South by the Indonesian and Malaysian areas.

The Northern part of Andaman Sea extend from Irrawaddy deltaic coast of the central Burma and extending about 800 kilometers from the western coast of the Thai-Malay Peninsula to the Andaman and the Nicobar Islands as showed in Figure 2.1. The Andaman Sea floor comprises two sedimentary basins as the Andaman basin which locates to the northwestern and the Mergui-North Sumatra basin to the southeastern part of the Andaman Sea. The water depth of the inner shelf along the western coast of the Malay Peninsula is less than 100 meters. A width of the northern end is about 130 kilometers. The width decreases toward the southern direction and is terminated by a minor slope which the relief is about 100 meters. The inner shelf of the Phuket Island is only 35 kilometers. The Mergui terrace is widened, flattened and deepened. The area is located at UTM 690000 to 1078786 North and 120000 to 411636 East in zone 47, and becomes concave, bifurcated into the Mergui bank on the western and the Sumatra shelf basin on the east. A width of the Mergui bank is about

70 kilometers, and the length is about 200 kilometers. The Sumatra shelf is bound to the east and the south by the slopes off the Sundaland shelf (Malacca strait) and the northern Sumatra, and it is opened to the continental slope at approximately 1,300 meters water depth as showed in Figure 2.1. The continental shelf break is deepened southward. The shelf break marker is pinnacle with about 200 meters of the relief on the western edge of the Mergui bank. Generally, the gradient is average 1.8° and steeper in the north. Between Sewell seamount and the Matabun canyon, the continental slope abruptly ends in 2,435 meters of the terrace, which gently in the west direction 60 kilometers to 2,670 meters depth, and the bottom of the central Andaman trough drops sharply to the 3,035 meters depth.

The Andaman Sea area is one of the largest modern back arc basins, which is associated with the Sundaland trench as showed in Figure 2.2. The Sunda arc, between Burma and the Sundaland to the east of Java represents a 5,000 kilometers long which it is subduction zone of the Indian oceanic plate beneath the Eurasian plate. The northern and southern parts of this elongate basin which extend into Burma and Sumatra, respectively, lie on the continental crust, but the center of the basin is floored by the young oceanic crust. Thus, the present day depositional environment of the basin changes from continental Burma to deltaic and the oceanic Andaman Sea, which display a variety of sediment types including coarse grained mass flow deposit, submarine fan turbidites and basinal turbidites, and again changes to continental condition in Sumatra.

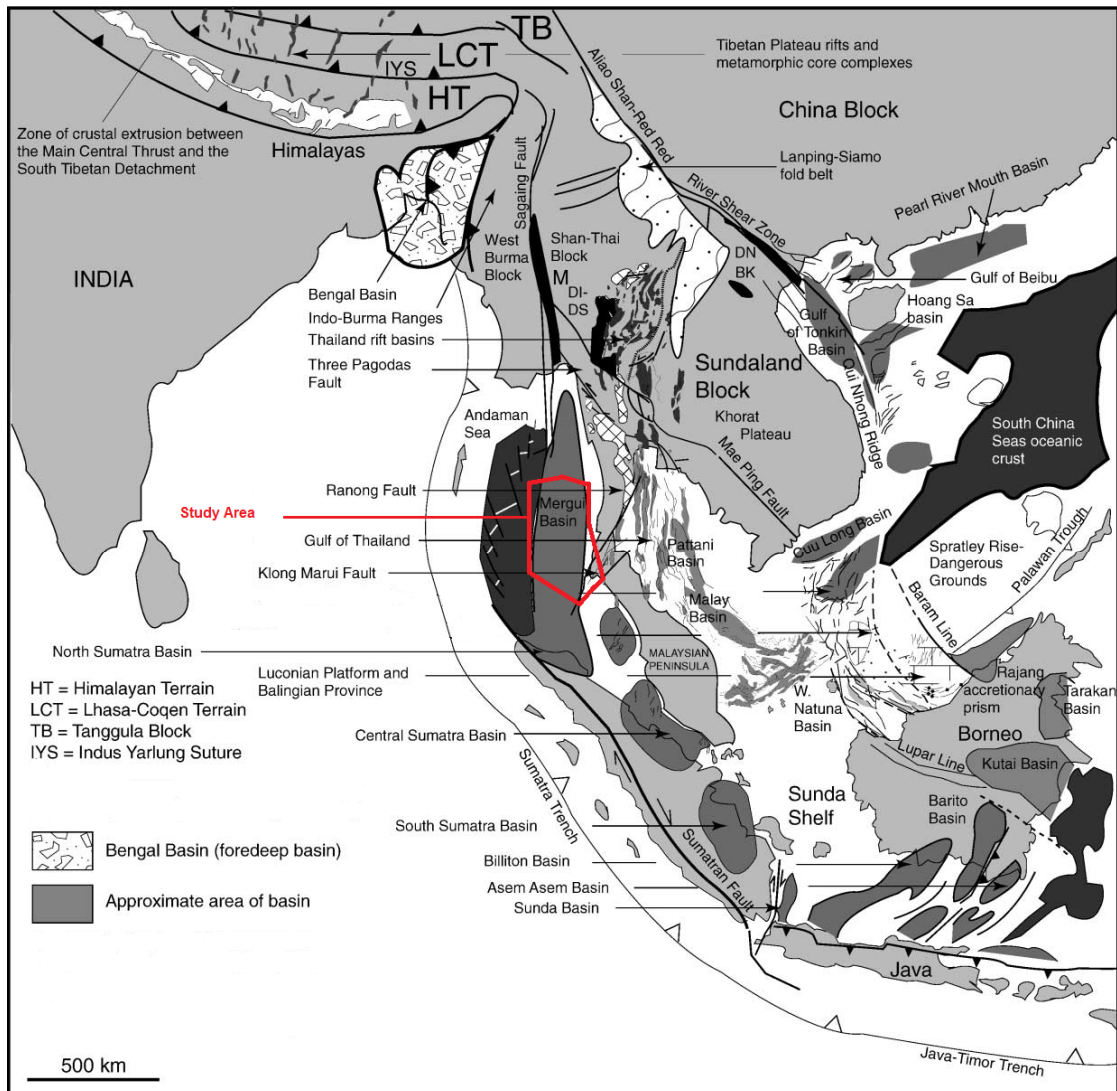


Figure 2.1 Physiography of the Andaman Sea (after C.K. Morley, 2002)

2.1.2 Geological setting

The Andaman Sea is a complex tectonic region. It lies at the intersection of the obliquely converging of Indian Ocean Plate and South East Plates showed in Figure 2.2. The Andaman Sea is presently opening in a northwest-southeast direction (Curry et al., 1979). Based on magnetic, gravity and seismic data, Peter et al. (1966) showed

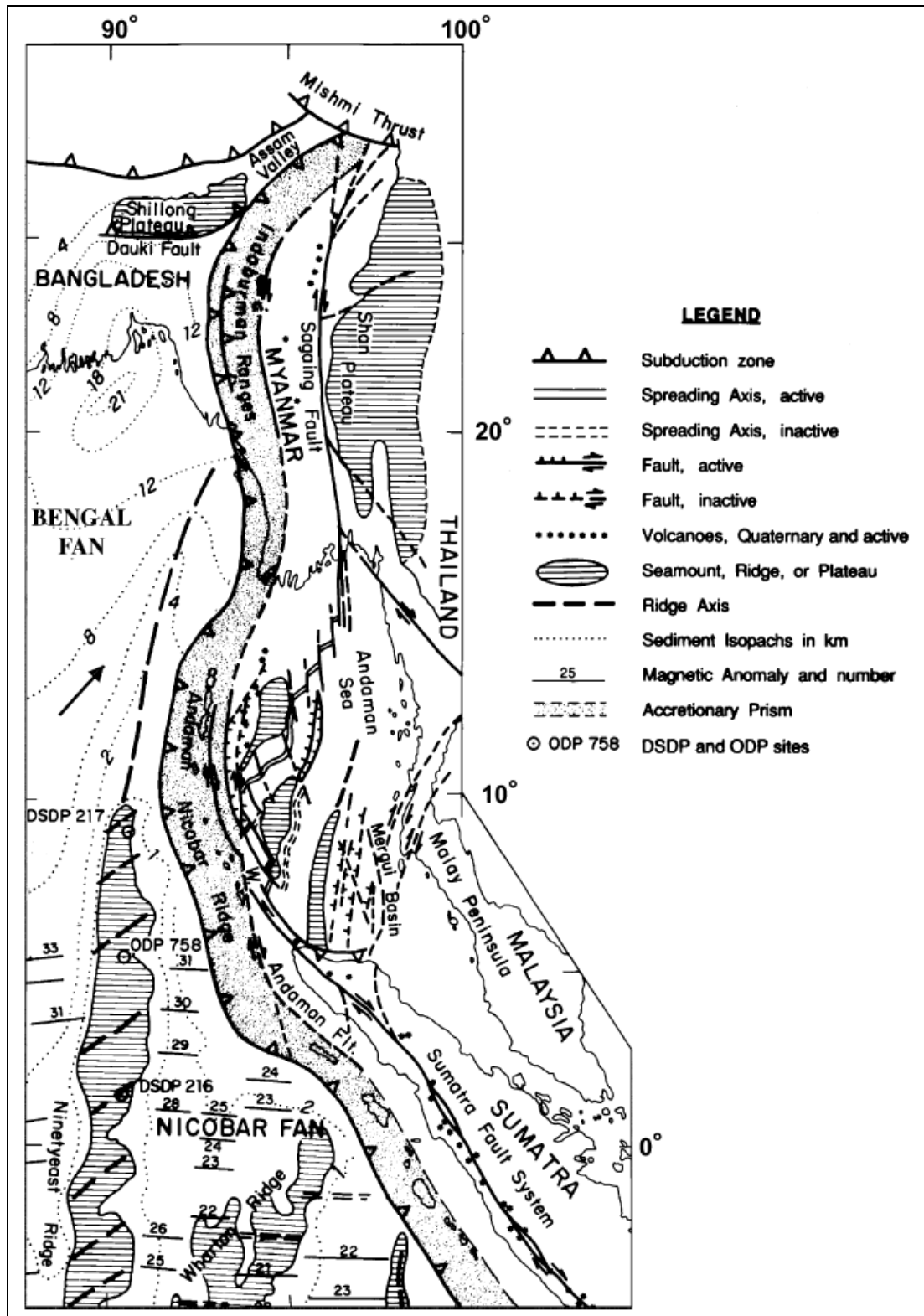


Figure 2.2 Tectonic map of the Mergui basin and Andaman Sea region

(after Curray et al., 2005)

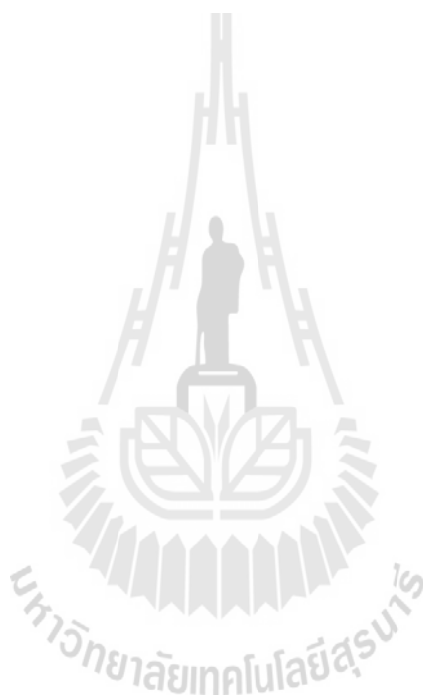
that the major tectonic trends of northern Sumatra and Burma can be linked through to the Andaman Sea. Weeks et al. (1967) further delineated major segments of the island arc system in the western part of the Andaman Sea. Rodolfo (1969) suggested that Tertiary differential movement between Indo-Australian and South East Asian Plates produced directional stress which opened up a rhombochasm in the Andaman Sea. Ridd (1971) postulated that the Mergui basin may have opened as a result of a dextral shear couple bounded to the east by the NE-SW trending Ranong-Klong Marui fault system and to the west by the Sagaing-Sumatra fault system. Shouls (1973), using earthquake foci data for the Andaman Sea, proposed a stress diagram with a dextral primary shear couple in a NW-SE direction to explain the rhombochasm opening with a NW-SE trending right-lateral wrench fault and a NW-SE trending antithetic left-lateral fault. Curry et al., (1979; 1982) concluded that subduction of the Indian oceanic crust beneath Sundaland Craton began in the Early Cretaceous. They suggested that the Andaman Sea Basin has developed by drifting of the Andaman-Nicobar ridge westwards over the eastern margin of the Indian Ocean Plate. They concluded that the Mergui basin started to open in Oligocene as a result of steepening of the subducted slab and westward movement of the Mergui ridge away from the Mergui shelf. Rapid extension occurred at the beginning, but ceased in Early Miocene time, at the commencement of sea-floor spreading in the Andaman Sea.

Molnar and Tapponnier (1975) and Tapponnier et al. (1982) suggested that the Mergui basin opened progressively northwards as a wedge-shaped gap, concurrently with strike-slip movements along the Ranong-Klong Marui and Sagaing-Sumatra fault system in the Oligocene.

Harding (1985) confirmed Shouls' (1973) model. The Mergui basin represents a transtensional basin which has a NNW-SSW trending dextral primary shear, coupled with NW-SE synthetic right lateral and NE-SW antithetic left-lateral fault sets. The structural style of the basin is dominated by negative flower structures along NW-SE trending wrench faults associated with parallel monoclines and series of north to NNE-trending oblique en échelon normal faults. Srikulwong (1986) studied the detailed structural development of the southern part of the Mergui basin (W9-E-1 well area). He concluded that the north-south trending normal faults were the main control on basin configuration, and that these faults had some degree of right-lateral movement related to NW-SE directed extensional dextral primary shear couple. Polachan (1988) studied the geological evolution of the Mergui basin based on seismic data in block W-8 and W-9 and geological data obtained from ten wells. He concluded that the Mergui basin is a transtensional back arc basin. The basin developed rapidly during the Late Oligocene as a series of N-S trending half-graben, and rifting developed progressively northward. Transtensional dextral shear along the NW-SE trending Sumatra fault system in the west and sinistral movement along Ranong and Klong Marui fault zones to the east led to the development of the Mergui basin are showed in Figure 2.3.

The Mergui basin is bounded by Ranong ridged to the east and the Mergui ridge to the west. The Mergui ridge represents the western edge of the Sundaland Craton (Curry et al., 1979). The basin can be divided into 3 sub-basins: the Western Mergui sub-basin, Eastern Mergui sub-basin and Ranong trough as showed in Figure 2.4. The eastern Mergui and western Mergui are separated by a central high which is a complex horst block extending along the Mergui fault zone.

The Ranong trough is separated from eastern Mergui by the Ranong ridge. During the early Miocene, three sub-basins coalesced to form a single basin. Sediments deposited of the Mergui ridge and Ranong ridge are generally thin and mainly of Pliocene-Pleistocene age (Polachan, 1988).



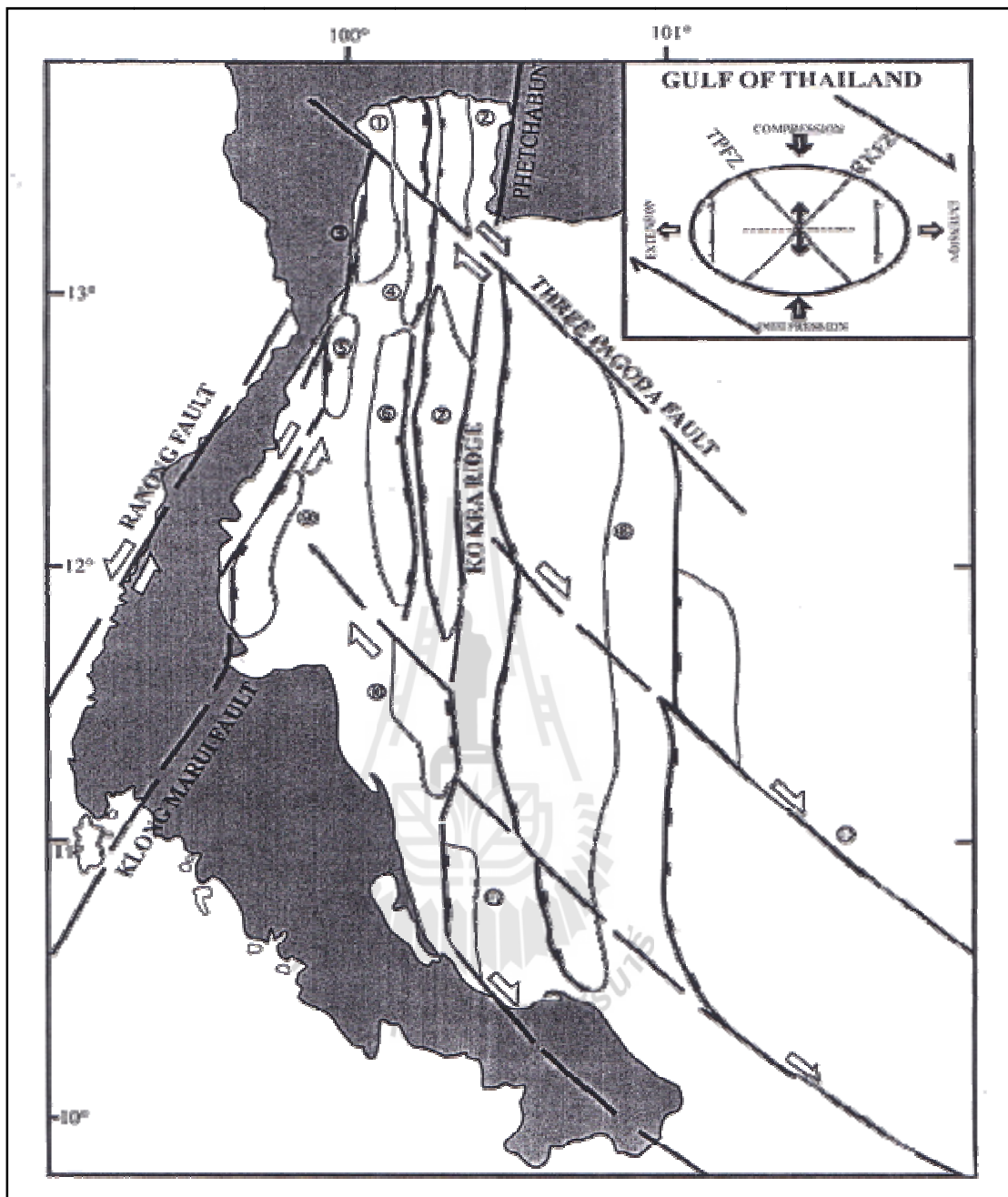


Figure 2.3 Model for the development of the Mergui basin through the combination of transtensional dextral shears along the NW-SE trending Sumatra Fault System (SFS) and the NNW-SSE trending Mergui Fault Zone (MFZ) (after Polachan, 1988)

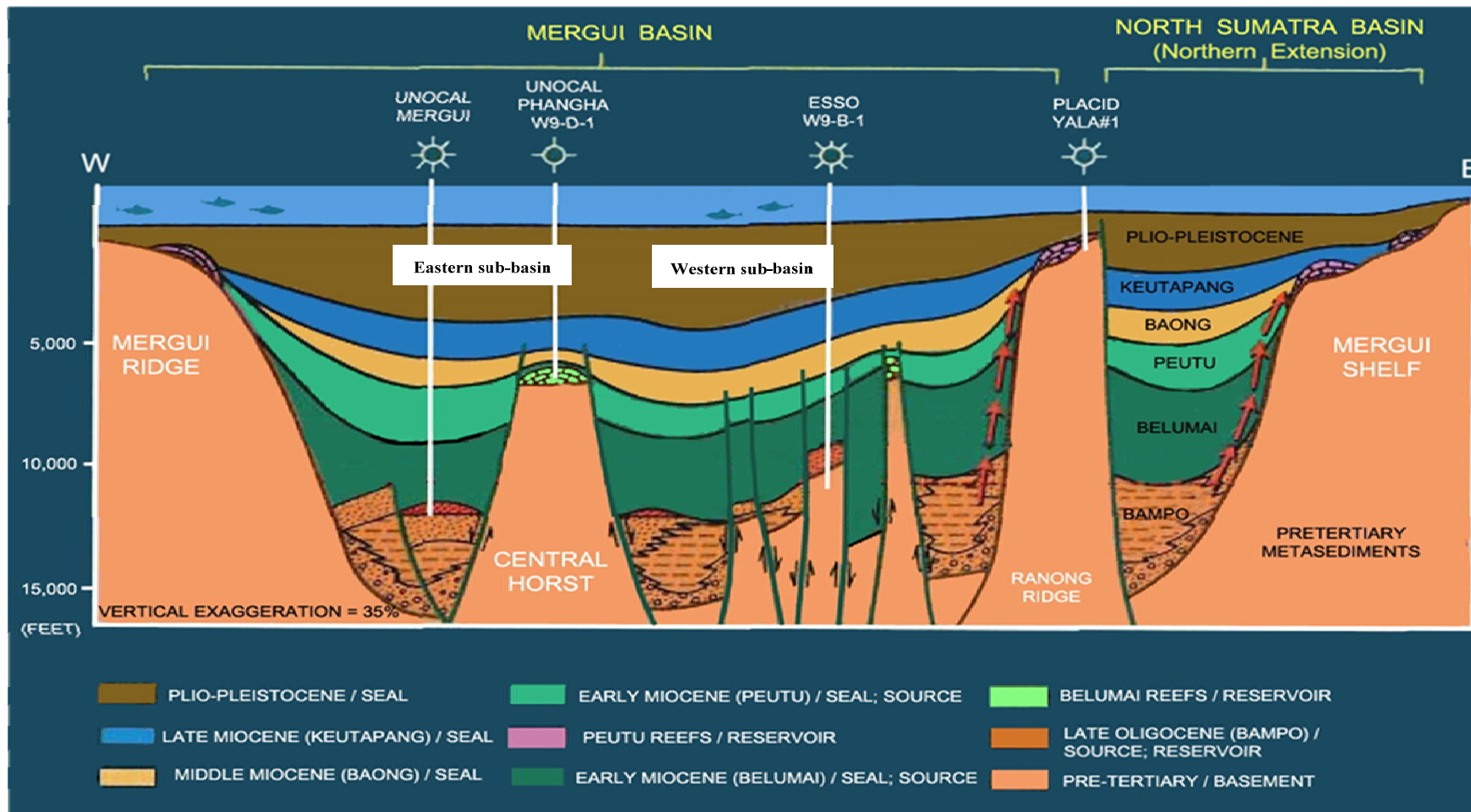


Figure 2.4 Physiography cross-section across the Mergui basin and the North Sumatra basin. (after Andreason et al., 1997)

2.1.3 Geological structure

The southern part of Mergui basin comprises three main sub basin namely Eastern sub-basin, Ranot trough and Ranong trough. They are small, narrow and elongate basins, which forms as a series of N-S trending half graben (Khurida, 2002).

1) Normal faults

The series of N-S trending normal faults is principally controlled by the development of the basin, then forming the N-S trending half graben geometry of the Ranong and Ranot troughs at the same time of sedimentation as showed in Figure 2.5. The depocenters, which influenced the sedimentation thickening into the western margin of the sub-basin, suggests that normal faults are growth fault as that affected rate of sedimentation and they themselves have been partly controlled by sedimentary loading which are known as growth faults (Khurida, 2002).

2) Rollover anticlines

Rollover anticline is the simplest structure that occurs associated to the listric normal fault. It is developed on the hanging wall of the listric normal fault. The surface at the top of the hanging wall formed an anticline or rollover as results of the sagging down of the sedimentary strata to the fault, therefore beds have been retated. and dips in hanging wall have been steeper than in the footwall. Basically, the rollover anticlines are clearly seen between the sequences of the Late Oligocene to Early Miocene in age particularly in Ranot trough (Khurida, 2002).

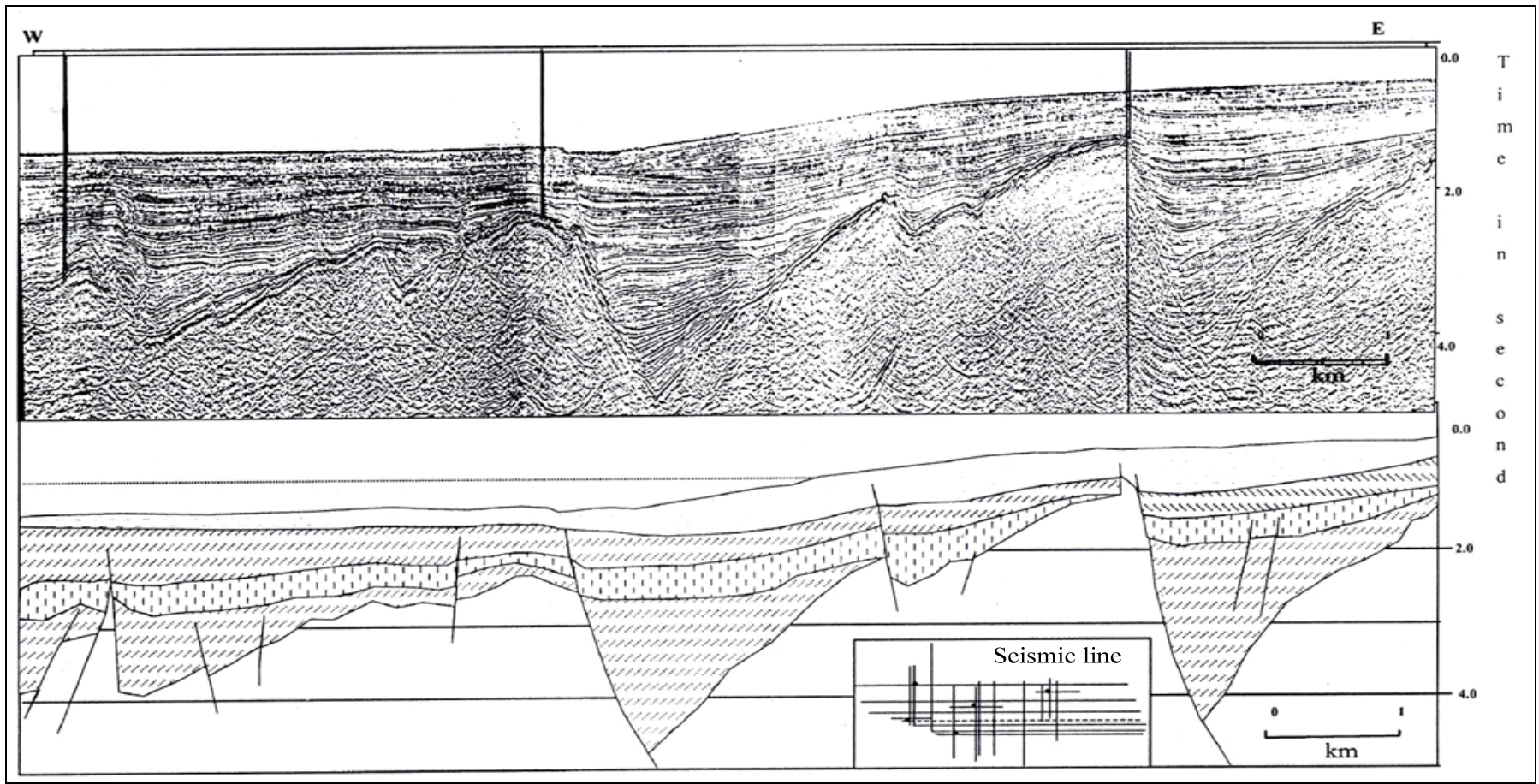
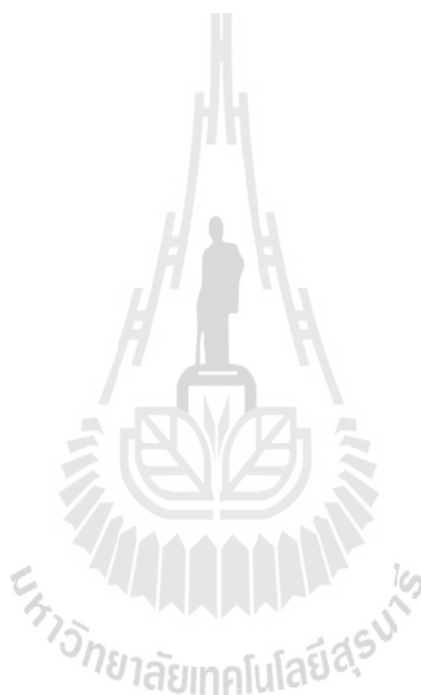


Figure 2.5 The seismic profile depicts half graben geometry sub-basin in the southern part of Mergui basin

after Khurida, 2002)

3) Negative flower structure

Negative flower structures are defined as linear, shallow synform that are displaced by upward-diverging strands of a wrench fault having normal separation which occur east side of Eastern sub-basin as showed in seismic profile of Figure 2.6. These structures demonstrate important criteria to identify the structure style of wrench fault of this region (Khurida, 2002).



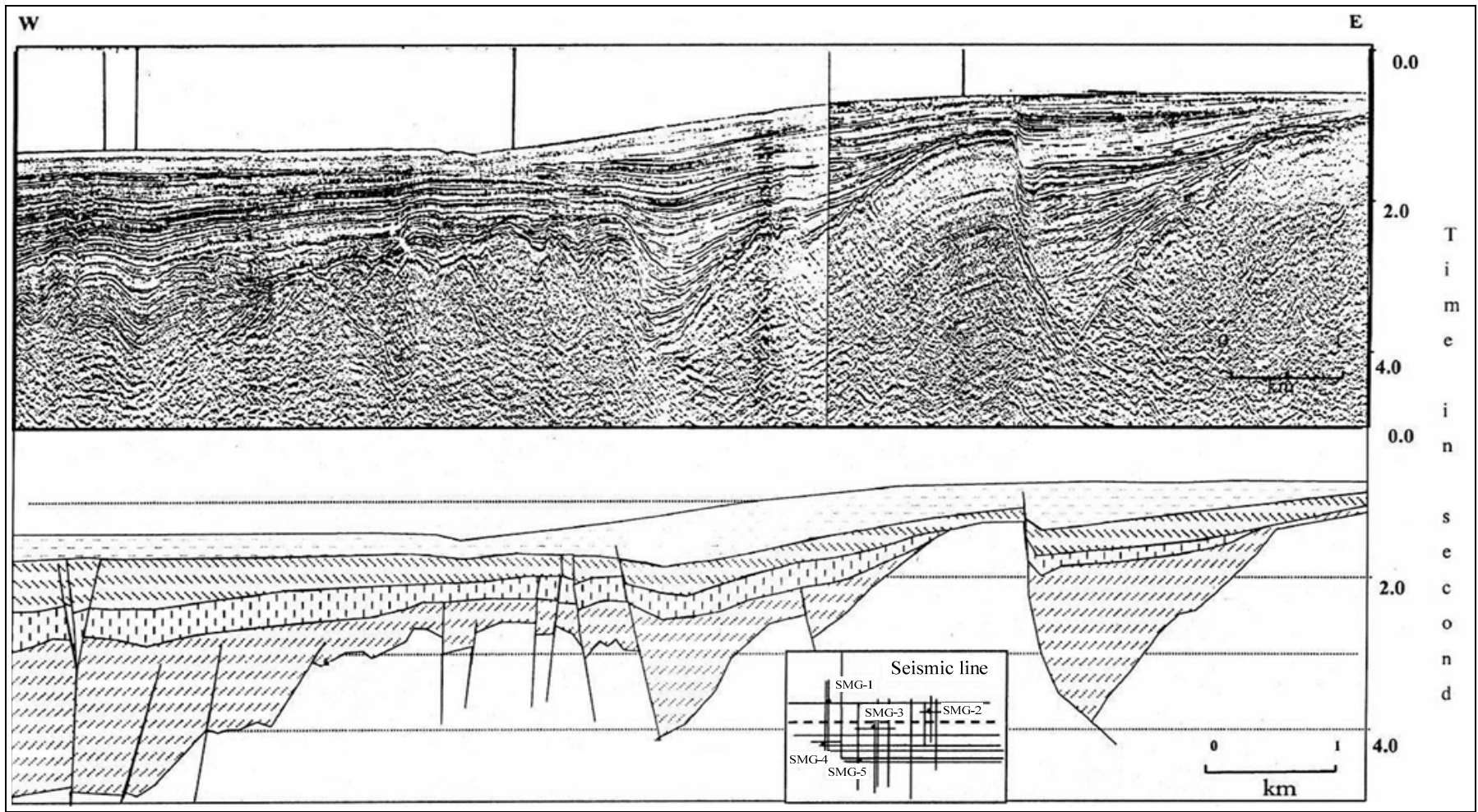


Figure 2.6 The seismic profile depicts negative flower structure in the southern part of Mergui basin (after Khurida, 2002)

2.1.4 Stratigraphy

Sedimentation in the Mergui basin began in the Late Oligocene with the onset of rifting. Sediment supplies were mainly transported from the Thai-Malay Peninsula and deposited into the deeper part of the basin (Polachan, 1994).

Generalized stratigraphic correlation of the Mergui basin and North Sumatra basin is showed in Figure 2.7. The basement of the Mergui basin in the study area is volcanic and meta-sedimentary rocks which vary in age from Late Cretaceous to Late Eocene. These Late Cretaceous-Late Eocene crystalline and volcanic basement units suggest that the basement was part of the magnetic arc of the Pre-Neogene Sunda arc subduction system (Polachan, 1994).

The stratigraphy discussed here is mainly derived from Polachan (1994). He established the stratigraphic correlation and environment of deposition based on seismic and well information obtained from ten wells. The stratigraphy of the Mergui basin can be broadly divided into nine formations within five time intervals and can be described in ascending order as follows;

1) **Ranong Formation**

This unit is divided into two formations on the basis of differences in lithology and environment of deposition. The Ranong Formation, named after the Ranong Fault, is composed mainly of shallow marine sandstones, which grade vertically and laterally into outer shelf to bathyal shales and submarine fan sediments of the Yala Formation. These formations can be correlated with the Bruksah and Bampo Formations respectively in the North Sumatra basin (Figure 2.7).

Lithology: The Ranong Formation consists of three lithological units. The basal unit comprises varicoloured (grey and red) massive or thick-bedded

sandstones and conglomerates. These sandstones are medium to very coarse-grained, have subangular to subrounded clasts, are poorly sorted and grade into conglomerate in their lower part. The conglomerates comprise white to milky quartz, chert, jasper, igneous and metamorphic pebbles in a red-brown to grey, silty clay matrix. The middle unit consists of interbedded green-grey sandstones, grey siltstones, dark grey shales and occasional thin coals. Sandstones are predominantly very fine to medium-grained, have subangular to subrounded clasts, are poorly to moderately sorted, and are often calcareous, micaceous and/or carbonaceous. The upper unit comprises massive green-grey, very fine to fine-grained, calcareous, micaceous, thick-bedded sandstones.

Palaeontology and Age: Oligocene palynomorph assemblages of conifer and mangrove (*Florschuetzia trilobata*) pollen are commonly found. The planktonic foraminifera *Globorotalia opima opima*, *Globigerina angulituralis* and *Globorotalia kugleri*, together with calcareous nannofossils, including *Sphenolithus ciproensis* and *Triquetrorhabdulus carinatus* were also recovered from this formation. These microfossils indicate a Late Oligocene to Early Miocene age.

Environment of Deposition: These lines of evidence suggest a near shore depositional environment, while palynology and benthic foraminiferal assemblages suggest a fluvial-deltaic to shallow-marine environment for the basal unit. Lithological and palaeontological data, together with sedimentary structures from the cores and log motifs, suggest that the lower part of the Ranong Formation was deposited in a fluvial environment, which was followed by a marine transgression resulting in a deltaic to shallow-marine environment of deposition for the middle and upper units. The Ranong Formation, named after the Ranong Fault, is composed

mainly of shallow marine sandstones, which grade vertically and laterally into outer-shelf to bathyal shales and submarine-fan sediments of the Yala Formation (see below). These formations can be correlated with the Bruksah and Bampo Formations, respectively, in the North Sumatra basin (Figure 2.7).

2) Yala Formation

The Yala Formation is a lateral equivalent of the Ranong Formation and can be correlated with the Bampo Formation of the North Sumatra basin (Figure 2.7).

Lithology: The formation can be broadly divided into two lithological units. The lower unit comprises grey glauconitic shales with abundant planktonic foraminifera and occasional thin calcareous and micaceous sandstones, siltstones and detrital limestones. Sandstones in the lower unit are white to light grey, very fine to fine-grained (occasionally medium to coarse-grained). The upper unit comprises white to light grey, very fine to fine-grained, very calcareous, micaceous, moderately to well sorted, glauconitic sandstones, containing abundant planktonic foraminifera and shell fragments.

Palaeontology and Age: The formation contains abundant deep-water planktonic and agglutinated benthic foraminifera, calcareous nannofossils and dinoflagellates. The planktonic foraminifera *Globigerina angulisuturalis* and *Globorotalia kugleri* and the calcareous nannoplankton *Sphenolithus ciperoensis* and *Triquetrorhabdulus carinatus* indicate a Late Oligocene to Early Miocene age for this formation.

Environment of deposition: The benthic foraminiferal assemblage suggests deposition in progressively-deepening upper/middle bathyal conditions in the

basal part of the lower unit, grading upwards to a lower bathyal environment towards the top of this unit. The upper unit shows a progressively shallowing-upwards profile from lower to middle/upper bathyal depths.

3) Payang Formation

The Payang Formation can be correlated with the Belumai Formation of the North Sumatra basin (Figure 2.7).

Lithology: The Payang Formation comprises white to light grey, medium to coarse-grained (occasionally fine-grained) calcareous, micaceous, glauconitic sandstones interbedded with grey shales. Benthic foraminifera and shell fragments are abundant in the upper part of the formation.

Palaeontology and Age: Benthic foraminifera are abundant from the top of the formation down to 1,020 meters. Thereafter, they are rare or absent. According to Union Oil, based on a combination of data from benthic foraminifera and palynomorphs, the Payang Formation is Early Miocene, although no further details were given.

Environment of Deposition: Rich benthic foraminiferal assemblages suggest a shallow-marine environment which progressively deepens upwards. Sediments below 1,080 meters contain abundant carbonaceous detritus and lignite, but no foraminifera.

4) Tai Formation

The Tai Formation can be correlated with the Peutu Formation of the North Sumatra basin (Figure 2.7).

Lithology: At the type locality, the formation is divisible into three units: A basal unit, comprising microcrystalline dolomite interbedded with anhydrite, dark grey shales and fine-grained sandstones.

A middle unit, consisting of white to light grey, recrystallized, massive, coral-algal reef limestones.

An upper unit, comprising thin-bedded calcarenites containing abundant angular to subangular, poorly-sorted limestone clasts, interbedded with grey, silty shales and fine-grained glauconitic sandstones.

Palaeontology and Age: The reefal limestones and sandstones of the basal unit in the W9-D-1 well contain abundant corals, algae, gastropods, brachiopods, bivalves and larger foraminifera, including representatives of the genera *Lepidocyclina*, *Spiroclypeus*, *Amphistegina*, *Heterostegina* and *Cycloclypeus* sp., indicating an Early Miocene age. Most of the fossils in the middle reefal unit have been destroyed by recrystallization. Abundant Early Miocene planktonic foraminifera including *Globoquadrina dehiscens dehiscens*, *Globigerinatella insueta* and *Globigerinoides sicanus* were found in association with Early Miocene nannoplankton, including *Discoaster druggi*, *Sphenolithus belemnos* and *Helicopontosphaera ampliaperta*. The age of the Tai Formation is thus Lower Miocene.

Environment of Deposition: Palaeoenvironmental interpretation based on foraminifera and calcareous algae suggests a progressive deepening from inner to outer shelf. The basal unit comprising fine-grained dolomite and anhydrite is interpreted to represent deposition in a high-salinity sabkha or lagoonal environment. The middle reefal unit represents shallow-marine carbonate buildups deposited on a structural high or in a shelf-edge shoal environment.

5) Kantang Formation

The Kantang Formation is a lateral facies equivalent of the Payang and Tai Formation and can be correlated with the Belumai Formation of the North Sumatra basin (Figure 2.7).

Lithology: The Kantang Formation comprises two major lithological units.

The lower shales and upper silty shales interbedded with sandstones. The lower unit consists mainly of grey to brown-grey glauconitic shales containing abundant planktonic foraminifera, and occasional thin siltstones, fine-grained glauconitic sandstones and detrital limestones.

The upper unit consists of grey, very silty, glauconitic shales interbedded with thin siltstones, fine-grained glauconitic sandstones and occasional calcarenites. Sandstone percentages are higher in the W9-A-1 and Trang wells. The unit contains abundant planktonic foraminifera, shell fragments and carbonaceous detritus. Conventional core comprises green-grey, very fine-to fine-grained, well-sorted, massive sandstones containing abundant broken juvenile planktonic foraminifera and green-grey clay rip-up clasts. Petrographically, these sands are mature arkoses containing abundant poikilotopic calcite cement. The abundant calcite cement may have been derived through alteration or dissolution of calcareous planktonic organisms.

Palaeontology and Age: Planktonic and benthic foraminifera, calcareous nannofossils and dinoflagellates are abundant throughout the formation, and include the Early Miocene planktonic foraminifera *Globoquadrina dehiscens*, *Globigerinatella insueta* and *Globigerinoides sicanus*, and the Early

Miocene calcareous nannofossils *Discoaster druggi*, *Sphenolithus belemnus* and *Helicopontosphaera ampliapertura*. The age of the Kantang Formation is therefore Lower Miocene.

Environment of Deposition: According to Union Oil, the benthic foraminifera indicate deposition in a fluctuating environment which progressively deepened from neritic shelf to upper bathyal in the Mergui and Trang wells suggest that the environment of deposition for this formation in the W9-A-1, W9-B-1 and W9-E-1 wells was lower bathyal in the lower unit, progressively shallowing to middle bathyal in the upper unit, on the basis of changes in benthic foraminiferal assemblages.

6) Surin Formation

The Surin Formation can be correlated with the Baong (sandstone) Formation of the North Sumatra basin (Figure 2.7).

Lithology: The Surin Formation mainly comprises green-grey, medium to coarse-grained, calcareous, micaceous and glauconitic sandstones interbedded with grey shales and brown-grey calcarenites. Abundant benthonic foraminifera, gastropod and bivalve fragments are present.

Palaeontology and Age: The Surin Formation contains abundant shallow-marine. Larger foraminifera (including *Lepidocyclina*, *Amphistegina*, *Heterostegina*), gastropod and shell fragments. According to Union Oil, it is Middle Miocene on the basis of foraminifera and palynology, although no further details were given.

Environment of Deposition: Larger foraminiferal assemblages indicate a very shallow-marine environment.

7) **Trang Formation**

The Trang Formation can be correlated with the shale unit of the Baong Formation of the North Sumatra basin (Figure 2.7).

Lithology: The Trang Formation can be subdivided into two major lithological units. The lower unit consists predominantly of grey to brown-grey, glauconitic shales containing abundant planktonic foraminifera and occasional thin siltstones, fine-grained glauconitic sandstones and limestone stringers. The upper unit comprises grey glauconitic shales, containing abundant planktonic foraminifera, shell fragments and carbonaceous detritus interbedded with siltstones, fine-grained glauconitic sandstones and calcarenites.

Palaeontology and Age: The Trang Formation contains abundant deep-water planktonic foraminifera, agglutinated benthic foraminifera, calcareous nannofossils and dinoflagellates. Planktonic foraminifera including *Globorotalia peripheroronda*, *G. peripheroacuta*, *Praefosi*, *G. fosi*, *Sphaeroidinellopsis subdehiscens* and *Globorotalia siakensis*, together with the calcareous nannofossils *Sphenolithus heteromorphus*, *Discoaster exilis*, *D. kugleri*, *Catinaster coalitus* and *Discoaster hamatus* indicate a Middle Miocene age.

Environment of Deposition: Benthic foraminifera suggest a bathyal environment for the lower unit with progressive shallowing to middle or upper bathyal environments in the upper unit.

8) **Thalang Formation**

The Thalang Formation can be correlated with the Keutapang Formation of the North Sumatra basin (Figure 2.7).

Lithology: The Thalang Formation at the type-locality comprises silty, glauconitic shales containing abundant planktonic, agglutinating and benthonic foraminifera, shell fragments and carbonaceous detritus interbedded with siltstones and fine-grained glauconitic sandstones. In the W9-B-1, W9-C-1 and W9-E-1 wells, it consists predominantly of grey, glauconitic shales containing abundant planktonic foraminifera, occasional siltstones and limestone stringers.

Palaeontology and Age: The Thalang Formation contains abundant planktonic and benthonic foraminifera, calcareous nannofossils and dinoflagellates. Planktonic foraminifera, including *Globorotalia linguaensis*, *G. acostaensis*, *G. tumida plesiotumida* and *G. sphaeroidinellopsis subdehiscens*, together with the nannoplankton *Discoaster calcaris* and *D. berggrenii* indicate a Late Miocene age.

Environment of Deposition: Foraminiferal faunas indicate a deep, lower bathyal environment at the base, shallowing to lower bathyal in the upper portion of the W9-A-1 and W9-E-1 wells, and middle bathyal in the W9-B-1 and W9-C-1 wells.

9) Takua Pa Formation

The Takua Pa Formation can be correlated with the Seurula and Julu Rayeu Formation of the North Sumatra basin (Figure 2.7).

Lithology: The Takua Pa Formation consists predominantly of green-grey, very soft, calcareous, glauconitic shales containing abundant planktonic foraminifera, and occasional siltstones.

Palaeontology and Age: The Takua Pa Formation contains abundant foraminifera, calcareous nannofossils and dinoflagellates. This formation is

a foraminiferal ooze. Based on the combination of planktonic foraminiferal markers and Pliocene-Pleistocene calcareous nannofossil marker zones, the age of Takua Pa Formation is Pliocene - Pleistocene to Recent.

Environment of Deposition: The foraminifera indicate a lower bathyal environment for the lower part of the unit, shallowing towards the upper part.

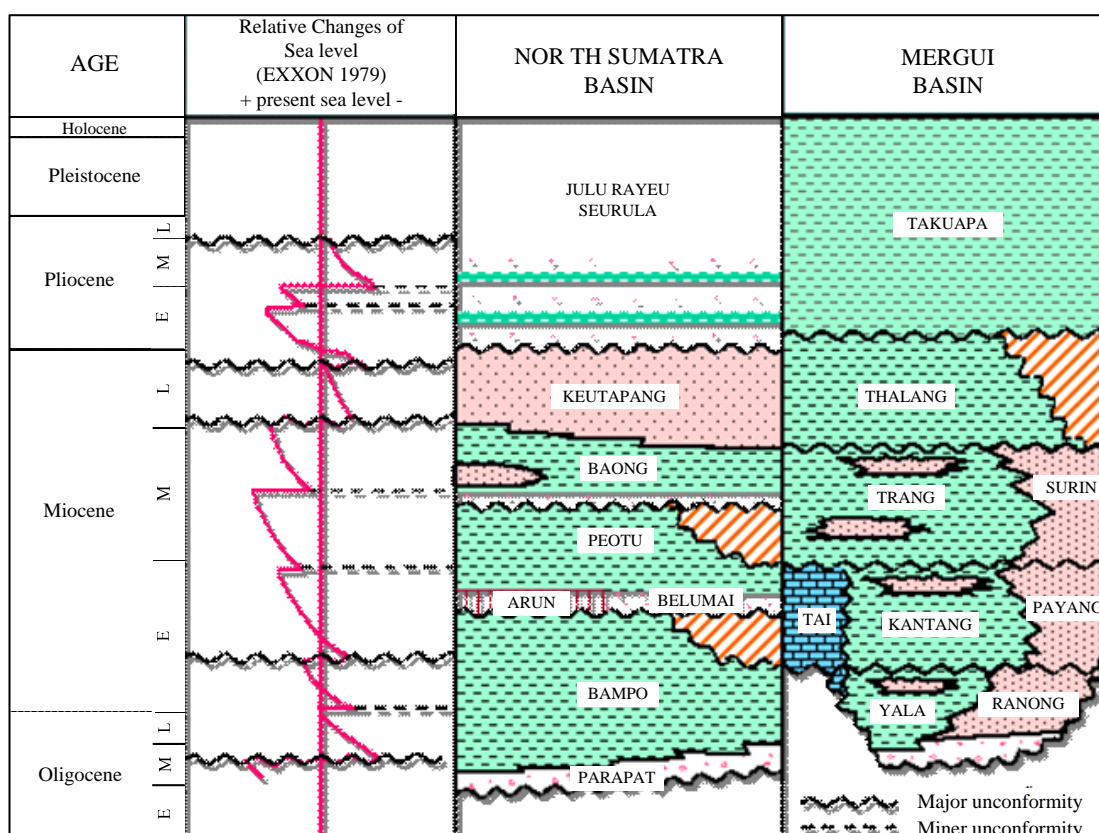


Figure 2.7 Generalized stratigraphy of the Mergui basin and stratigraphic correlation to the North Sumatra basin (modified after Polachan, 1988)

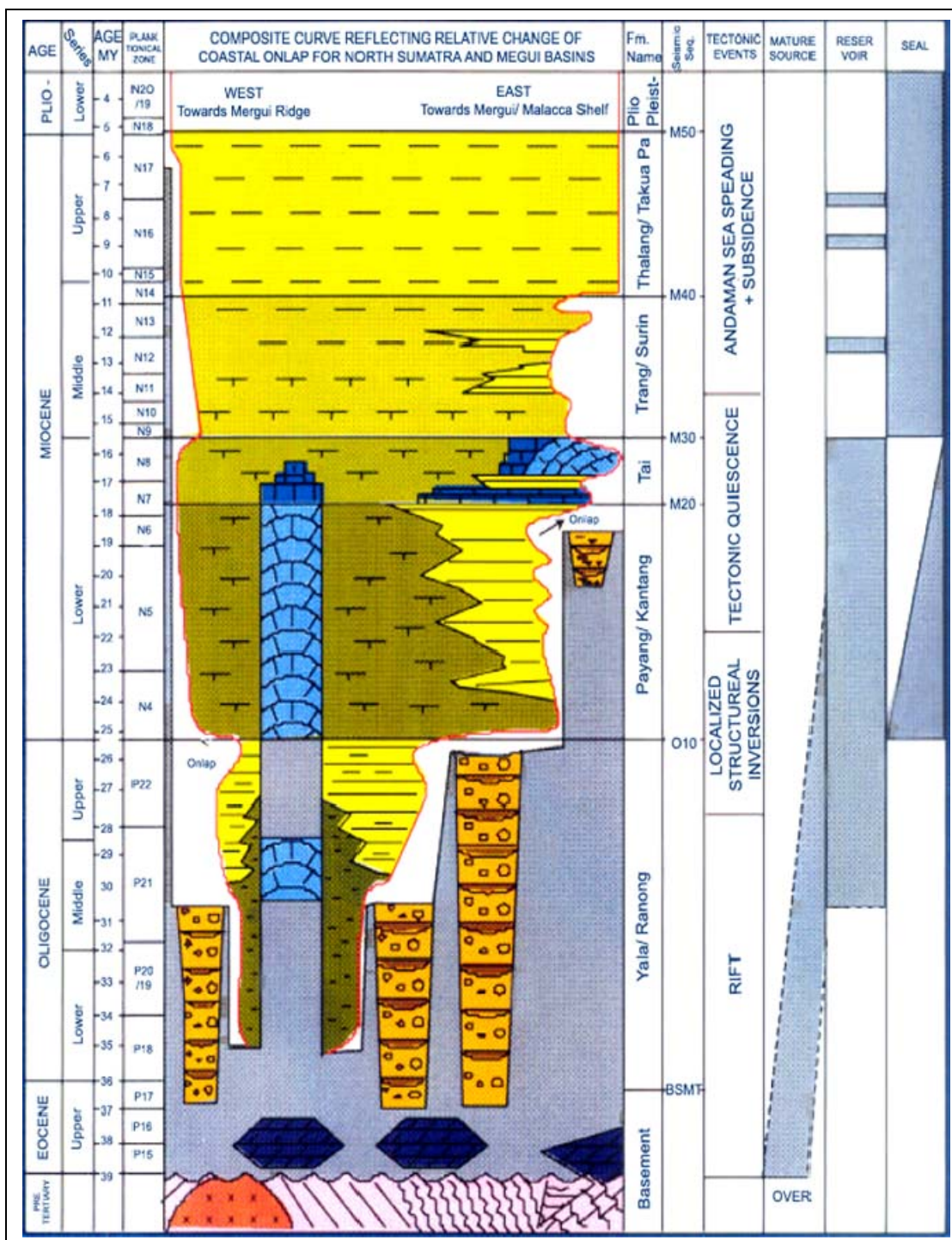


Figure 2.8 Stratigraphy of the Mergui basin (modified after Unocal, 1997)

2.2 Petroleum system of the Mergui basin

Based on studies of Polachan and Racey (1993) and Polachan (1994), petroleum system of the Mergui basin can be summarized as follows.

2.2.1 Source rocks

Results from study of the following wells: W9-A-1, W9-B-1, W9-C-1, W9-D-1, W9-E-1, Trang, Mergui, Tai, Phangha and Payang indicate that potential source rocks are presented in the Thalang, Trang, Kantang and Yala Formations. However, the Thalang, Trang and Kantang were immature in the studied wells, whilst the Yala was mature only in the W9-E-1 and W9-C-1 wells. Thinner mature source rocks may be present in the middle unit of the Ranong Formation. Yala Formation has total organic carbon (TOC) values of less than 0.5%, and generally comprise Type III terrestrial, gas-prone kerogen. The shallow-marine shales of the Ranong Formation have TOC values of 0.5-1.0%, and consist of a mixture of Type II and Type III kerogens, which would be gas-prone. The Kantang Formation has fair-to-good TOC values (average 1.0%), and consists of mainly Type I kerogen. The Trang and Thalang Formations have average TOC values of 1.2%, and consist of Type I.

2.2.2 Reservoir rocks

Sandstone potential reservoirs occur throughout most of the succession, especially in the Ranong, Payang and Surin Formations to a lesser extent in the Yala, Kantang, Trang and Takua Pa Formations. Thick, deltaic and shallow-marine sandstones of the Ranong Formation probably rate as the most promising reservoir intervals, while mid-fan turbidite sands of the Yala Formation and shallow-marine sandstones of the Payang Formation may also form potential reservoirs. The limestones of the Tai Formation may also constitute a potential reservoir where they

have been fractured and/or karstified. Although petrographically these limestones are “tight”, most of the wells which have penetrated the Tai Formation to date have lost circulation due to the presence of large cavities which may have formed through karstification during exposure in the Middle Miocene.

2.2.3 Migration

Hydrocarbon is the movement from source rock to reservoir rock or from reservoir rock to the surface. The main migration path way in this basin is possibly along the faults, resulting from movement along the Mergui fault zone.

2.2.4 Seals and Traps

Potential seals include a number of structural “plays” (e.g. anticlinal and rollover structures) and thick Middle Miocene to Recent deep-marine shale units. The majority of the traps are stratigraphic or combination structural stratigraphic types.

2.3 Exploration history in the Mergui basin, Andaman Sea

In 1971-1972, petroleum exploration began when six shallow waters (less than 200 meters deep) block Nos. W-1, W-2, W-3, W-4, W-5 and W-6 were awarded to oil companied. Minor seismic surveys were undertaken although further exploration was abandoned due to the presence of a thin (<1000 meters) sedimentary succession.

In 1974, the concession block No.W-7 was awarded to Oceanic Exploration S.E.A., the concession block No.W-8 to Union oil Company of Thailand, and the concession block No.W-9 to Esso Exploration Inc. In that year, 2D seismic survey was carried out on the concession block No.W-7.

From late 1975-1976, 2D seismic surveys of totally 5,100 line kilometers were conducted on the concession block No.W-9. Five exploratory wells in the water

depths ranged from 583 to 1,055 meters were drilled. They are W9-A-1, W9-B-1, W9-C-1, W9-D-1 and W9-E-1 with total depth of 16,535 meters. Non-commercial hydrocarbon was presented and Esso Exploration Inc. fully relinquished its concessions in 1982.

In 1976, 2D seismic surveys were carried out on the concession block No.W-8. Six exploratory wells were drilled in the water depth ranged from 410 to 621 meters they are Trang-1, Tai-1, Thanlang-1, Mergui-1 and Payang-1. Only in Mergui-1 and Trang-1 wells was abandoned because of mechanical problems. Only in Mergui-1 and Trang-1 wells that gas shows and trace were found. The grantee, Union Oil Company of Thailand relinquished this concession block in 1977.

In 1987, two exploratory wells were drilled in the concession block No.W-8 that had the same name but different in shapes from the previous W-8. The water depths were ranged from 618 to 655 meters they are Yala-1 and Ranong-1. Before those wells were drilled, hunt International Corp. carried out minor 2D seismic surveys of totally 834 line kilometers in 1984. Both wells were found dry, with only minor gas shows was observed in Yala-1 well.

In 1995, The Department of Mineral Resource carried out the 2D seismic surveys covering the Andaman Sea using Geco-Prakla service.

In 1996, the concession W-8 and W-9 were again awarded to Unocal, Total and Staoil. Extensive 2D seismic surveys of total 11,737 line kilometers were conducted, and five exploratory wells, namely Kantang-1, Thalang-1, Sikao-1, Kathu-1 and Kraburi-1 were drilled with the total depth of 10,648 meters. Non-commercial hydrocarbon was presented and then that concession was relinquished.

CHAPTER III

METHODOLOGY

3.1 Introduction

Based on available data, this research conducted some geochemical, mapping, and reservoir modeling techniques in order to study potential source rocks and potential petroleum migration pathway of the Mergui basin which can be described in details as follows.

3.2 Petroleum source rock

In order to study maturity and organic richness of potential source rocks of the Mergui basin, some essential geochemical data including kerogen types, hydrocarbon index (HI), oxygen index (OI), total organic carbon (TOC), Production Index (PI) and, Tmax etc., were collected and analyzed from available sources. Some concerning theory and background on these geochemical data are briefly presented as follows.

3.2.1 Element for petroleum source rock study

1) Kerogen

Petroleum source rock is defined as any rock that has the capacity to generate and expel enough hydrocarbons to form an accumulation of oil or gas. The most important factor controlling the generation of oil and gas is the hydrogen content of the organic matter (Hunt and Jamieson, 1956).

Geochemists (Tissot and Welte, 1984) define kerogen as the fraction of sedimentary organic constituent of sedimentary rocks that is insoluble in the usual organic solvents (Table 3.1). Kerogens are composed of a variety of organic materials, including algae, pollen, wood, vitrinite, and structureless material. The types of kerogens present in a rock largely control the type of hydrocarbons generated in that rock. Different types of kerogen contain different amounts of hydrogen relative to carbon and oxygen. The hydrogen content of kerogen is the controlling factor for oil vs. gas yields from the primary hydrocarbon generating reactions.

Table 3.1 Classification of kerogen (after Tissot and Welte, 1984)

Kerogen Type	Kerogen Composition	Hydrogen Index (HI)	Main product expelled at peak maturity
		Mg HC/g TOC)	
I	Amorphous/alginate	>600	Oil
II	Exinite	300-600	Oil
II/III	Exinite/vitrinite	200-300	Mixed oil and gas
III	Vitrinite	50-200	Gas
IV	Inertinite	<50	None

These four types are based on chemical composition and the relative amounts of carbon, hydrocarbon, and oxygen present in the sample. The higher the hydrogen contents in kerogen the higher the oil-generative potential of the source rock. During burial and resulting thermal maturation as oil and gas from or crack from the source rock the kerogen becomes depleted in hydrocarbon and oxygen relative to carbon.

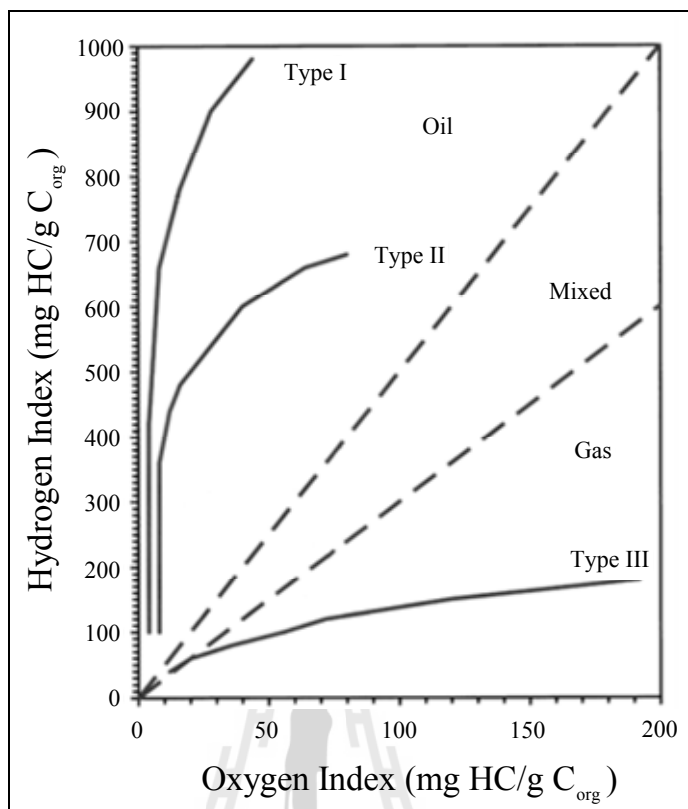


Figure 3.1 Classification of the source rock type by using hydrogen and oxygen indices (after Espitalie et al., 1977)

Plotting of atomic H/C-O/C as showed in Figure 3.1 (Van Krevelen Plot) is the best method for evaluating the quality and maturation state of the source rock in the subsurface. As this technique is time consuming and expensive it is unsuitable for onsite drilling operations or screening large sample populations. A quicker and less expensive method utilizes a modified Van Krevelen diagram that utilizes Rock-Eval parameters and TOC analysis. Modified Van Krevelen diagrams plot atomic HI versus OI. The three kerogen types mature along different evolutionary paths with the arrows pointing towards higher maturation states.

2) Rock-Eval

As being noted above, organic carbon content alone does not provide a reliable indicator of source potential because type of organic matter and the level of maturity influence the actual hydrocarbon yield. Pyrolysis is a more direct indicator and widely accepted among exploration geologists as a rapid and effective mean of evaluating hydrocarbon potential of prospective source rocks. The method follows a special pyrolysis device sketched is showed in Figure 3.2.

“Rock-Eval” pyrolysis as being described by Espitalie et al., (1977) provides information on the quantity, type, and thermal maturity of associated organic matter. Pyrolysis is the program heating of rock samples in an inert atmosphere and measuring the amounts of the different products evolved as showed in Figure 3.3.

Products are released from the organic matter in the rocks in two phases:

a) Free hydrocarbons, oil and gas, contained in the organic matter are vaporized at around 300 °C. This thermo-vaporization for a period of the minutes gives a peak, called the S₁ peak, expressed in mg HC/g of rock.

b) Between 300 and 500 °C, hydrocarbons and oxygen containing compounds are expelled from the rock during the cracking of both kerogen and heavy extractible compounds such as resins and asphaltenes. Hydrocarbons from the S₂ peak which corresponds to the present potential of the rock sample. S₂ is expressed in mg HC/g of rock. Oxygen compounds decomposed between 300 and 390 °C, and the resulting CO₂ is measured as the S₃ peak expressed in mg CO₂/g of rock.

c) The temperature for which the peak is maximum (T_{max} , expressed in $^{\circ}C$) was found to vary with the thermal evolution formerly undergone by the rock sample under analysis.

d) The organic carbon remaining after the recording of the S_2 peak (C_R) is measured by oxidation under air (or oxygen) atmosphere at $600^{\circ}C$. The CO_2 obtained is the peak, expressed in $mg\ CO_2/g$ of rocks. The total organic carbon (TOC, expressed in weight %) is automatically computed from peaks S_1 , S_2 and S_4 .

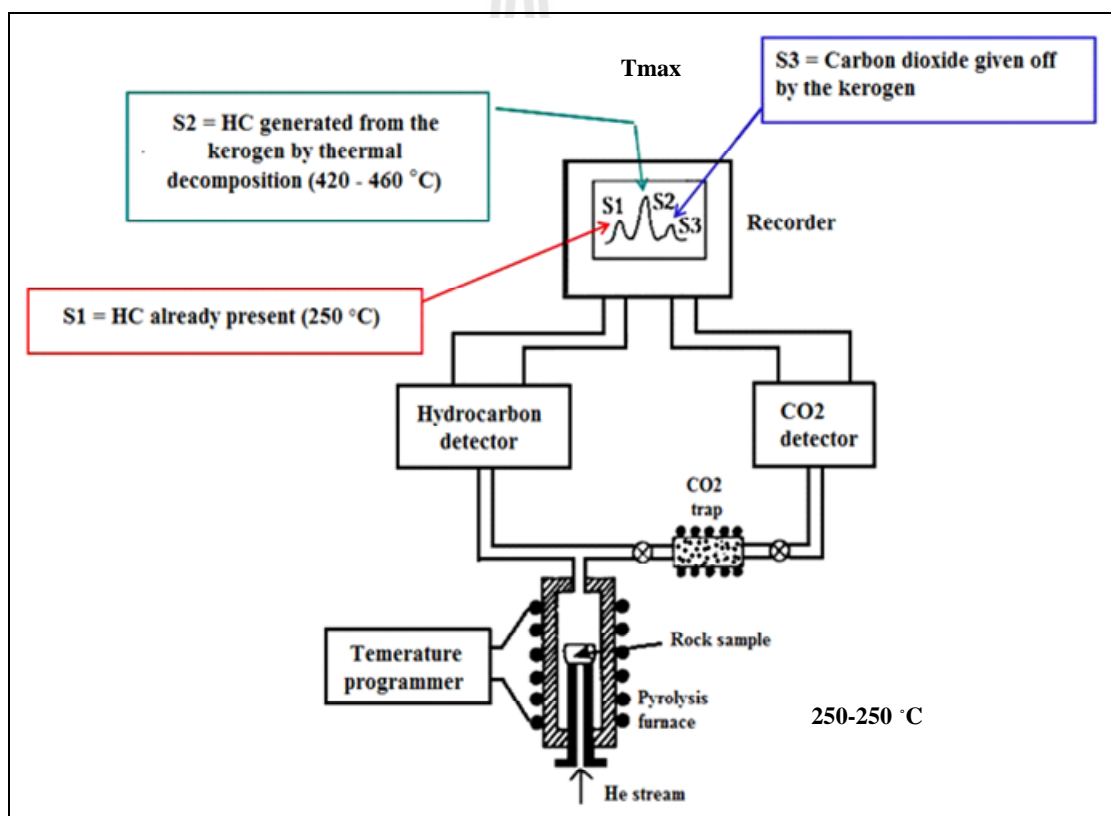


Figure 3.2 Principle of the Rock-Eval pyrolysis (after Waples, 1985)

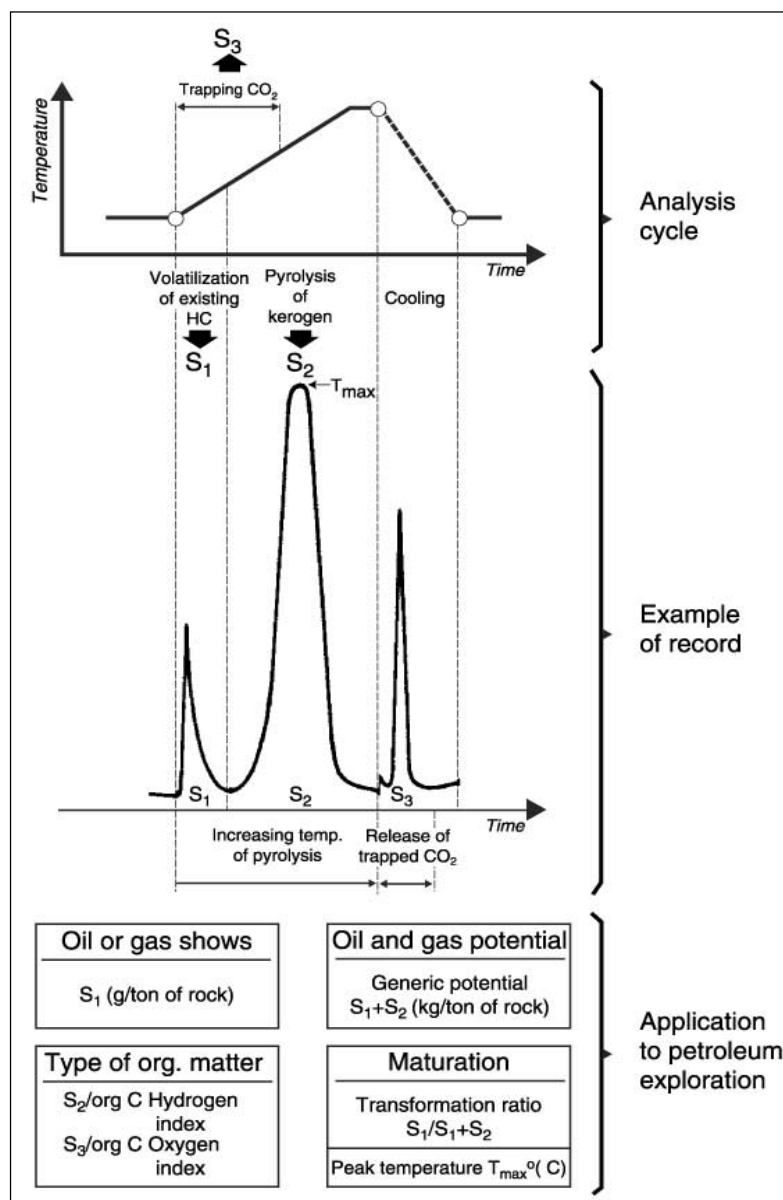


Figure 3.3 Cycle of analysis and example of record obtained by the pyrolysis method of Espitalie et al., 1977 (after Espitalie et al., 1977)

Pyrolysis also provides an indicator of the kerogen type. The conventional approach (Espitalie et al., 1977) utilizes a modified Van Krevelen diagram in which the Hydrogen Index (S_2/TOC , mg HC/gTOC) and the Oxygen Index (S_3/TOC , mg HC/gTOC) are substituted for the H/C and O/C ratios of the original

Van Krevelen diagram. This method assumes that the S_2 hydrocarbon yield is solely dependent on the level of hydrogen enrichment of the kerogen and that $S_3(\text{CO}_2)$ yield is derived solely from organic matter.

The maturation parameters derived from pyrolysis are transformation ratio (KTR), or production index (PI) which is the ratio of the free hydrocarbons to total hydrocarbons ($S_1/(S_1 + S_2)$) ; and T_{max} , the temperature at the point of maximum S_2 hydrocarbons generation during the pyrolysis process.

The transformation ratio ($S_1/(S_1 + S_2)$) is a measure of the hydrocarbons available for accumulation. This ratio will increase as a function of depth and make it a valuable index of maturation. From the example of the maturation of kerogen with depth as monitored by pyrolysis is show in Figure 3.4 (Espitalie et al., 1977). The free hydrocarbon (S_1) are seen to increase steadily with depth, while the generatable hydrocarbon (S_2) are steadily decreased. The transformation ratio increases accordingly. KTR values of 0.1 and 0.4 mark the entrance to and exit from the oil window (Tissot and Welte, 1978). In rocks with low hydrocarbon yield ($S_1 + S_2$) less than 1 mg HC/g rock), the KTR values are highly variable and do not correlate with other maturity indices.

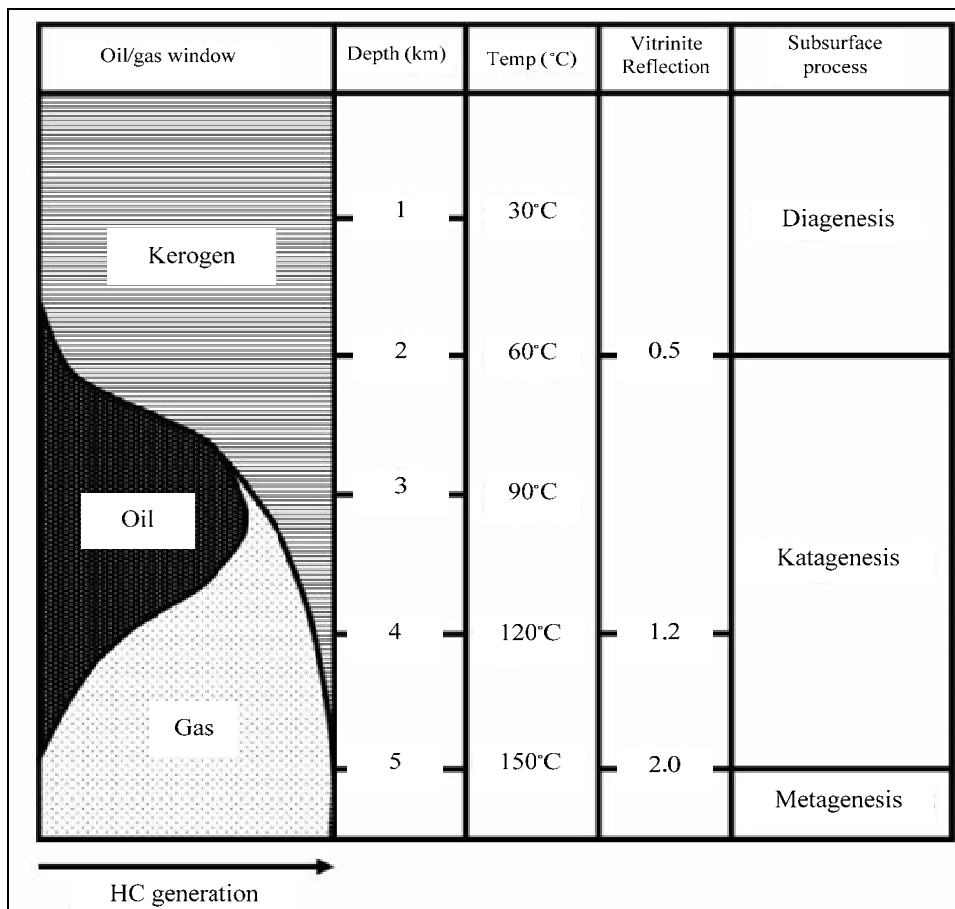


Figure 3.4 Characterization of source rock maturity by pyrolysis methods.

Transformation ratio and/or peak temperature T_{max} may be used as indicators of thermal evolution

(after Tissot and Welte, 1978)

3) T_{max}

T_{max} is temperature which recorded for the minimum of the S_2 peak varies as a function of the thermal maturity of the organic matter (Tissot and Espitalie, 1975). Mature organic matter, which is more condensed is more difficult to pyrolyze and requires higher activation energy, i.e. a higher temperature. Actually, chemical bonds that survived in most highly mature kerogens are those requiring the

highest energy to be broken. Tmax is linked to the kinetics to have relatively simpler molecular structures than type III. It implies a narrower distribution of cracking activation energies and a smaller temperature range (Tissot and Espitalie, 1976).

Tmax variation has been studied for each type of organic matter as a function of its thermal evolution, taking as a reference the vitrinite reflectance R_o of particular interest in the determination for each type of organic matter of the Tmax which corresponds to the being of both the oil and gas window

a) For type I oil genesis beings for a R_o of about 0.70% (measured in interbedded coals) and at a Tmax of 440 °C. the cracking is sudden and all the kerogen is already transformed when 1.0%, while the Tmax remined roughly constant.

b) For type II. The beginning of the oil genesis seems to occur at around 0.60% R_o equivalent, although some examples would show that a most of the kerogen is transformed for $R_o = 1.0$ which corresponds to a Tmax of 455°C. The gas and condensate zones correspond to a range of Tmax of 455-470°C.

c) For type III. Hydrocarbons are formed from $R_o = 0.60\%$ or even 0.70% for a Tmax higher than 435°C. The transition to the condensate zone corresponds to $R_o = 1.30\%$ and Tmax = 470 °C. For type III organic matter, thermal degradation is not yet completed at $R_o = 1.60\%$, which corresponds to Tmax values higher than 600 °C. Dry gas is produced for Tmax higher than 540 °C.

Then, Tmax can also be derived from vitrinite reflectance (R_o) by using Baker and Pawlewicz's (1986) equation below.

$$T_{\max} = [\ln(R_o) + 1.2] / 0.0078 \quad (3.1)$$

Bearmore and Cull (2001) have mentioned that two aspects of pyrolysis related to the increasing of maturity. First, the location of the S_2 peak moves progressively to the right. Second, the amplitude of the S_1 peak increases relative to the S_2 peak. Both of the effects have been correlated with TTI and other maturity indicators, transformation ratio (TR) defined as the height of S_1 divided by the sum of S_1 and S_2

$$TR = S_1 / (S_1 + S_2) \quad (3.2)$$

The specific results of pyrolysis significantly depend on the heating rate and the recording equipment. A faster heat rate gives the reactions less time to proceed; therefore they require higher temperature or a higher heating rate will result in a higher value of T_{\max} for same sample.

4) Thermal maturity modeling

The history of maturity modeling has been discussed in detail elsewhere (Waples, 1984; Ungerer, 1990) and is only summarized here.

- **Time Temperature Index (TTI)**

Lopatin's method is one of used of useful is one of useful applications for petroleum exploration by commonly used of Time Temperature Index or TTI. Location believes that two factors, time and temperature, are important in oil generation and destruction. The effect of both time and temperature could be considered in calculating the thermal maturity of organic material in sediment. The time temperature index of maturity is developed to model, which could predict the

thermal conditions under which hydrocarbon could be generate and preserved. These two factors are interchangeable: high temperature acting for a shot time while a low temperature acting over a long time. The rate of the chemical reactions involved in thermal maturation of organic matter appears to double with every 10°C rise in temperature.

The total maturation or TTI of sediment is given by the sum of the maturities acquired each interval. Thus

$$TTI = \sum_{n_{min}}^{n_{max}} (\Delta T_n)(r^n) \quad (3.3)$$

Where n is index values, n max and n min are the n-values of highest and lowest temperature intervals encountered. ΔT_n is the length of time in million years spent by sediment in temperature interval n. r^n is temperature factor where r is 2 (Waples, 1980).

The values of Lopatin's time temperature index of maturation correlating with important stages of oil generation and preservation are shown in table. Thus, the present day TTI values could be used for finding preserved accumulations of hydrocarbon in suspected reservoir, answering of the time of generation and whether or not the thermal maturity necessary for hydrocarbon generation.

The time and temperature related to kerogen maturity which based on a burial history curve. The burial depth is plotted against geologic time for particular region.

The total maturity is expressed by TTI which the sum of the interval maturity:

TTI	Hydrocarbon generation
15	Onset of oil generation
75	Peak oil generation
160	End of oil generation
500	40 °API oil preservation deadline
1000	50 °API oil preservation deadline
1500	Wet gas preservation deadline
>65000	Dry gas preservation deadline

5) Thermal maturity indicator

There are many methods to reveal the thermal history of sedimentary basin which derive from specific, non-reversible, temperature-dependent, chemical or physical processes that act on one or more components of the sediment. The products of these processes are termed paleotemperature indicators (Beardsmore and Cull, 2001).

- **Vitrinite Reflectance (R_o)**

Reflectance measurements have been extended to particles of disseminated organic matter (kerogen) occurring in shale and other rocks. Histograms showing the frequency distribution of reflectance are established, the reflectance increase from liptinite particles to vitrinite and finally to inertinite.

In order to determine vitrinite reflectance, the cutting or pulverized rock fragments are embedded in an epoxy resin plug. The hardened plug is polished and the reflectance measurement of the individual vitrinite particles is made on randomly oriented particles under a microscope. The reflectance data collected from

each sample were plotted as histograms in an attempt to identify the mean value for the indigenous population. When mean vitrinite reflectance values are plotted as a function of depth on semi-log paper, a linear profile is commonly created. The construction of linear profiles may be complicated by several factors including: marked increases in the rate of deposition and/or reductions in the geothermal gradient, intrusive, faults and major unconformities.

The general reaction leads to the assumption that vitrinite to residual vitrinite and some condensate (Hantschel and Kauerauf, 2009). The vitrinite reflectance models were proposed by Waples (1980) and Sweeney and Burnham (1990) respectively.

The notation used is % R_o (R=reflectivity, o-oil). For kerogen maturity, the approximately maturity boundaries between different levels of maturation are:

- a) $R_o < 0.5$ to 0.7% diagenesis stage, source rock is immature
- b) $0.6-0.7\% < R_o < 1.3\%$ catagenesis stage, main zone of oil generation, also referred to as oil windows.
- c) $1.3\% < R_o < 2\%$ catagenesis stage, zone of wet gas and condensate.
- d) $R_o > 2\%$ metagenesis stage, methane remains as the only hydrocarbon (dry gas zone).

- **Time temperature index or TTI model**

This model was proposed by Waples (1980). It calculated TTI maturity, which is converted to reflectance. The definition of the TTI is based on the

assumption that the maturity rate of vitrinite almost doubles every 10 °C. This thermal maturity indicator has been explained in detail in 3.2.1.4.

- **Molecular biomarkers**

Hantschel and Keuerauf (2009) have described the molecular characteristics of kerogen and petroleum during catagenesis. They are controlled by the types of deposited organisms, the environmental and preservation conditions and the thermal maturity. Gas chromatography and gas chromatography-mass spectrography show the relative abundance of individual biomarkers during kerogen pyrolysis. Chromatographic fingerprints and correlations can therefore be used to determine the organic facies types, the thermal maturation state and the degree of biodegradation.

Table 3.2 A cyclic biomarkers as indicators of biological input or depositional environment; assumes high concentration of component (after Hantschel and Keuerauf, 2009).

Compound	Biological Origin	Environment
2-Methyldocosane	Bacteria?	Hypersaline
Mid-chain monomethylalkanes	Cyanobacteria	Hot springs, marine
Pristane/phytane (low)	Phototrophs, archaea	Anoxic, high salinity
PMI (PME)	Archaea, methanogens and methanotrophs	Hypersaline, anoxic
Crocetane	Archaea, methanotrophs?	Methane seeps?
C ₂₅ HBI	Diatoms	Marine and lacustrine
Squalane	Archaea	Hypersaline?
Botryococcane polymethylsqualanes	Green algae Botryococcus	Lacustrine-brackish-saline

Table 3.3 Generalized geochemical properties differ between nonbiodegraded crude oils from marine, terrigenous, or lacustrine source-rock organic matter (after Hantschel and Keuerauf, 2009).

Property	Marine	Terrigenous	Lacustrine
Sulfur (wt.%)	High (anoxic)	Low	Low
Pristane/phytane	< 2	> 3	~1 – 3
C ₂₇ – C ₂₉ steranes	High C ₂₈	High C ₂₉	High C ₂₇
C _{30,24} -n-propylcholestane	Low	Low or absent	Absent
Steranes/hopanes	High	Low	Low
Bicyclic sesquiterpanes	Low	High	Low
Tricyclic diterpanes	Low	High	High
Tetracyclic diterpanes	Low	High	Low
Lupanes, bisnorlupanes	Low	High	Low
28,30-bisnorhopane	High (anoxic)	Low	Low
Oleananes	Low or absent	High	Low
β -carotane	Absent	Absent	High (arid)
Botryococcane	Absent	Absent	High (brackish)
V/(V + Ni)	High (anoxic)	Low or absent	Low or absent

Table 3.4 Generalized correlation of level of maturity (after Peters and Cassa, 1994).

Level of Thermal Maturity				
Stage of Thermal Maturity for Oil	Maturation		Generation	
	R _o	Tmax	Bitumen	Production Index
	(%)	°C	(mg/g rock)	[S ₁ / (S ₁ + S ₂)]
Immature	0.2-0.6	< 435	< 50	< 0.10
Mature				
Early	0.6-0.65	435-445	50-100	0.10-0.15
Peak	0.65-0.9	445-450	150-250	0.25-0.40
Late	0.9-1.35	450-470	-	> 0.40
Overmature	> 1.35	> 470	-	-

3.2.2 PetroMod 1D modeling workflow

1) Introduction of PetroMod

PetroMod (Schlumberger, 2010) is a program system modeling software that combines seismic information, well data, and geological knowledge to model the evolution of sedimentary basin. PetroMod 1D modeling workflow is demonstrated in Figure 3.5. The software will predict if, and how a reservoir has been charged with hydrocarbon generation, migration routes, quantities, and hydrocarbon type in the subsurface conditions. Petroleum systems modeling is a vital additional component in assessing exploration risk prior to drilling. It helps to predict which traps are most likely to contain hydrocarbons and which type of hydrocarbon can be expected as well as their properties. In 2008 Schlumberger acquired IES (Integrated Exploration System), which was founded in 1982 by Prof. Dietrich Welte as a service company for the oil and gas exploration industry to utilize a newly emerging technology called “Basin modeling” that could improve predictions of when and where oil and gas were generation modeling, technology is now commonly described as “Petroleum Systems Modeling”.

PetroMod software was donated by Schlumberger to the School of Geotechnology, Institute of Engineering Suranaree University of Technology, Thailand, in 2011.

The outputs in PetroMod ID Basin and Petroleum Systems Modeling are; Generation: the burial of source rocks through geological time, from their deposition at the surface until they reach sufficient depth to generate first oil and eventually gas as they descend deeper into the earth.

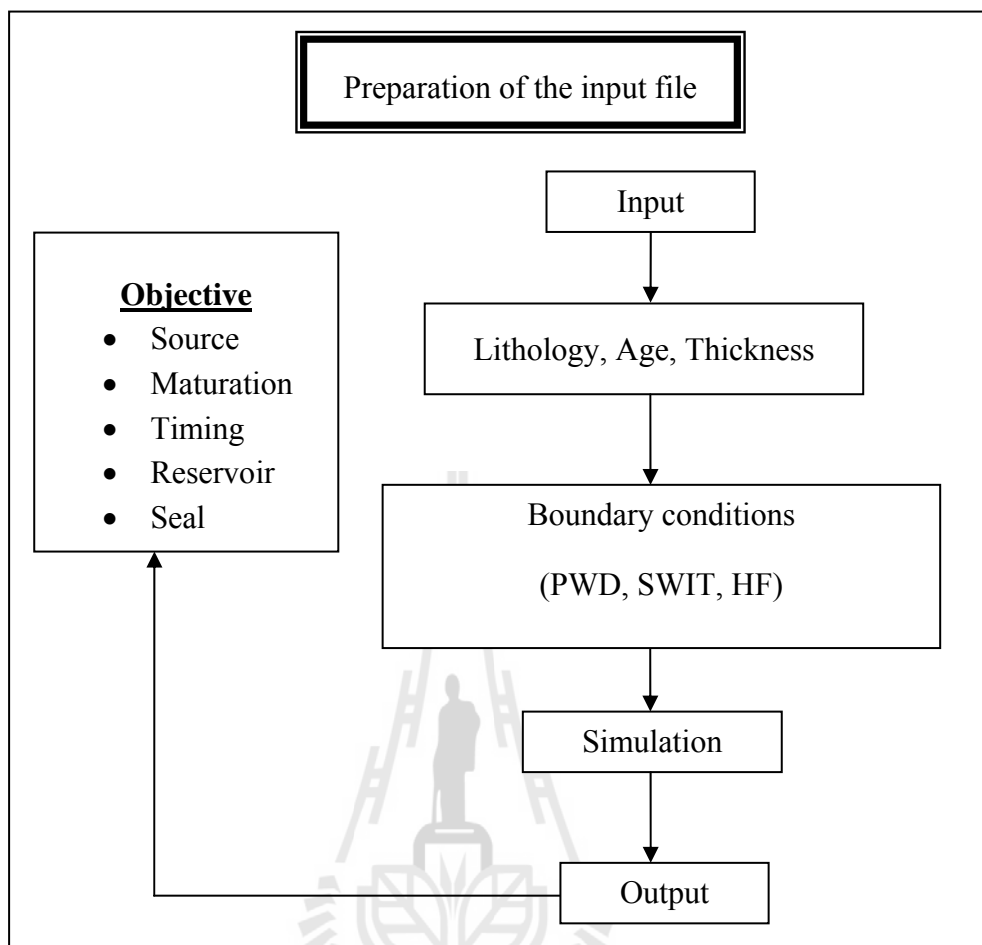


Figure 3.5 PetroMod 1D modeling workflow (modified after Schlumberger, 2010)

Where PWD = Paleo Water Depth,

SWIT = Sediment Water Interface Temperature,

HF = Heat Flow

3.3 Petroleum migration pathway

Petroleum migration pathways can be seen as invisible “bridges” between source rocks and traps. The migration pathways control the distribution of oil and gas in sedimentary basins. Clear understanding of petroleum migration pathways is therefore of great significance for optimizing petroleum exploration in an intensively

explored area. The physical mechanics of oil and gas migration in carrier beds (secondary migration) has been well established. The driving forces for secondary petroleum migration are buoyancy and groundwater flow. In addition, the restraining force is capillary pressure, which increases with decreasing pore-throat size, increasing interfacial tension and wettability.

In order to study the potential petroleum migration pathway of the Mergui basin, this research had conducted some studies on porosity, permeability distribution and also correlated their relationship within the potential reservoirs. In addition, some theories and background on petroleum migration pathway study also briefly presented as follows.

3.3.1 Element for petroleum migration pathway

1) Reservoir rock properties

- **Porosity**

Porosity is percentage of pore volume or void space, or that volume within rock that can contain fluids. Porosity can be a relic of deposition

Primary porosity: such as space between grains that were not compacted together completely or can develop through alteration of the rock

Secondary porosity: such as when feldspar grains or fossils are preferentially dissolved from sandstones).

Porosity can be generated by the development of fractures, in which case it is called fracture porosity. Effective porosity is the interconnected pore volume in a rock that contributes to fluid flow in a reservoir. It excludes isolated pores. Total porosity is the total void space in the rock whether or not it contributes to fluid flow.

Thus, effective porosity is typically less than total porosity.

Characteristics of porosity in other rocks are showed in Figure 3.6.

Shale gas reservoirs tend to have relatively high porosity, but the alignment of platy grains such as clays makes their permeability very low.

Rocks porosity is classified as

a) Absolute porosity: total of rock.

b) Effective porosity: only that porosity due to voids which are time of formation.

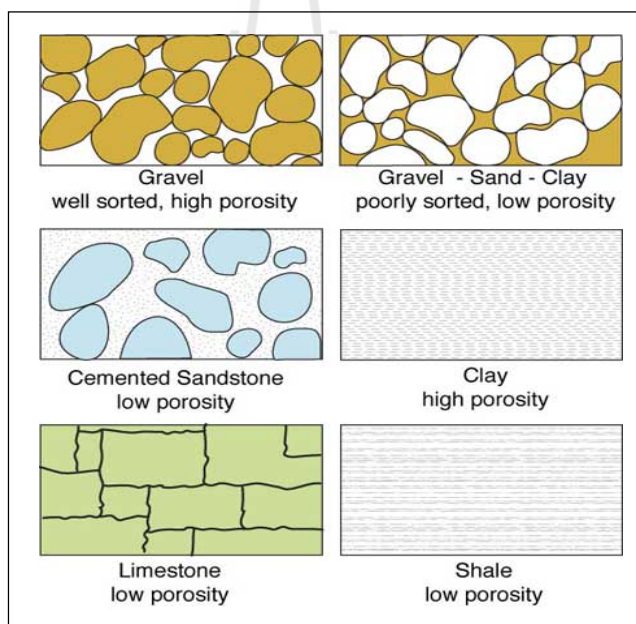


Figure 3.6 Characteristics of porosity in other rocks (after Kansas Ground Water,

<http://www.kgs.ku.edu/Publications/Bulletins/ED10>

/gifs/fig2.jpg, 2012)

- **Permeability**

Permeability is defined as a measurement of a rock's ability, to transmit fluids, typically measured in darcies or millidarcies. The term was basically defined by Henry Darcy, who showed that the common mathematics of heat transfer could be modified to adequately describe fluid flow in porous media. Formations that transmit fluids readily, such as sandstones, are described as permeable and tend to have many large, well-connected pores. Impermeable formations, such as shales and siltstones, tend to be finer grained or of a mixed grain size, with smaller, fewer, or less interconnected pores. Relationships of porosity and permeability in other rocks are showed in Figure 3.7.

Absolute permeability is the measurement of the permeability conducted when a single fluid, or phase, is present in the rock.

Effective permeability is the ability to preferentially flow or transmit a particular fluid through a rock when other immiscible fluids are present in the reservoir (for example, effective permeability of gas in a gas-water reservoir). The relative saturations of the fluids as well as the nature of the reservoir affect the effective permeability.

Relative permeability is the ratio of effective permeability of a particular fluid at a particular saturation to absolute permeability of that fluid at total saturation. If a single fluid is present in a rock, its relative permeability is 1.0.

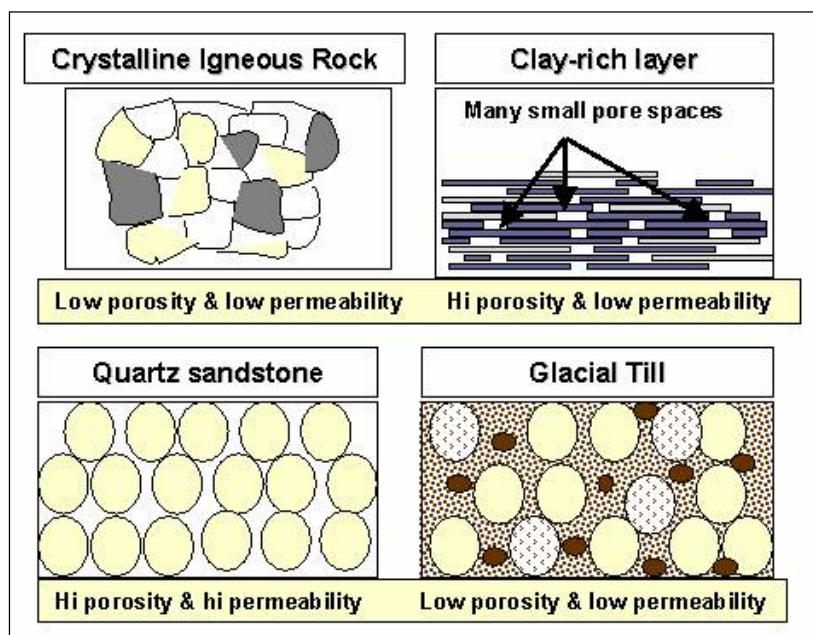


Figure 3.7 Relationship of porosity and permeability in other rocks (after University of Wisconsin, <http://www.co.pepin.wi.us/roundwater%20website/New%20Folder/Slide4.gif>, 2012)

3.3.2 Oil and gas reservoirs

Hydrocarbons and their associated impurities occur in rock formations called reservoir that are usually buried thousands of feet or meters below the surface. Further, not every rock can hold hydrocarbons. To serve as an oil and gas reservoir, rocks have to meet several criteria.

Oil and gas usually stored in small voids called “pores” as showed in Figure 3.8. A rock with pores is "porous" and a porous rock has "porosity." Reservoir rocks must be porous, because hydrocarbons can occur only in pores.

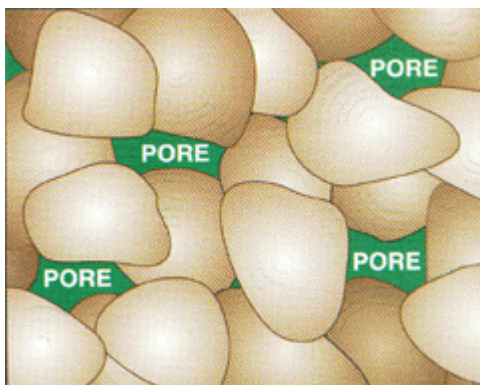


Figure 3.8 Pores in rock (after MPG petroleum, <http://mpgpeteroleum.com/images/pores.gif>, 2012)

A reservoir rock is also permeable—that is its pores are connected as showed in Figure 3.9. If hydrocarbons are in the pores of a rock, they must be able to move out of them. Unless hydrocarbons can move from pore to pore, they remain locked in place, unable to flow into a well. A suitable reservoir rock must therefore be porous, permeable, and contain enough hydrocarbons to make it economically feasible for the operating company to drill for and produce them.

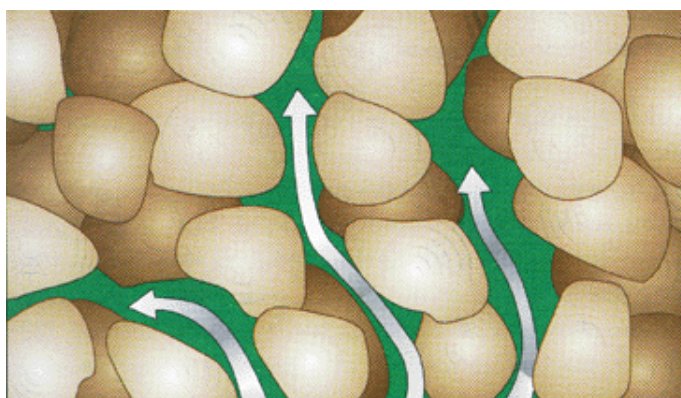


Figure 3.9 Connected pores in rock (after MPG petroleum, <http://mpgpeteroleum.com/images/pores2.gif>, 2012)

3.3.3 Introduction to migration and accumulation of oil and gas

Petroleum accumulations are generally found in relatively coarse grained porous and permeable rocks that contain little or no insoluble organic matter. It is highly improbable that the huge quantities of petroleum found in these rocks could have originated in them from solid organic matter of which now to trace remains. The processes of petroleum migration are still under discussion and not very well understood. Reservoir engineering and production modeling, which are usually based on Darcy type separate phase flow and mass conservation, are successfully applied to model petroleum flow, at least in reservoirs (Peaceman, 1977; Aziz and Settari, 1979; Barenblatt *et al.*, 1990; Dake, 2001).

The principles of hydrocarbon migration, discussed in this section, can be summarized as follows:

- Hydrocarbons migrate as a separate phase, primarily due to buoyancy. This force causes them to move vertically at geologically rapid rates.
- Lithologic layers slow or restrict the vertical movement of hydrocarbons. Seals deflect the hydrocarbons laterally updip through underlying beds to a trap or spill point. Lateral migration is also facilitated by meteoric groundwater flow. Flow rates for compaction- driven water generally are too slow to significantly affect hydrocarbon flow.
- The properties of reservoirs and carrier beds (dip, relative permeability, etc.) control the rate of migration and thus the specific direction of the bulk of hydrocarbons under seals.

3.3.4 Migration stages

Hydrocarbon migration consists of four stages: primary, secondary, tertiary, and remigration. The list below contains their definitions.

- Primary migration; The process of loss of hydrocarbons from the source rock.
- Secondary migration; Migration from source to reservoir along a simple or complex carrier system. Includes is migration within the reservoir rock itself.
- Tertiary migration; Migration to the surface, either from a reservoir or source rock. Also called dismigration.
- Remigration; Migration from one reservoir position through an intervening section into another reservoir position in the same or a different reservoir.

3.3.5 Factors that cause migration

Hydrocarbons migrate from a position of higher potential energy to one of lower potential energy. The spatial location of these energy differences defines the expected migration path. There are many sources for this energy that causes oil and gas migration.

- **Sources of energy**

Three factors primarily cause hydrocarbon migration. All may be active at the same time during the migration process. Each factor produces energy from one or more sources. The table below lists these factors and their corresponding energy sources.

Table 3.5 Factors primarily cause hydrocarbon migration

Factors	Energy Sources
Presence of oil or gas	<ul style="list-style-type: none"> • Buoyancy • Chemical potential (related to concentration differences) • Expansion due to a phase change (related to maturation) • Volume increase due to maturation • Sediment compaction (squeezing the oil or gas from collapsing pore space)
Indirect effects on oil or gas due to burial	<ul style="list-style-type: none"> • Thermal expansion • Water motion due to compaction • Topographically driven flow
Decrease in pressure and temperature as a result of the upward migration of oil or gas	<ul style="list-style-type: none"> • Phase change • Gas expansion

2) Compositional changes during primary migration

i) Factors favoring oil expulsion from a source rock:

Type I or II kerogen

- Sufficient time in the oil window
- High levels of TOC
- Concentration of organic matter in lamina
- Low-capillary-pressure conduits

ii) Factors favoring gas expulsion from a source rock:

Type III kerogen

- Rapid burial through the oil window
- Low TOC
- Dissemination of organic matter
- High-capillary-pressure conduits

3.3.6 Migration Pathways

Hydrocarbon migration appears to occur in spatially limited areas (always unsampled because of their small size) and in discrete time intervals. It leaves either no trace or a trace that is continually modified or destroyed by later events. Effective hydrocarbon migration occurs along discrete pathways, not along broad, uniform fronts. These pathways are determined by the pore networks, the interaction of these networks between formations, and the stratigraphic variation within the basin. Within the carrier/reservoir bed, the migration pathway is controlled by the structural configuration of the contact with the overlying seal and the continuity of both the carrier permeability network and the overlying seal. This section discusses the general characteristics of these paths and shows several examples.

3.3.7 Defining Migration Pathways from Source to Trap

The general flow of petroleum from a mature source rock to a trap can be estimated using a few simple assumptions:

- The dominant force causing petroleum to move is buoyancy.
- Petroleum is deflected laterally through sand-rich sections by overlying shale-rich sections.
- Where there are closed traps along this pathway, petroleum will accumulate until the trap is full and spills, or leaks, any additional migrating petroleum.

The exact flow paths generally require more detailed information about stratigraphic variability, distribution of fractures, and permeability of faults than is generally available to geologists.

Table 3.6 Procedure for defining migration pathways

Step	Action
1	Identify stratigraphic units with high permeability that could serve as carrier beds.
2	Identify stratigraphic units with low permeability that could serve as regional seals.
3	Make a structure contour map at the top of carrier beds or the base of regional seal. Highs focus flow so lows diffuse flow.
4	Locate source rocks and map the location of the upper boundary of the oil and gas maturation windows.
5	Locate other geologic features that could influence flow pathways, e.g., fault segments, fractures, unconformities, boundaries of intrusions, flanks of salt domes.
6	Draw migration vectors based on the above information.

i) Data requirements

A map of the structure at the top of the main sand-rich section is required to make a petroleum migration map. Generally, a map showing the present structure is used. However, a much better result can be obtained by using a map showing the structure at the time of main hydrocarbon expulsion. The location of mature source rock is projected vertically onto this map.

3.3.8 Reservoir of the Mergui basin

UNOCAL (1997) suggested that The first sediment from nine formations started deposition in the Late Oligocene above the basement is the Ranong

and Yala Formations. Ranong Formation was deposited in a fluvio-deltaic to shore-face environment whereas Yala Formation which interfinger with Ranong Formation was deposited in a shallow marine environment, carbonate and turbidite can be found locally. Ranong Formation corresponds to the maximum rifting and extension of the basin during Oligocene lowermost Miocene. The map reflects the general configuration of the basin during this period. The main depocenters correspond to the present ones: northern and southern part of the Ranong Trough bounded to the west by the Ranong Fault, Ranot Trough and its northern prolongation, Eastern Mergui Basin, Western Mergui Basin (3 main depocenters). Central High bounded by steep faults, northernmost part of the basin. According to the work of UNOCAL (1997), Ranong Formation is divided into 3 Sub-Formations; Lower, Middle, and Upper Ranong Sub-Formation.

In this study, the reservoir parameter maps were specifically produced only in these 3 Sub-Formations which included the porosity, permeability distribution map, and structural time contour map. Procedures for reservoir studying are as follows;

1) Porosity mapping

The porosity distribution or porosity maps of the Ranong 3 Sub-Formations had been generated according to the following steps;

- i) Collected porosity data of the Ranong sub-formation based on the log re-evaluation report (5 % porosity cut off) and placed into the base map.
- ii) Produced the map by hand contouring. The porosity distribution model based on environmental deposition was also taken into account.

2) Porosity plot versus depth

The relationship between porosity and depth of the Ranong Sub-Formations had been generated as following steps;

i) Collected the porosity data of each well from the wireline log re-evaluation report (with $\geq 5\%$ porosity cut off) and plotted versus the true vertical depth for each particular sub formation.

ii) Added the trend line to generate the linear relationship of each sub-formation.

3) Permeability mapping

The permeability distribution or permeability maps of the Ranong 3 Sub-Formations had been generated according to the following steps;

i) Collected permeability data of the Ranong Sub-Formation based on relationship the porosity plotted versus permeability from original well reports and placed into the base map.

ii) Produced the map by hand contouring. The porosity distribution model based on environmental deposition was also taken into account.

4) Permeability plot versus porosity

The relationships between permeability and porosity of the Ranong Sub-Formations have been generated as following steps;

i) Collected the permeability and porosity data of each well from the relationship porosity plotted versus permeability from original well reports and plotted versus the true vertical depth for each particular sub formation.

ii) Added the trend line to generate the linear relationship of each sub-formation.

5) Structural mapping

The structural time contour (TWT) map of the Ranong horizon had been generated according to the following petroleum migration pathway based on regional geology and main structure of the Mergui basin.



CHAPTER IV

RESULT OF THE STUDY

4.1 Petroleum source rock

Results from petroleum source rocks study of the Mergui basin based on available data, geochemical techniques and PetroMod program, some issues can be summarized as follows.

4.1.1 Petroleum source rock of the Mergui basin

Based on previous study of source rock richness and kerogen type of the Mergui basin that was evaluated using standard Rock-Eval pyrolysis and visual kerogen analyses, all of petroleum geochemical studied were reported and reinterpreted. Unfortunately, Rock-Eval pyrolysis was analyzed only the sidewall cores and cuttings from the Yala, Kantang and Trang Formations. As a result, the range and frequency of total organic carbon (TOC) measurements in weight percent, Tmax, production index (PI) = $[S_1 / (S_1 + S_2)]$, vitrinite reflectance (%R_o), hydrogen index (mg HC/g TOC) and oxygen index (mg HC/g TOC).

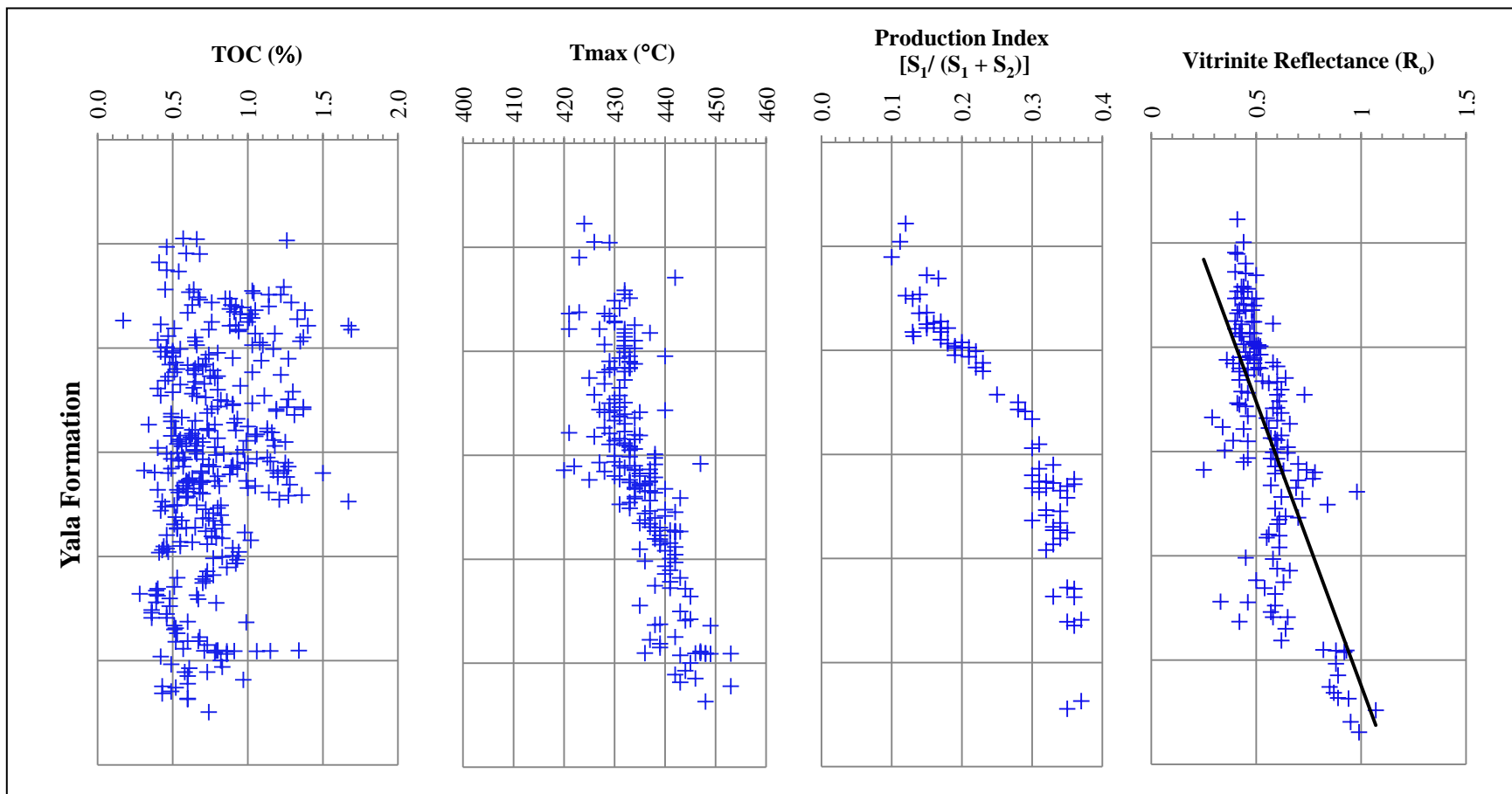


Figure 4.1 Results of pyrolysis (Rock-Eval) cutting samples of the Yala Formation; TOC in wt. %, Tmax (°C), Production index $[S_1 / (S_1 + S_2)]$, Vitrinite reflectance ($\%R_o$)

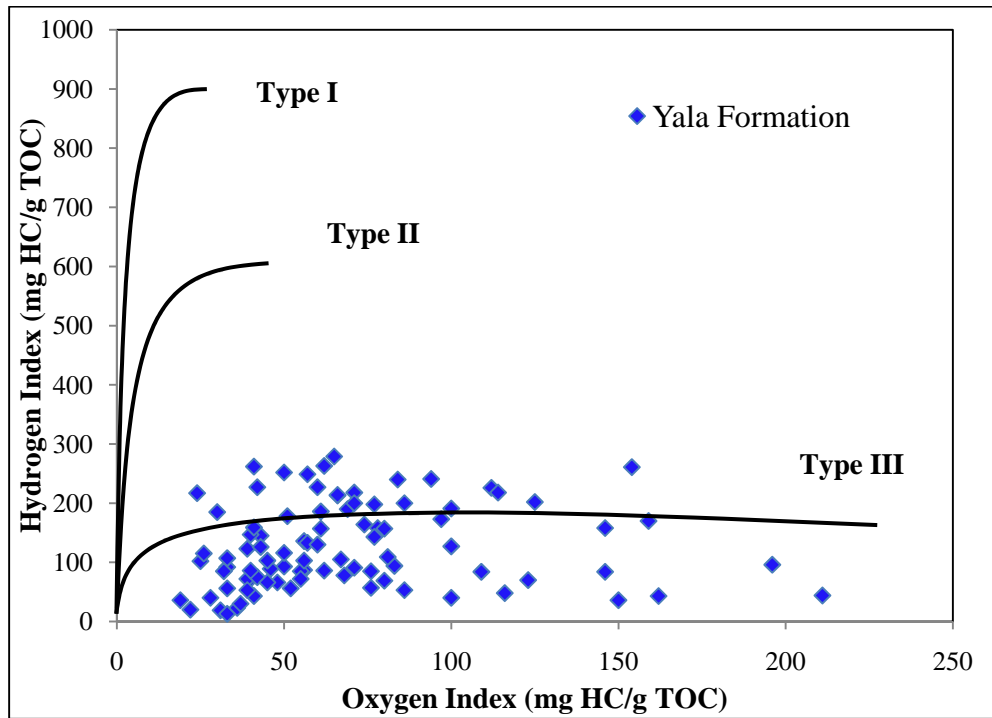


Figure 4.2 Hydrogen Index (HI) versus Oxygen Index (OI) of the Yala Formation plotted

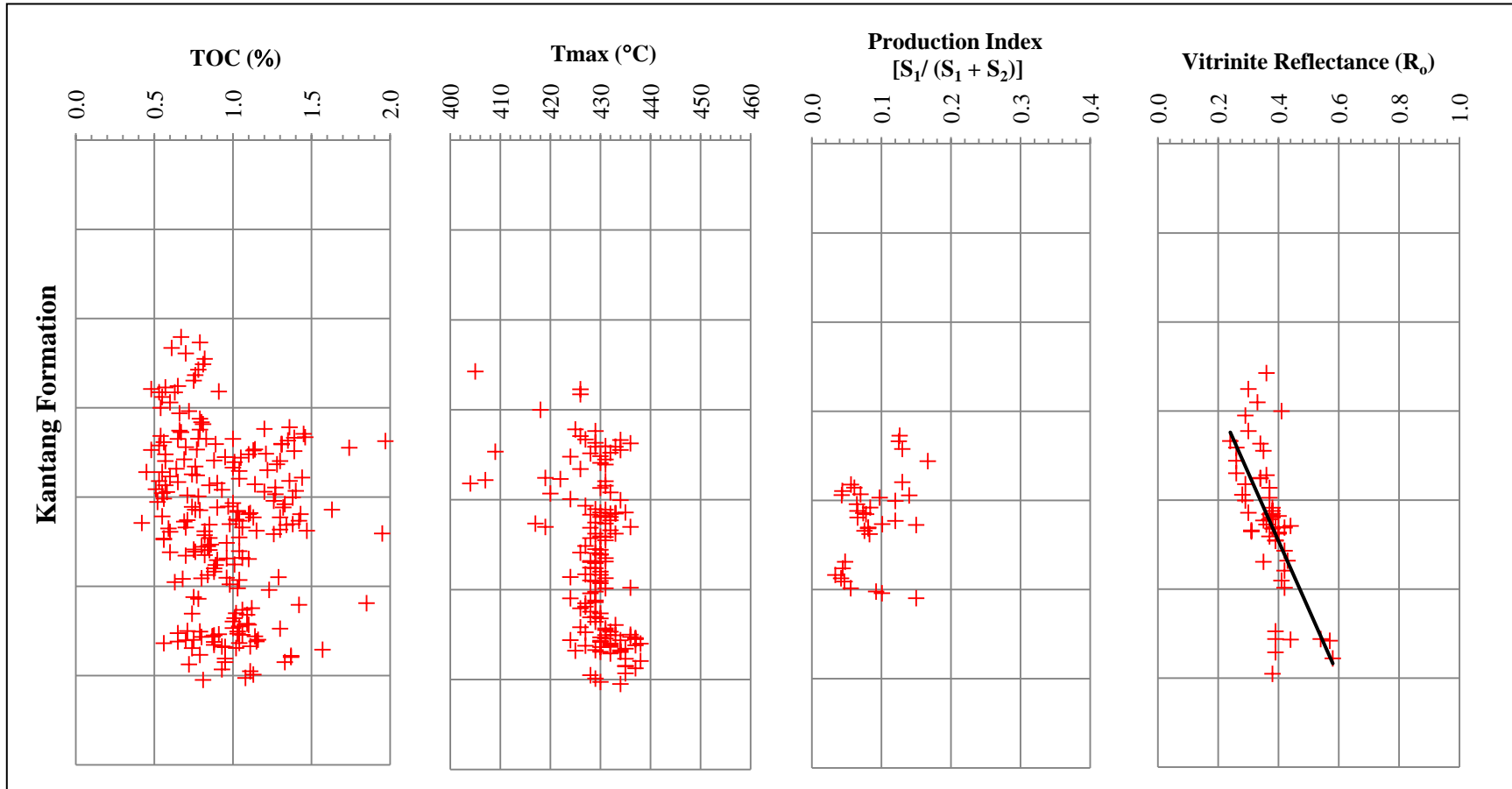


Figure 4.3 Results of pyrolysis (Rock-Eval) cutting samples of the Kantang Formation; TOC in wt. %, Tmax (°C), Production index $[S_1 / (S_1 + S_2)]$, Vitrinite reflectance ($\%R_o$)

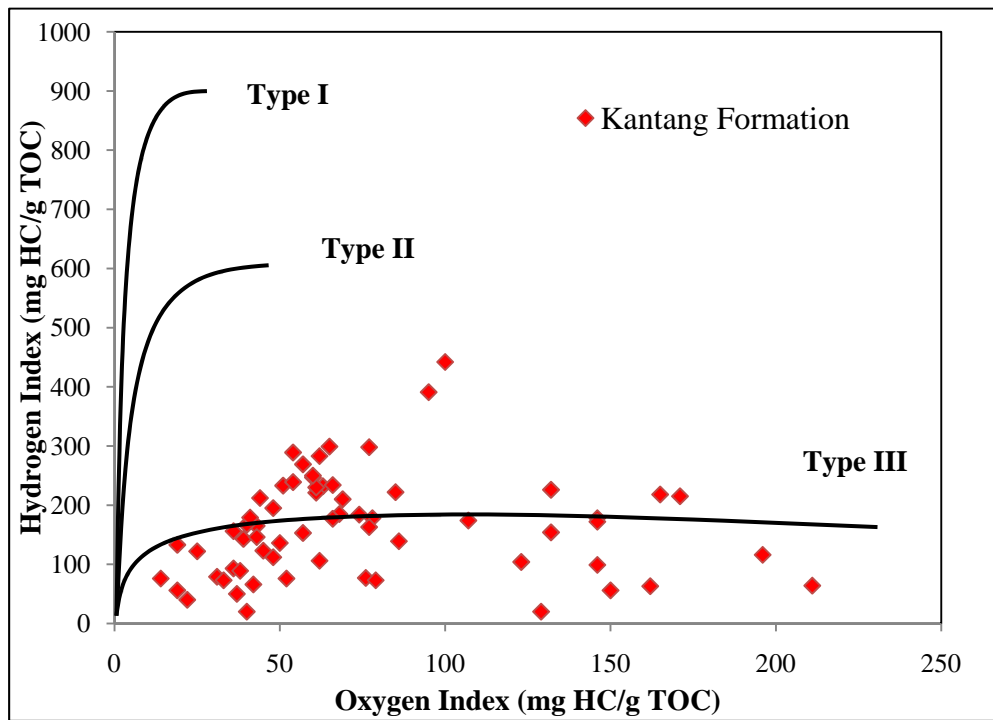


Figure 4.4 Hydrogen Index (HI) versus Oxygen Index (OI) of the Kantang Formation plotted

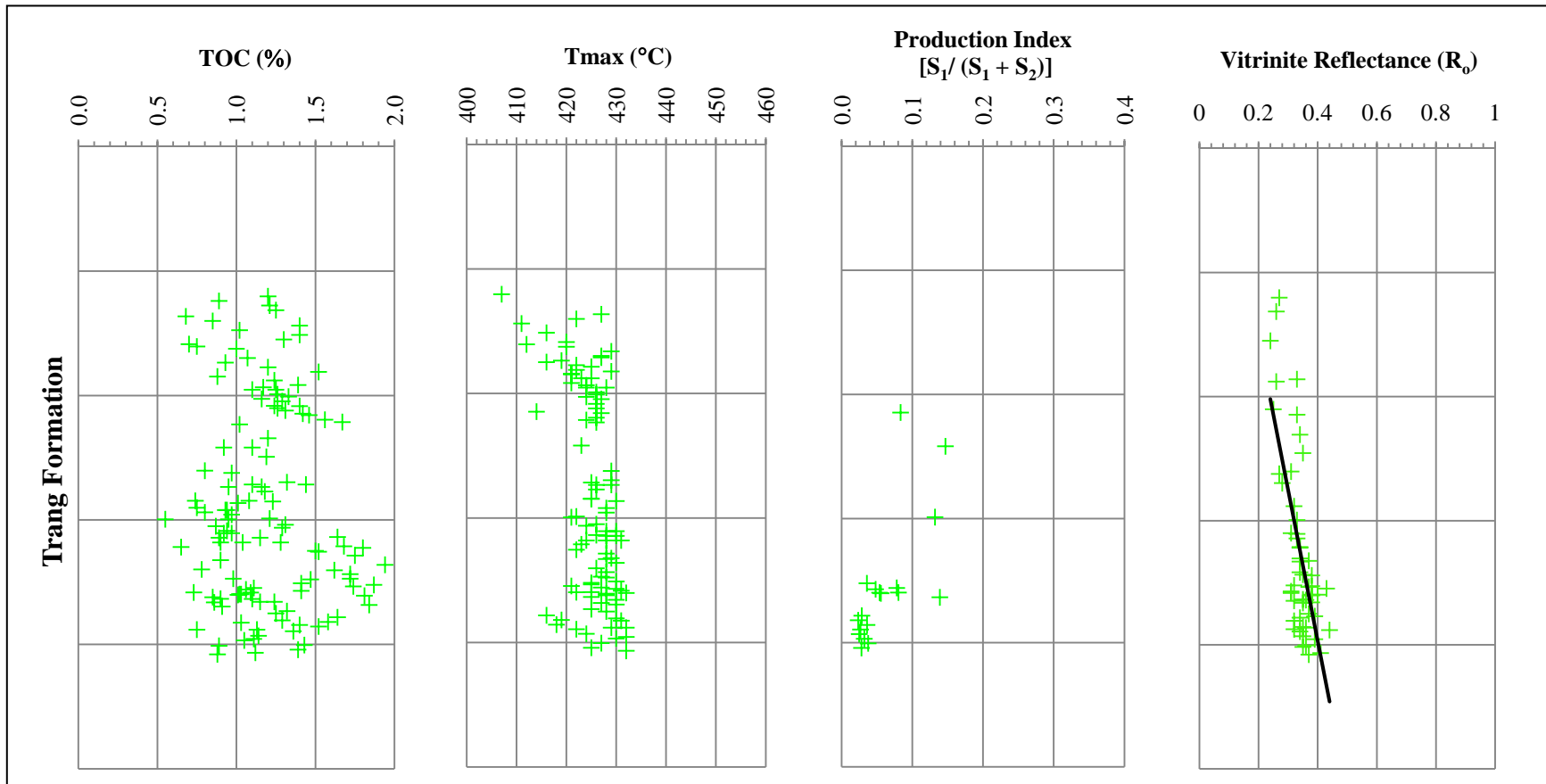


Figure 4.5 Results of pyrolysis (Rock-Eval) cutting samples of the Trang Formation; TOC in wt. %, Tmax (°C), Production index $[S_1 / (S_1 + S_2)]$, Vitrinite reflectance ($\%R_o$)

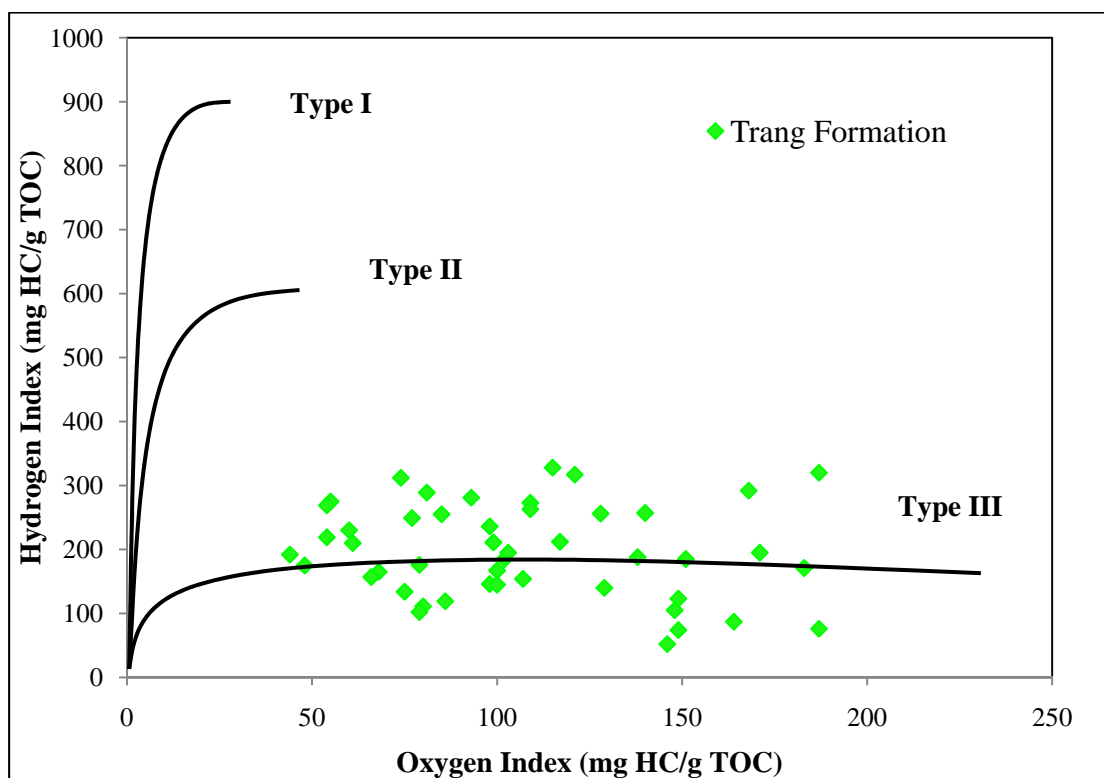


Figure 4.6 Hydrogen Index (HI) versus Oxygen Index (OI) of the Trang Formation plotted

- **Organic matter content**

Total organic carbon (TOC) content of the Yala, Kantang, and Trang Formation (Figure 4.1, 4.3 and 4.5) are show. The Yala Formation (Figure 4.1) indicated that the marine shales of the Late Oligocene to Early Miocene have total organic carbon (TOC) values of range 0.5-1.5% which the Early Miocene Kantang Formation (Figure 4.3) have fair to good TOC value average 0.5-1.5% and the Middle Miocene Trang Formation (Figure 4.5) has fair to very good average TOC 0.5-2.0 %.

- **Organic matter type**

Results a standard modified Van Krevelen diagram comparing hydrogen index (mg HC/g TOC) and oxygen index (mg HC/g TOC) obtain from

Rock-Eval pyrolysis assay reported of the Yala, Kantang, and Trang Formation (Figure 4.2, 4.4 and 4.6) are plotting.

The Yala Formation (Figure 4.2) plotting indicates type of organic matter is Type III terrestrial, gas prone kerogen. Like the Kantang Formation (Figure 4.4) is mixing of Type II/ III, oil/gas prone kerogen. And the Trang Formation (Figure 4.6) is mixing of Type II/ III, oil/gas prone kerogen.

4.1.2 Thermal maturation and timing of hydrocarbon generation and migration

Thermal maturity of source rocks is using Rock-Eval pyrolysis, hydrocarbon geochemistry, and vitrinite reflectance (R_o , in percent). Results of T_{max} and R_o data are plotted for the Yala, Kantang, and Trang Formations as show in Figure 4.1, 4.3 and 4.5, respectively.

The Yala Formation (Figure 4.1) has R_o about 0.6-1.0 and T_{max} of from 430 to nearly 450 °C, the Kantang Formation (Figure 4.3) has R_o about 0.2-0.6 and T_{max} of from 420 to 440 °C, and the Trang Formation (Figure 4.5) has R_o about 0.2-0.4 and T_{max} of from 400 to 430 °C.

Production index (PI) (Figure 4.1) for the Yala Formation (Figure 4.1) has increase regularly with depth from 0.10 to nearly 0.4, the Kantang Formation (Figure 4.3) has PI about 0.02-0.15, and the Trang Formation (Figure 4.5) has PI about 0.1-0.14. Although PI value 0.15-0.40 is indicate hydrocarbon generation (Peters and Cassa, 1994). Primary migration may proceed simultaneously or in episodic pulses as hydrocarbons are generated and source rock threshold saturation levels are reached. The Yala Formation, these ranges are characteristic of maturities corresponding to main hydrocarbon generation zone (cut off: R_o about 0.6-0.8, T_{max} of from 435 - 445

°C and production index 0.30 - 0.36) at depths of approximately 3,000 – 3,500 m, whereas the Kantang and Trang Formation are somewhat immature.

4.1.3 Hydrocarbon indications

Based on well completion report of drilled wells in the Mergui basin and geochemical re-evaluation report, some hydrocarbon indications can be summarized as follows;

Payang-1 well

No hydrocarbon shows were reported. No cores were taken and no tests were recorded.

Kantang-1 well

Migration gas, with some associated liquid hydrocarbons, is observed in the sediments overlying the Oligocene carbonate reservoir. Headspace gas wetness, ethane abundance and benzene anomalies in drilling fluid samples indicated that migrated hydrocarbons were encountered between 1,938 m and the top of the gas reservoir. The shallower gas has a higher proportion of wet gas components than the gas collected from the carbonate, meaning that it may have a different source or maturity, and thus not be a product of straightforward leakage of gas through the cap rock.

Kraburi-1 well

No migrated oil or condensate was detected in the well. It is possible that migrated gas may occur in Upper Ranong sandstone, but isotopic measurements were not carried out to confirm the source character of this gas.

Ranot-1 well

It does contain a small percentage of gas particularly in top well where the water saturations are the lowest. They water saturations have average 87%. The reef has probably no seal. According to electrical log calculations, the Ranong sandstones generally have a few of water saturations.

Thalang-1 well

In the absence of vertical gas migration, headspace gas in shallow, immature sediments is derived from bacterial utilization of sedimentary organic matter. This gas is very dry. When increasing burial depth and thus increasing maturity. The headspace gas becomes increasingly wet due to the generation of ethane and heavier hydrocarbons from kerogen.

Yala-1 well

No oil staining, fluorescence, or cut was seen in the well cuttings. Minor gas shows were observed in the Middle Miocene sandstone. These minor show where indicated by an increase in the percentage of methane as these sections of the well were drilled.

W9-A-1 well

No hydrocarbon shows were encountered and the section was normally pressured.

W9-B-1 well

Gas shows were encountered from sandstones at the top of Ranong Formation. This section was cored and the sandstones were described as very fine to medium grained, quartzite, clean, locally calcareous and with generally fair to good porosity. The gas-water contact is considered from log and core.

W9-C-1 well

Only minor fluorescence was noted in core taken to evaluate a weak hydrocarbon show in cuttings (Lower Ranong Sub-Formation).

W9-E-1 well

A number of hydrogen shows were reported in the Ranong Formation. One core was taken to evaluate a hydrocarbon show observed in cuttings and on the gas detector. The sandstone had light yellow fluorescence which gave a moderately strong yellow cut. Retorted oil from this core had a gravity of 46° API.

Mergui -1 well

Light yellow fluorescence was observed. In the Ranong Formation no show cut fluorescence had been reported in the cutting description. Chromatograph readings have not significant shows. However, hydrocarbon shows are present in the Ranong sandstones beds.

Phangha-1 well

The sandy intercalations of the Trang shales are all water wet according to log analysis. Concerning the Tai Formation, minor gas shows are associated with two limestones.

Trang-1 well

The fluorescence was predominantly faint to dull pale golden yellow indicating that the observed oil was a low gravity. No significant gas peaks were associated with these shows, because no test was recorded.

W9-D-1 well

No hydrocarbon shows were reported. The section is normally pressured. Log analysis indicates all potential reservoirs to be water wet.

4.1.4 Biomarker

In this study the biomarker founded in Kantang-1 and Thalang-1 wells had been re-evaluated and can be summarized below.

Katang -1 well

The biomarker distributions observed an increasing proportion of C₂₉ steranes in the deeper samples may indicate increasing terrestrial influence with depth. Trough, the abundance of land plant-derived biomarkers (oleanane, bicadinances) suggesting the contribution of terrestrial organic matter. High values of the C₂₉/C₃₀ hopane ratio and low diasterane abundances are the typicality of bitumen that derived from carbonate or marl sediments. Low concentration of C₃₅ homohopanes represents that strong reducing conditions were not developed during deposition of the Miocene sediments.

Thalang-1 well

The biomarker compositions of the four samples were broadly similar indicating relatively minor changes in the type of organic matter input into the basin at the Thalang-1 well during Oligocene-Late Miocene time. Samples have a biomarker trace that shows the typicality of marine shale with the minor contribution of terrestrial organic matter. The terrestrial contribution is shown by slightly higher proportions of C₂₉ steranes than expected. Oleanane is the most abundant in the sample from the Ranong/Yala sequence (2,430 m.) indicating that the influence of terrestrial organic matter was strongest at the time. Level of the C₃₅ homohopaned indicates that the depositional environment was not strongly anoxic at the sediments accumulation.

4.1.5 Modeling of the Mergui basin by using PetroMod 1D

In order to study the Mergui basin modeling, PetroMod 1D computer program was used and the Mergui basin was divided into 3 sub-areas as northern, eastern, and western Mergui physiographically.

Required data for basin modeling were obtained from 16 wells, including Payang-1, Kantang-1, Kathu-1, Kraburi-1, Ranot-1, Sikao-1, Thalang- 1, Yala-1, W9-A-1, W9-B-1, W9-C-1, W9-E-1, Mergui-1, Phanga-1, Trang-1, and W9-D-1. Some collected geochemical data required for PetroMod 1D are listed in Table 4.1. The results were burial history, Temperature Index (TI), and Time Temperature Index (TTI) of each sub-basin.

Table 4.1 Geochemical analysis data of rocks

Well	TOC % (average)	Geothermal gradient (°C/100m)	Kerogen			Source rock type	Potential petroleum source rock
			I	II	III		
Northern the Mergui basin							
1. Payang-1	-	1.46	-	-	-	-	None
Eastern the Mergui basin							
1. Kantang-1	1.12	5.21		X	X	Oil/Gas prone	Fair
2. Kathu-1	0.65	4.39			X	Gas prone	Poor
3. Kra Buri-1	1.16	4.42			X	Gas prone	Fair
4. Ranot-1	0.70	-			X	Gas prone	Poor
5. Sikao-1	0.10	4.19			X	Gas prone	Poor
6. Thalang-1	1.15	5.82			X	Gas prone	Fair
7. W9-A-1	0.36	4.37		X	X	Gas prone	Poor
8. W9-B-1	1.43	5.06		X	X	Oil/Gas prone	Good
9. W9-C-1	1.31	5.02			X	Gas prone	Good

Table 4.1 Geochemical analysis data of rocks (Continued)

Well	TOC % (average)	Geothermal gradient (°C/100m)	Kerogen			Source rock type	Potential petroleum source rock
			I	II	III		
10. W9-E-1	0.57	4.91			X	Gas prone	Poor
11. Yala-1	2.35	-			X	Gas prone	Very good
Western the Mergui basin							
1. Mergui-1	0.70	4.10		X	X	Oil/Gas prone	Poor
2. Phangha-1	-	1.46	-	-	-	-	None
3. Trang-1	-	3.51	-	-	-	-	None
4. W9-D-1	0.23	4.93			X	Gas prone	Poor

In addition, vitrinite reflectance (R_o) is commonly used to indicate if and when migration occurred. Expulsion of hydrocarbons is related to the amount of hydrocarbon generated and the porosity and permeability of the source rock (England et al., 1991; Palciauskas, 1991). The amount of hydrocarbon generated is dependence on the amount and type of organic matter in the sediments. These constraints on expulsion, vitrinite reflectance can not directly indicate when the migration occurred or how much was expelled. The vitrinite reflectance can only suggest when expulsion might be possible.

Consequently results of basin modeling on burial history, TI, TTI, and vitrinite reflectance (R_o) study of each selected well in each sub-area were illustrated as following figures.

Northern Mergui

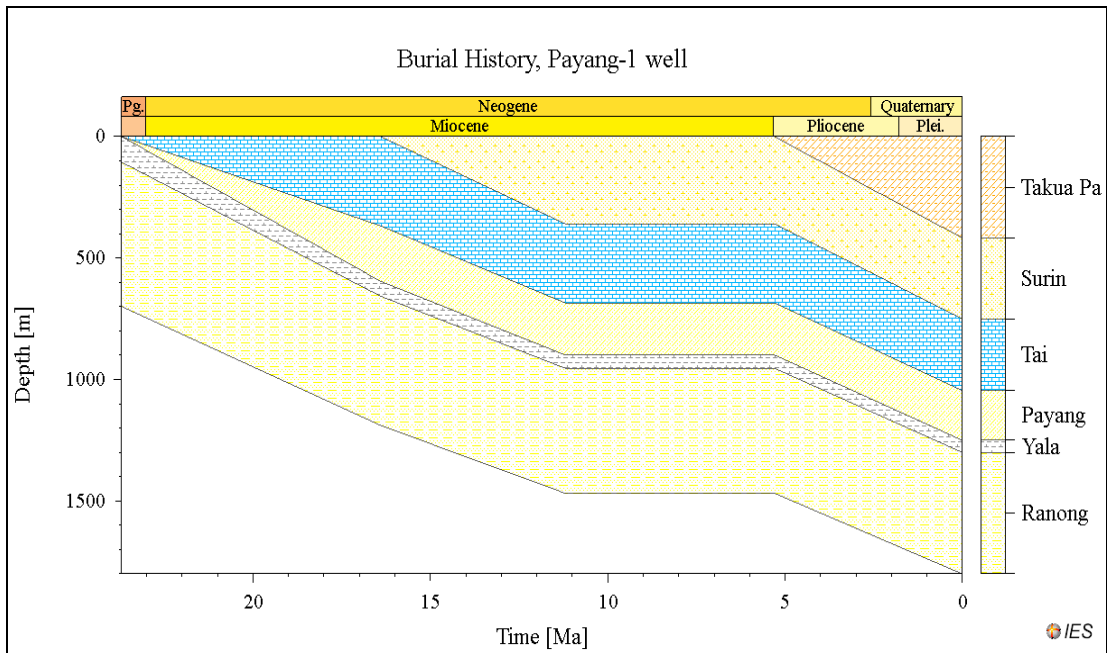


Figure 4.7 Burial history of the Payang-1 well

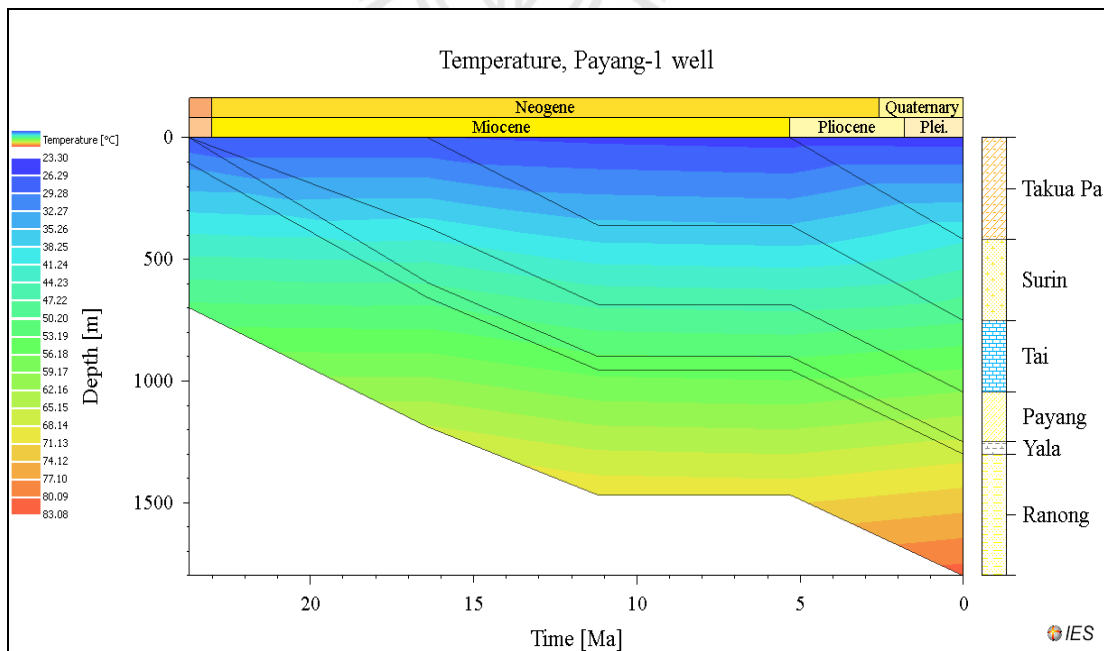


Figure 4.8 Temperature Index (°C) of the Payang-1 well

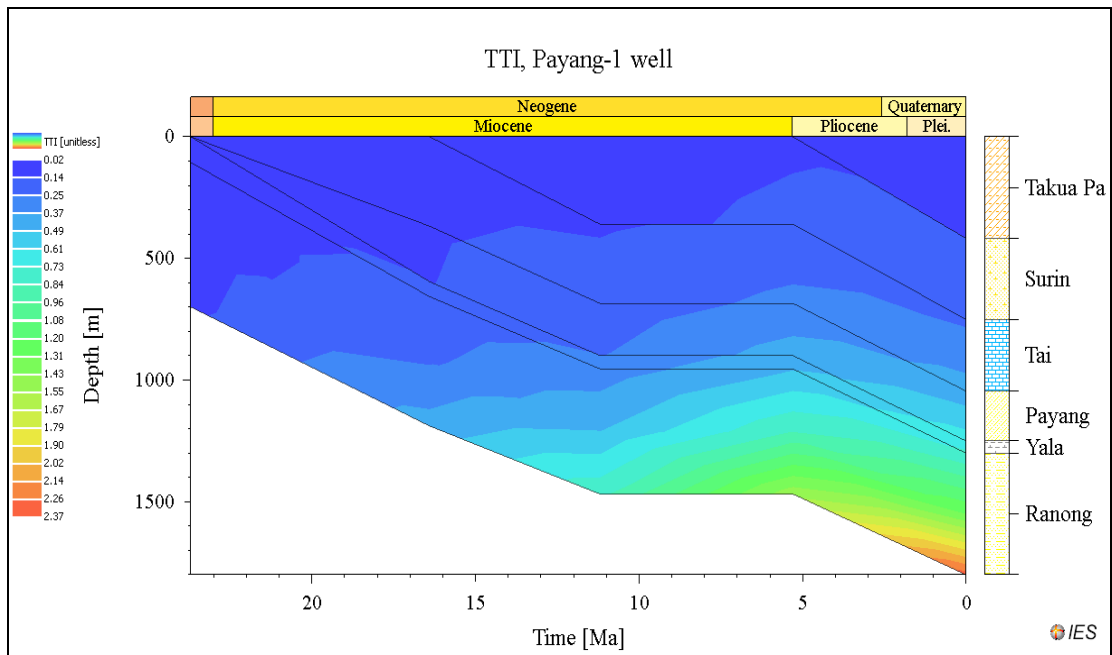
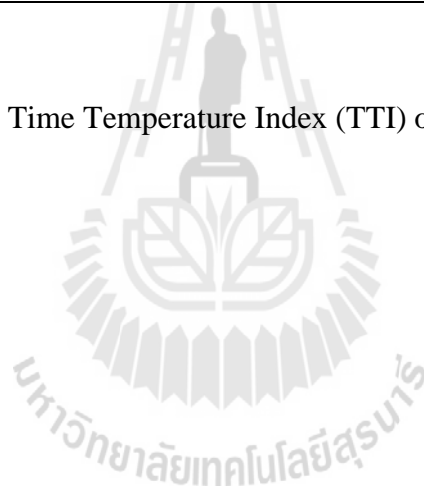


Figure 4.9 Time Temperature Index (TTI) of the Payang-1 well



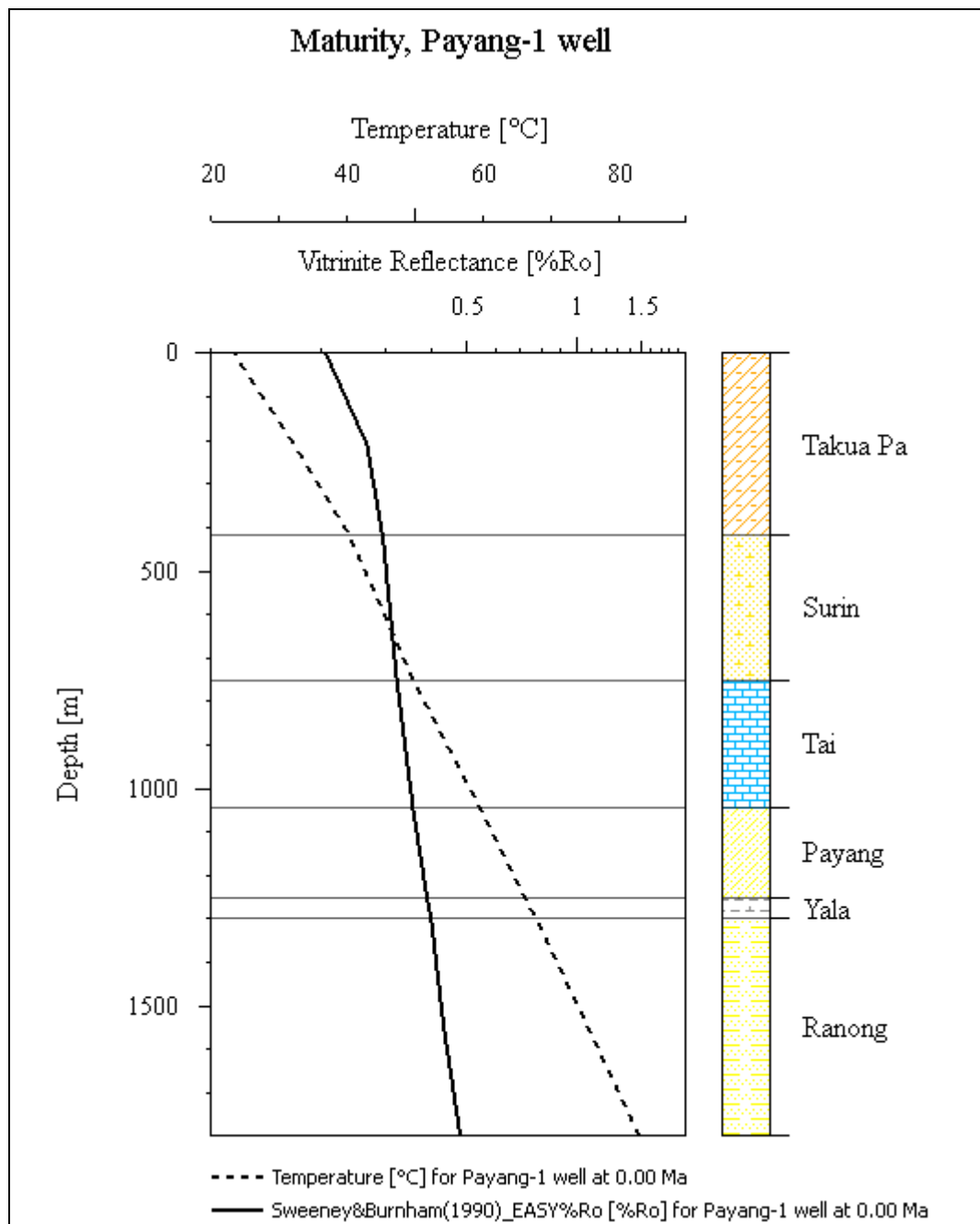


Figure 4.10 Maturity overlay R_o compare with temperature and depth of the Payang-1 well

Eastern Mergui

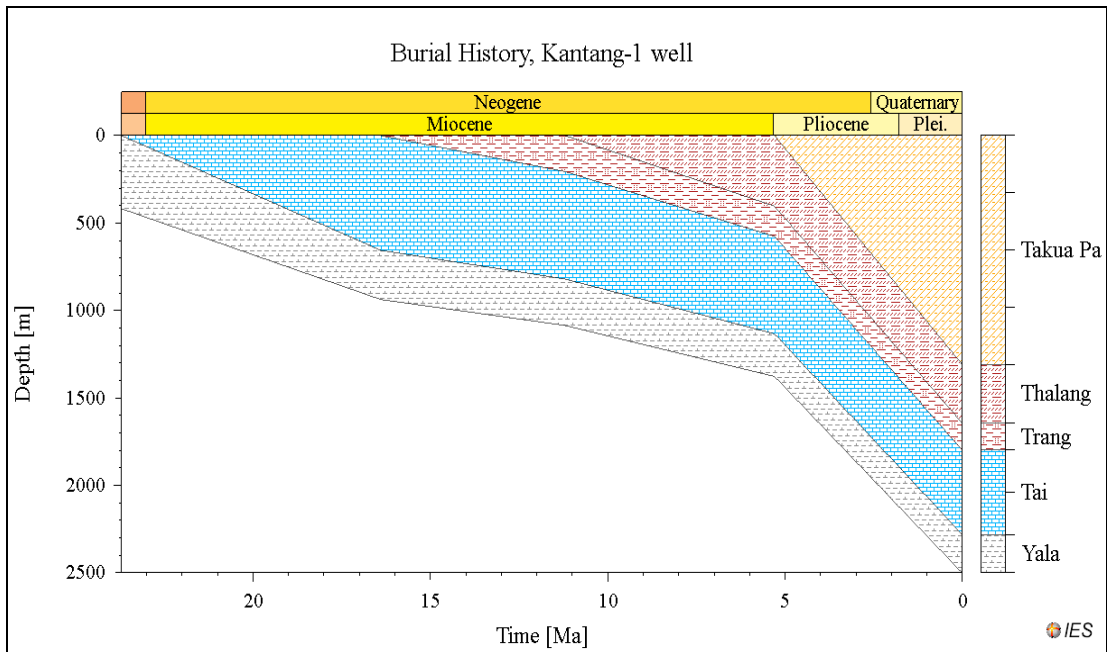


Figure 4.11 Burial history of the Kantang-1 well

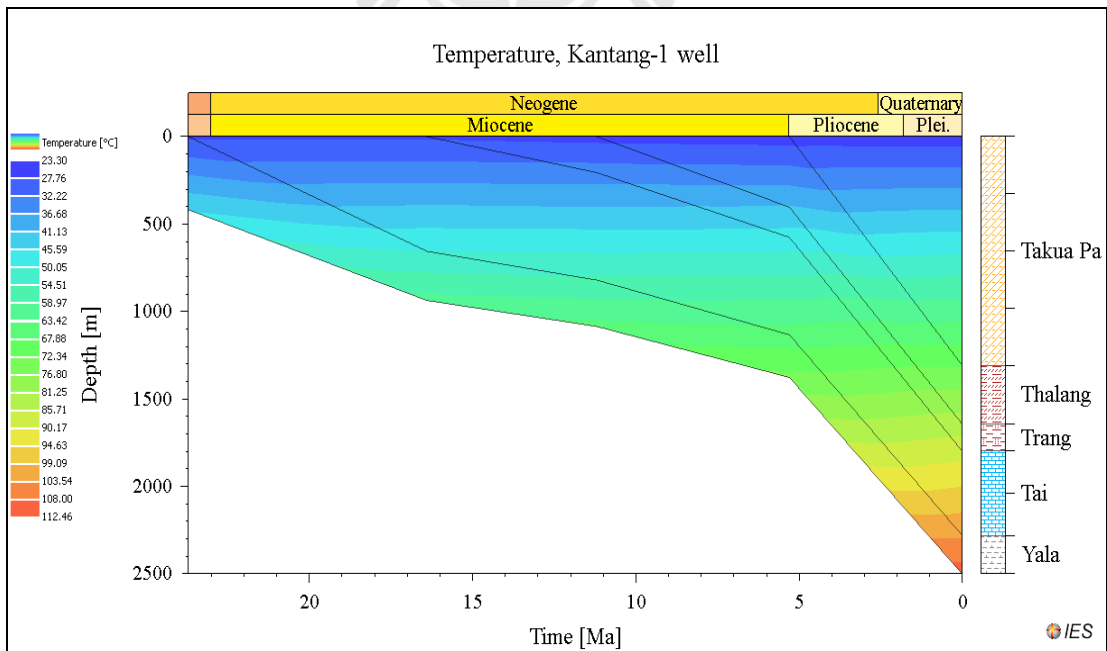


Figure 4.12 Temperature Index (°C) of the Kantang-1 well

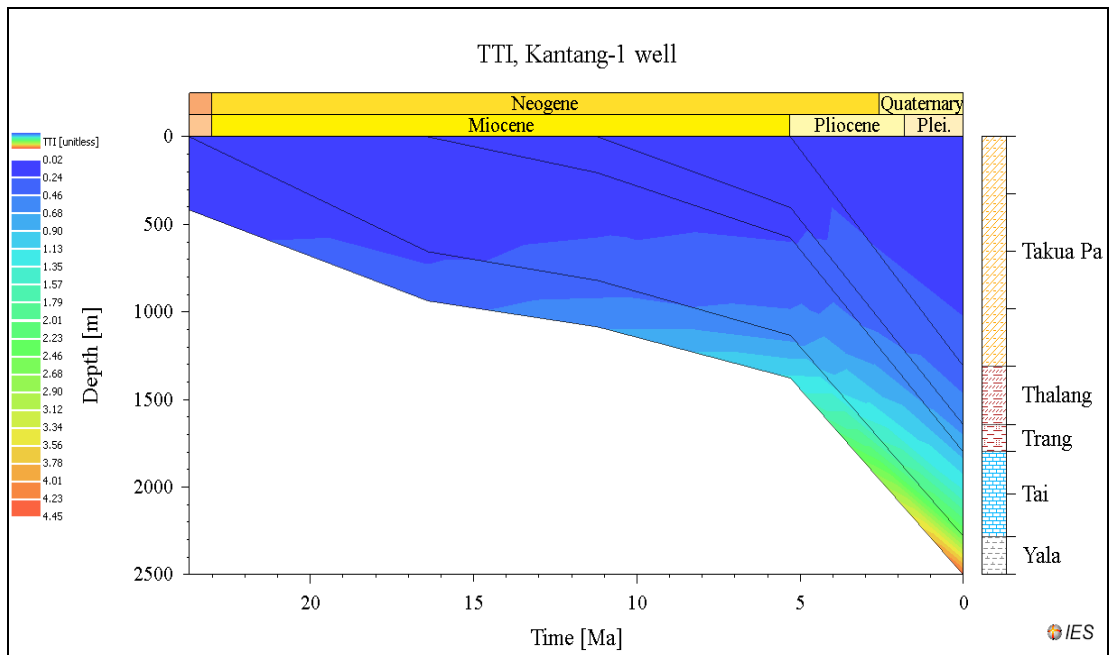
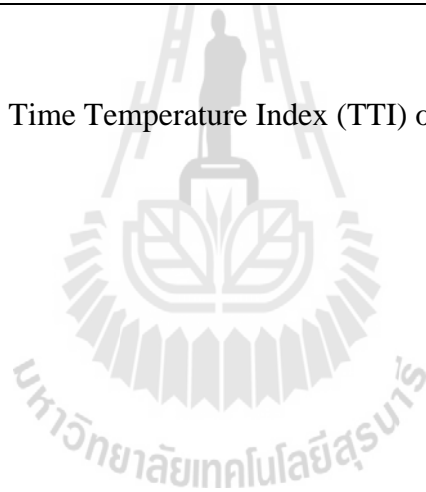


Figure 4.13 Time Temperature Index (TTI) of the Kantang-1 well



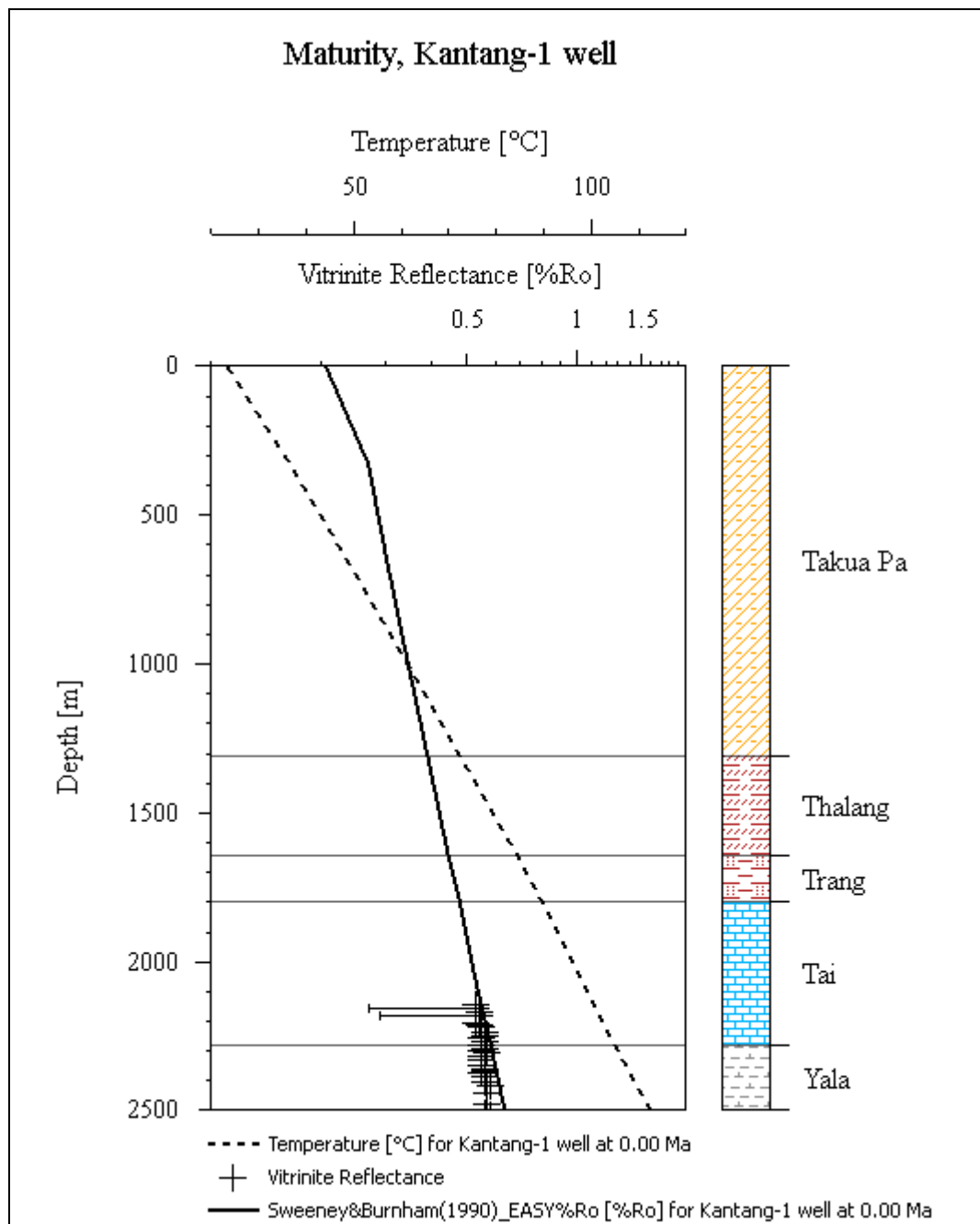


Figure 4.14 Maturity overlay R_o compare with temperature and depth of the Kantang-1 well

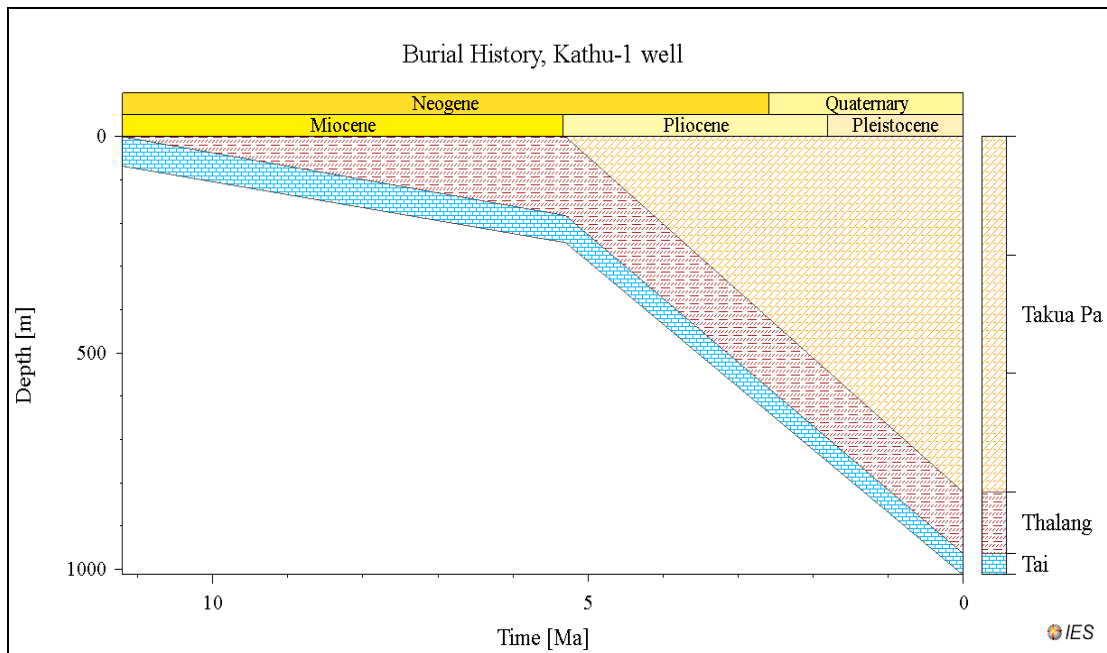


Figure 4.15 Burial history of the Kathu-1 well

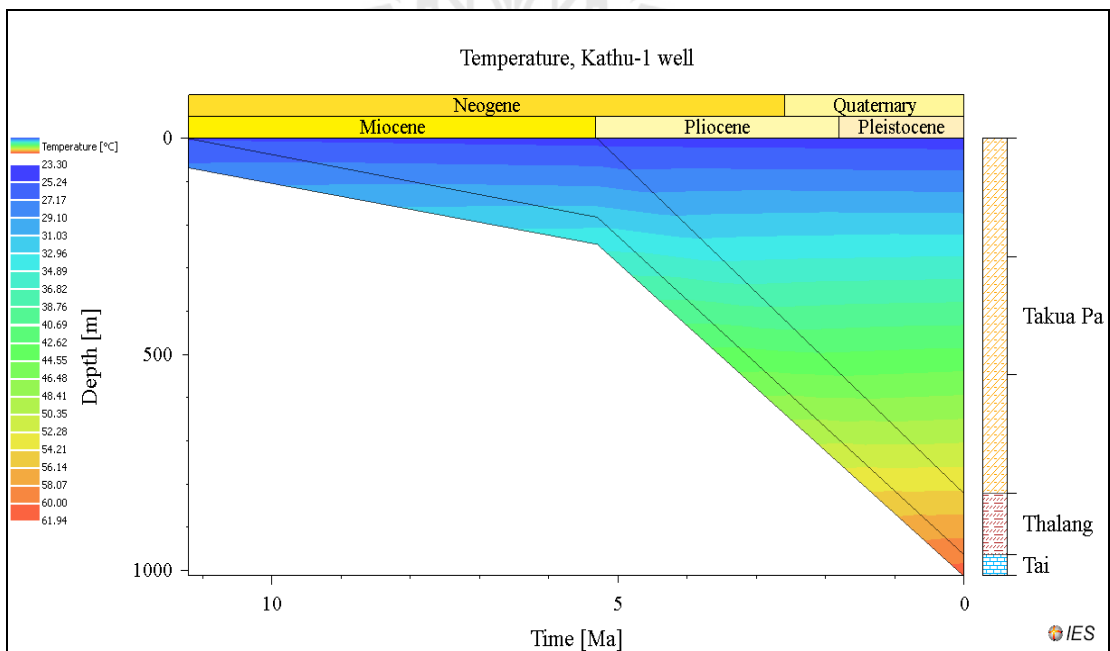


Figure 4.16 Temperature Index (°C) of the Kathu-1 well

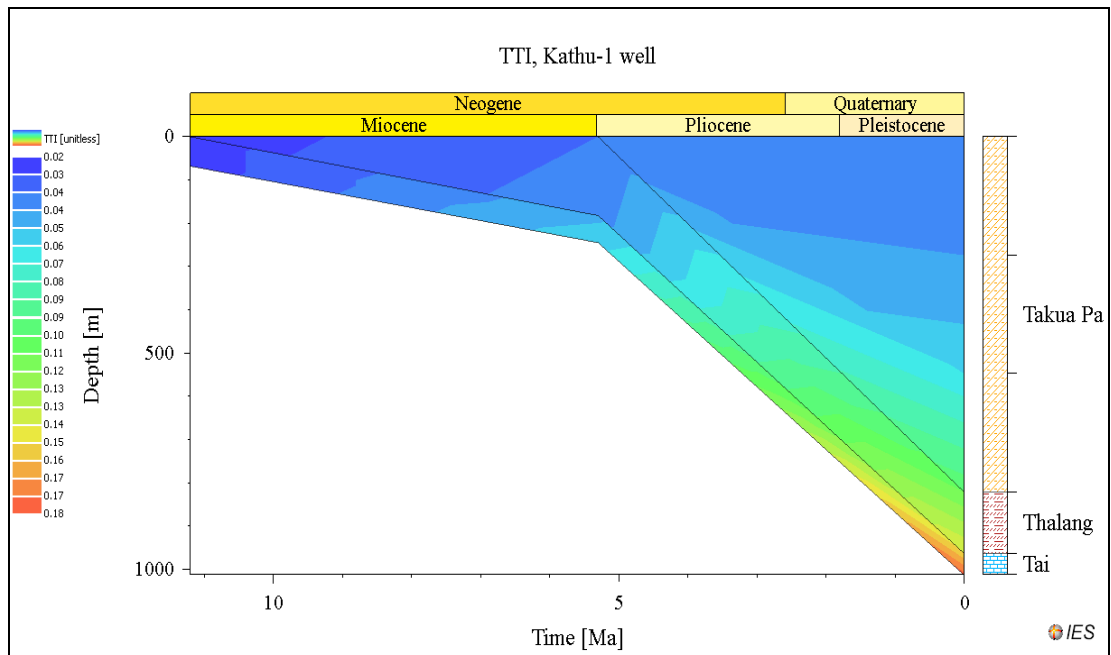
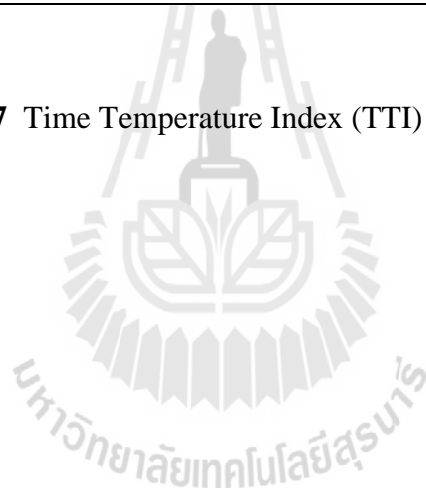


Figure 4.17 Time Temperature Index (TTI) of the Kathu-1 well



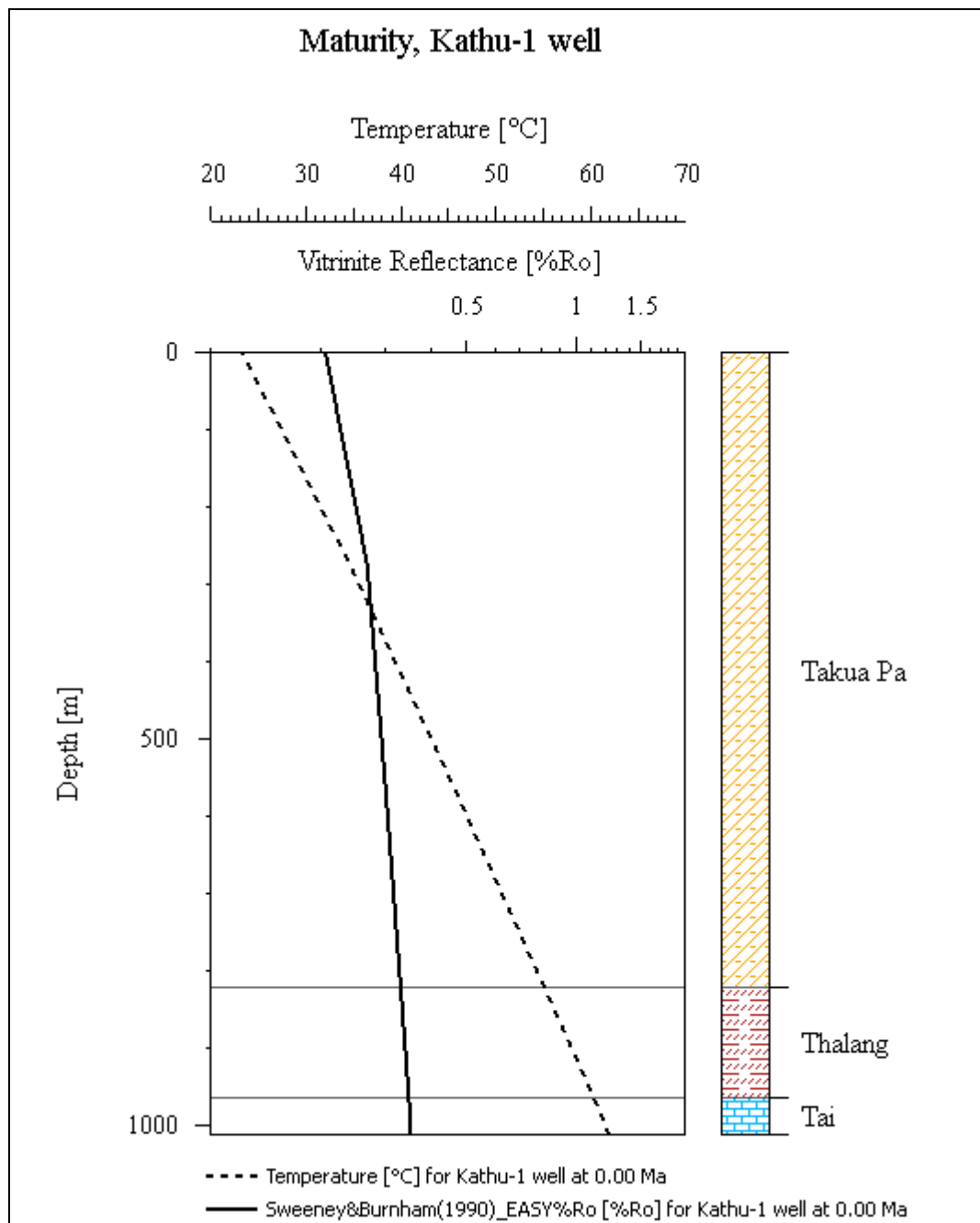


Figure 4.18 Maturity overlay R_o compare with temperature and depth of the Kathu-1 well

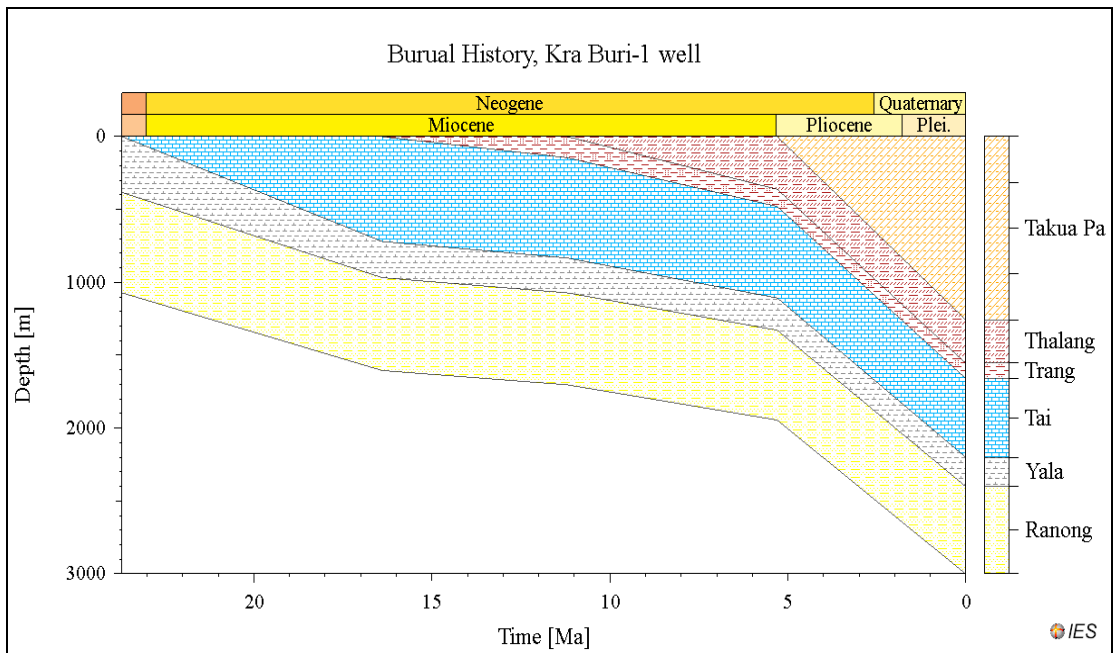


Figure 4.19 Burial history of the Kra Buri-1 well

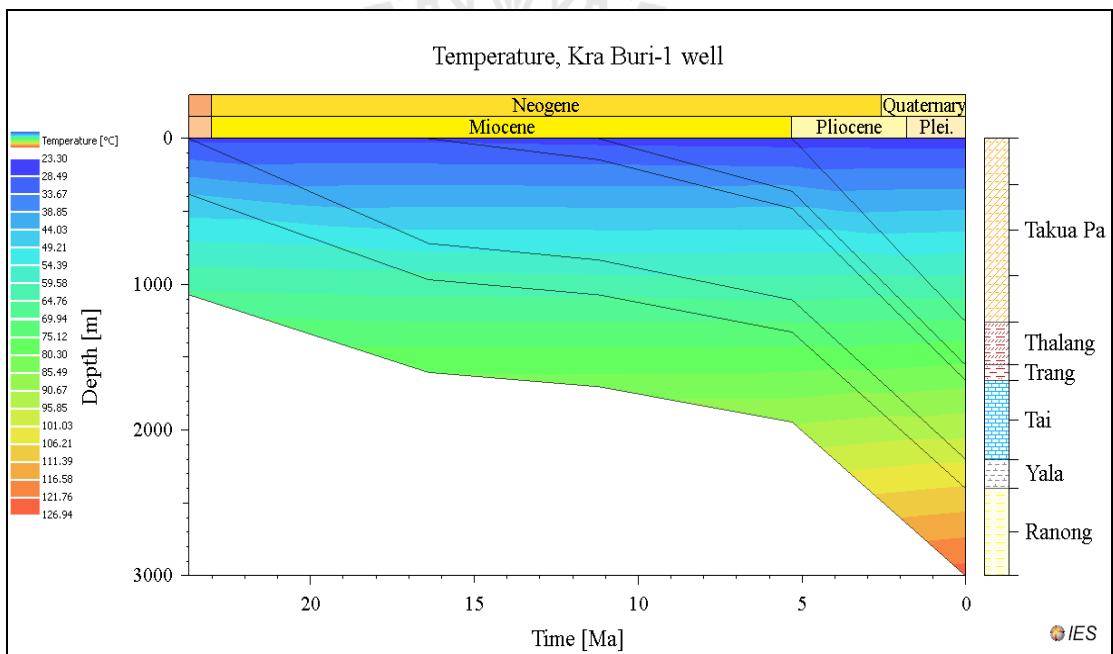


Figure 4.20 Temperature Index (°C) of the Kra Buri-1 well

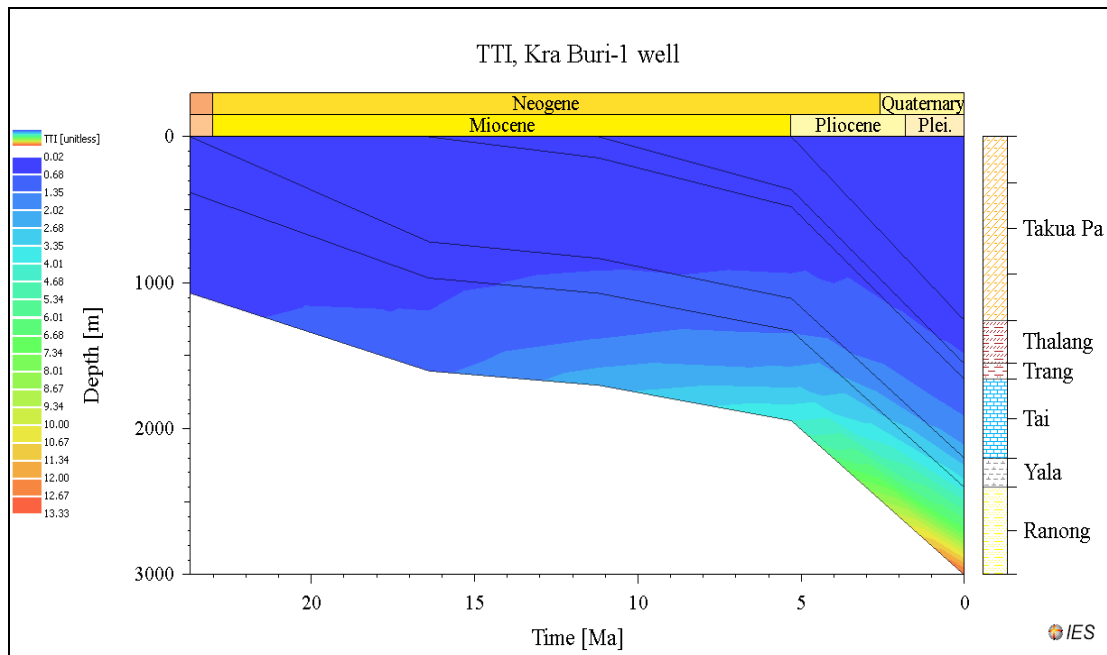
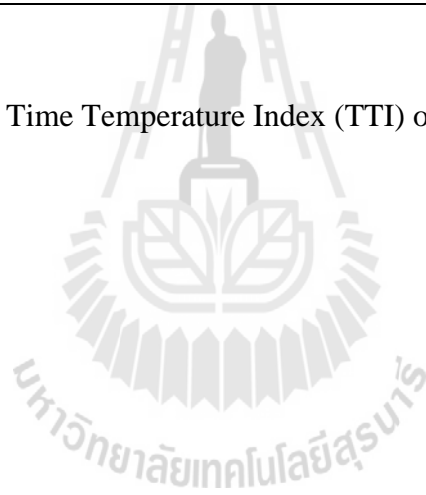


Figure 4.21 Time Temperature Index (TTI) of the Kra Buri-1 well



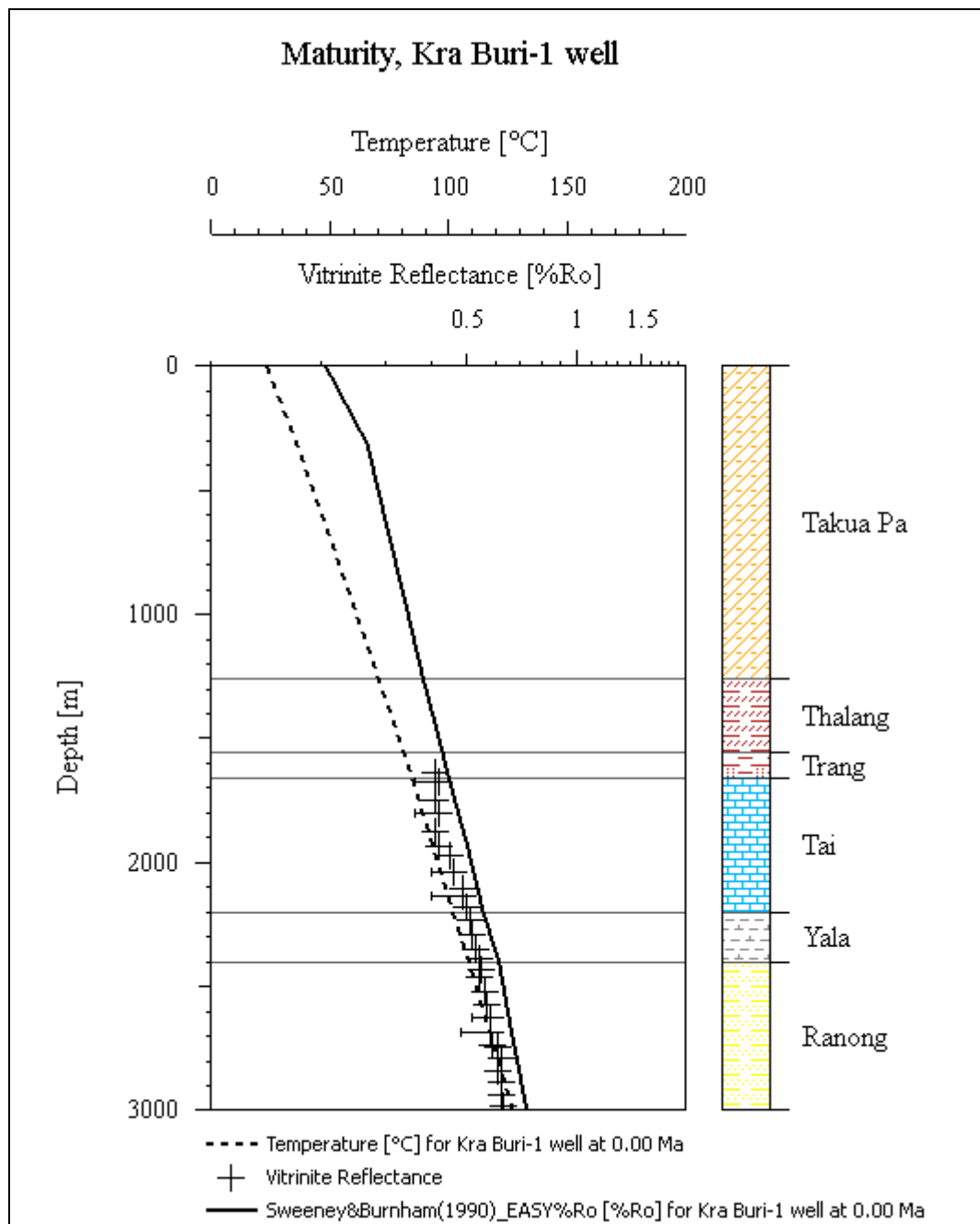


Figure 4.22 Maturity overlay R_o compare with temperature and depth of the Kra Buri-1 well

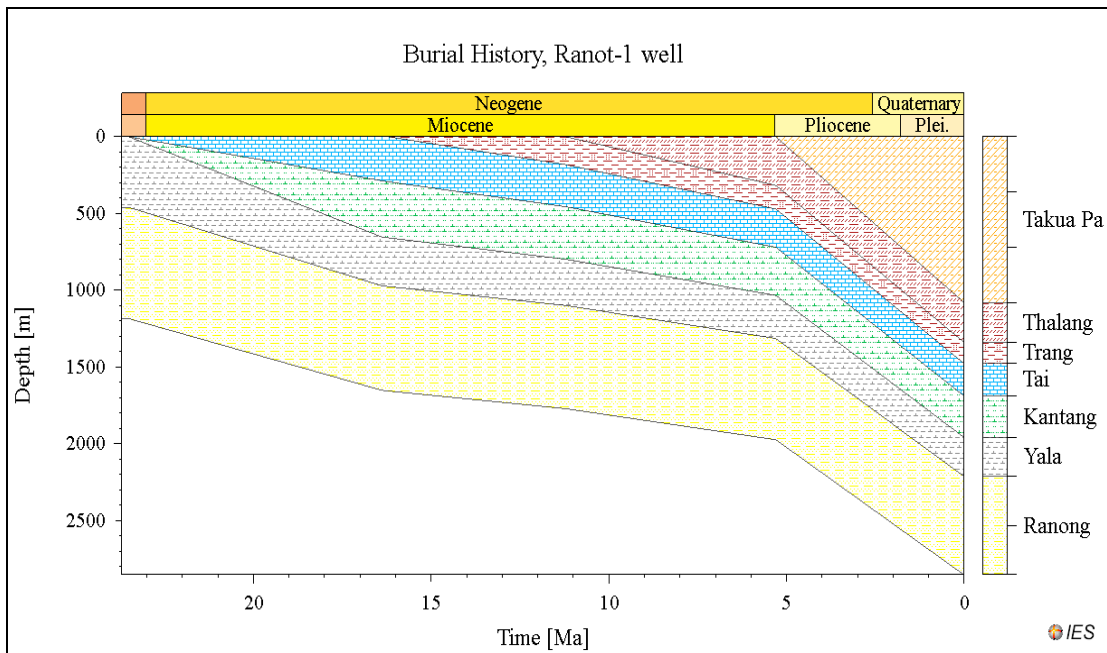


Figure 4.23 Burial history of the Ranot-1 well

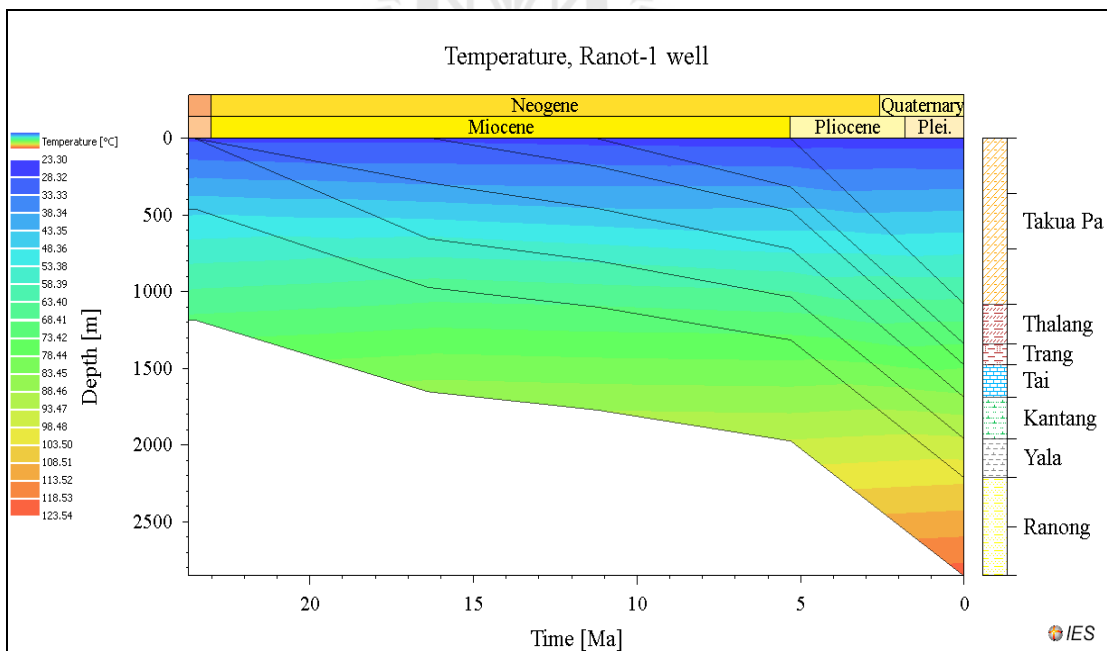


Figure 4.24 Temperature Index (°C) of the Ranot-1 well

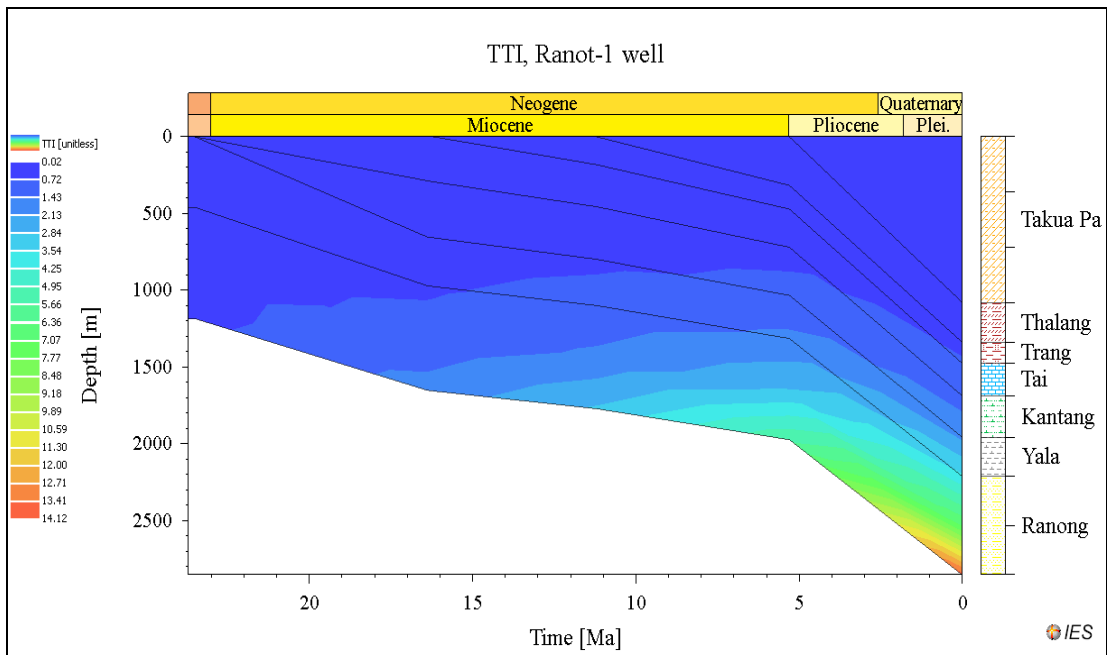
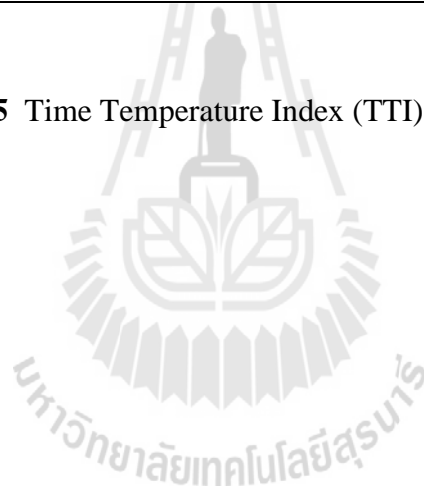


Figure 4.25 Time Temperature Index (TTI) of the Ranot-1 well



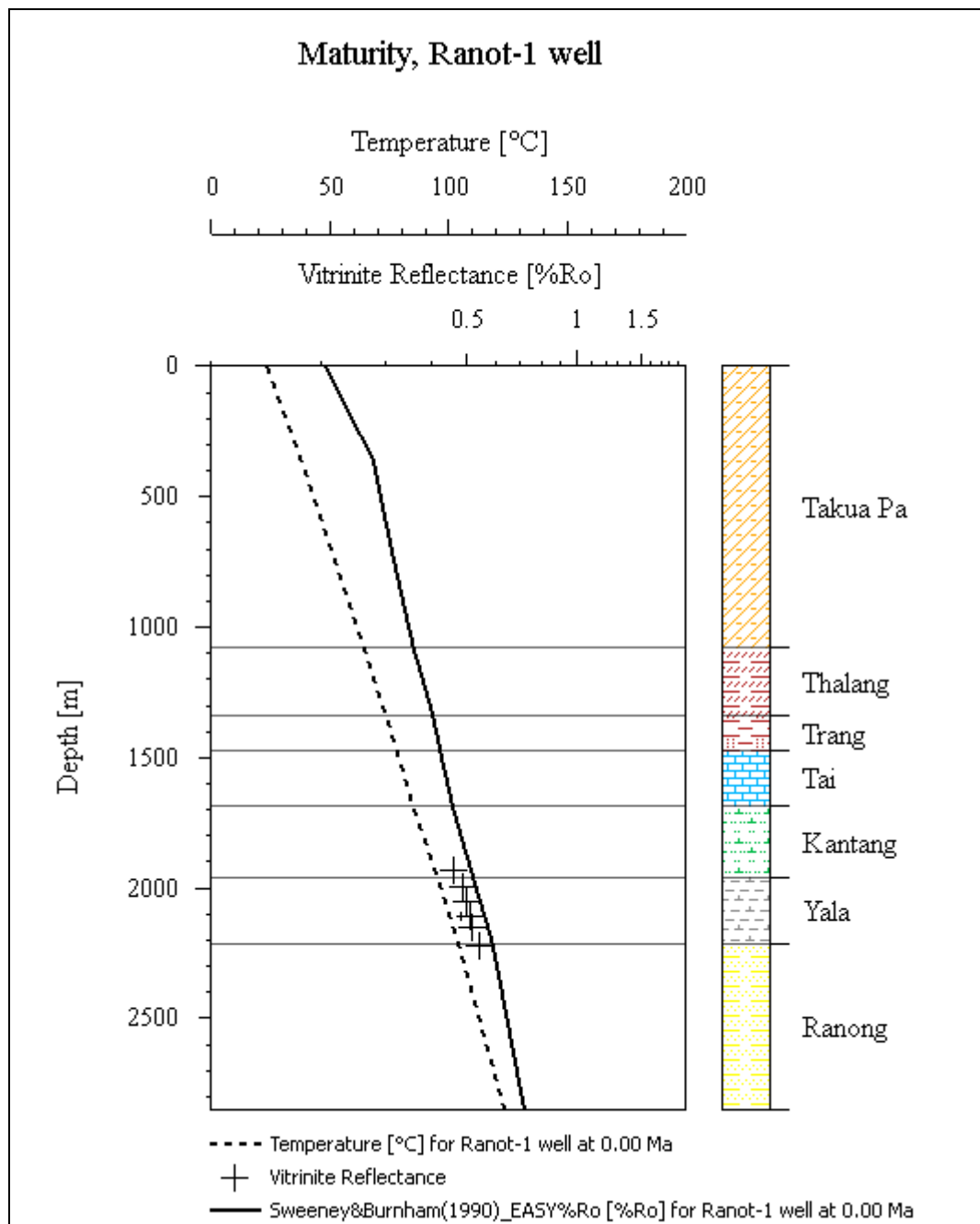


Figure 4.26 Maturity overlay R_o compare with temperature and depth of the Ranot-1 well

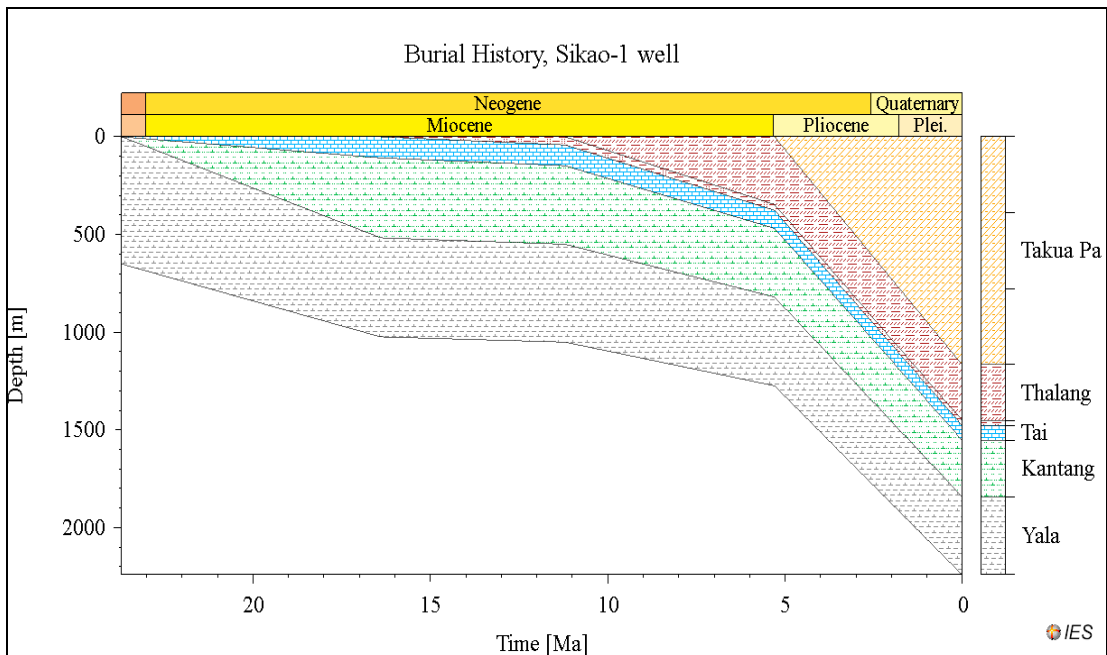


Figure 4.27 Burial history of the Sikao-1 well

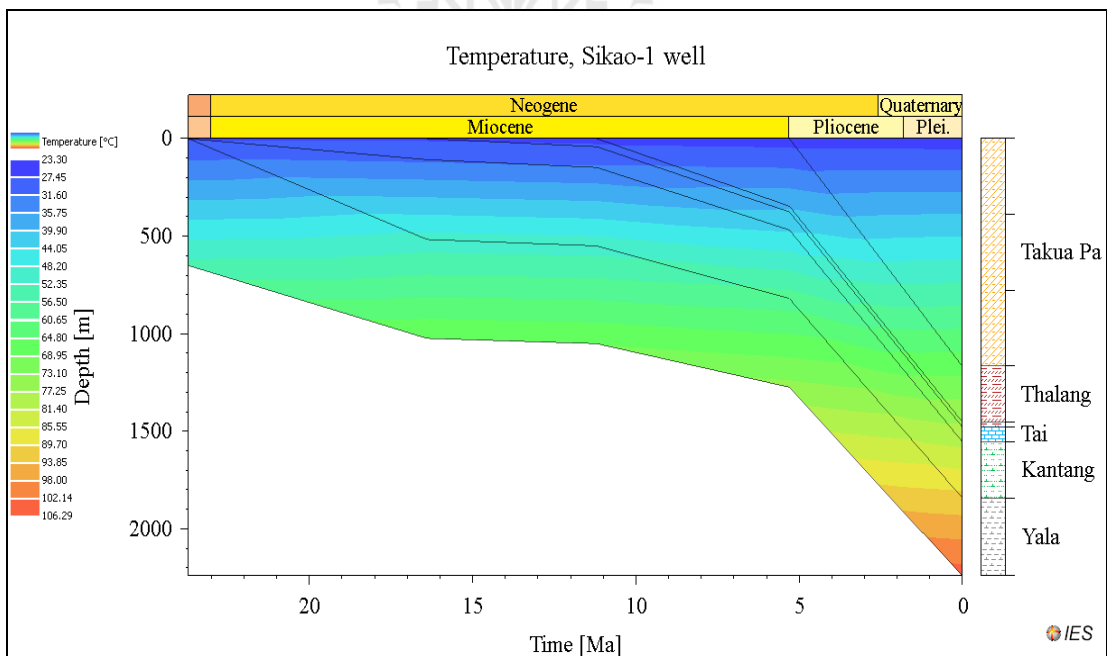


Figure 4.28 Temperature Index (°C) of the Sikao-1 well

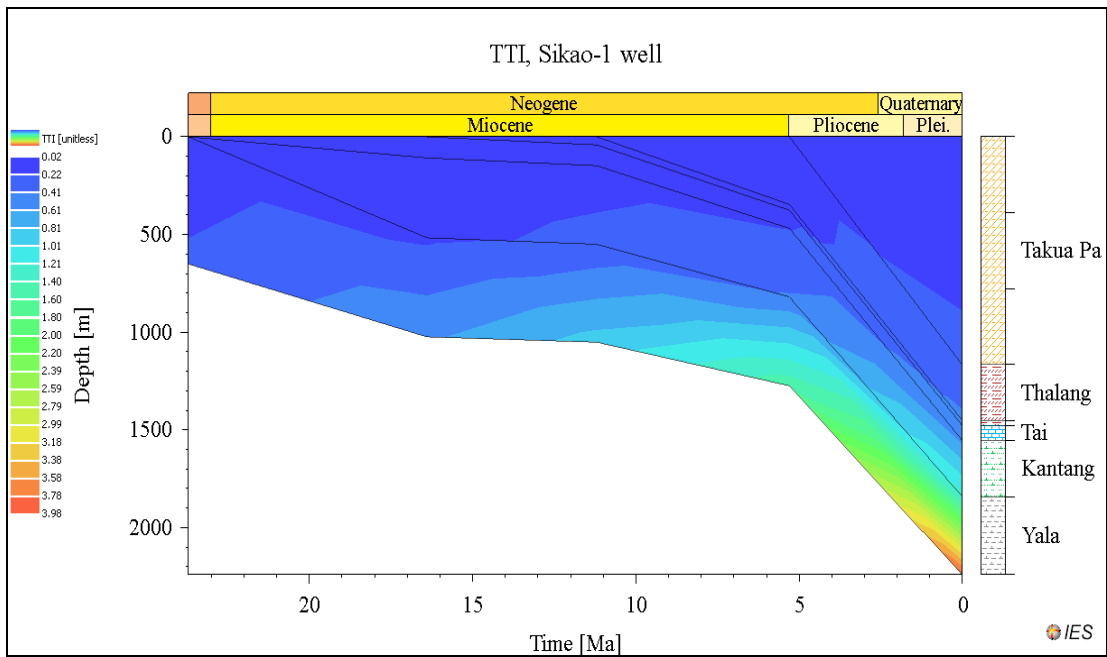
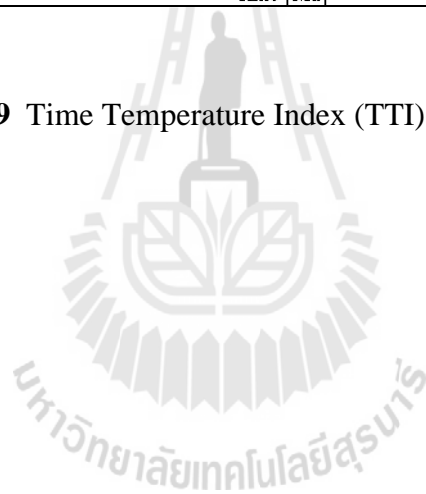


Figure 4.29 Time Temperature Index (TTI) of the Sikao-1 well



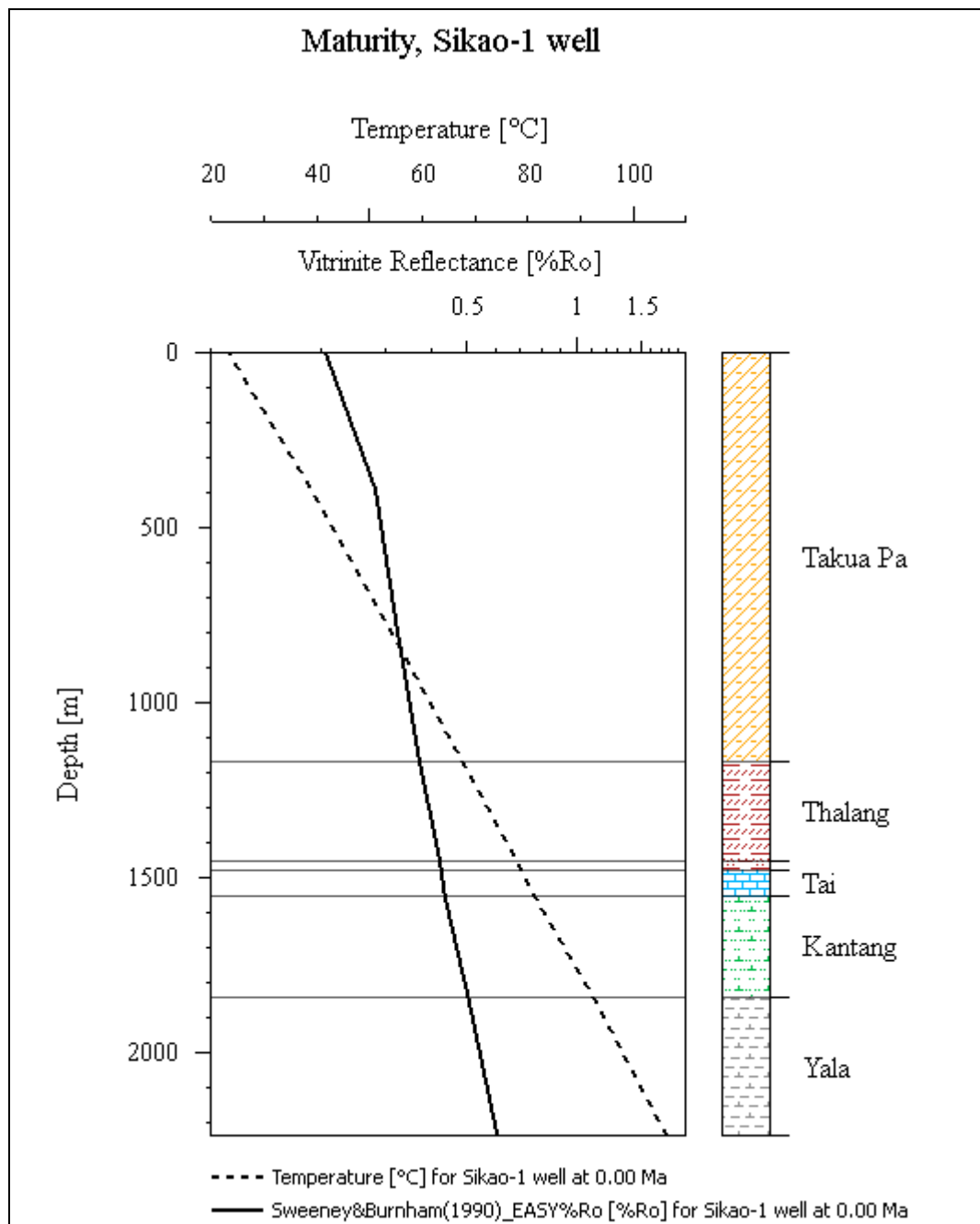


Figure 4.30 Maturity overlay R_o compare with temperature and depth of the Sikao-1 well

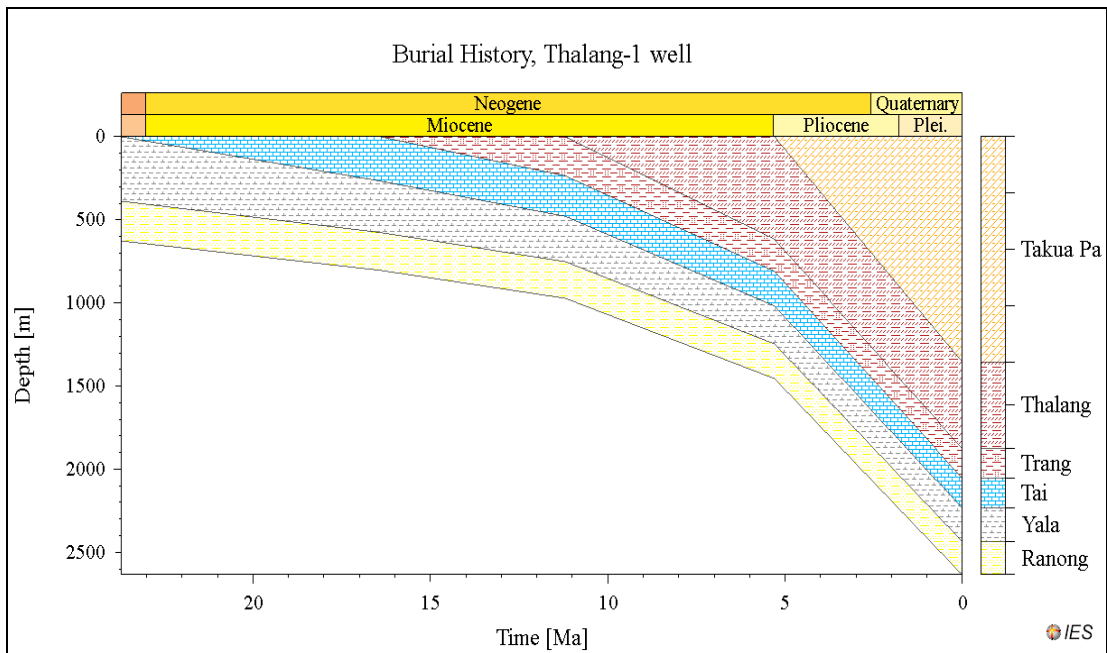


Figure 4.31 Burial history of the Thalang-1 well

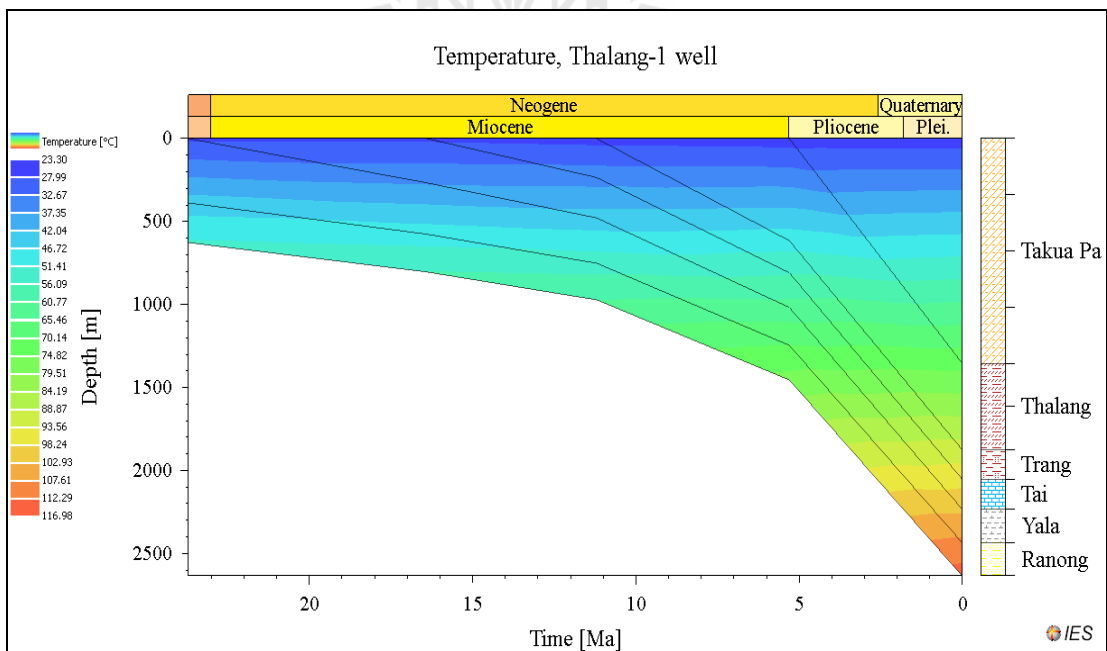


Figure 4.32 Temperature Index (°C) of the Thalang-1 well

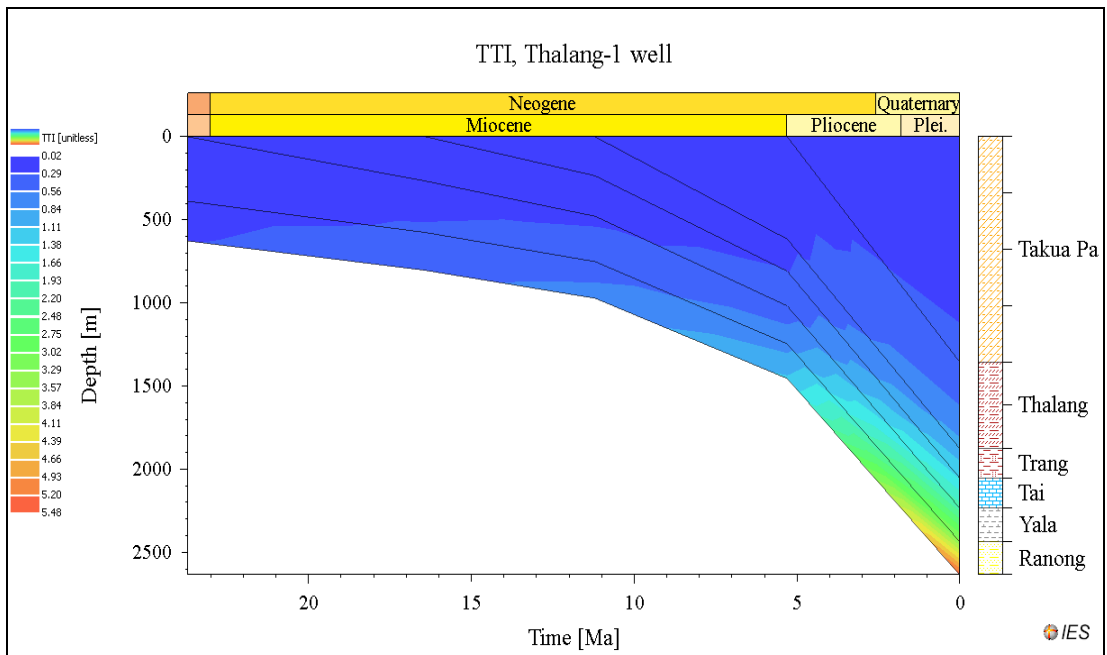
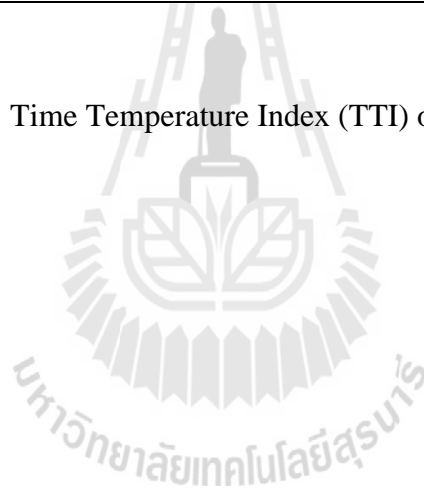


Figure 4.33 Time Temperature Index (TTI) of the Thalang-1 well



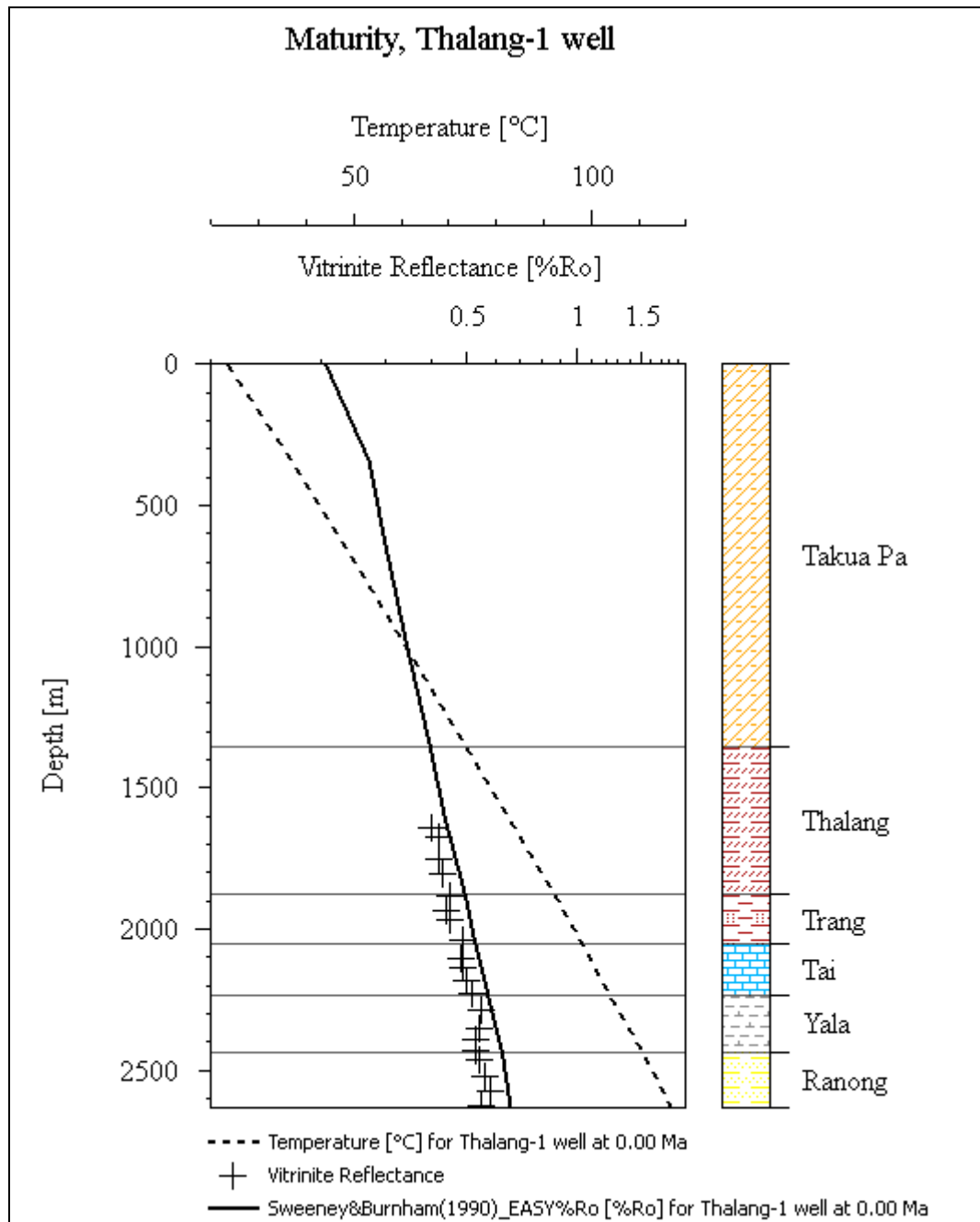


Figure 4.34 Maturity overlay R_o compare with temperature and depth of the Thalang-1 well

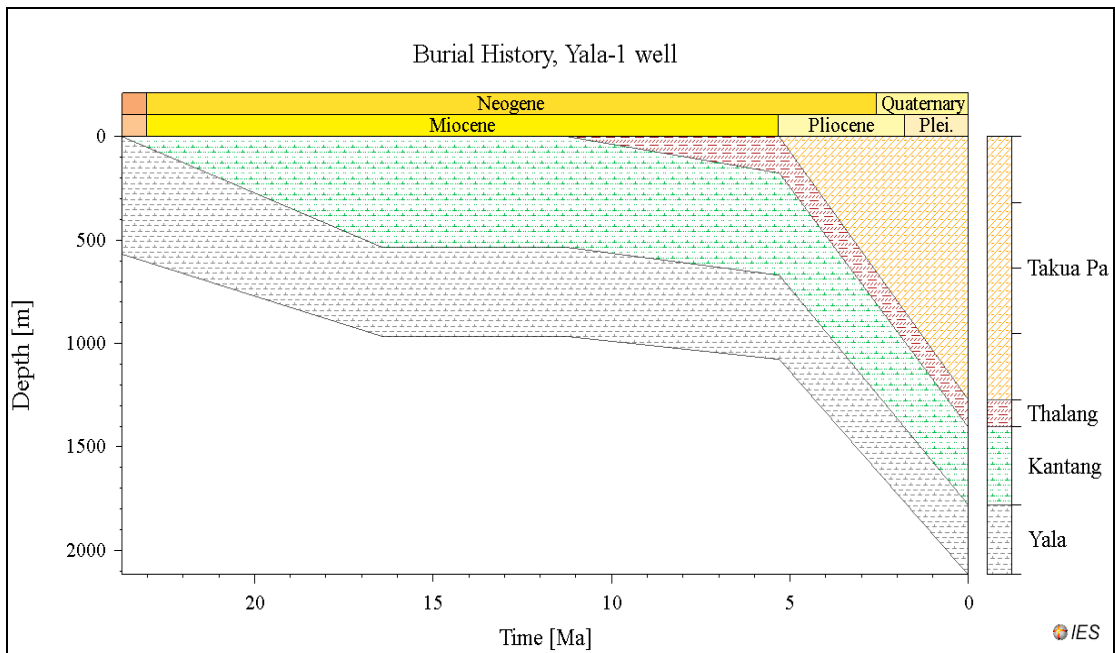


Figure 4.35 Burial history of the Yala-1 well

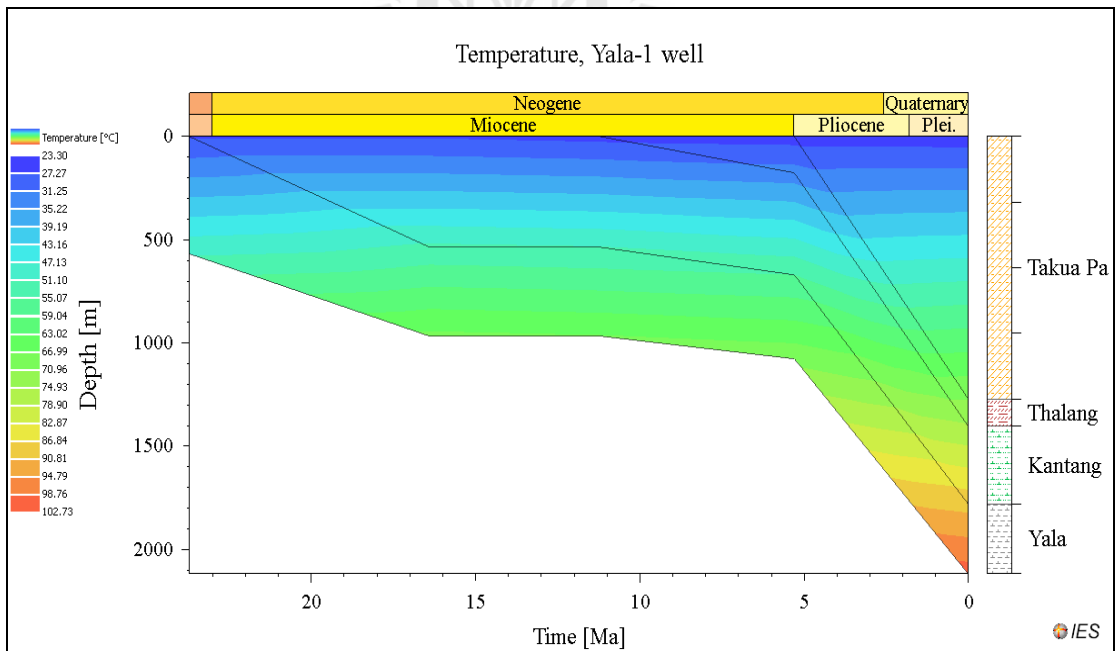


Figure 4.36 Temperature Index (°C) of the Yala-1 well

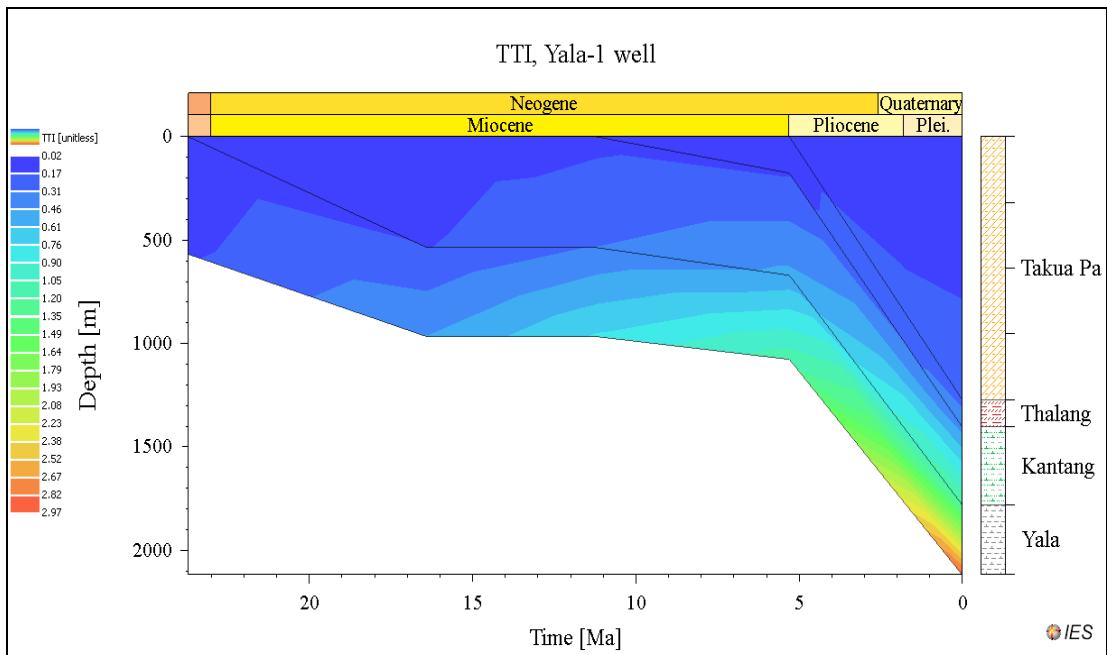
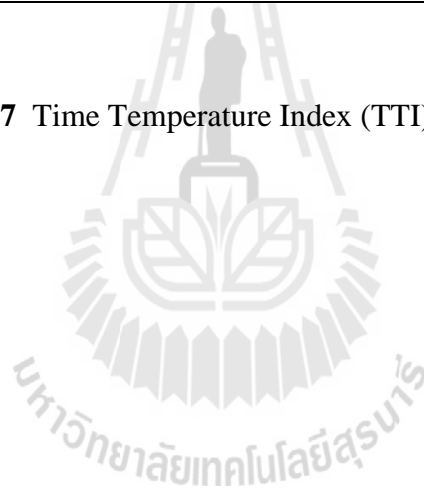


Figure 4.37 Time Temperature Index (TTI) of the Yala-1 well



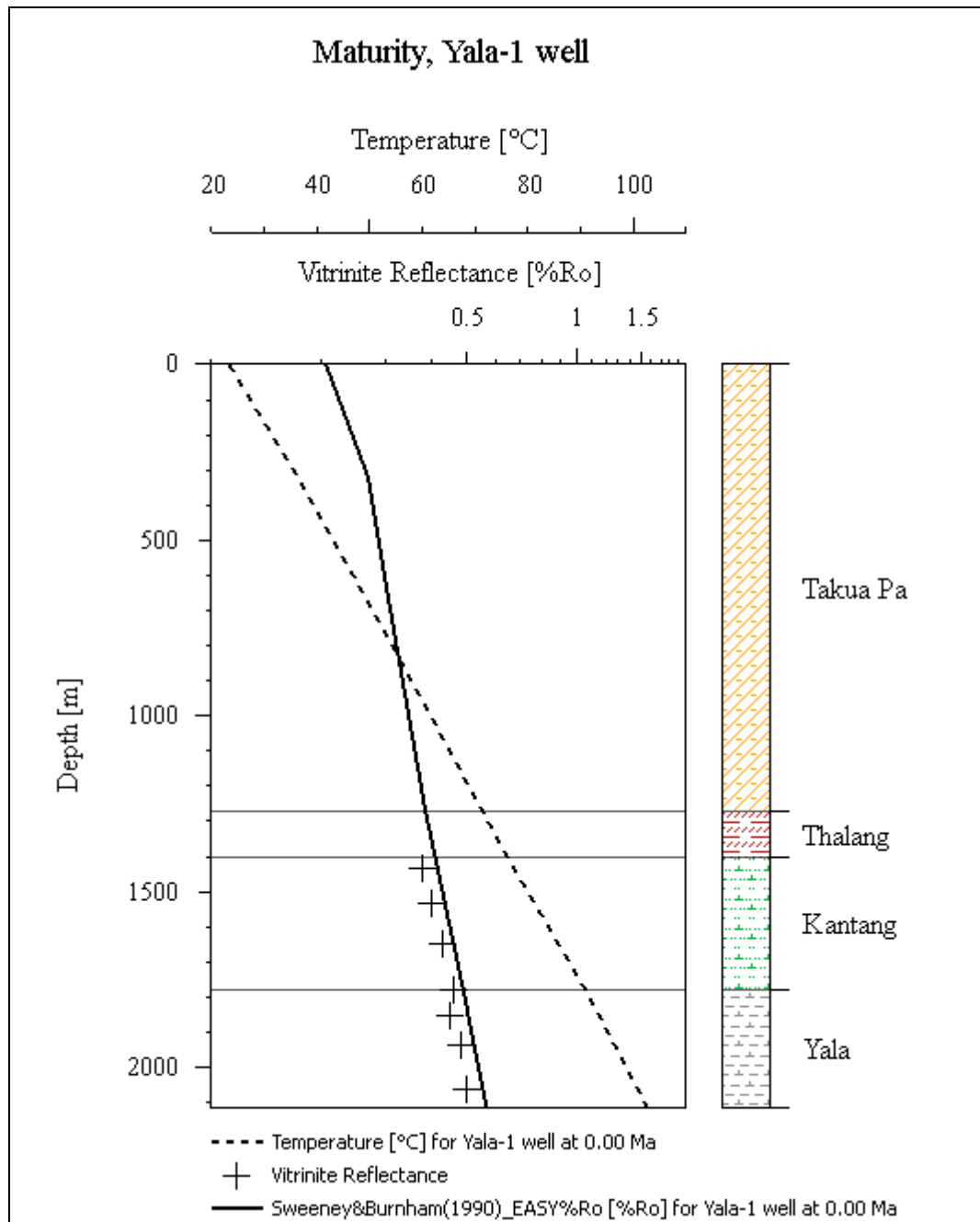


Figure 4.38 Maturity overlay R_o compare with temperature and depth of the Yala-1 well

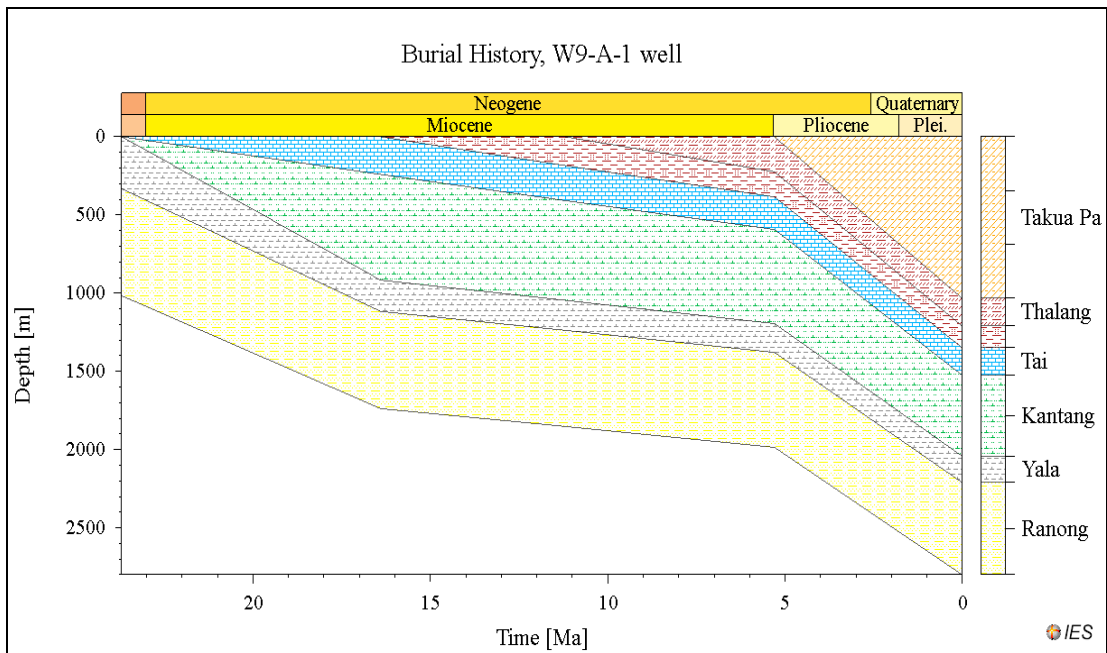


Figure 4.39 Burial history of the W9-A-1 well

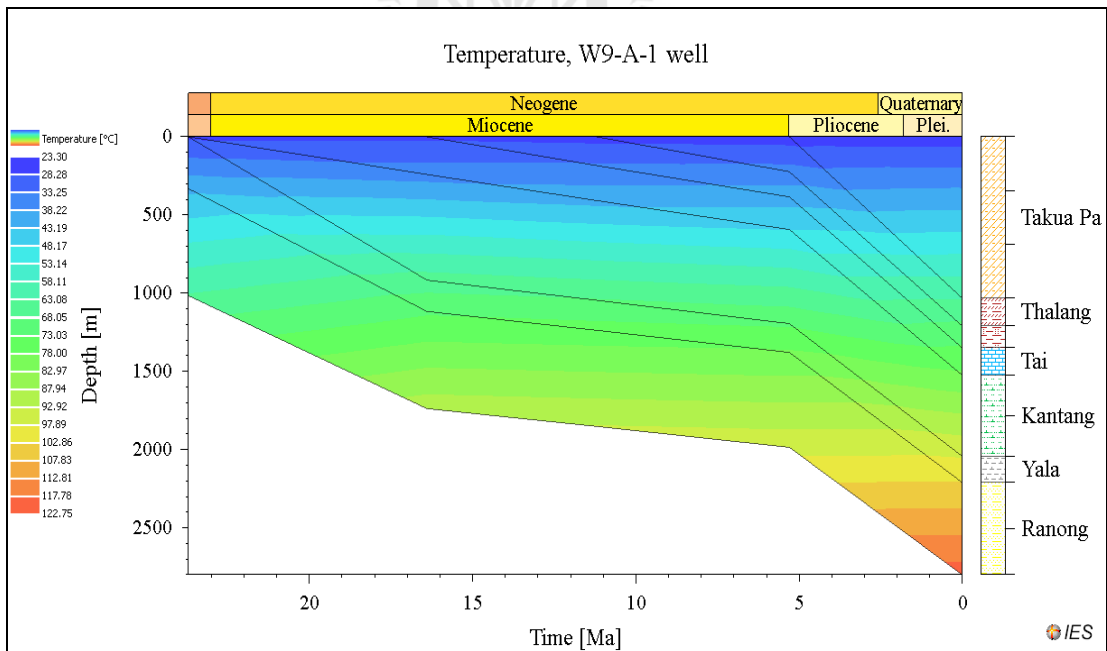


Figure 4.40 Temperature Index (°C) of the W9-A-1 well

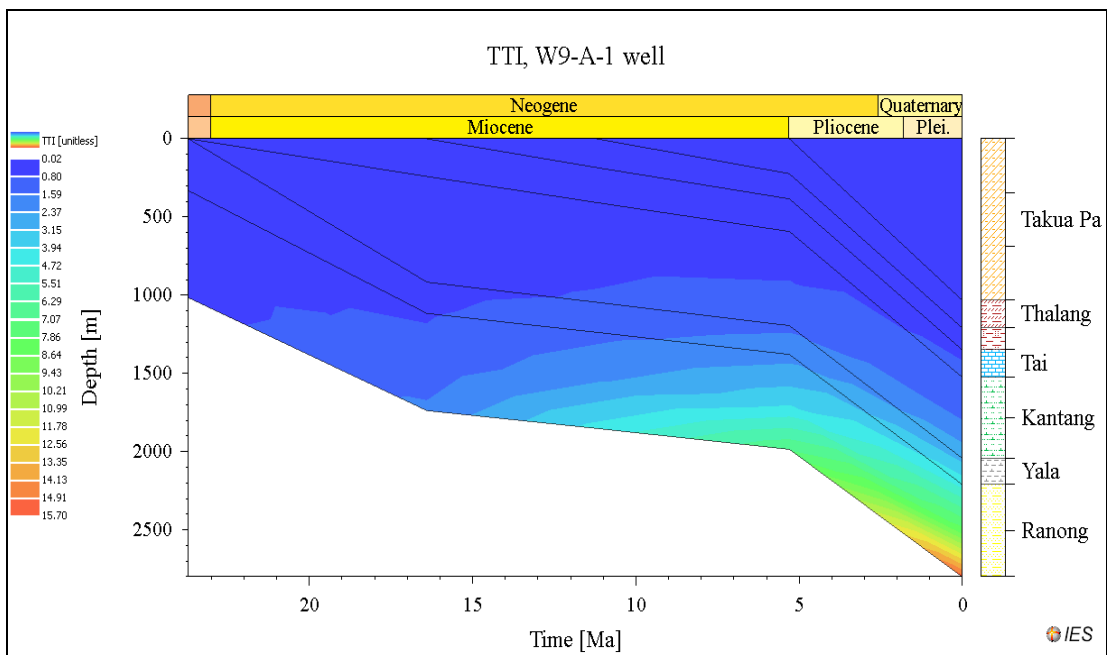
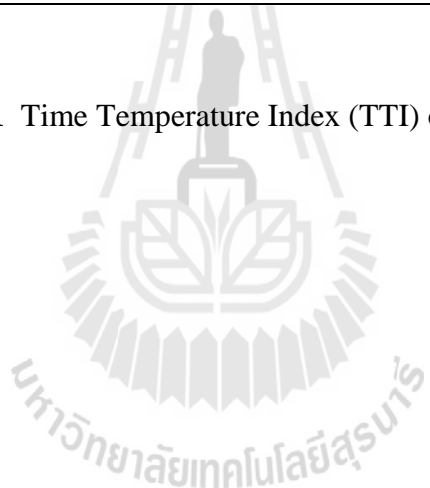


Figure 4.41 Time Temperature Index (TTI) of the W9-A-1 well



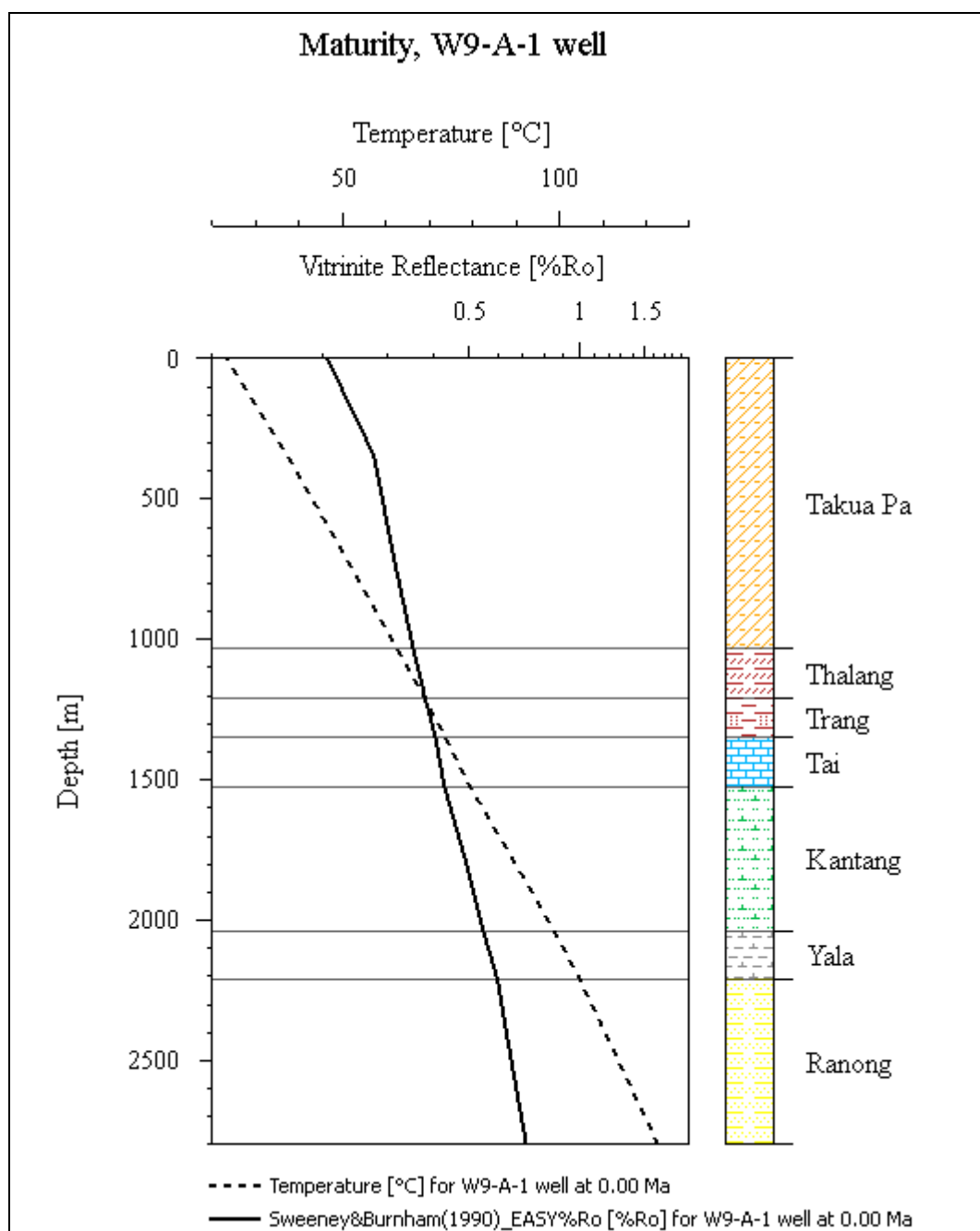


Figure 4.42 Maturity overlay R_o compare with temperature and depth of the W9-A-1 well

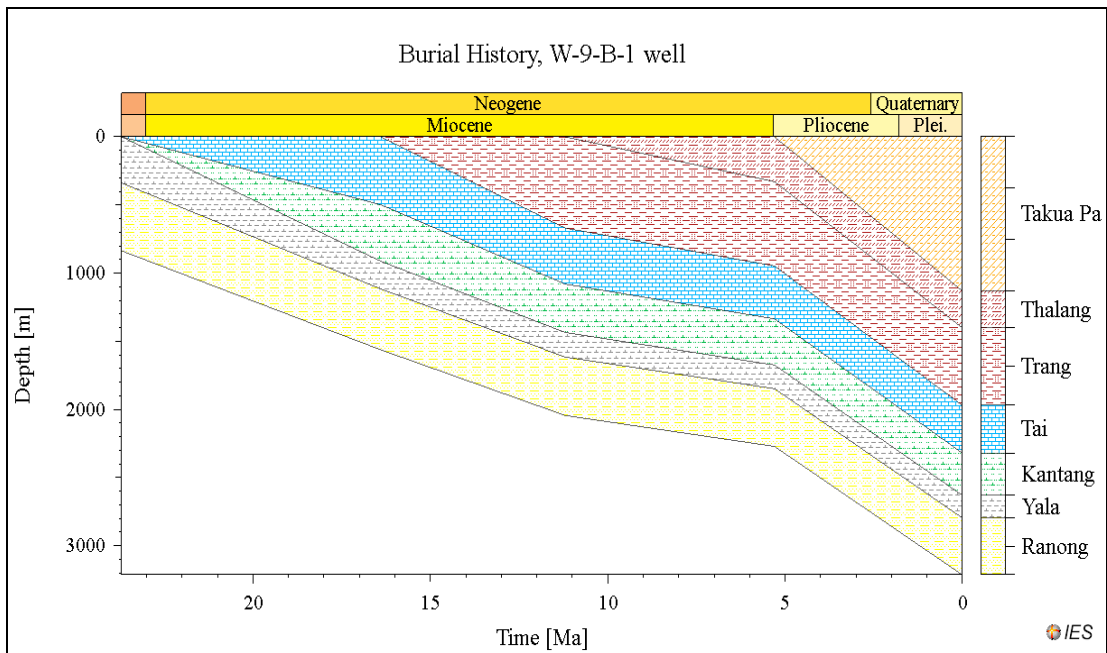


Figure 4.43 Burial history of the W9-B-1 well

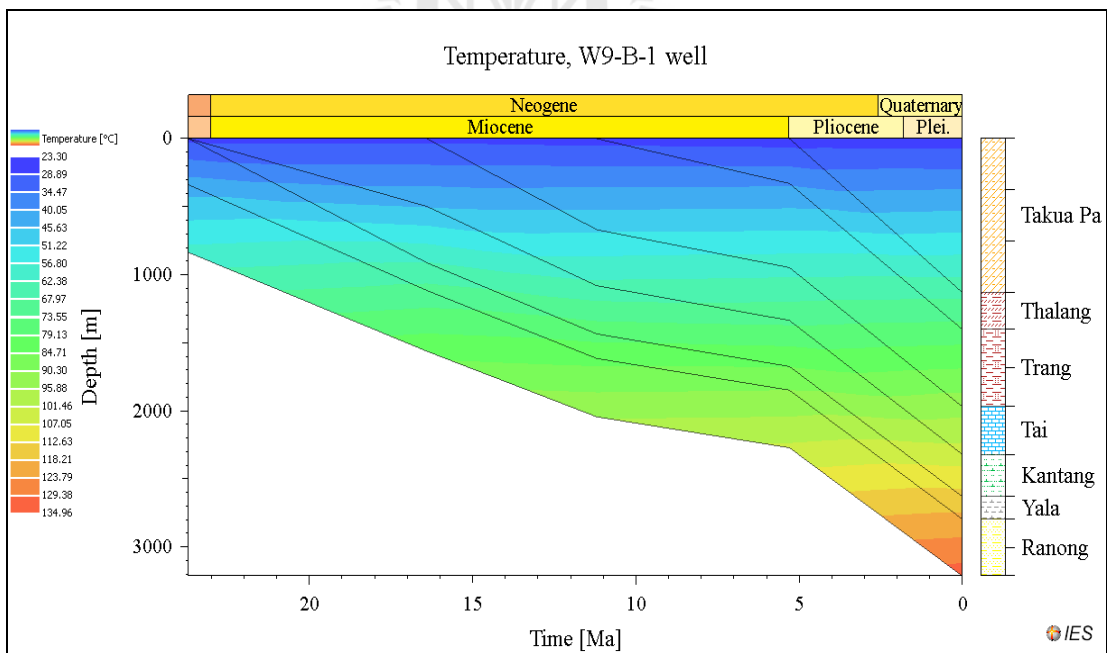


Figure 4.44 Temperature Index (°C) of the W9-B-1 well

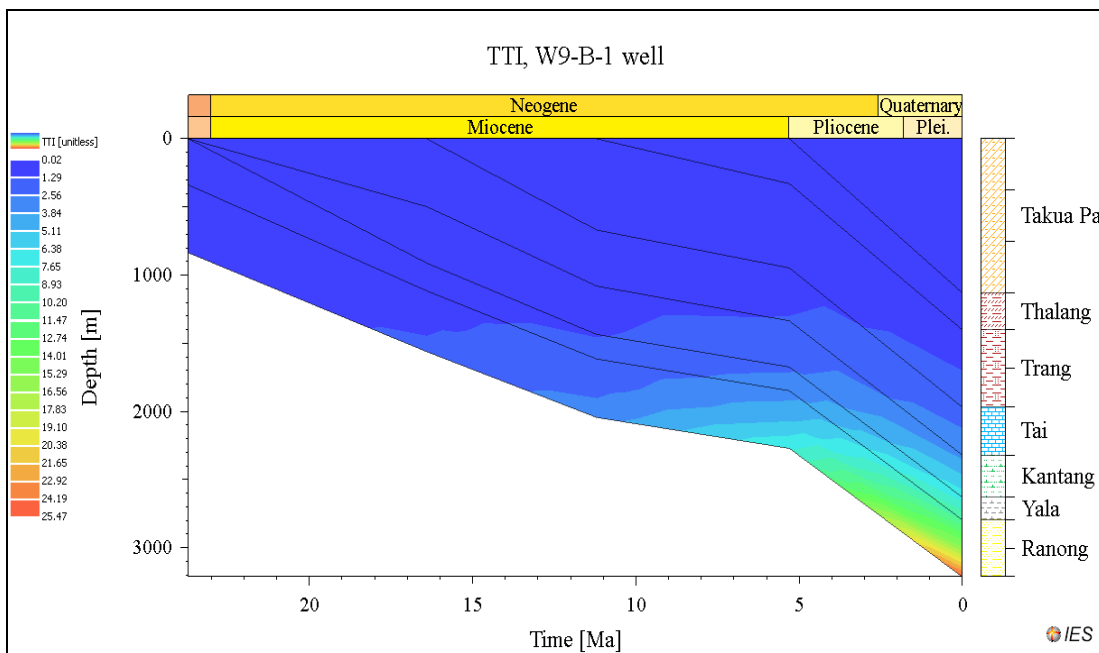
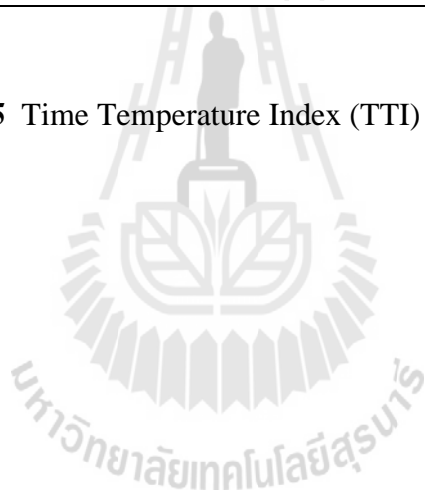


Figure 4.45 Time Temperature Index (TTI) of the W9-B-1 well



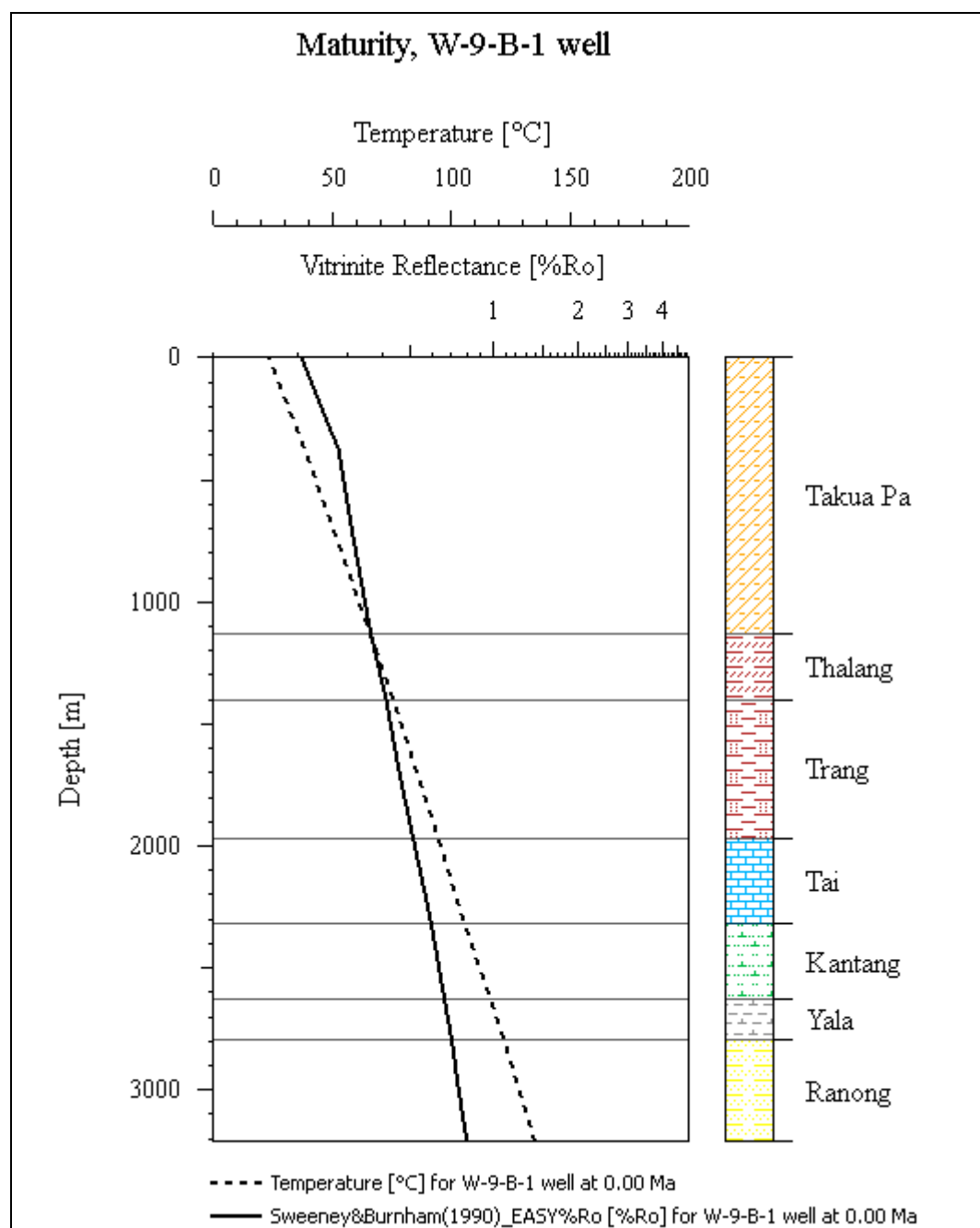


Figure 4.46 Maturity overlay R_o compare with temperature and depth of the W9-B-1 well

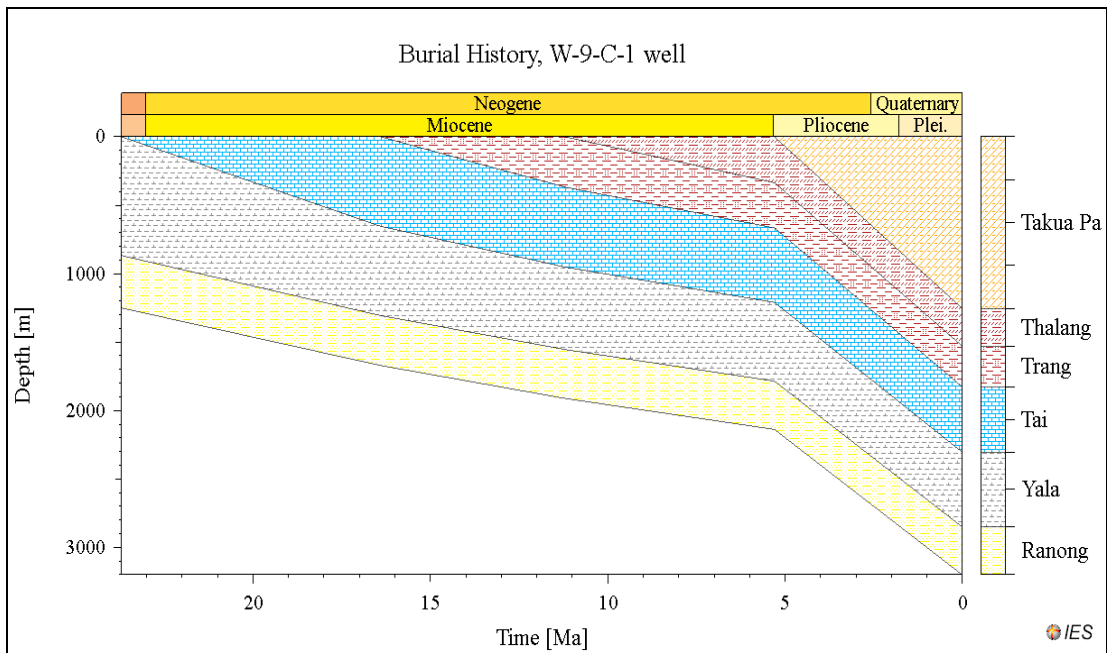


Figure 4.47 Burial history of the W9-C-1 well

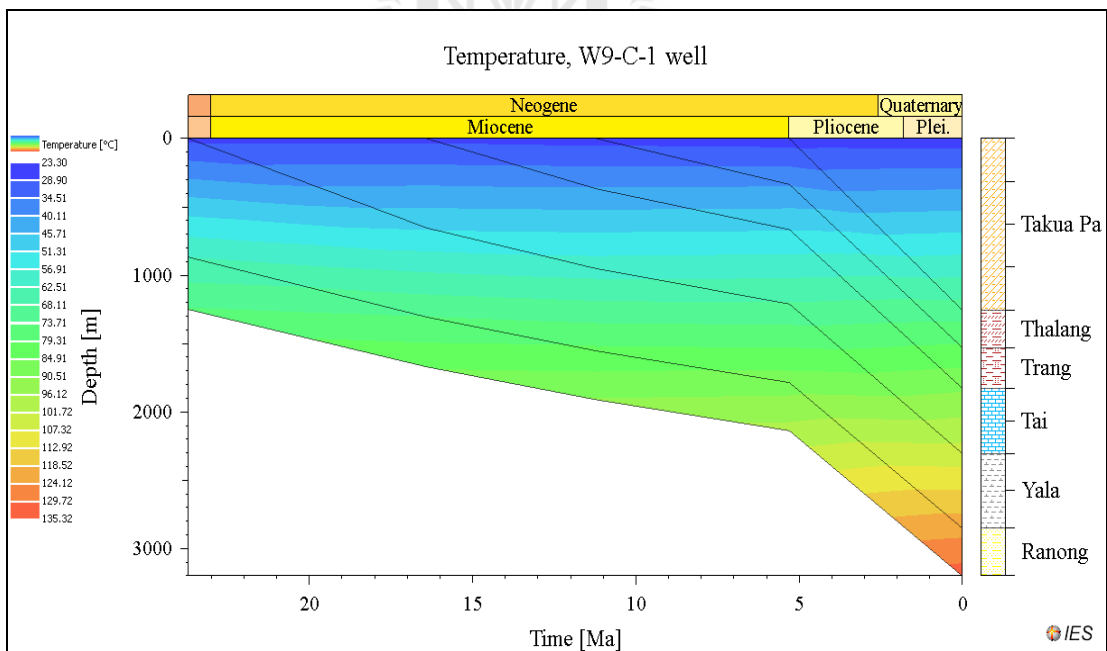


Figure 4.48 Temperature Index (°C) of the W9-C-1 well

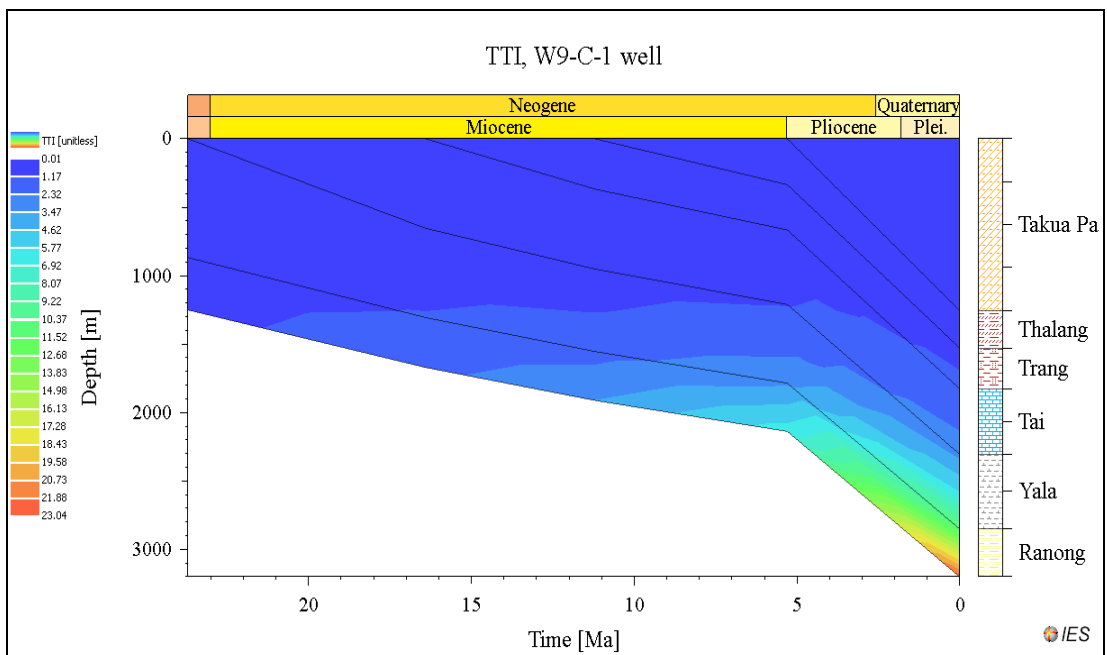
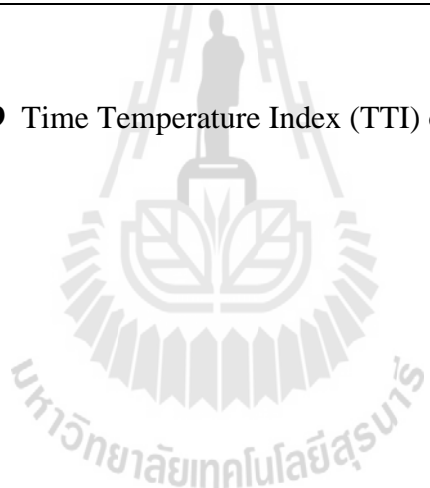


Figure 4.49 Time Temperature Index (TTI) of the W9-C-1 well



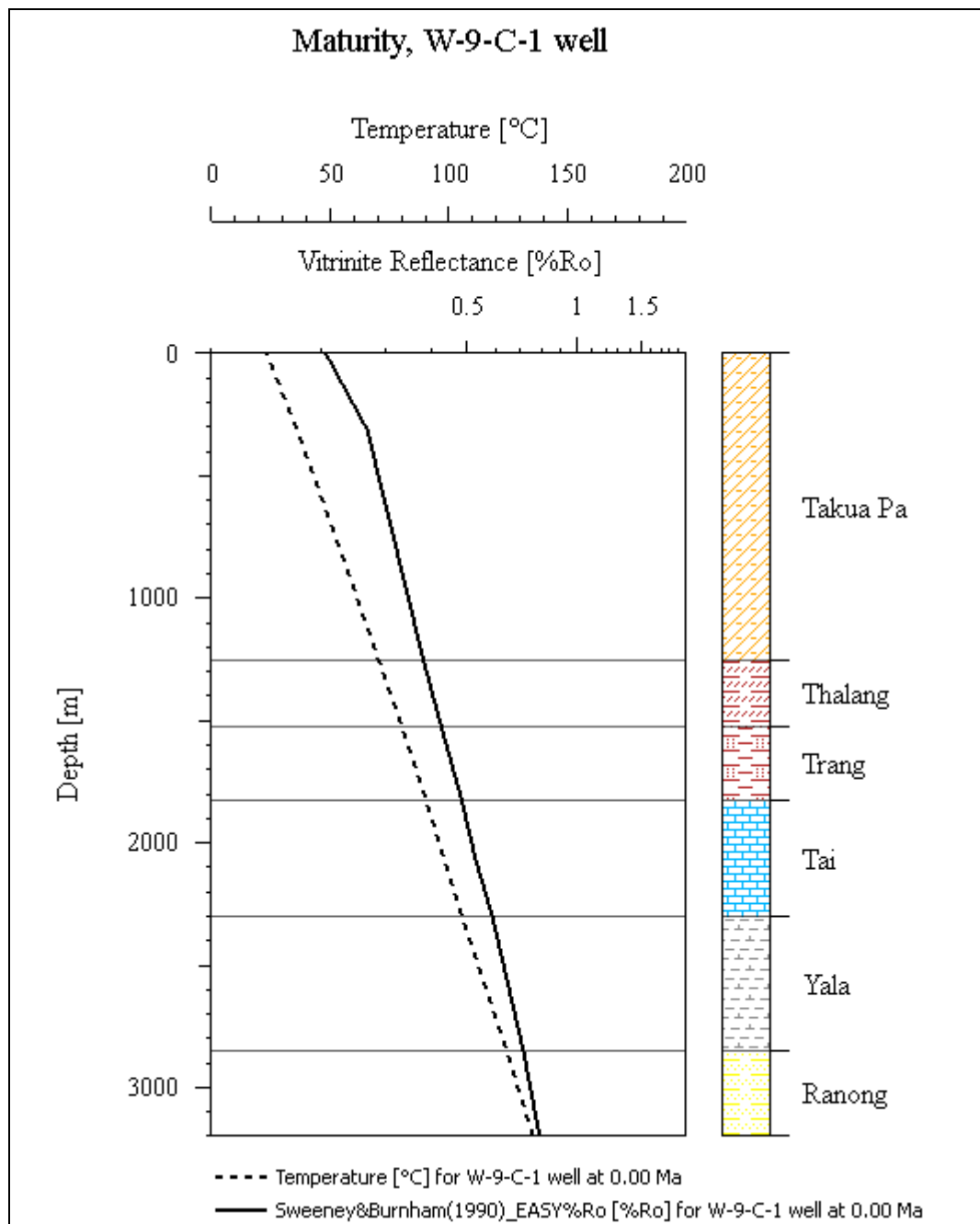


Figure 4.50 Maturity overlay R_o compare with temperature and depth of the W9-C-1 well

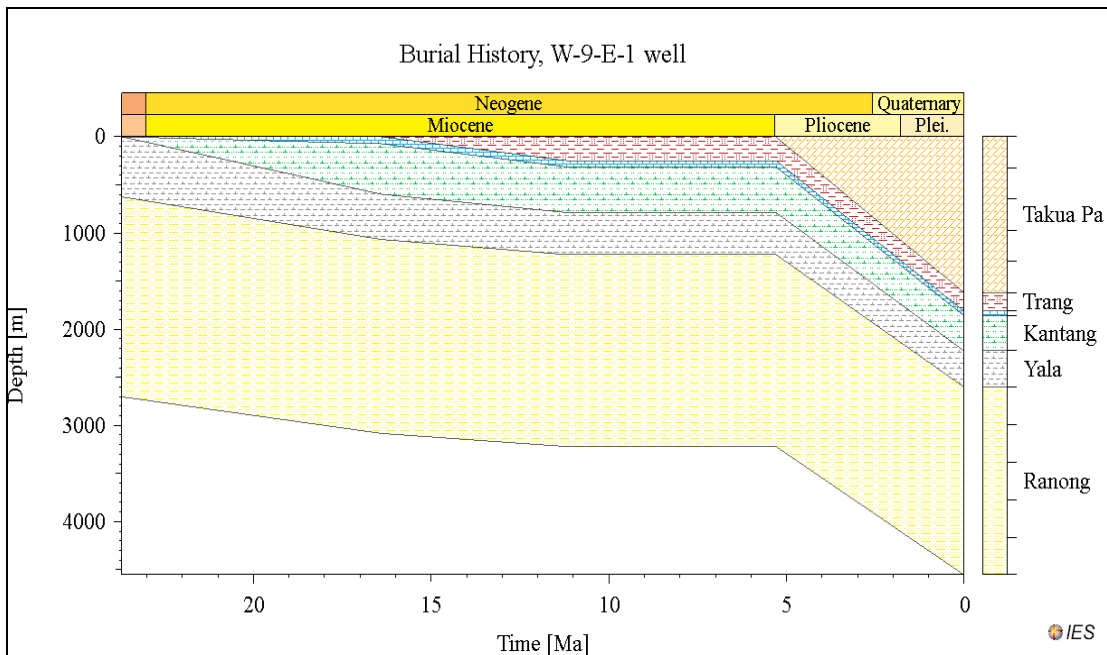


Figure 4.51 Burial history of the W9-E-1 well

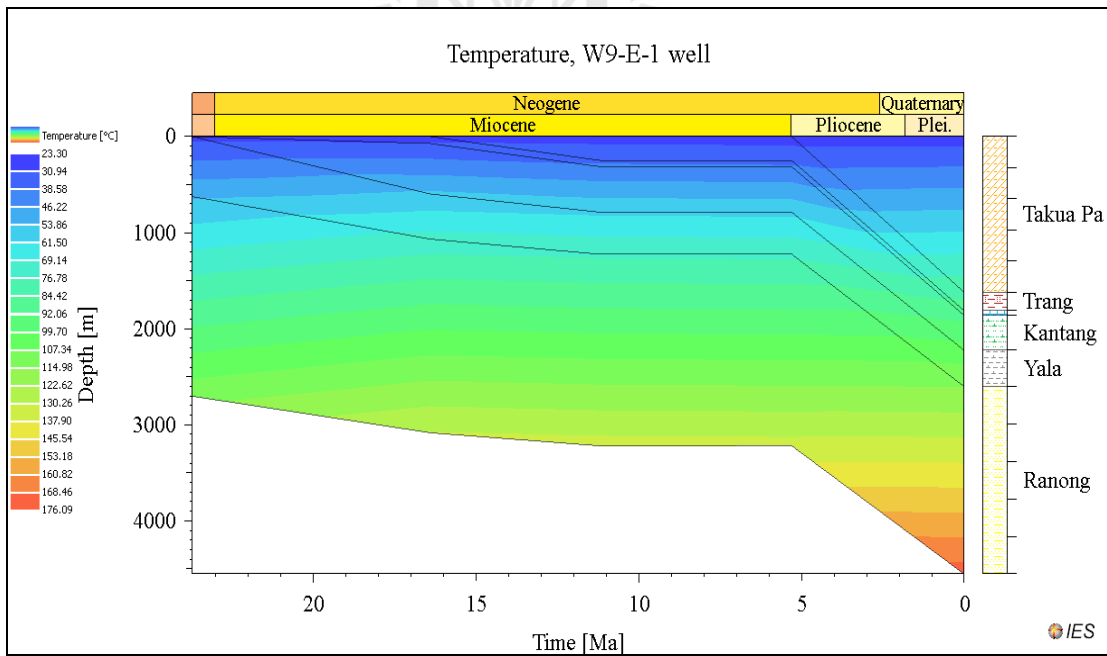


Figure 4.52 Temperature Index (°C) of the W9-E-1 well

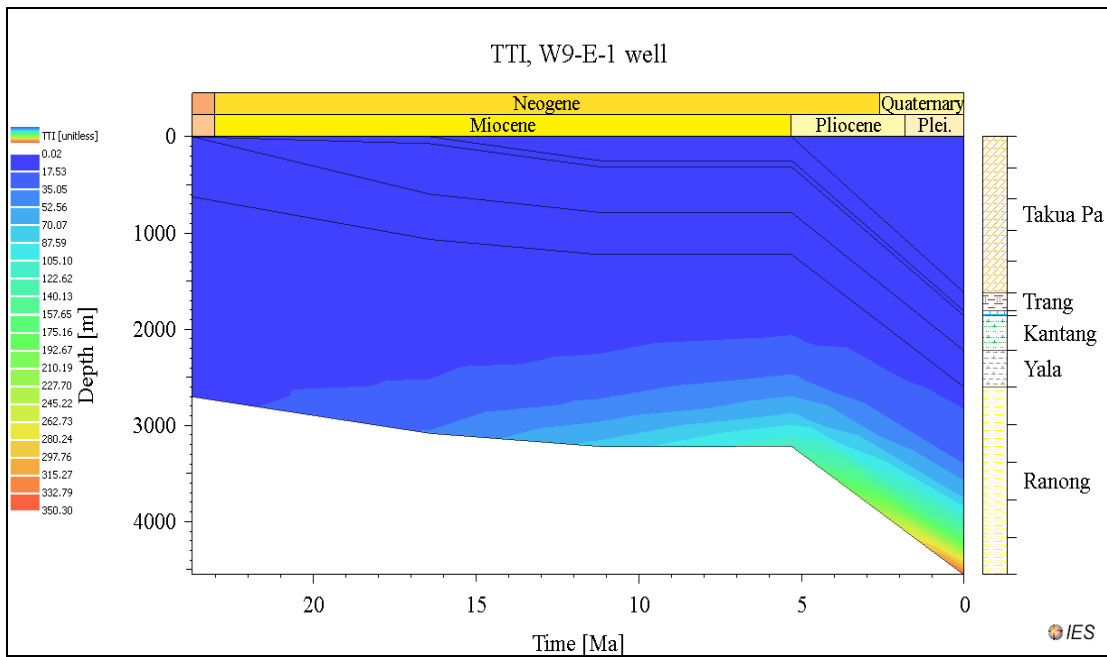
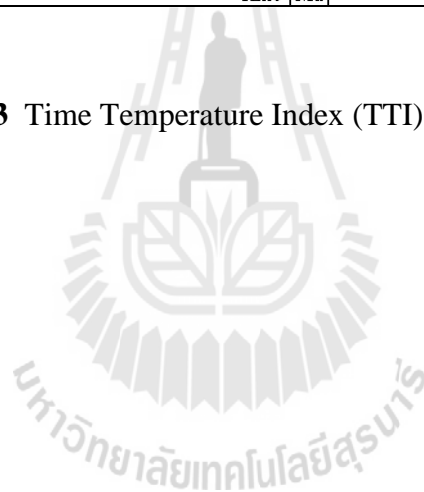


Figure 4.53 Time Temperature Index (TTI) of the W9-E-1 well



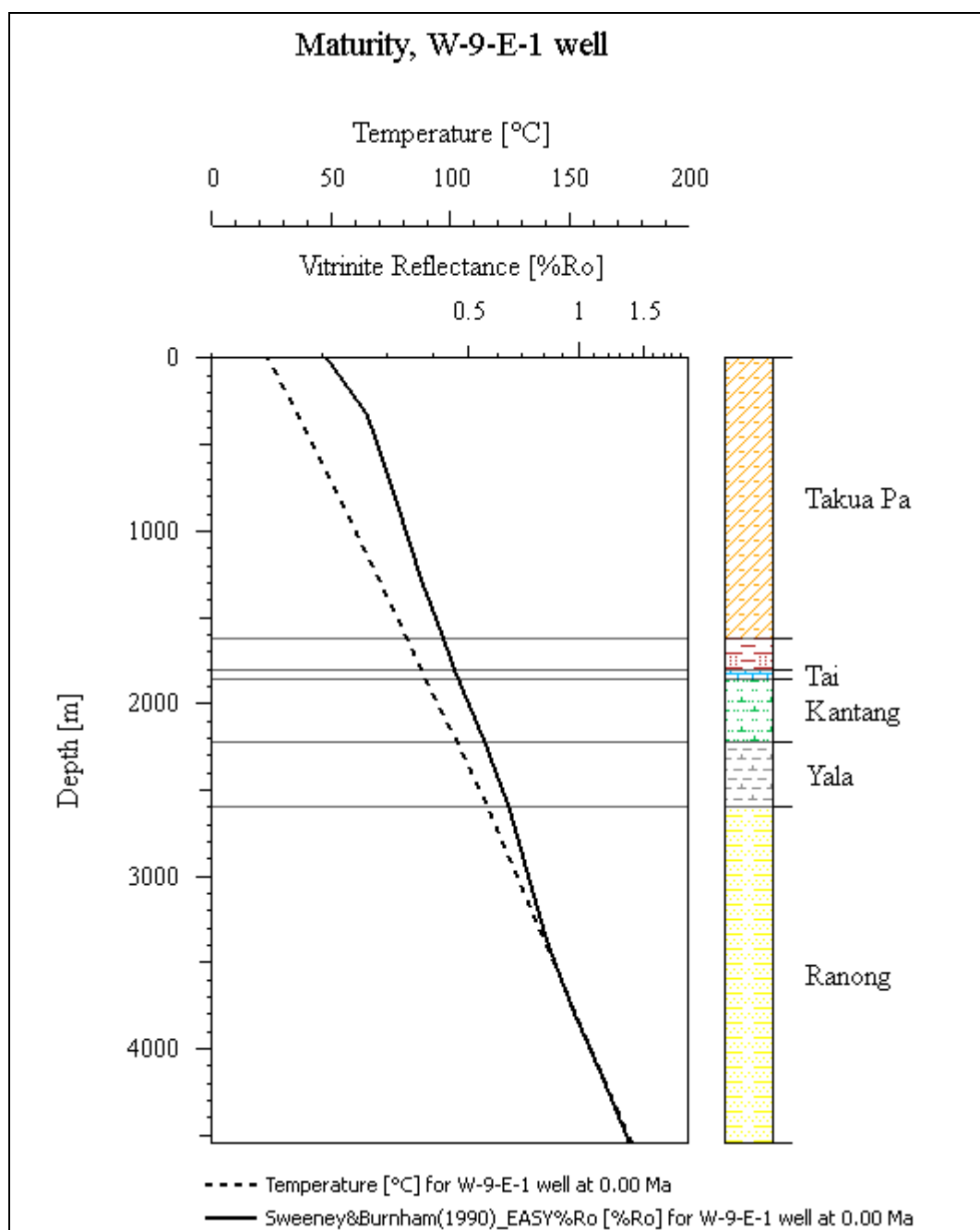


Figure 4.54 Maturity overlay R_o compare with temperature and depth of the W9-E-1 well

Western Mergui

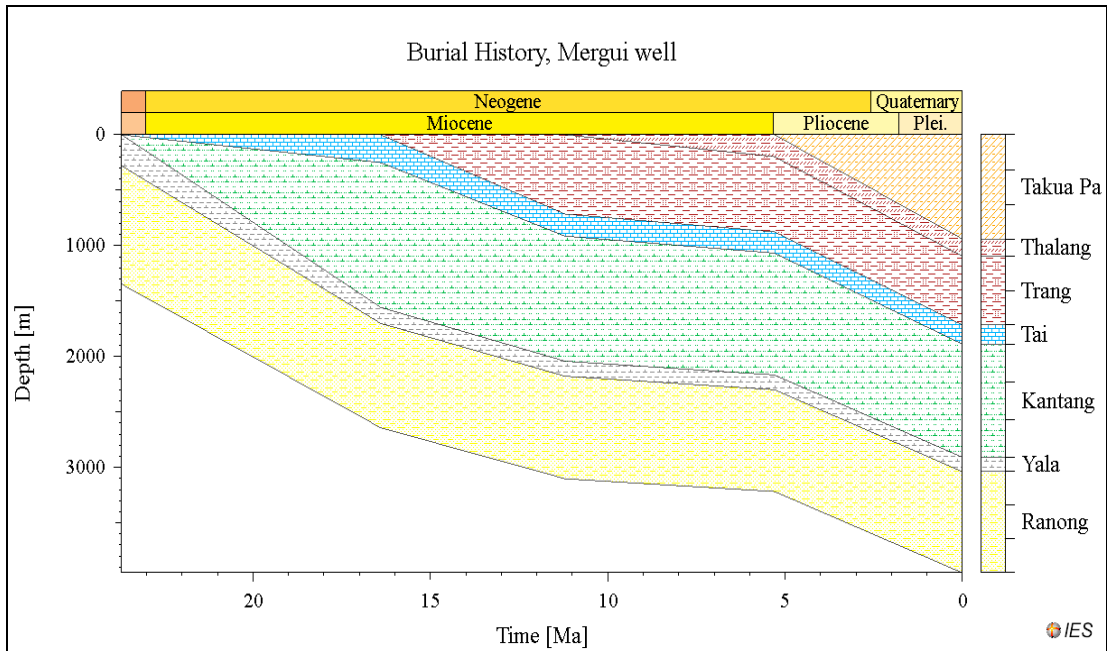


Figure 4.55 Burial history of the Mergui-1 well

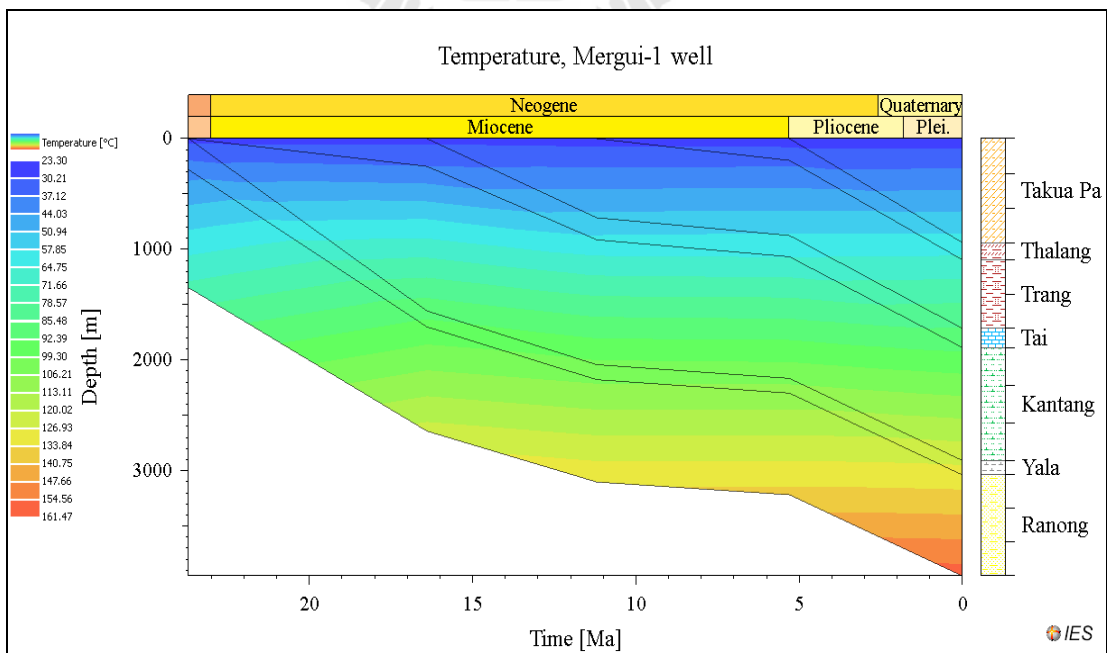


Figure 4.56 Temperature Index (°C) of the Mergui-1 well

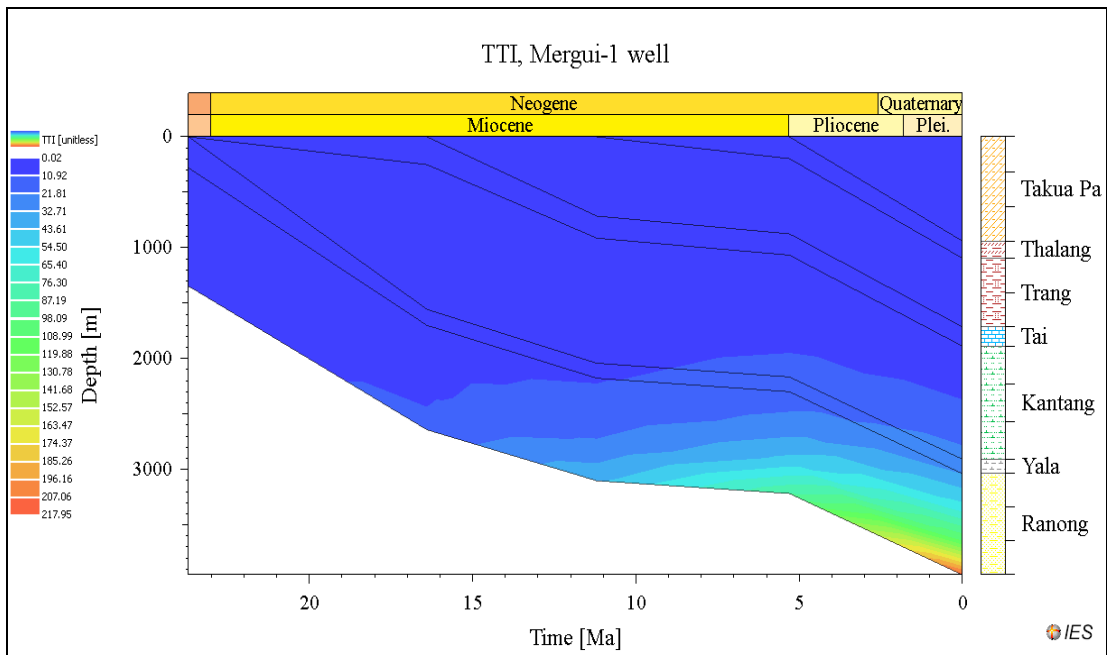
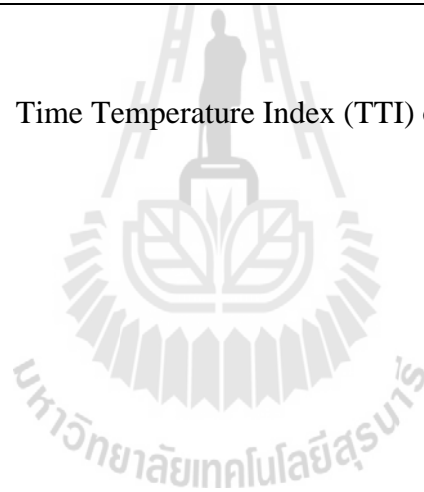


Figure 4.57 Time Temperature Index (TTI) of the Mergui-1 well



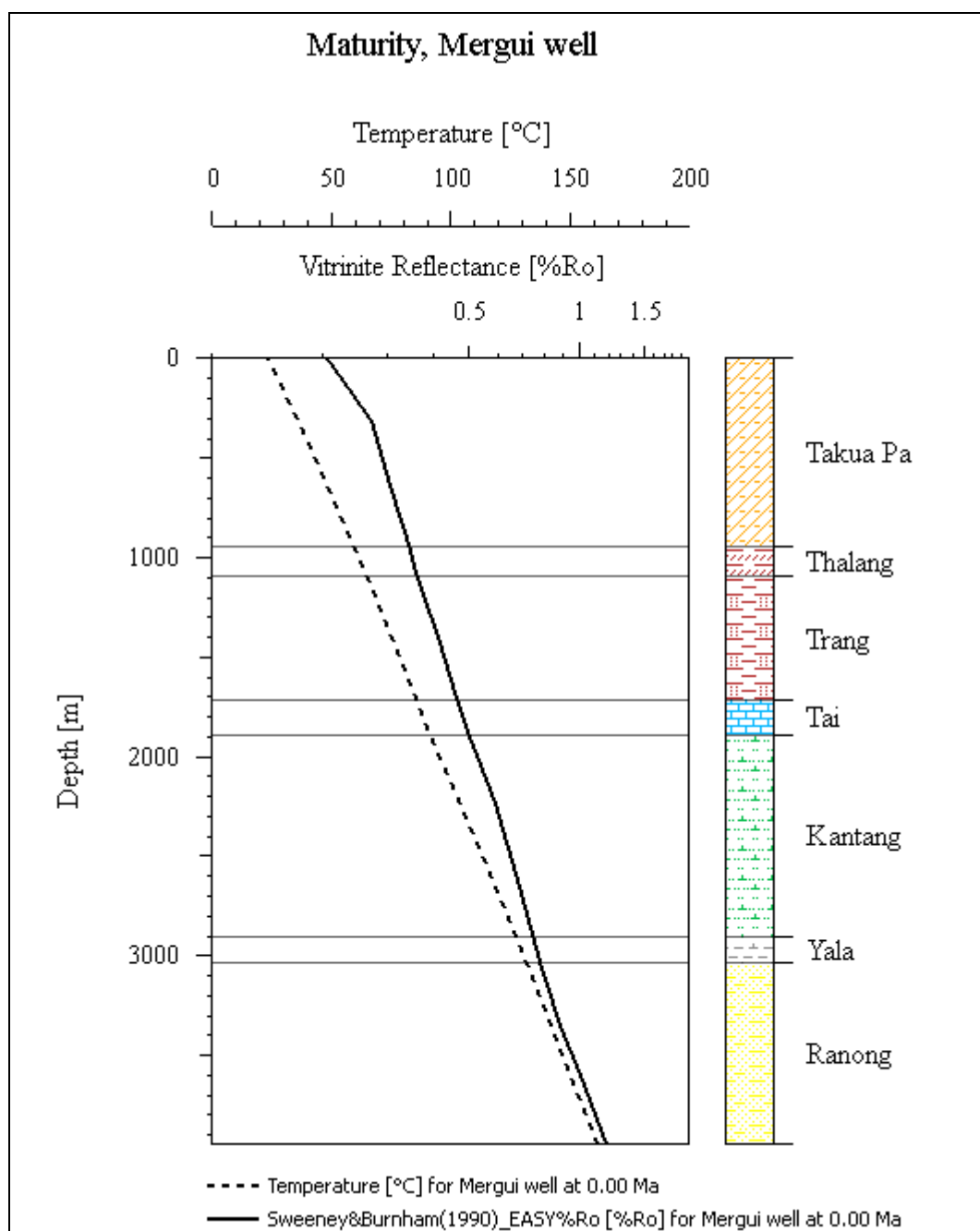


Figure 4.58 Maturity overlay R_o compare with temperature and depth of the Mergui-1 well

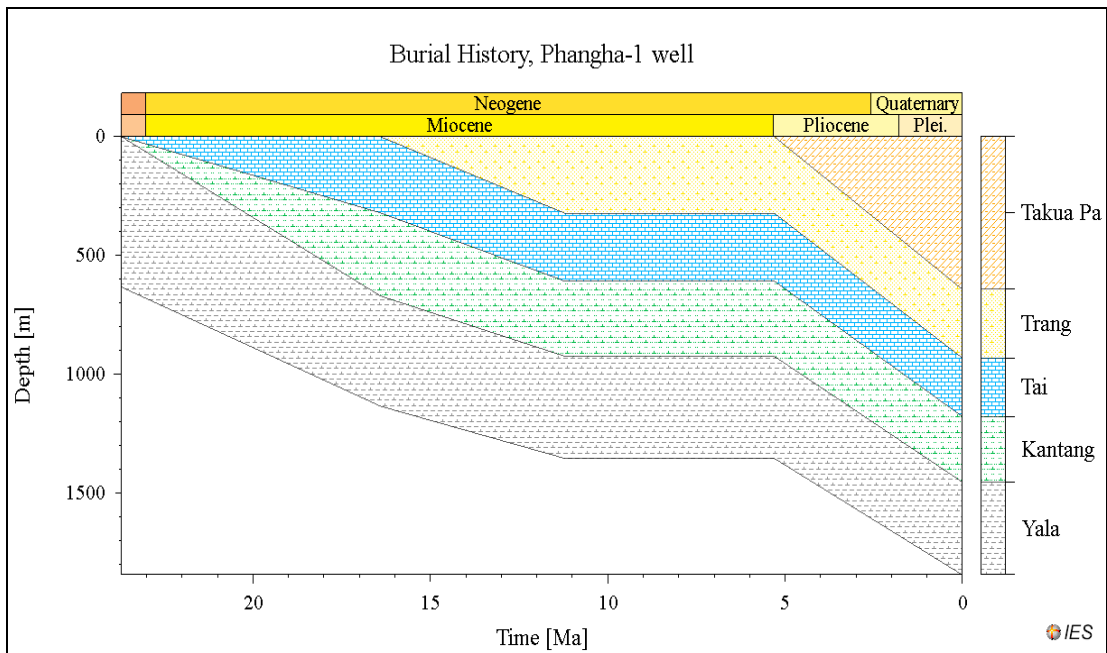


Figure 4.59 Burial history of the Phangha-1 well

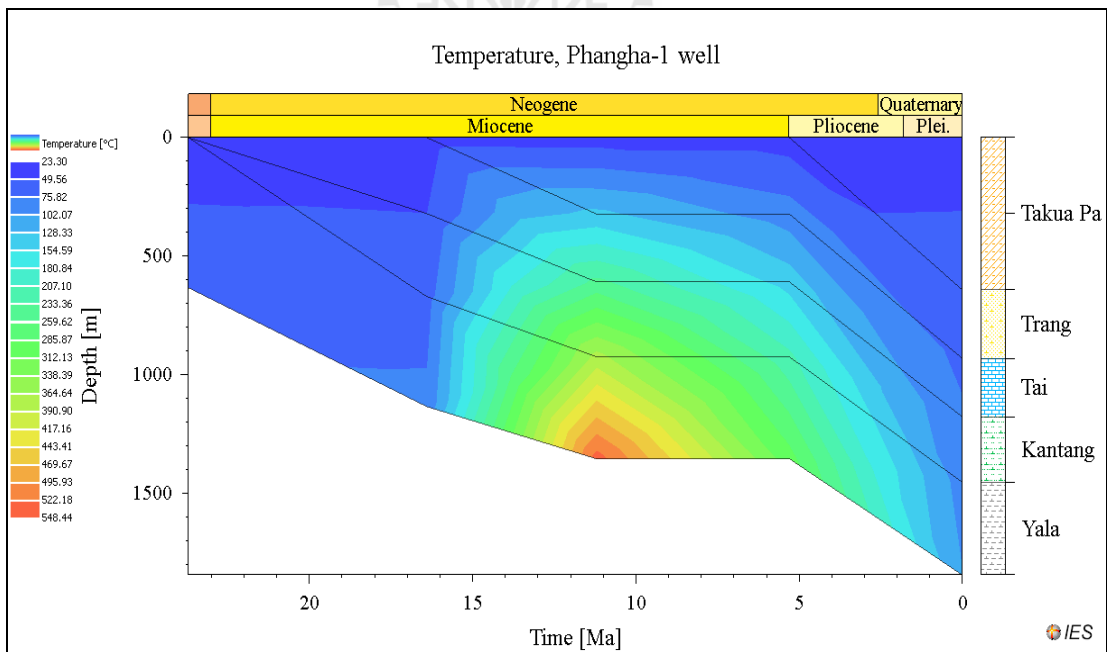


Figure 4.60 Temperature Index (°C) of the Phangha-1 well

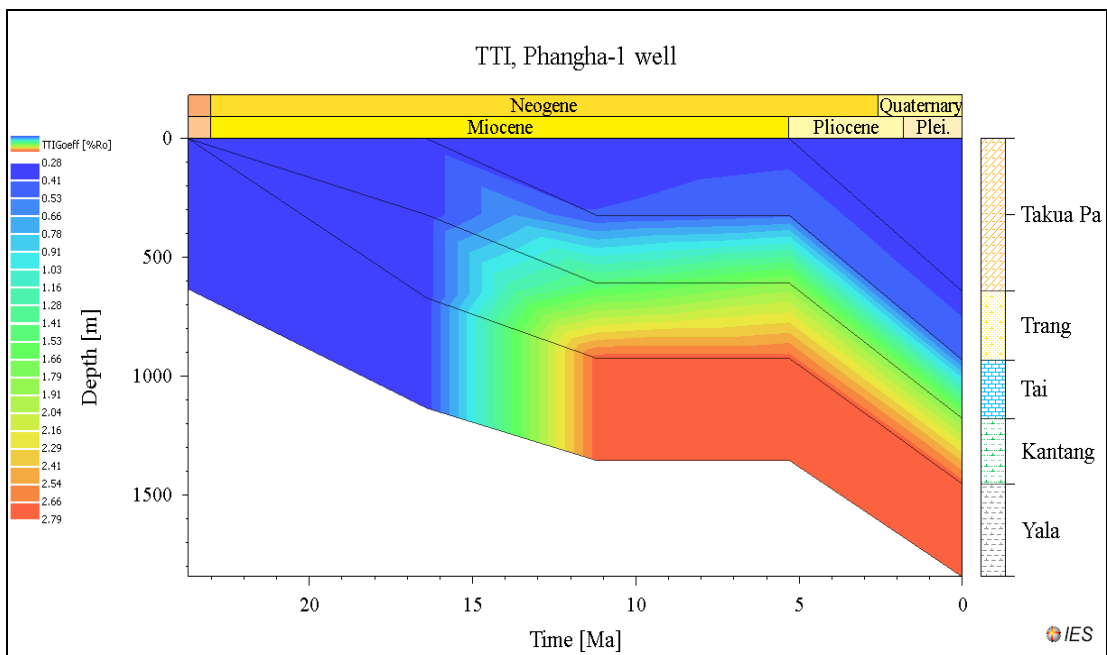
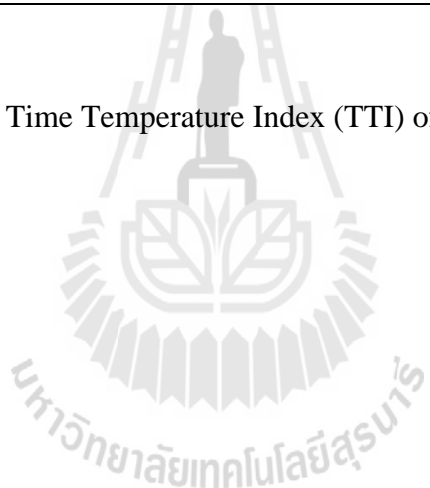


Figure 4.61 Time Temperature Index (TTI) of the Phangha-1 well



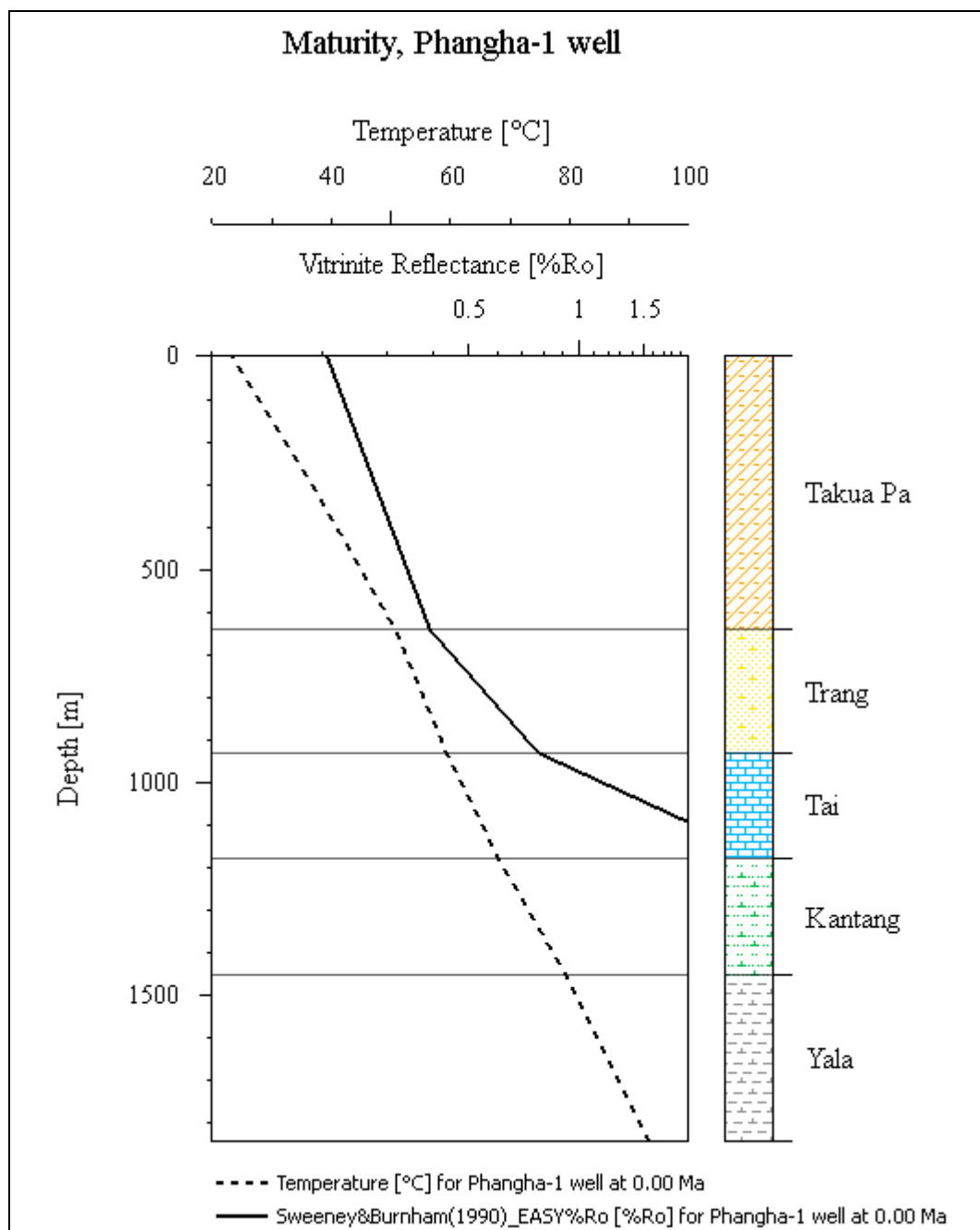


Figure 4.62 Maturity overlay R_o compare with temperature and depth of the Phangha-1 well

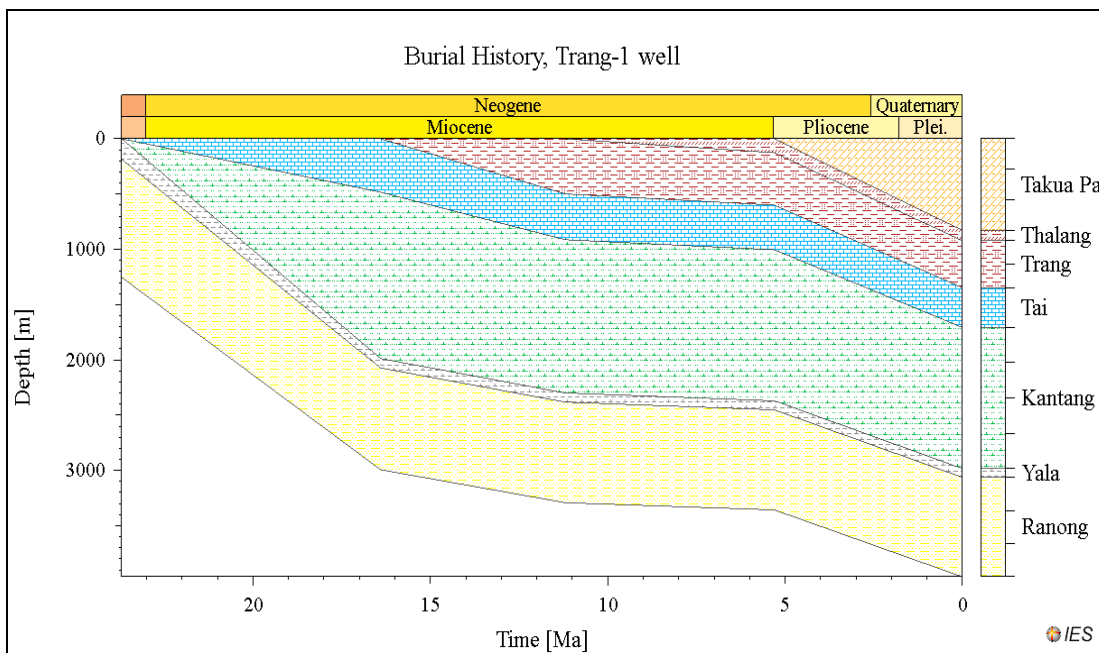


Figure 4.63 Burial history of the Trang-1 well

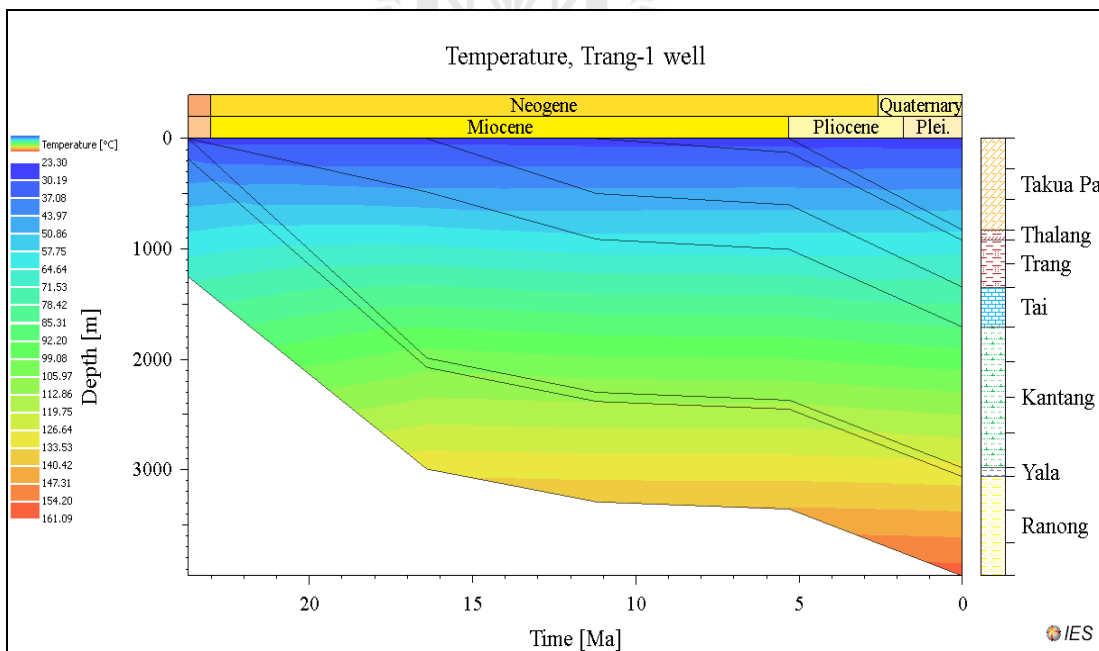


Figure 4.64 Temperature Index (°C) of the Trang-1 well

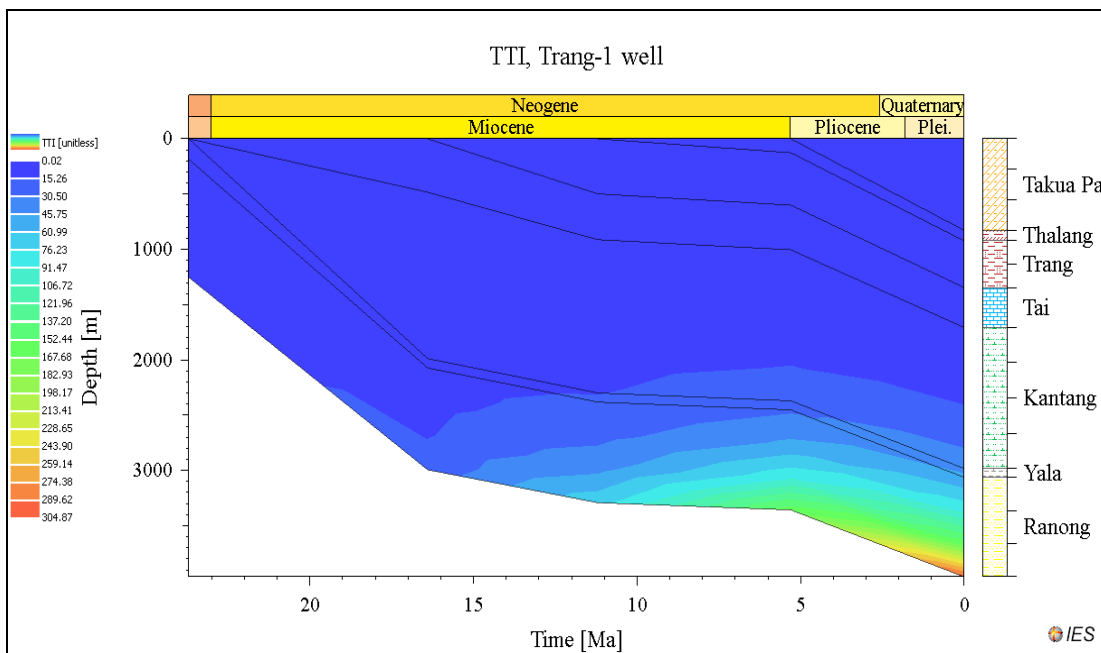
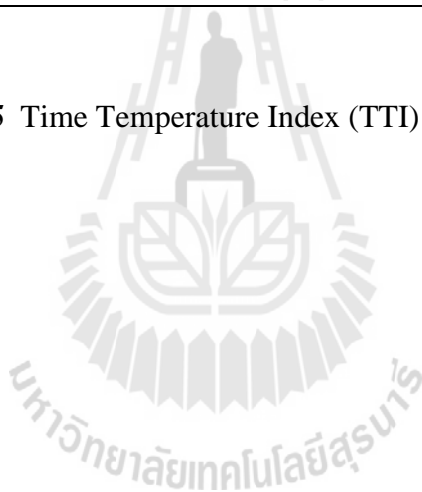


Figure 4.65 Time Temperature Index (TTI) of the Trang-1 well



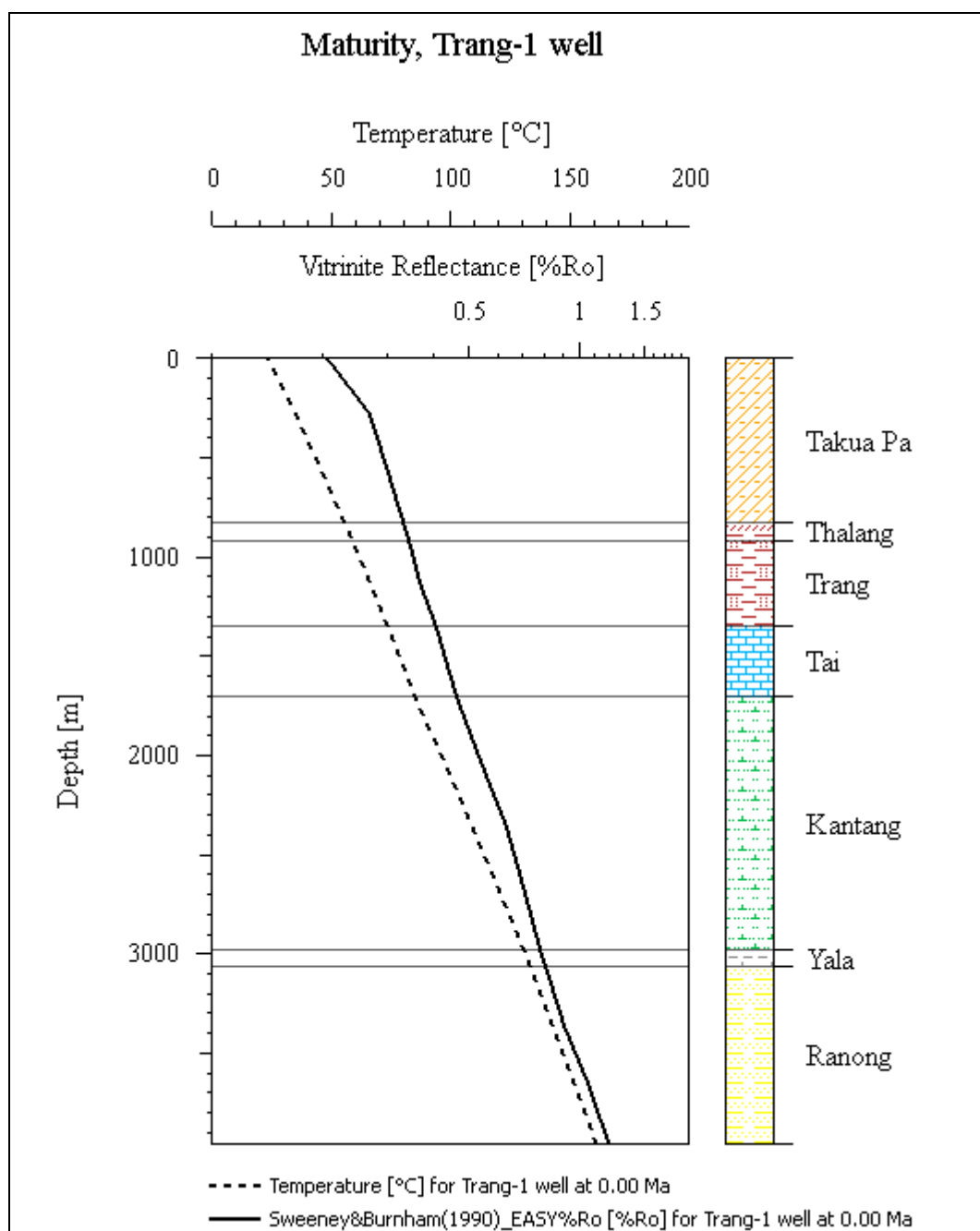


Figure 4.66 Maturity overlay R_o compare with temperature and depth of the Trang-1 well

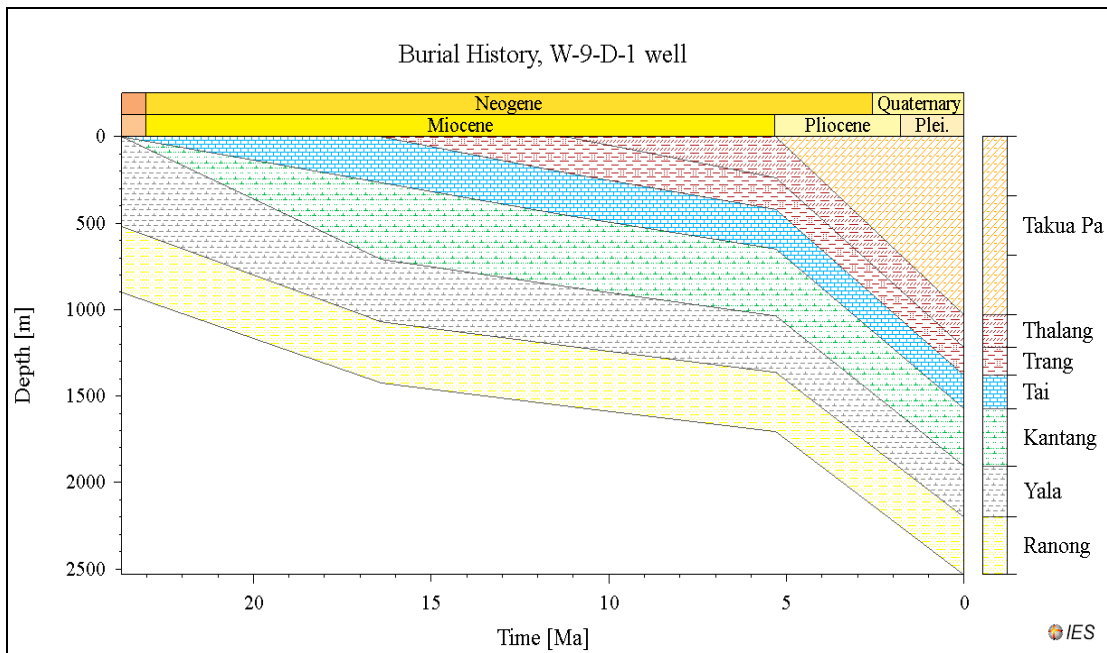


Figure 4.67 Burial history of the W9-D-1 well

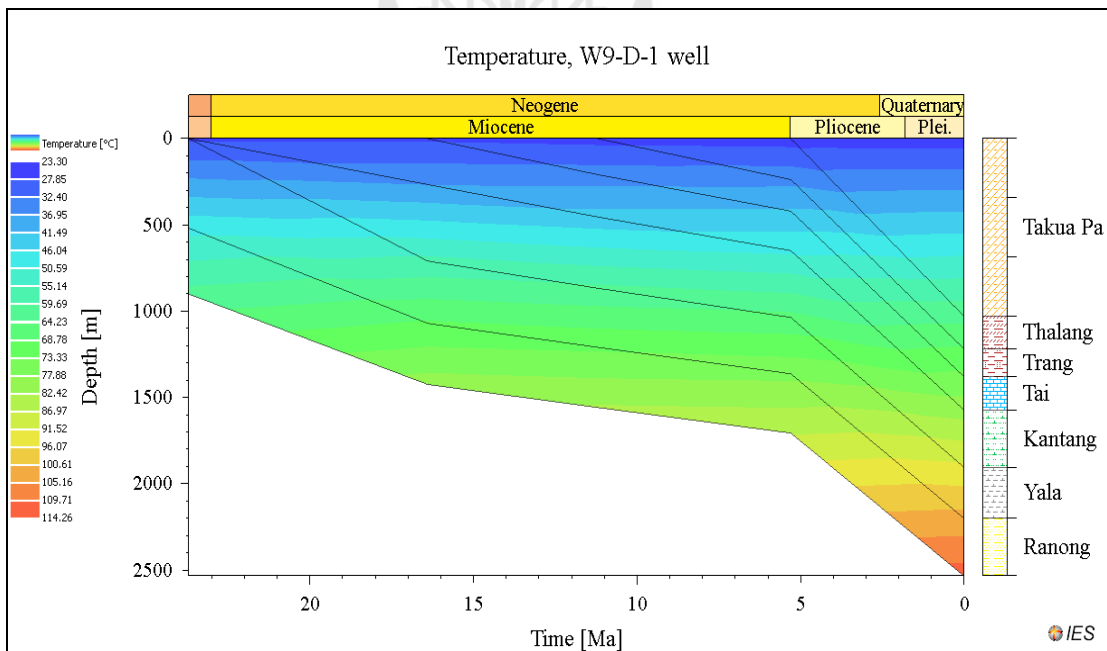


Figure 4.68 Temperature Index (°C) of the W9-D-1 well

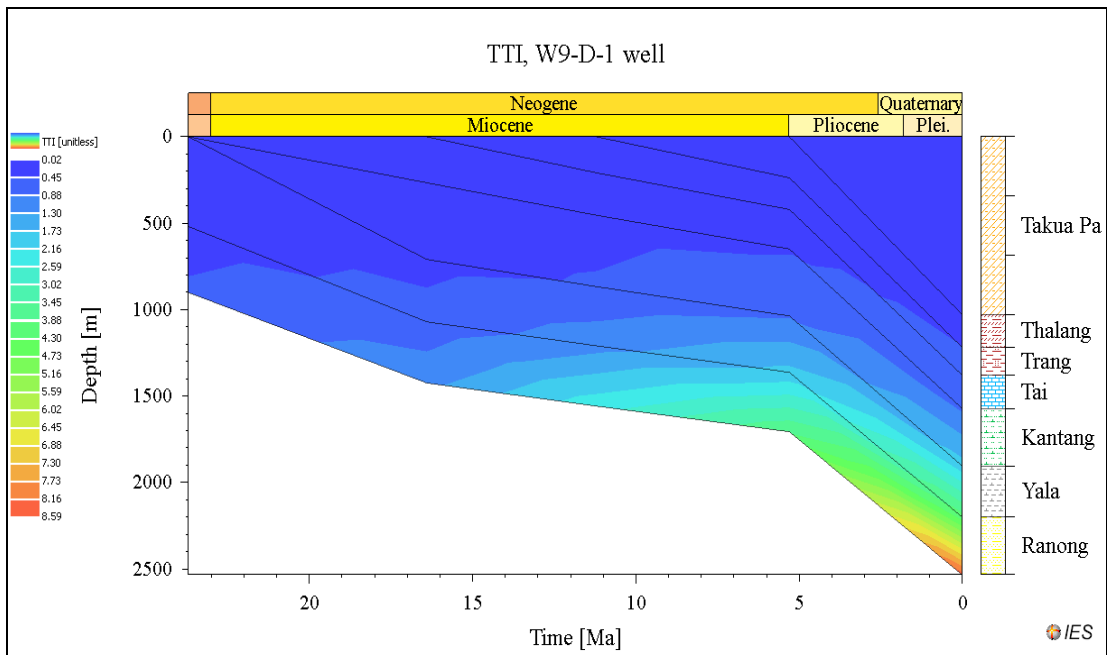
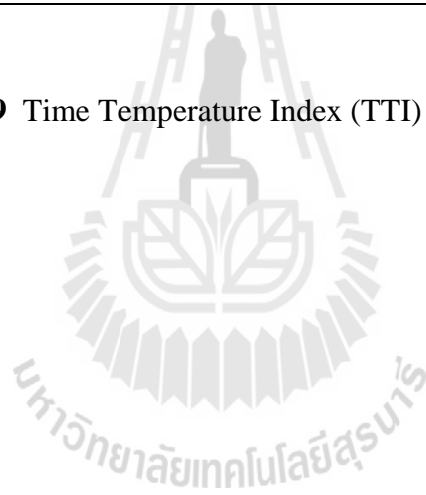


Figure 4.69 Time Temperature Index (TTI) of the W9-D-1 well



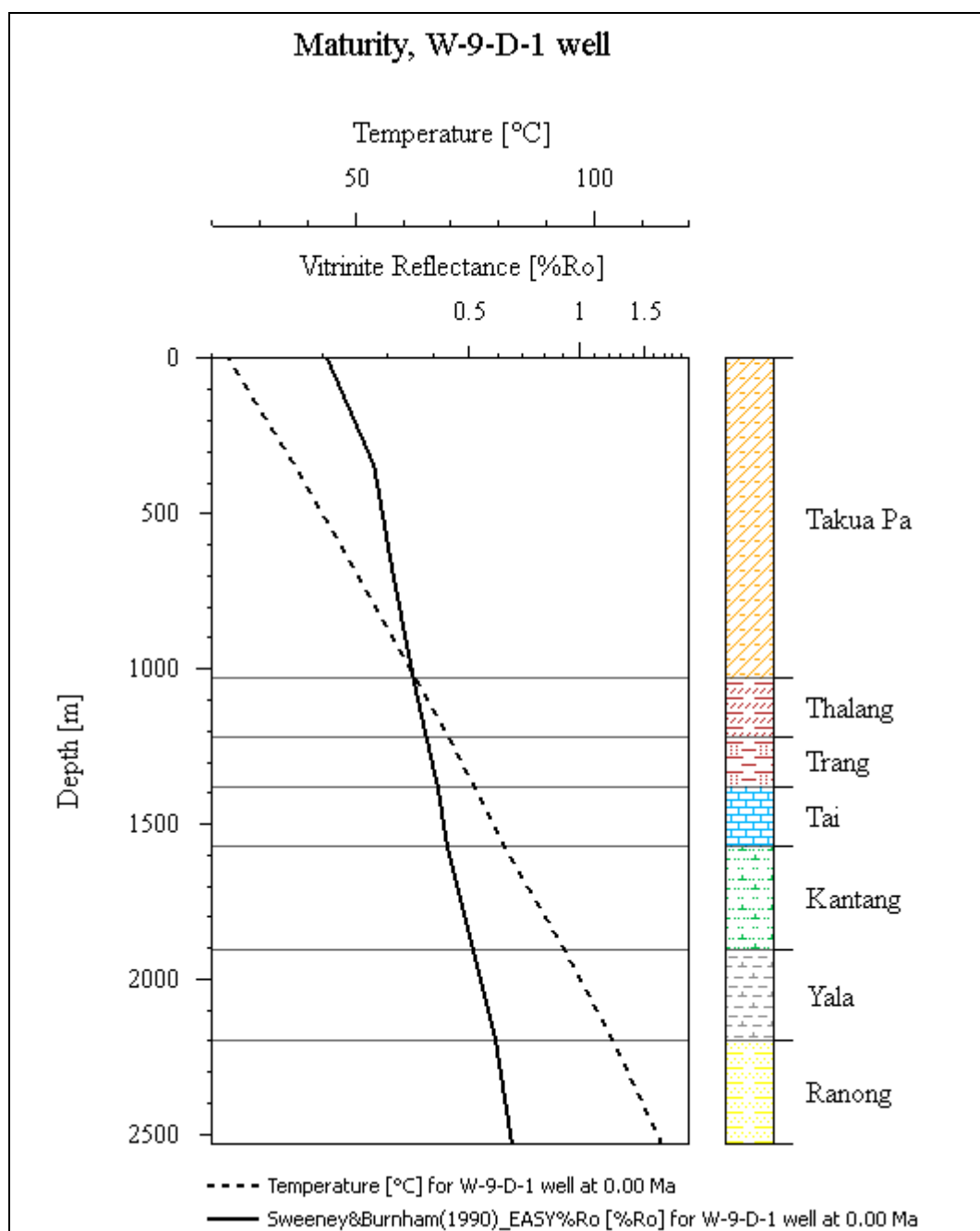


Figure 4.70 Maturity overlay R_o compare with temperature and depth of the W9-D-1 well

Results from PetroMod 1D basin modeling of each well can be interpreted and discussed as follows:

Northern Mergui

Payang-1 well (Figure 4.7-4.10)

- Miocene and Oligocene sediments of Payang-1 well at the depth range from 417 m to 1,800 m were analyzed to determine their hydrocarbon source potential, thermal maturity and the occurrence of migrated hydrocarbons.
- The source potential was not found in this well.

Eastern Mergui

Kantang-1 well (Figure 4.11-4.14)

- Miocene and Oligocene sediments of Kantang-1 well at the depth range from 1,310 m to 2,500 m were analyzed to determine their hydrocarbon source potential, thermal maturity and the occurrence of migrated hydrocarbons.
- The source potential of the Oligocene sediments is poor to fair in the Yala Formation (average TOC 1.22%). The TOC content of Miocene sediment in the Trang Formation is 1.02%.

- Organic matter within the sediments is predominantly gas-prone, representing Type III or mixed II/III kerogen, composed of varying proportion of amorphinite & herbaceous/woody kerogen with minor coaly and algal organic matter.

Kathu-1 well (Figure 4.15-4.18)

- Sediment in studied depth almost clastic overlying the carbonate reef. Miocene and Oligocene sediments of Kathu-1 well at the depth range from 821 m to 1,013 m were analyzed to determine their hydrocarbon source potential, thermal maturity and the occurrence of migrated hydrocarbons.

- The source potential of the Oligocene sediments is poor to fair in the Yala Formation (average TOC 0.65%).
- The organic matter within the sediments has few hydrocarbon source potential and is generally gas prone/Type III.

KraBuri-1 well (Figure 4.19-4.22)

- Miocene and Oligocene sediment of KraBuri-1 well at depth range from 1,280 m to 3,000 m were analyzed to determine their hydrocarbon source potential, thermal maturity and the occurrence of migrated hydrocarbons.
- The potential source rock was found to be mostly shale in Oligocene sediments is poor to fair. The average TOC throughout the well is 1.16% found in the Yala Formation.
- The organic matter within the sediments has few hydrocarbon source potential and is generally gas prone/Type III.

Ranot-1 well (Figure 4.23-4.26)

- Miocene and Oligocene sediments of Ranot-1 well at the depth range from 1,079 m to 2,854 m were analyzed to determine their hydrocarbon source potential, thermal maturity and the occurrence of migrated hydrocarbons.
- The source potential of the Miocene sediments is poor in the Trang Formation with TOC 0.70%.
- The organic matter within the sediments is predominantly gas-prone, representing Type III kerogen. The kerogen is dominated by terrestrial matter.

Sikao-1 well (Figure 4.27-4.30)

- The sediment at depth range from 1,166 m to 2,241 m were analyzed to determine their hydrocarbon source potential, thermal maturity and the occurrence of migrated hydrocarbons.
- The source potential of the Oligocene sediments is poor to fair in the Yala Formation with TOC 0.32%.
- The organic matter within the sediments has few hydrocarbon source potential and is generally gas prone/Type III.

Thalang-1 well (Figure 4.31-4.34)

- Miocene and Oligocene sediments of Thalang-1 well at the depth range from 1,354 m to 2,435 m were analyzed to determine their hydrocarbon source potential, thermal maturity and the occurrence of migrated hydrocarbons.
- The source potential of the Miocene and Oligocene sediments is poor to fair. The TOC is 0.76% in the Yala Formation, 1.12% in the Kantang Formation, and 1.58% in the Trang Formation.
- The organic matter within the sediments is predominantly gas-prone, representing Type III kerogen.

Yala-1 well (Figure 4.35-4.38)

- Miocene and Oligocene sediments of Yala-1 well at the depth range from 1,271 m to 2,118 m were analyzed to determine their hydrocarbon source potential, thermal maturity and the occurrence of migrated hydrocarbons.
- The source potential of the Miocene sediments is good in the Kantang Formation with TOC 2.35%.

- The organic matter within the sediments is predominantly gas-prone, representing Type III kerogen.

W9-A-1 well (Figure 4.39-4.42)

- Miocene and Oligocene sediments of W9-A-1 well at the depth range from 1,032 m to 2,800 m were analyzed to determine their hydrocarbon source potential, thermal maturity and the occurrence of migrated hydrocarbons.

- The source potential of the Oligocene sediments is poor in the Yala Formation with TOC 0.16%. The TOC of Miocene sediment in the Kantang Formation is 0.55%.

- The organic matter within the sediments is composed of mixed Type II/III kerogen that would generate gas

W9-B-1 well (Figure 4.43-4.46)

- Miocene and Oligocene sediments of W9-B-1 well at the depth range from 1,130 m to 3,214 m were analyzed to determine their hydrocarbon source potential, thermal maturity and the occurrence of migrated hydrocarbons.

- The source potential of the Oligocene sediments is poor to fair in the Yala Formation with TOC 1.25%. The TOC content of Miocene sediment in the Kantang Formation is 1.61%.

- The kerogen is predominantly of woody and coaly material. Organic matter within the sediments is predominantly gas-prone, representing Type III or mixed II/III kerogen.

W9-C-1 well (Figure 4.47-4.50)

- Miocene and Oligocene sediments of W9-C-1 well at the depth range from 1,254 m to 3,200 m were analyzed to determine their hydrocarbon source potential, thermal maturity and the occurrence of migrated hydrocarbons.
- The source potential of the Oligocene sediments is poor to fair in the Yala Formation with TOC 0.82%. The TOC content of Miocene sediment in the Trang Formation is 1.80%.
- The kerogen is predominantly of woody and coaly material. Organic matter within the sediments is predominantly gas-prone (Type III).

W9-E-1 well (Figure 4.51-4.54)

- Miocene and Oligocene sediments of W9-E-1 well at the depth range from 1,618 m to 4,552 m were analyzed to determine their hydrocarbon source potential, thermal maturity and the occurrence of migrated hydrocarbons.
- The source potential of the Oligocene sediments is poor to fair in the Yala Formation with TOC 0.40%. The TOC content of Miocene sediment in the Kantang Formation is 0.74%.
- The kerogen is predominantly of woody and coaly material. Organic matter within the sediments is predominantly gas-prone (Type III).

Western Mergui**Mergui-1 well** (Figure 4.55-4.58)

- Miocene and Oligocene sediments of Mergui-1 well at the depth range from 939 m to 3,950 m were analyzed to determine their hydrocarbon source potential, thermal maturity and the occurrence of migrated hydrocarbons.

- The source potential of the Oligocene sediments is poor to fair in the Yala Formation with TOC 0.48%. The TOC content of Miocene sediment in the Kantang Formation is 0.91%.

- The kerogen is predominantly of woody and coaly material. Organic matter within the sediments is predominantly gas-prone, representing Type III or mixed II/III kerogen.

Phangha-1 well (Figure 4.59-4.62)

- Miocene and Oligocene sediments of Phangha-1 well at the depth range from 642 m to 1,845 m were analyzed to determine their hydrocarbon source potential, thermal maturity and the occurrence of migrated hydrocarbons.

- The source potential of the Miocene sediment is the Tai Formation with TOC 0.58%. Clastic sediment overlying the carbonate reefs were deposited in environments. The reef was deposited in an inner neritic environment.

- The kerogen is predominantly gas-prone.

Trang-1 well (Figure 4.63-4.66)

- Miocene and Oligocene sediments of Trang-1 well at the depth range from 939 m to 3,950 m were analyzed to determine their hydrocarbon source potential, thermal maturity and the occurrence of migrated hydrocarbons.

- The source potential was not found in this well.

W9-D-1 well (Figure 4.67-4.70)

- Miocene and Oligocene sediments of W9-D-1 well at the depth range from 1,029 m to 2,354 m were analyzed to determine their hydrocarbon source potential, thermal maturity and the occurrence of migrated hydrocarbons.

- The source potential of the Oligocene sediments is poor in the Yala Formation with TOC 0.23%.
- The kerogen is predominantly of woody and coaly material. Organic matter within the sediments is predominantly gas-prone (Type III).

4.1.6 Hydrocarbon expulsion

In this study hydrocarbon expulsion studies were conducted in the Mergui basin as in sub-area separately. Results of the study can be listed as follows.

Northern Mergui

The simulation was based on Payang-1 well data. The maximum thickness of sediments is reached at 1,800 m. There are no hydrocarbon shown and no core sample at 1,800 m depth based on the well completion and geochemical re-evaluation report.

Eastern Mergui

The simulation was based on Kantang-1, Kathu-1, Kraburi-1, Ranot-1, Sikao-1, Thalang- 1, Yala-1, W9-A-1, W9-B-1, W9-C-1, and W9-E-1 wells data. The sedimentary thickness reaches 4,552 m in the deepest fictitious well W9-E-1 based on well completion and geochemical re-evaluation report. Almost hydrocarbons were observed in the Ranong Formation. Hydrocarbons were showed in the cuttings and on the gas detector. Absence of the vertical gas migration, headspace gas in the shallow depth, immature sediments are derived from bacterial utilization of sedimentary organic matter. The hydrocarbon product in this formation is a dry gas (dominate with Methane). Increasing of burial depth and maturity, the headspace gas becomes increasingly wet gas due to the generation of ethane and heavier hydrocarbons from kerogen.

The oil window appeared in the Early Miocene (16.4 Ma) and the gas zone in the Late Miocene (5.3 Ma). Expulsion of hydrocarbon from the Ranong and Yala Formations started in Middle Miocene (11.2 Ma).

Western Mergui

The simulation was based on Mergui-1, Phanga-1, Trang-1, and W9-D-1 wells data. Fictitious wells represent the deepest part of the basin based on well completion and geochemical re-evaluation report. The fluorescence was observed and range from light yellow to dull pale golden yellow. The oil showed was low gravity and minor gas peak. Almost hydrocarbon was observed in the Ranong sandstone. Only W9-D-1 well has log analysis indicates all potential reservoirs to be water wet.

Maturation of the organic matter of the Ranong and Yala Formations was began during the Early Miocene (16.4 Ma) for oil and for gas (3.6 Ma) in the Pliocene.

4.1.7 TOC distribution map

In order to study the potential source rock distribution, observed and collected TOC from selected wells were compiled and mapped as TOC distribution map in the Yala, Kantang, and Trang Formation. Results of mapping are illustrated in Figure 4.71 to 4.73. Moreover, geothermal gradient map of the Mergui basin was also created (Figure 4.74) in order to study the relationship between temperature and amount of TOC. Consequently, it was notified that geothermal was direct proportion to the amount of TOC.

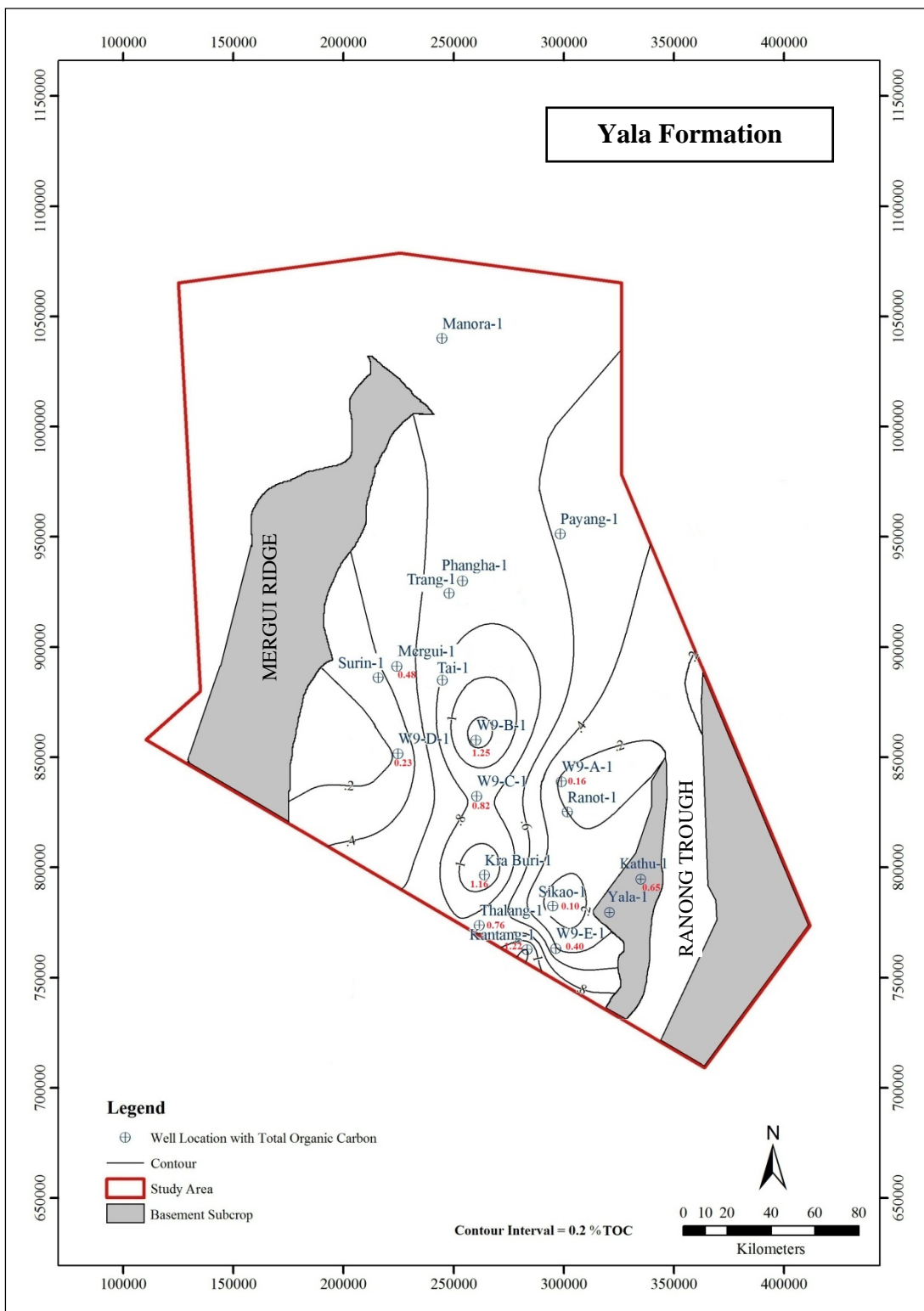


Figure 4.71 TOC distribution map of the Yala Formation

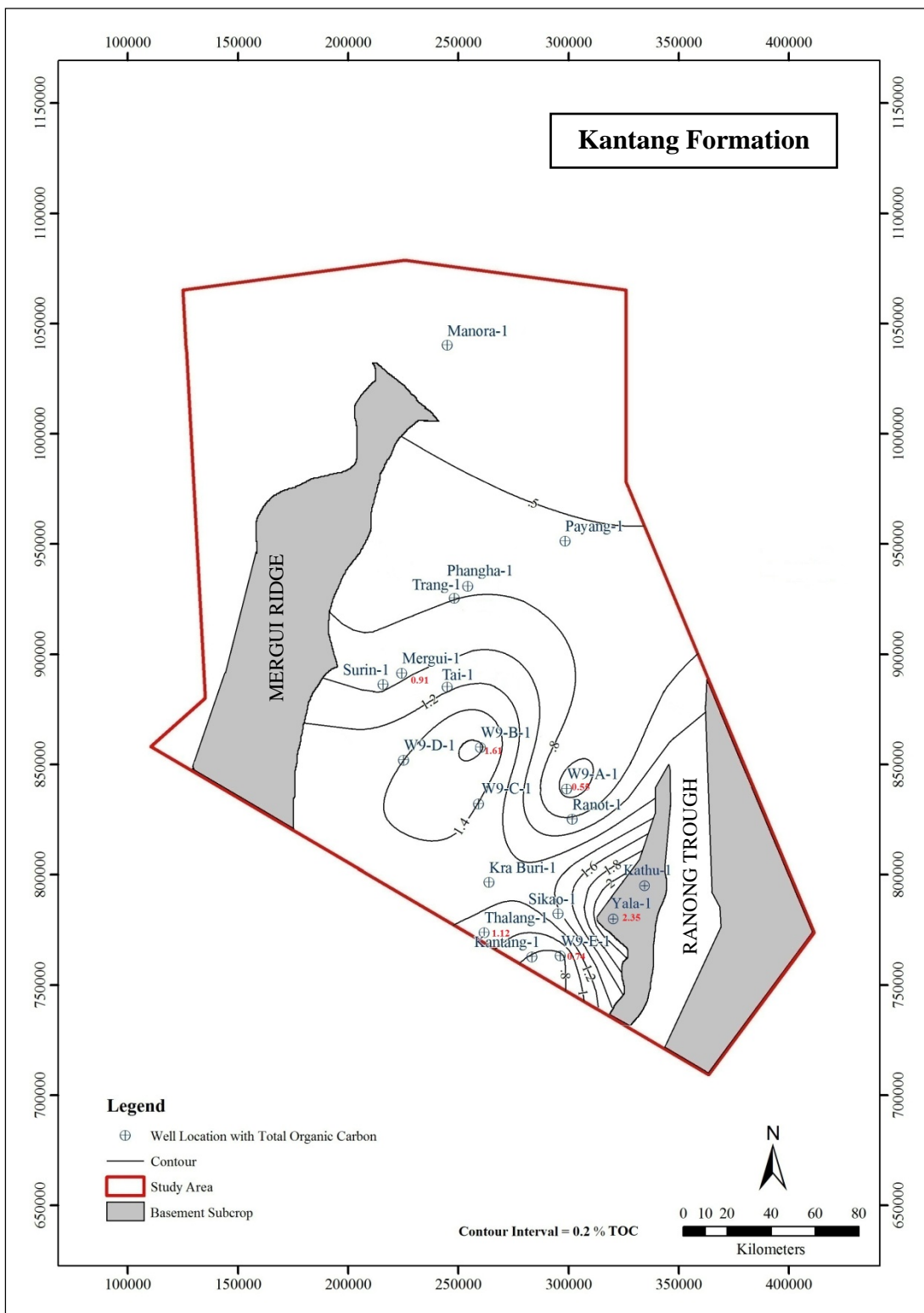


Figure 4.72 TOC distribution map of the Kantang Formation

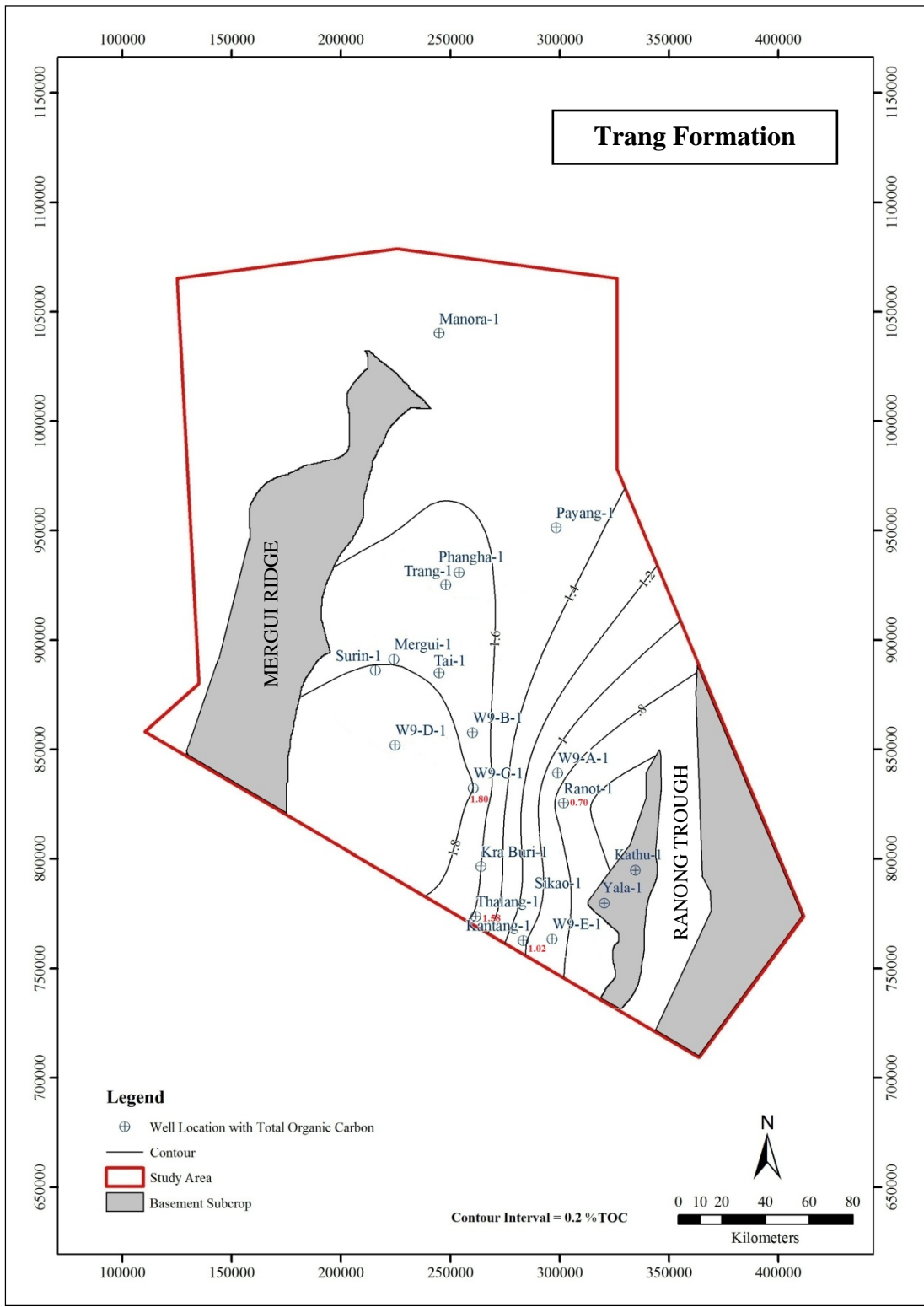


Figure 4.73 TOC distribution map of the Trang Formation

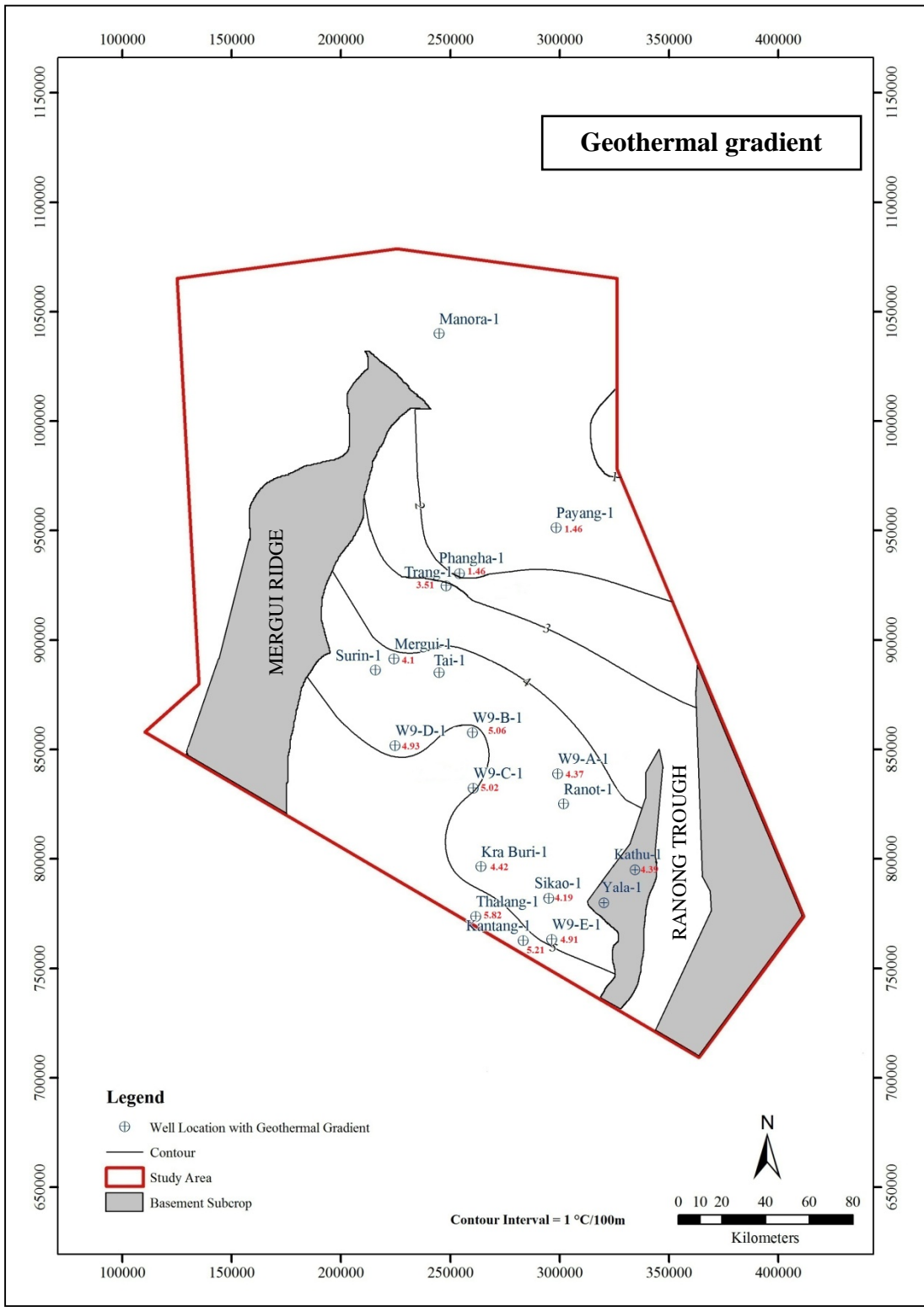


Figure 4.74 Geothermal gradient distribution map of the Mergui basin

4.2 Petroleum migration pathway

In order to study the potential petroleum migration pathway of the Mergui basin porosity, permeability distribution and their relationship with depth were mapped, plotted, and analyzed as follows.

4.2.1 Porosity

- **Porosity maps**

Based on log re-evaluation report (5% porosity cut off), the three porosity maps have been generated by Arc View 3.0 software to evaluate the porosity distribution in the study area. The porosity model was used to extrapolate and generated the porosity pattern in the deep water area. The output maps are consisted of Lower Ranong, Middle Ranong and Upper Ranong Sub-Formations. The resulted porosity maps are shown in Figure 4.75-4.77. Some information on porosity data can be summarized as follows.

Lower Ranong Sub-Formation porosity map

The porosity distribution map of the Lower Ranong Sub-Formation was initially generated only in the southern part of the Mergui basin (Figure 4.75), where the sedimentation was initially occurred. It is obvious that the porosity in Lower Ranong Sub-Formation is relatively high in the eastern part of the Mergui basin with the maximum porosity of 19% found in W9-A-1 well. This may imply that the sediment source was mainly from the eastern part of the Mergui basin. Poor sorting sandstone is expected corresponding to the early stage of syn-rift sedimentation model.

Middle Ranong Sub-Formation porosity map

The porosity in Middle Ranong (Figure 4.76) is relatively high in the eastern Mergui basin and conforms to the Lower Ranong Sub-Formation with slightly eastward shift. The maximum porosity is 18% found in Kra Buri-1 and W9-A-1 wells. Relatively low porosity of Middle Ranong Sub-Formation can be explained in term of shaley sand deposited during transgression period (Atop Technology, 2006).

Upper Ranong Sub-Formation porosity map

The porosity map of Upper Ranong can be generated throughout the area (Figure 4.77) corresponding to the sedimentation was deposited widely spread. The higher porosity towards the eastern and northern Mergui basin can be observed with higher porosity is Middle and Lower Ranong Sub-Formation. The maximum porosity of 28% is recorded in Thalang-1 well.



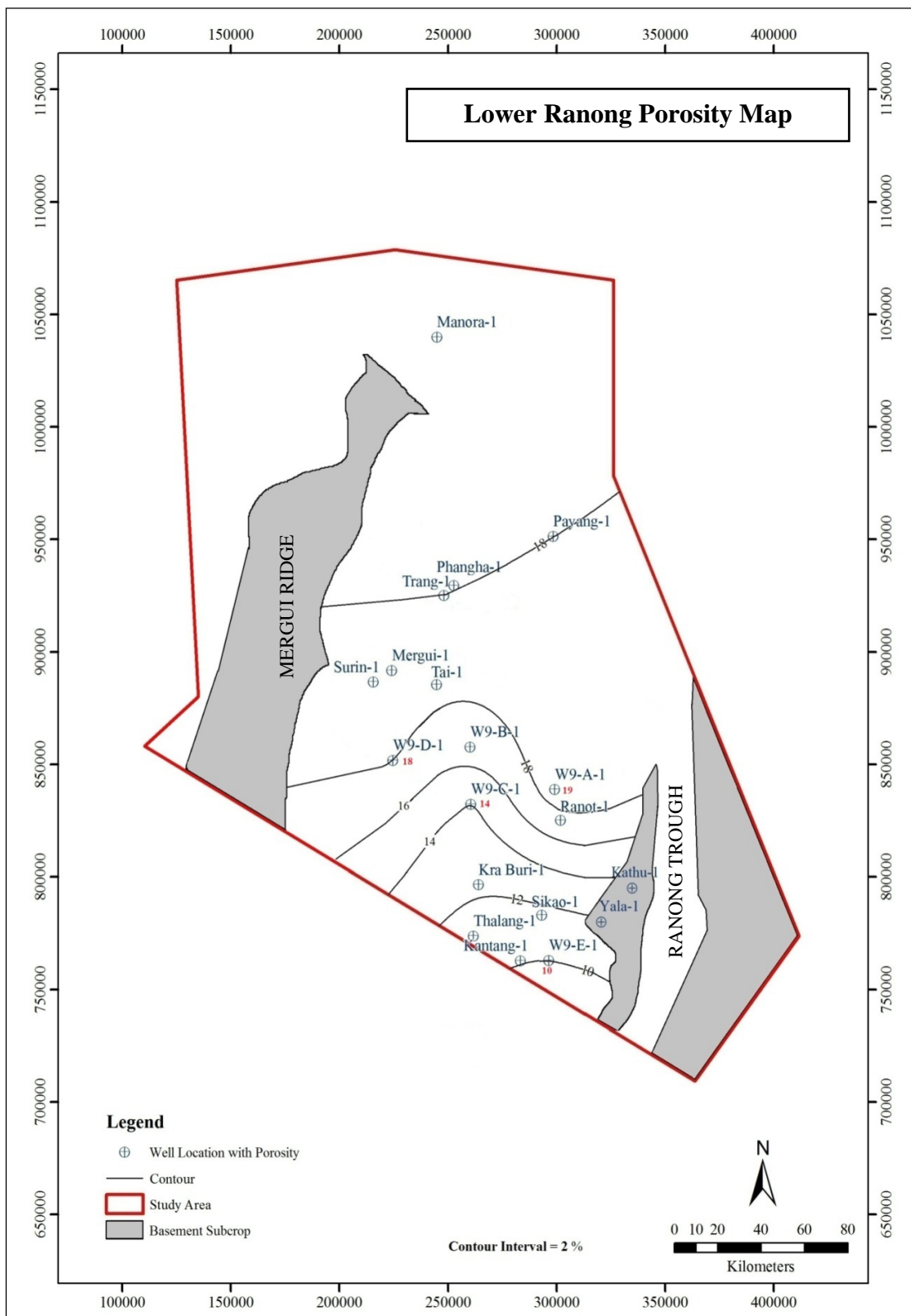


Figure 4.75 Lower Ranong Sub-Formation porosity map

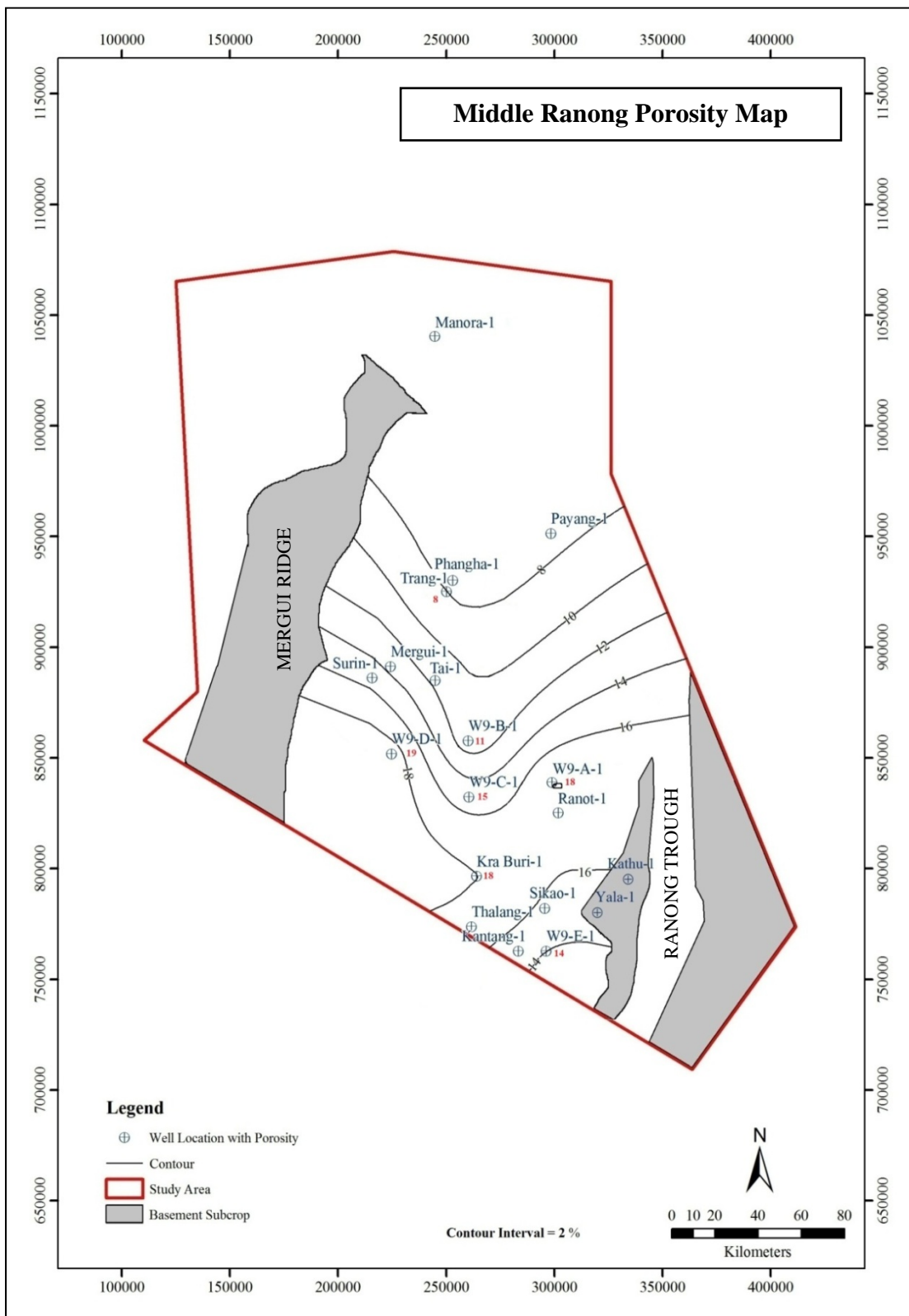


Figure 4.76 Middle Ranong Sub-Formation porosity map

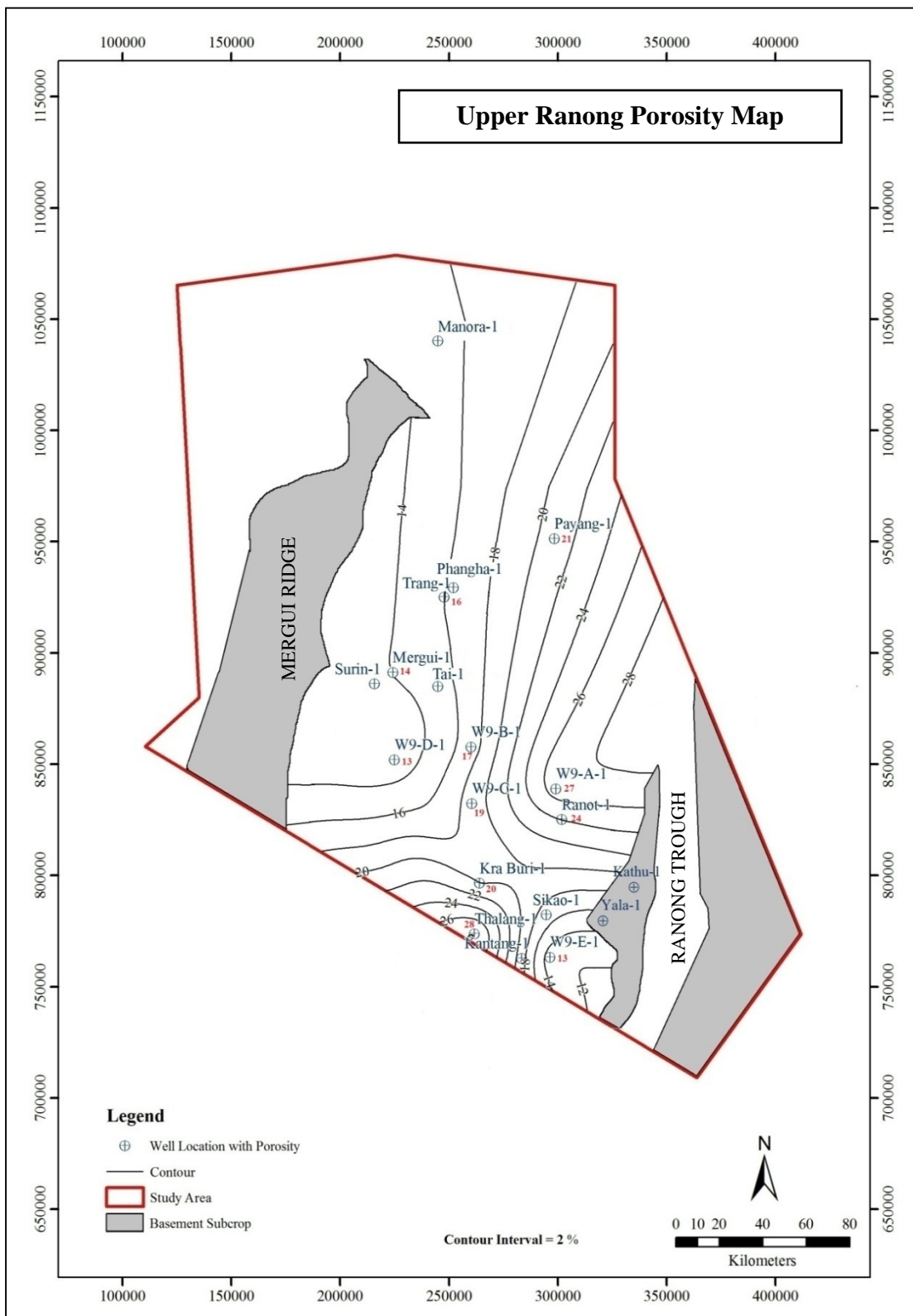


Figure 4.77 Upper Ranong Sub-Formation porosity map

- **Porosity plot versus depth**

Three porosity plots versus depth had been produced in the Ranong three Sub-Formations separately, including Lower Ranong, Middle Ranong and Upper Ranong Sub-Formations. Porosity plot versus depths are showed in Figure 4.78-4.80 and some information can be summarized as follows.

Lower Ranong Sub-Formation porosity plot vs. depth

The syn-rift sediment have poor sorted sandstone corresponding in mixing sediments deposited during the opening of sub basins could be a reason to cause a large variation of porosity. Relationship between depth and porosity of Lower Ranong Sub-Formation is a linear function (Figure 4.78) and can be expressed as following equation;

$$y = -173.1x + 5580 \quad (4.1)$$

Where y = depth (meter),

X = porosity (percent)

Middle Ranong Sub-Formation porosity plot vs. depth

The porosity in this formation is ranged between 8 – 19%. A narrow shape of porosity range implies the grained sorting is higher than lower Ranong Sub-Formation. Noticeable from the trend line, the porosity less than 10% can be expected at below 3,300 m. Relationship between depth and porosity of Middle Ranong Sub-Formation is a linear function (Figure 4.79) and can be expressed as following equation;

$$y = -119.5x + 4342 \quad (4.2)$$

Where y = depth (meter),

x = porosity (percent)

Upper Ranong Sub-Formation porosity plot vs. depth

The porosity in this formation is quite high with a wide range between 13 – 28%. The porosity trend in this formation is dramatically decreased with depth and good fit to a number of porosity from many well data. A wide range of porosity implies that the grain had been well sorted compared to Middle Ranong Sub-Formation. Relationship between depth and porosity of Upper Ranong Sub-Formation is a linear function (Figure 4.80) and can be expressed as following equation;

$$y = -50.80x + 3161 \quad (4.3)$$

Where y = depth (meter),

x = porosity (percent)



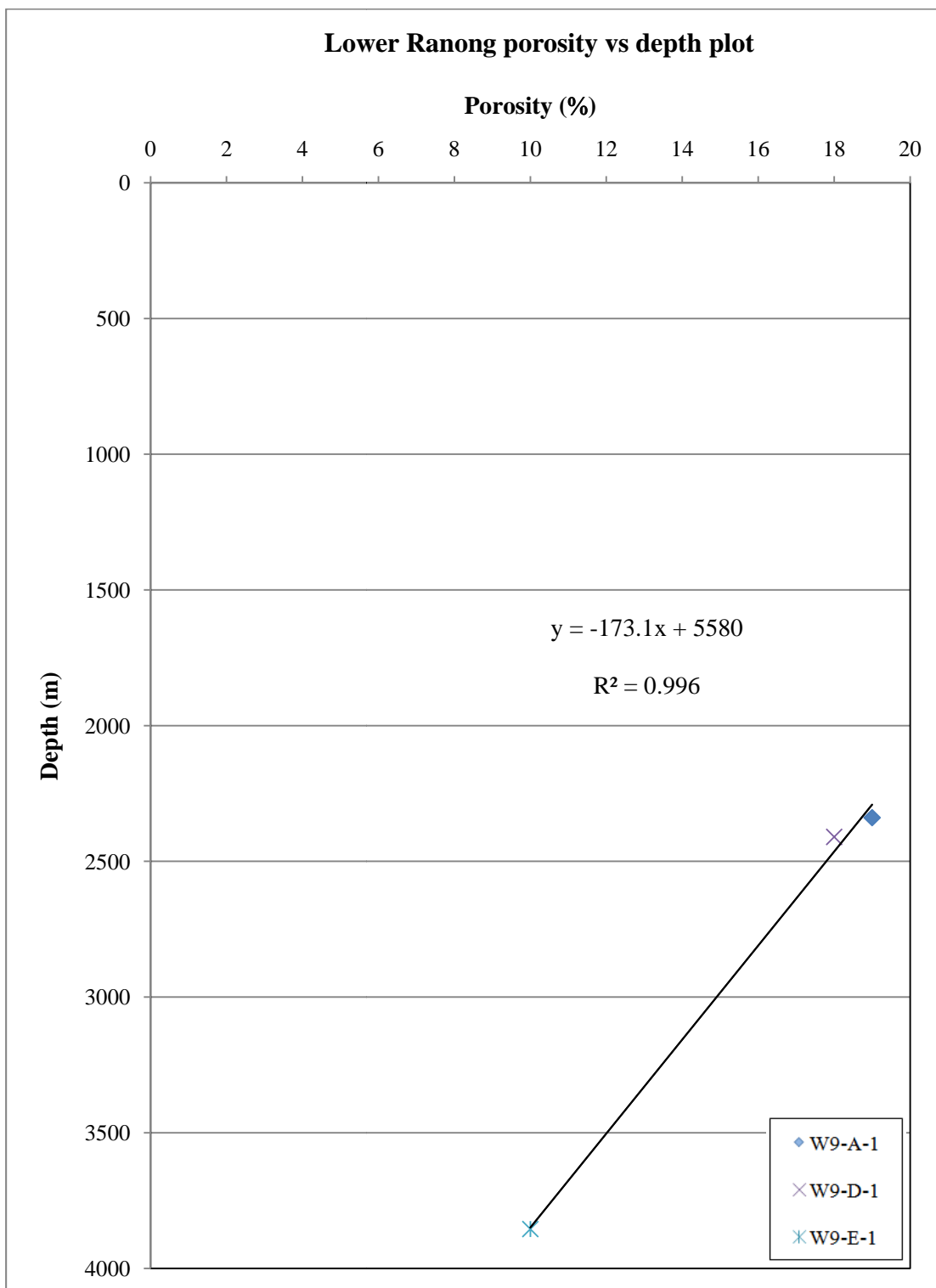


Figure 4.78 Lower Ranong porosity vs. depth plot

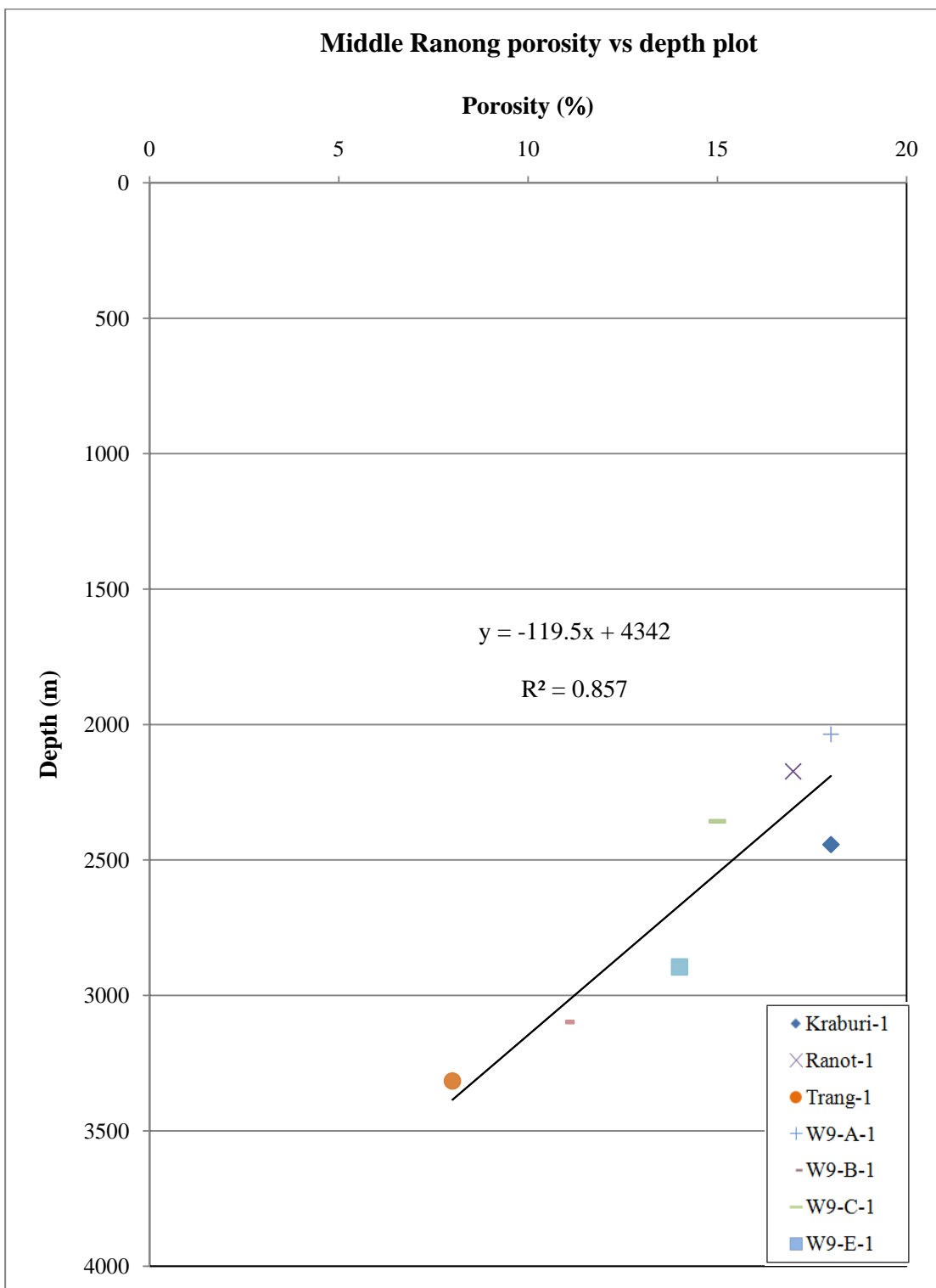


Figure 4.79 Middle Ranong porosity vs. depth plot

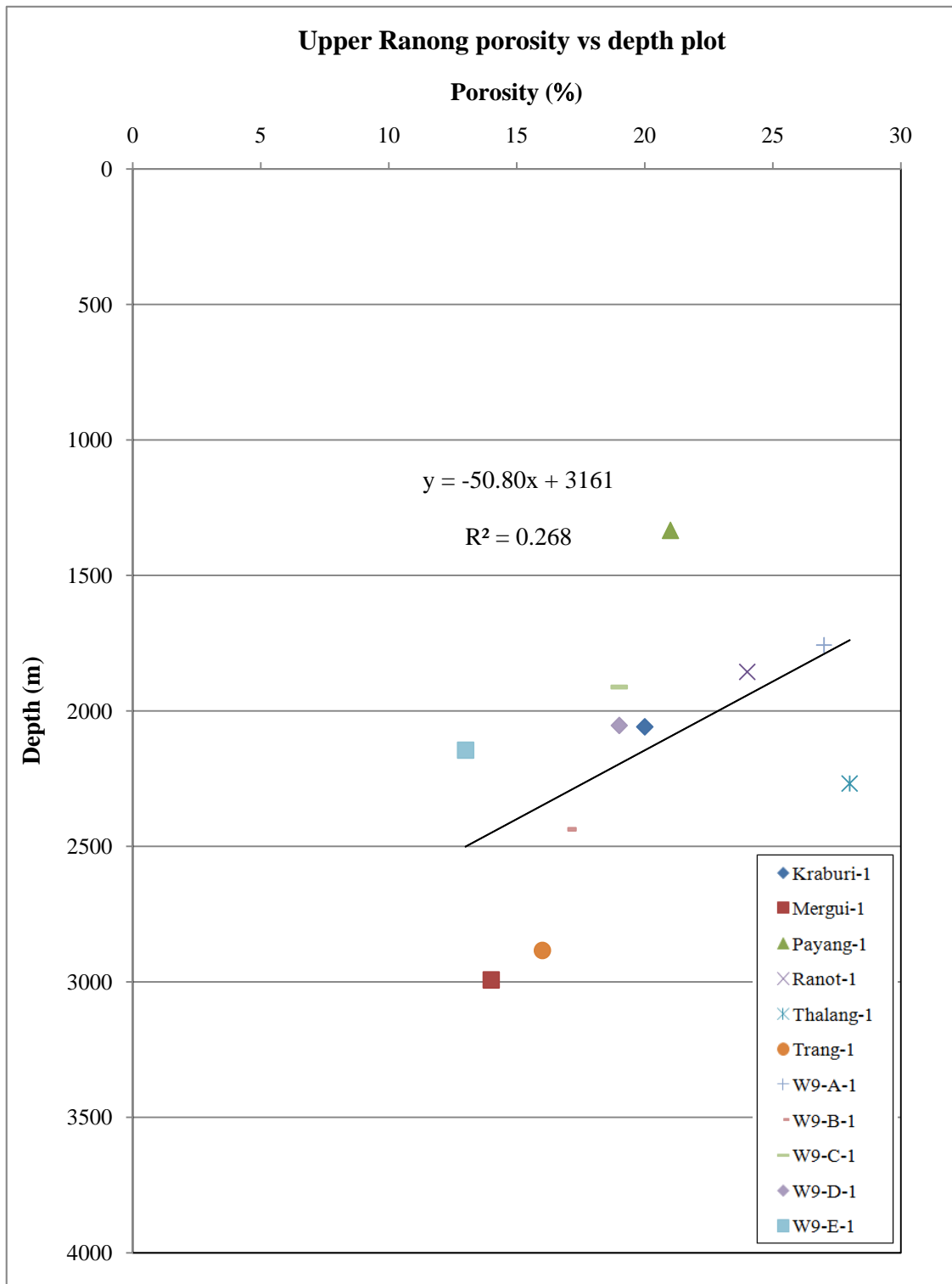


Figure 4.80 Upper Ranong porosity vs. depth plot

4.2.2 Permeability

Based on permeability and porosity data collected from selected wells, the relationship between porosity and permeability of the Ranong formation had been plotted on semi-log graph as showed in Figure 4.81. Results from porosity and permeability relationship analysis indicated that the relationship between porosity and permeability of the Ranong Formation is an exponential function. The corresponding exponential function can be expressed as the following equation;

$$y = 0.0001e^{0.576x} \quad (4.4)$$

Where y = permeability (md),

x = porosity (percent)

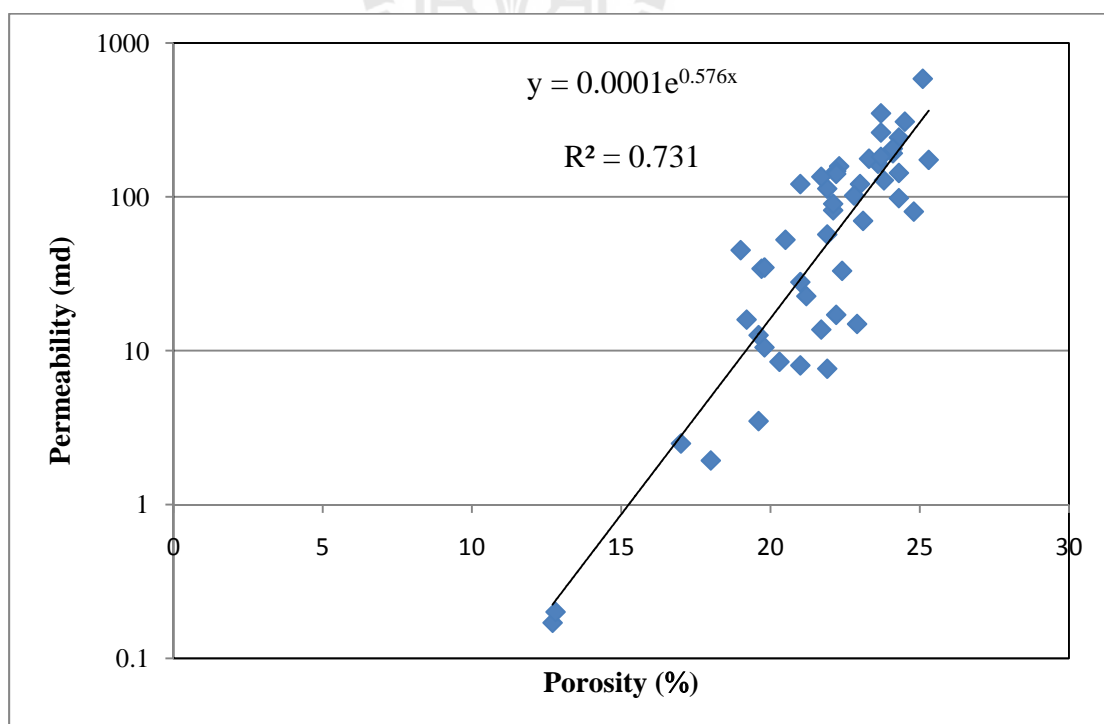


Figure 4.81 Relationship between porosity and permeability plot

- **Permeability map**

In order to study the distribution of permeability of each the Ranong Sub-Formations, permeability data of each the Ranong Sub-Formation was mapped separately as showed in Figure 4.82-4.84 respectively. Some information can be summarized as follows.

Lower Ranong Sub-Formation permeability map

The permeability in Lower Ranong Sub-Formation is relatively high in the eastern part of the Mergui basin (Figure 4.82) with the maximum permeability of 5.7 md found in W9-A-1 well. This may imply that the sediment source was mainly from the eastern part of the Mergui basin. Poor sorting sandstone is expected corresponding to the early stage of syn-rift sedimentation.

Middle Ranong Sub-Formation permeability map

The permeability in Middle Ranong is relatively high in the eastern Mergui basin (Figure 4.83) conforms to the Lower Ranong Sub-Formation with slightly eastward shift. The maximum permeability is 3.2 md found in Kra Buri-1 and W9-A-1 wells.

Upper Ranong Sub-Formation permeability map

The permeability map of Upper Ranong can be generated throughout the area corresponding to the sedimentation was deposited widely spread (Figure 4.84). The higher permeability towards the eastern and northern Mergui basin can be observed and average permeability is higher than Middle and Lower Ranong Sub-Formation. The maximum permeability of 1,010 md is recorded in Thalang-1 well.

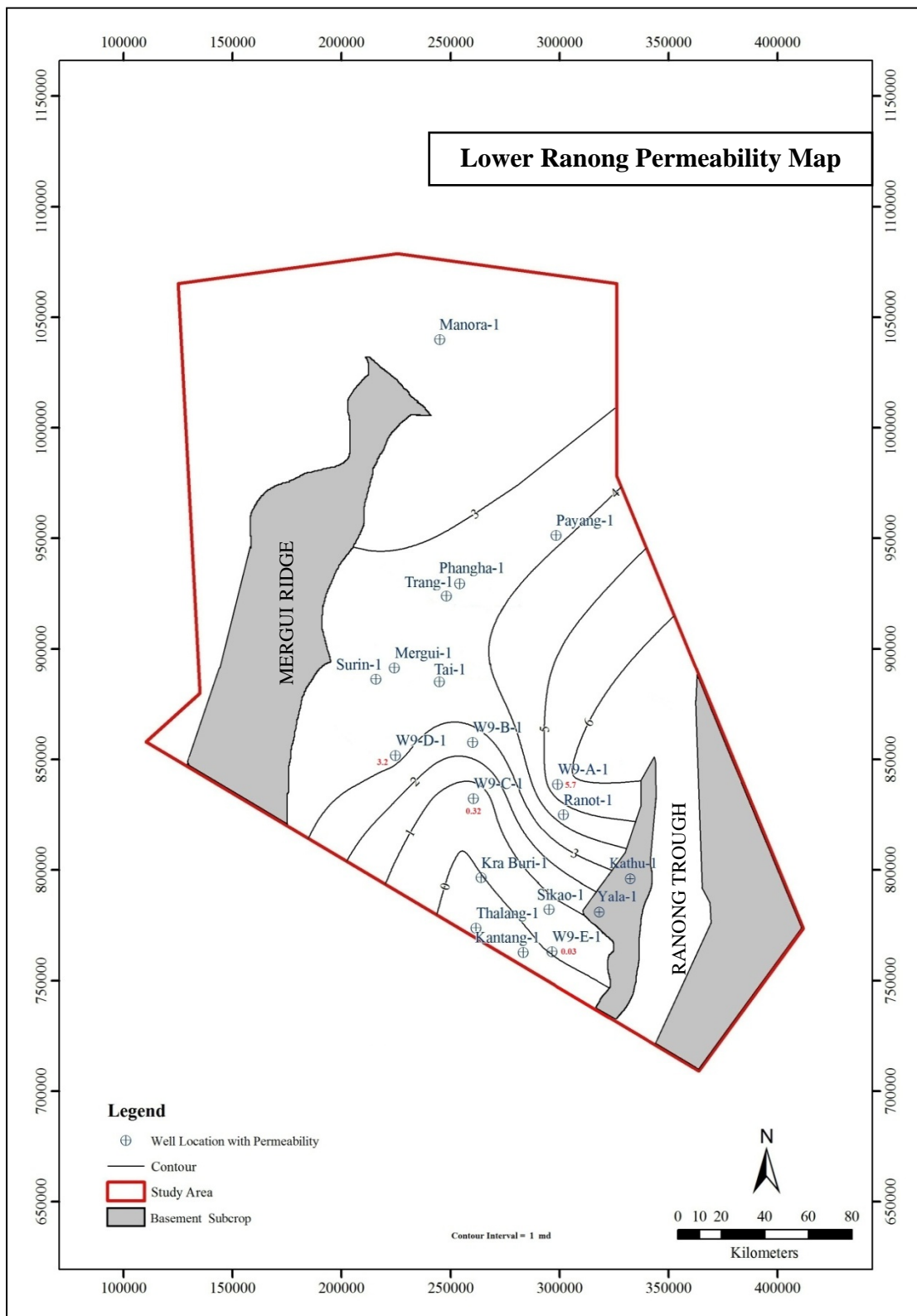


Figure 4.82 Lower Ranong Sub-Formation permeability map

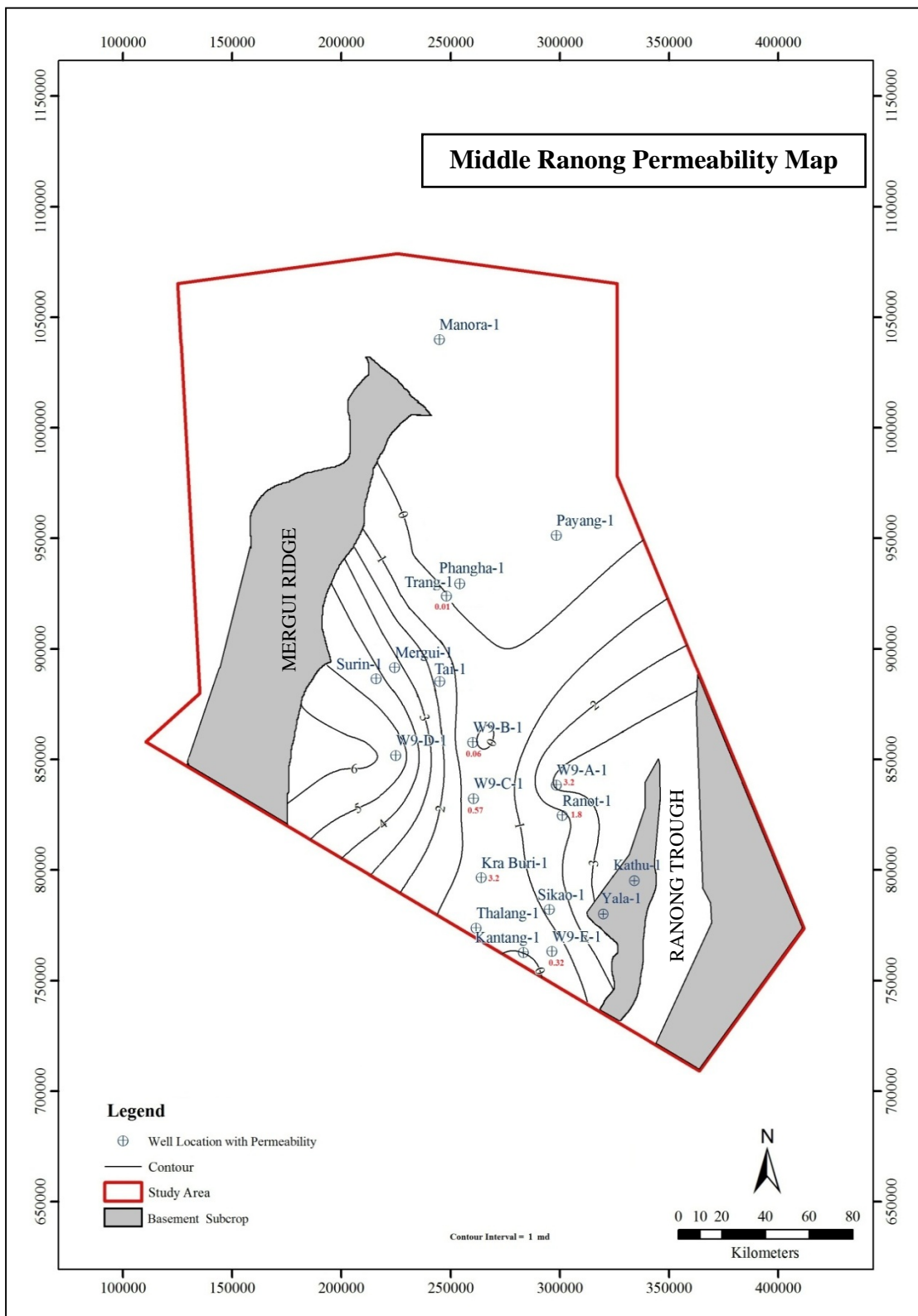


Figure 4.83 Middle Ranong Sub-Formation permeability map

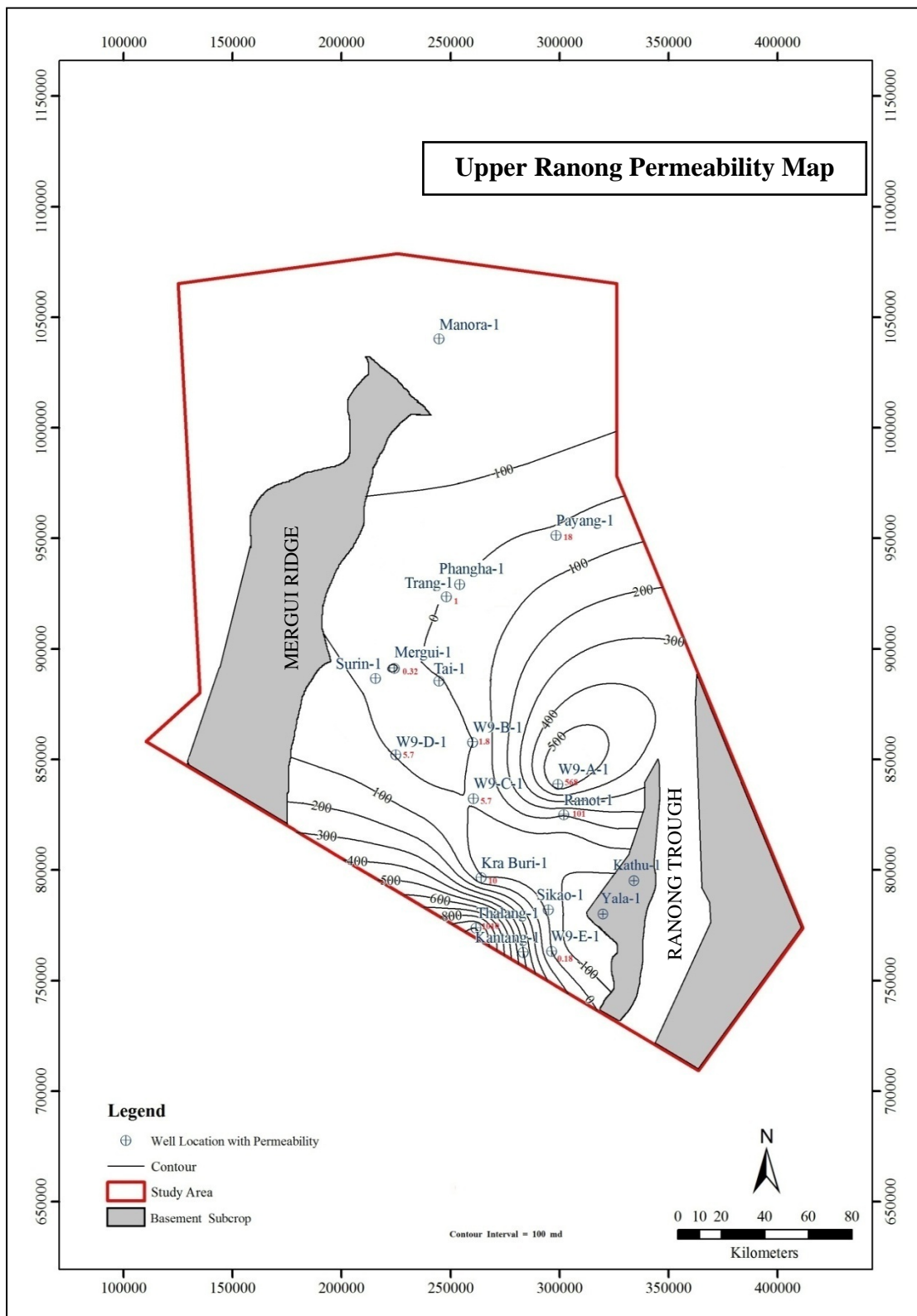


Figure 4.84 Lower Ranong Sub-Formation permeability map

- **Permeability plot versus porosity**

Permeability and porosity depend on pores in the rock. There are two discerned typologies of pores in rocks: closed and open pores. Closed pores are completely isolated from the external surface, not allowing the access of external fluids in either the liquid or gaseous phase. Closed pores influence parameters such as density and mechanical and thermal properties. Open pores are connected to the external surface and are therefore accessible to fluids, depending on the pore characteristics/size and the nature of fluid. Open pores can be further divided into dead-end or interconnected pores. The percentage of interconnected pores within the rock is known as effective porosity. Effective porosity excludes isolated pores and pore volume occupied by water adsorbed on clay minerals or other grains. In this study three permeability plots versus porosity had been produced in the Ranong Sub-Formations and separated into sub-basins in order to study their relationship. Results from porosity and permeability relationship of each the Ranong Formation analysis plotted on semi-log graph are showed in Figure 4.85- 4.87 it was found that the relationship between porosity and permeability of the Ranong Formation is an exponential function some details can be given as follows.

**Lower Ranong Sub-Formation permeability plots
vs. porosity**

Result from plotting indicates that relationship between permeability and porosity of the Lower Ranong Sub-Formation is an exponential function (Figure 4.85) which can be expressed as a following equation.

$$y = 0.0001e^{0.576x} \quad (4.5)$$

Where y = permeability (md),

x = porosity (percent)

Middle Ranong Sub-Formation permeability plots vs. porosity

Like the Lower Ranong Sub-Formation, the relationship between permeability and porosity of the Middle Ranong Sub-Formation is also an exponential function (Figure 4.86) and can be expressed as an equation below.

$$y = 0.0001e^{0.574x} \quad (4.6)$$

Where y = permeability (md),

x = porosity (percent)

Upper Ranong Sub-Formation permeability plots vs. porosity

Relationship between permeability and porosity of the Upper Ranong Sub-Formation is also an exponential function (Figure 4.87) as its lower sub-formations and can be expressed as an exponential equation.

$$y = 0.0001e^{0.575x} \quad (4.7)$$

where y = permeability (md),

x = porosity (percent)

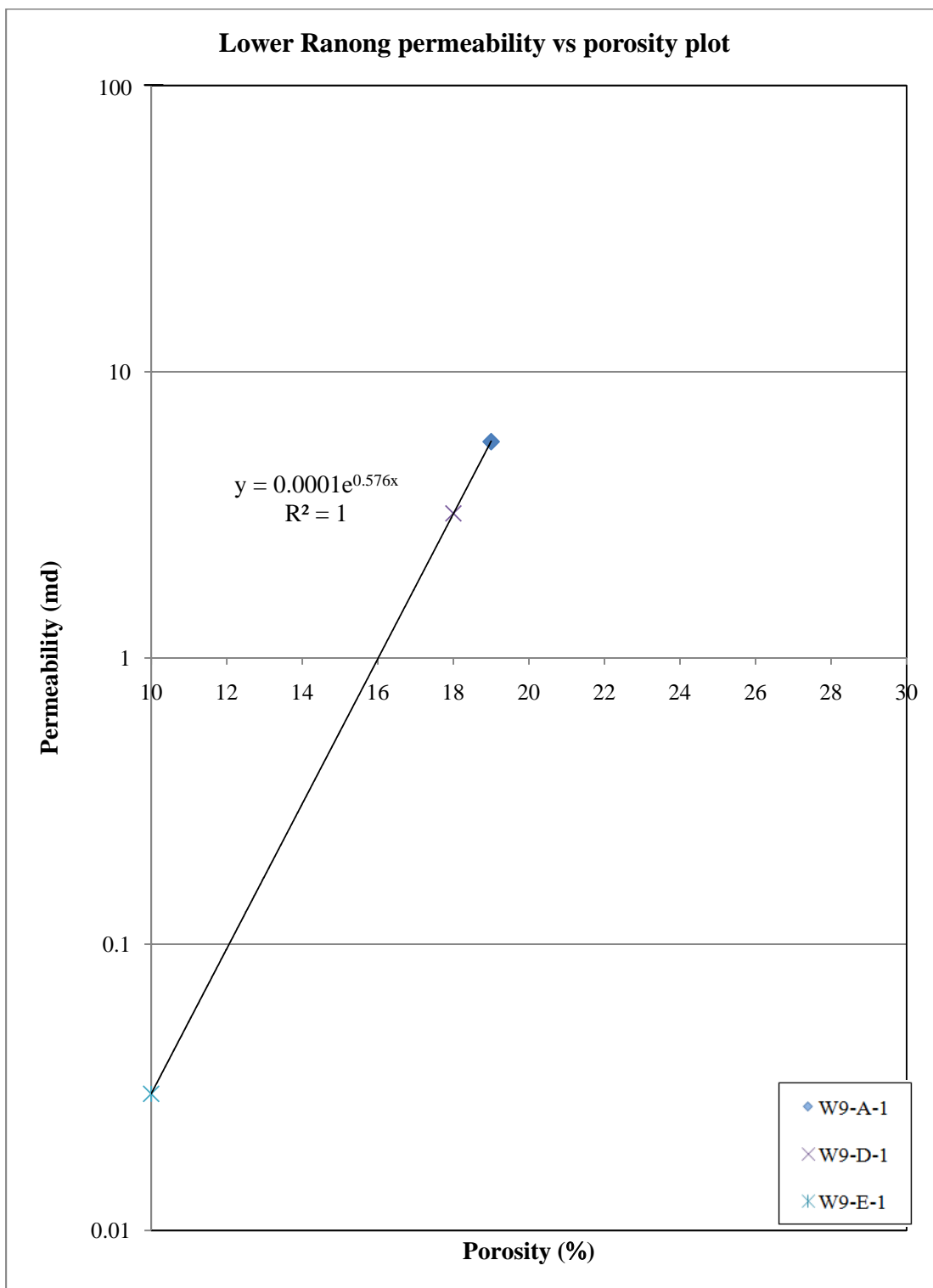


Figure 4.85 Lower Ranong Sub-Formation permeability vs. porosity plot

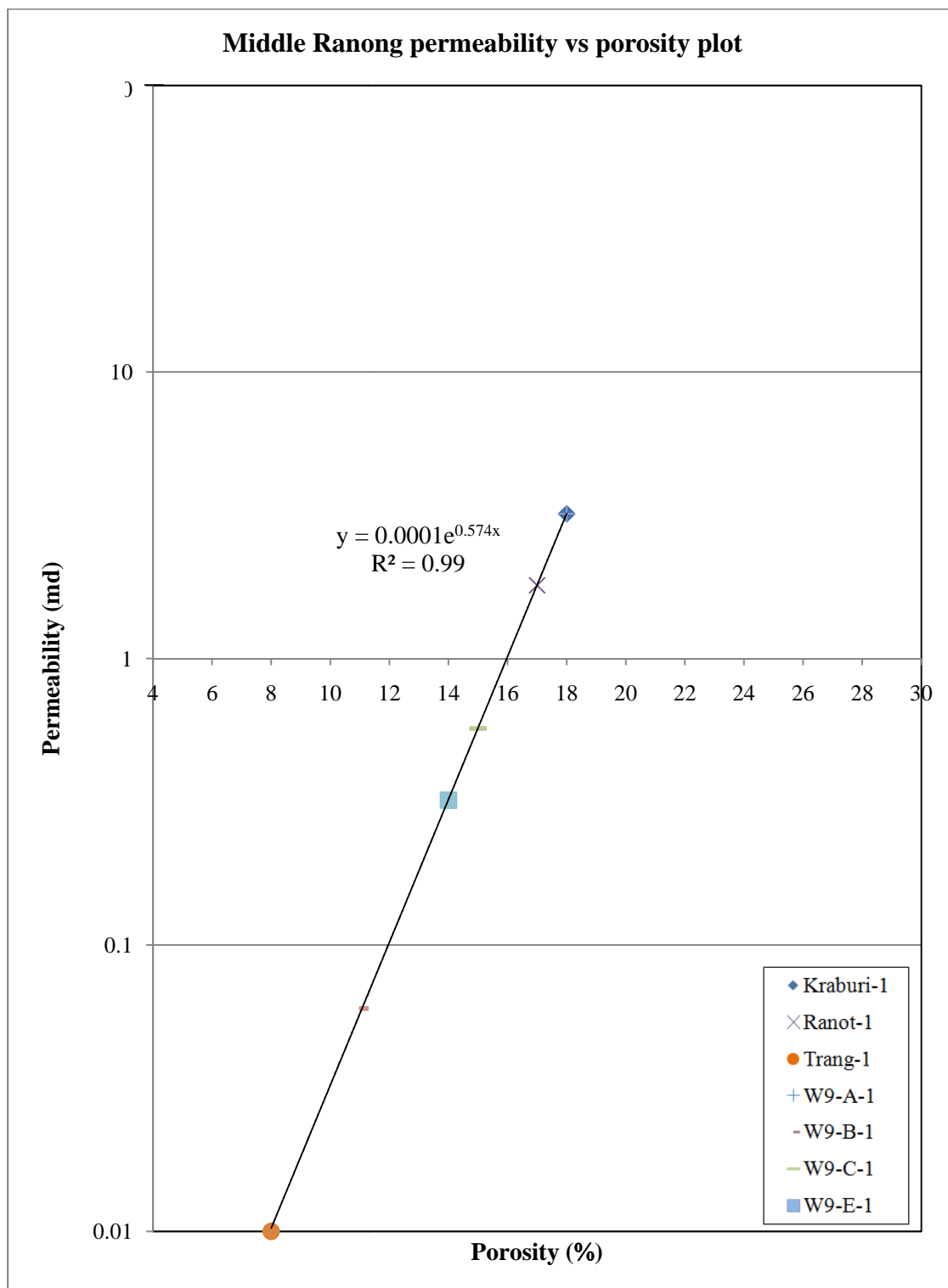


Figure 4.86 Middle Ranong Sub-Formation permeability vs. porosity plot

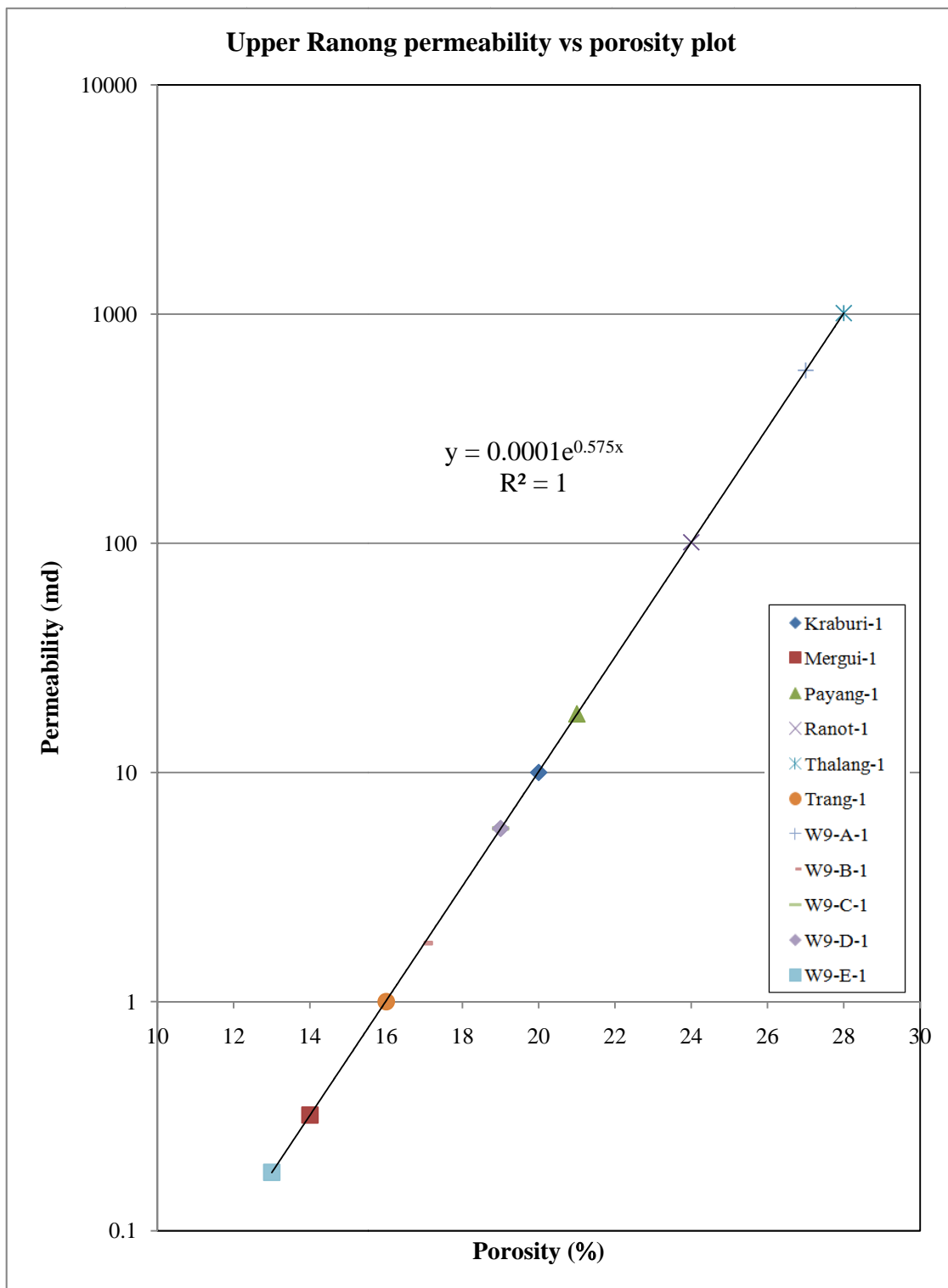


Figure 4.87 Upper Ranong Sub-Formation permeability vs. porosity plot

Petroleum migration pathway

Petroleum migration results from a buoyancy force which is the main driving force. The buoyancy force is the principle of density difference, low density material can move over high density material, so oil and gas drive over the water formation. Obstacle to migration is a capillary force, if the rock has smaller pore, oil or gas migrates hardly or trap under this rock. Fault can act to support or obstruct oil and gas migration. The appropriate area for drilling should be considered from local structure, stratigraphy and distribution of the reservoir rocks.

In order to study the potential petroleum migration pathway, structural time contour map of the Ranong horizon, structural time contour map showing Lower, Middle, and Upper Ranong Sub-Formations were mapped and illustrated in Figure 4.88 through Figure 4.91 respectively. As a result the possible migration pathway and suggested drilling area can be determined from overlaying main structures (Mergui Fault Zone, Ranong Fault Zone, Khlong Marui Fault Zone and east Andaman Fault Zone) with porosity maps (Figure 4.75-4.77), permeability maps (Figure 4.82-4.84), and structure geology maps (Figure 4.88-4.91) as illustrated in Figure 4.92. Result of overlying indicated that the potential petroleum migration pathway of the Mergui basin were mainly toward central high structure located in the central part of the Mergui basin.

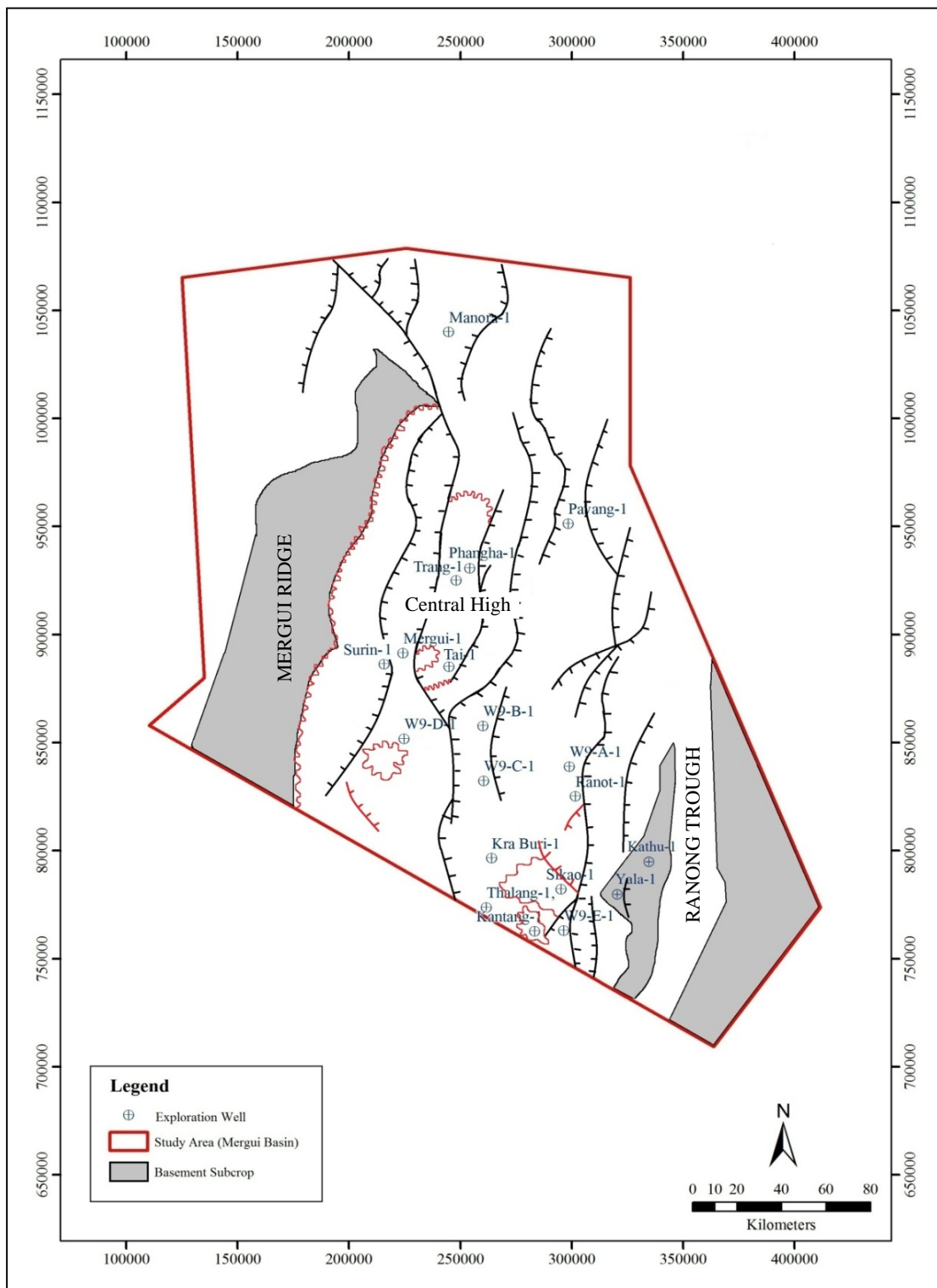


Figure 4.88 Structural map of the Ranong Formation of the Mergui basin

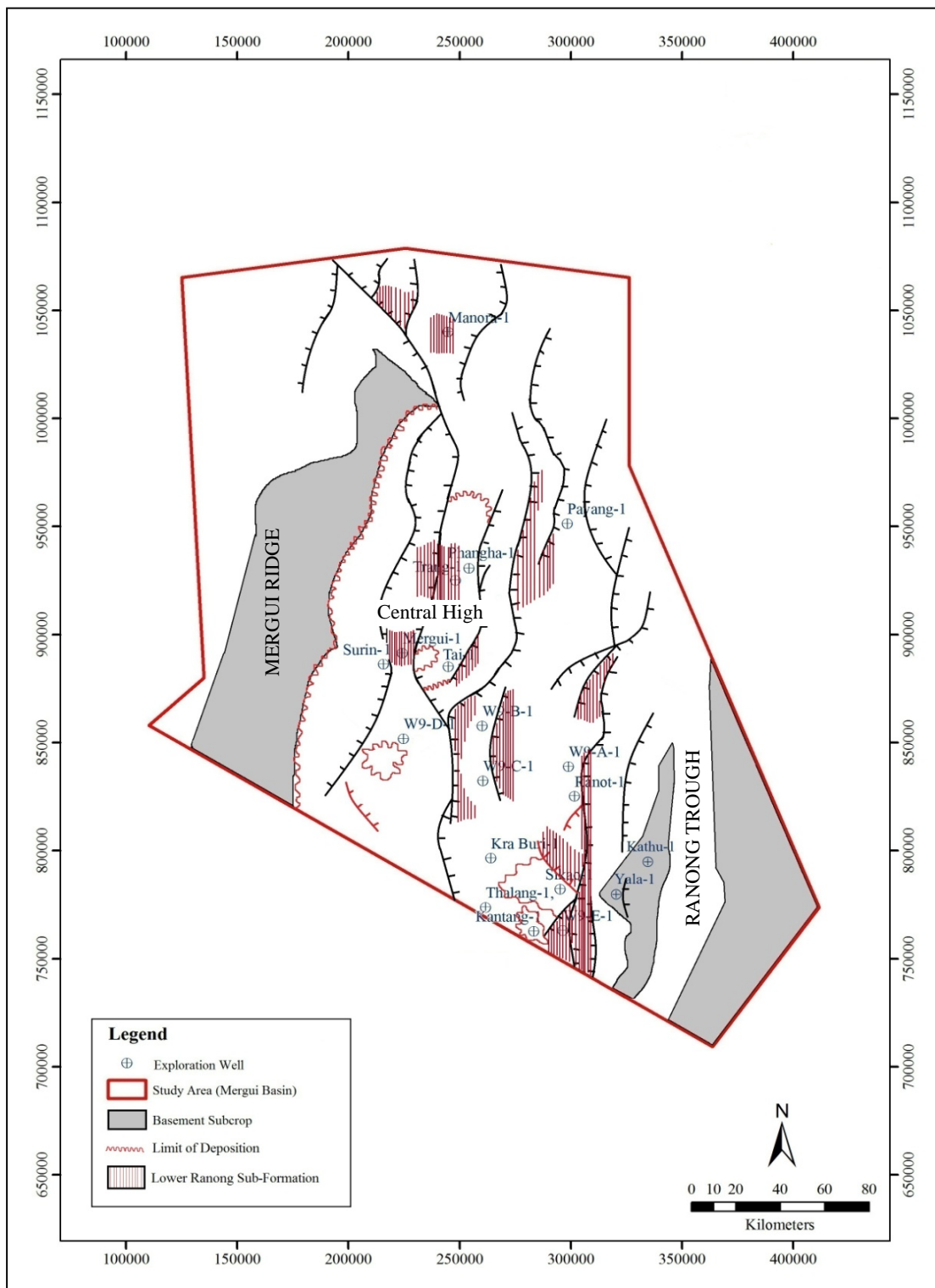


Figure 4.89 Structural map of the Ranong Formation showing Lower Ranong Sub-Formation

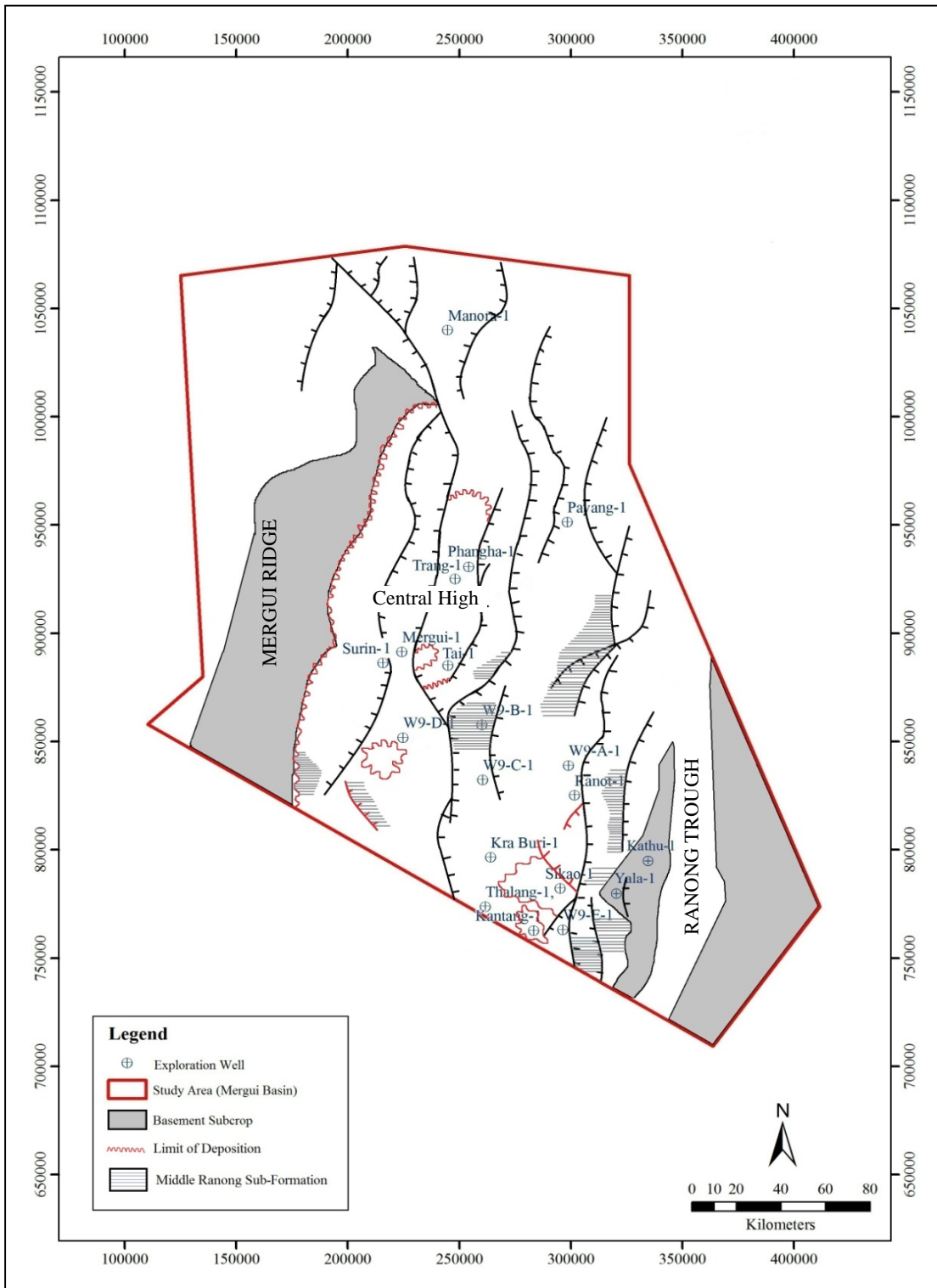


Figure 4.90 Structural map of the Ranong Formation showing Middle Ranong Sub-Formation

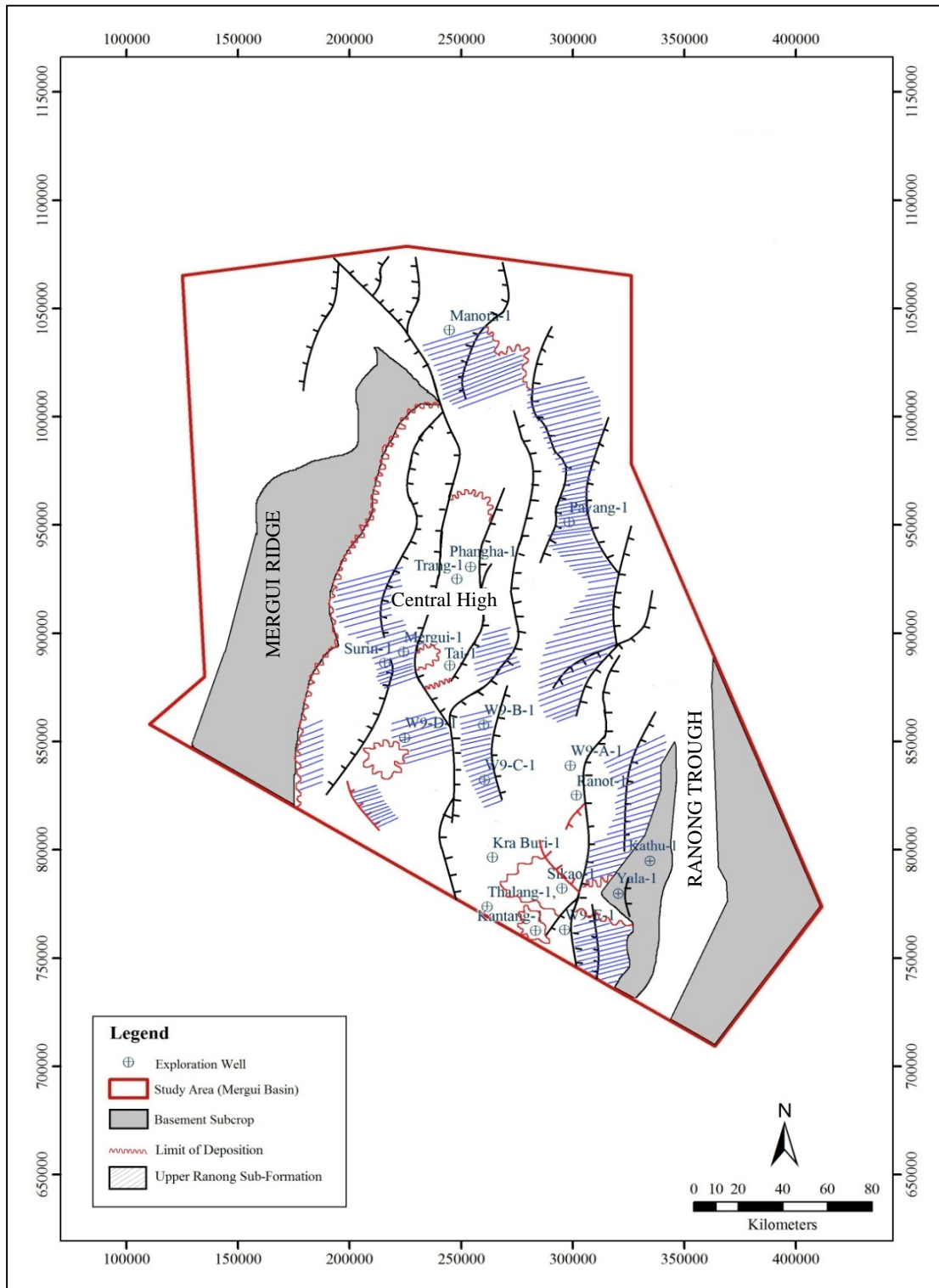


Figure 4.91 Structural map of Ranong Formation showing Upper Ranong Sub-Formation

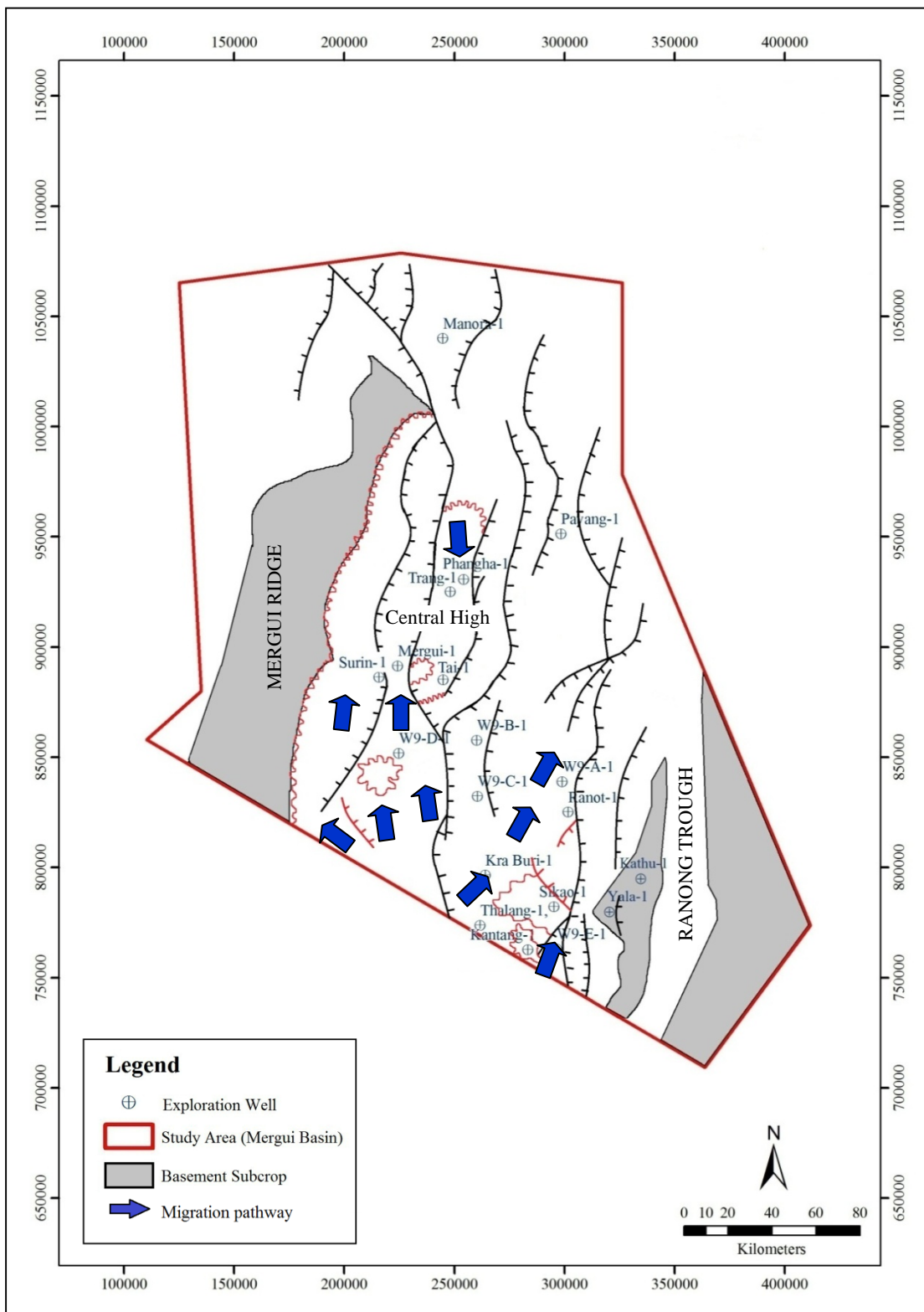


Figure 4.92 Migration pathway in the Mergui basin

CHAPTER V

CONCLUSIONS AND RECOMMENDATIONS

5.1 Conclusions

5.1.1 Petroleum system of the Mergui basin

Based on literature review and results from this study, petroleum system of the Mergui basin can be summarized as illustrated in Figure 5.1.

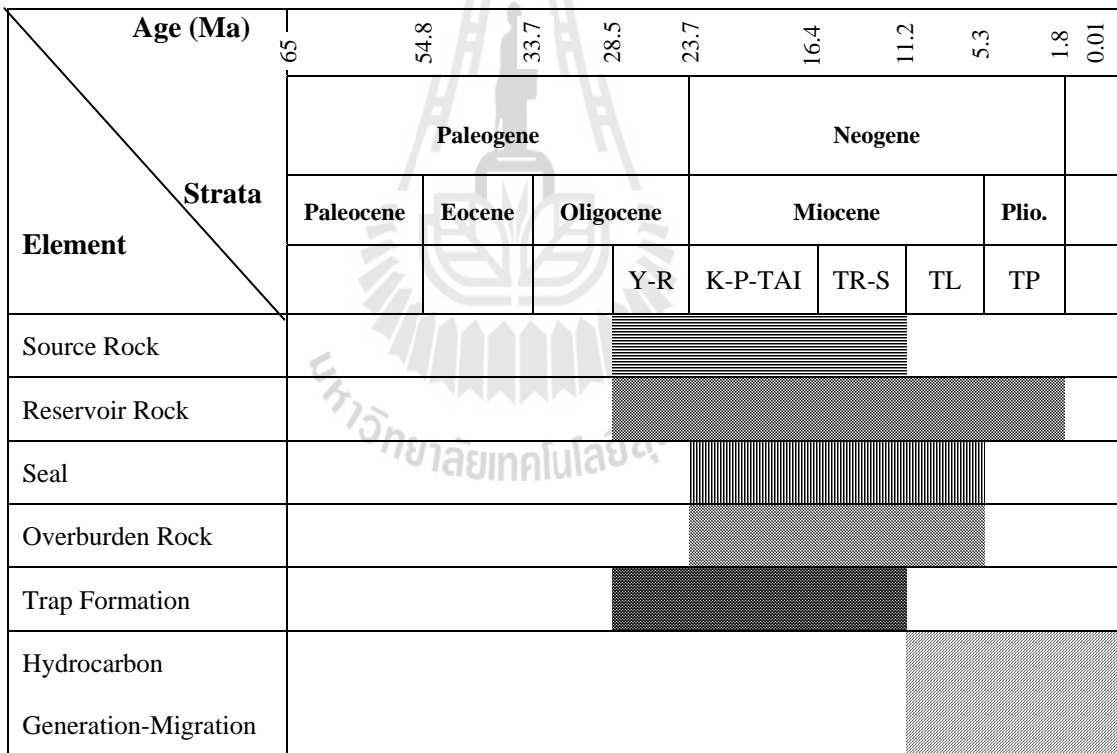


Figure 5.1 Event chart of the petroleum system from the Mergui basin; R:Ranong Fm.; Y:Yala Fm.; TAI;Tai Fm.; P:Payang Fm.; K:Kantrang Fm.; S:Surin Fm.; TR:Trang Fm.; TL:Thalang Fm.; TP:TakuaPa Fm.

5.1.2 Petroleum source rock of the Mergui basin

- The Yala Formation has total organic carbon (TOC) values of range 0.5-1.5%. Organic matter is Type III terrestrial, gas prone kerogen. Thermal maturity has R_o about 0.6-1.0, T_{max} of from 430 to nearly 450 °C and production index 0.10 - 0.4.
- The Kantang Formation has fair to good TOC value average 0.5-1.5%. Organic matter is mixing of Type II/ III, oil/gas prone kerogen. Thermal maturity has R_o about 0.2-0.6, T_{max} of from 420 to 440 °C and production index 0.02-0.15.
- The Trang Formation has fair to very good average TOC 0.5-2.0%. This organic matter is mixing of Type II/ III, oil/gas prone kerogen. Thermal maturity has R_o about 0.2-0.4, T_{max} of from 400 to 430 °C and production index 0.1-0.14.
- The Yala Formation, these ranges are characteristic of maturities corresponding to main hydrocarbon generation zone at depths (cut off: R_o about 0.6-0.8, T_{max} of from 435 - 445 °C and production index 0.30 - 0.36) of approximately 3,000 – 3,500 m in most of the depressions of the Mergui basin, whereas the Kantang and Trang Formation are somewhat immature.
- Peak generation for gas occurred in Late Tertiary times (between 12 and 5.5 Ma: Late Miocene to Early Pliocene).
- Modeling results indicate that gaseous hydrocarbons are the primary migratory (expulsion) products where they are limited to deepest parts of the eastern and the western Mergui basins.
- The biomarker can be indicated that the depositional environment was not strongly an anoxic and reducing condition at the time the sediments were deposited. The source potential of Miocene sediments is poor to fair.

- Peak generation for hydrocarbon occurred during the Middle Miocene to Pliocene period. Expulsion of hydrocarbon took place during Late Miocene to Pliocene.

5.1.3 Petroleum migration pathway of the Mergui basin

Migration of hydrocarbons from neighbouring kitchens area is problematic (particularly from kitchens located in the southwestern part of basin). Migration pathways were started from the Ranong sandstones mostly located in basinal areas, the flanks of blocks, and had extensional faults limiting the blocks. The amount of hydrocarbons that had been generated from the mature source rocks and then migrated towards the traps was limited. Because of the type of the organic matter and the great depth of hydrocarbon generation and expulsion, the entire area is considered as the gas-prone. Hydrocarbons generation expulsion and migration occurred mainly in Late Miocene-Pliocene after main trap were formed and exceeds 2,400 – 3,500 m. possible petroleum pathways in this basin are mainly toward the central high structure which is located in the central part of the basin.

5.2 Recommendations for future studies

This study had been conducted under limited data, thus results may have some errors. Therefore, when there are more geochemical and/or well data in the future, source rock potential and migration pathway should be restudied. According to the advantages in seismic survey and seismic processing techniques in present day, new seismic survey should be conducted and/or old seismic data should be re-processing with new technologies in order to identify potential reservoir and migration pathway of the Mergui basin.

REFERENCES

- Allen, A.P. and Allen, R.J. (2005). **Basin Analysis: Principles and Applications (2nd Edition)**. Malden, USA: Blackwell.
- Andreason, M.W., Mudford, Brett, and St. Onge, J.E. (1997). Geologic evolution and petroleum system of the Thailand Andaman Sea basins. In **Proceedings of an International Conference on Petroleum Systems of SE Asia and Australasia**. May 1997: (pp. 337-350). Jakarta, Indonesia.
- Atop Technology Co., Ltd. (2006). **Petroleum Assessment in Northeastern Thailand**: Department of Mineral Fuels, Ministry of Energy. (Confidential Report).
- Beardsmore, G.R. and Cull, J.P. (2001). **Crustal Heat Flow: A Guide to Measurement and Modelling**. Cambridge University Press, Cambridge.
- Bordenave, M.L. (1992). **Applied petroleum geochemistry**. Paris, France: Imprimerie Nouvelle.
- Charusirisawad, R., 1966. **Reprocessing of Seismic Data from the Murgui Basin, Andaman Sea, Thailand**. Master Thesis, Discipline of Geophysics, Graduate School, The University of Tulsa, Japan.
- Curry, J.R., Moore, D.G., Lawver, L.A., Emmel, F.J., Raitt, R.W., Henry, M. and Kieckhefer, R. (1979). **Tectonics of the Andaman Sea and Burma**. In: Watkins, J. and Montadert, L.(Eds), **Geological and Geophysical Investigations of Continental Margins**. AAPG Bull, 29, 189-198.

- Curry, J.R. (2005). **Tectonics and history of the Andaman Sea region**. Journal of Asian Earth Sciences, 25, 187-232.
- Einsele, G. 1992. **Sedimentary basins**. Berlin, Germany: Springer-Verlag.
- England, W.A., Mann, A.L. and Mann, D.M. (1991). Migration from source to trap. in Merrill, R.K. **Source and migration processes and evaluation techniques**. AAPG Bull, Handbook of Petroleum Geology, 23–46 pp.
- Espitalie J., Madec, M., Tissot, B., Mennig, J.J., and Leplat, P., 1977. **Source rock characterization method for petroleum exploration**. Proc. Offshore Technology Conference, pp. 439-443.
- Esso Exploration & Production. (1976a). **Well completion report W9-A-1: Thai Andaman Sea**. Mineral Fuels Division, Department of Mineral Resources, Ministry of Industry, Thailand. (Confidential Report).
- Esso Exploration & Production. (1976b). **Well completion report W9-B-1: Thai Andaman Sea**. Mineral Fuels Division, Department of Mineral Resources, Ministry of Industry, Thailand. (Confidential Report).
- Esso Exploration & Production. (1976c). **Well completion report W9-C-1: Thai Andaman Sea**. Mineral Fuels Division, Department of Mineral Resources, Ministry of Industry, Thailand. (Confidential Report).
- Esso Exploration & Production. (1976d). **Well completion report W9-D-1: Thai Andaman Sea**. Mineral Fuels Division, Department of Mineral Resources, Ministry of Industry, Thailand. (Confidential Report).
- Esso Exploration & Production. (1976e). **Well completion report W9-E-1: Thai Andaman Sea**. Mineral Fuels Division, Department of Mineral Resources, Ministry of Industry, Thailand. (Confidential Report).

Exxon Production Research Company. (1976a). **Hydrocarbon source analysis of samples from the W9-A-1: Thai Andaman Sea.** Mineral Fuels Division, Department of Mineral Resources, Ministry of Industry, Thailand. (Confidential Report).

Exxon Production Research Company. (1976b). **Hydrocarbon source analysis of samples from the W9-B-1: Thai Andaman Sea.** Mineral Fuels Division, Department of Mineral Resources, Ministry of Industry, Thailand. (Confidential Report).

Exxon Production Research Company. (1976c). **Hydrocarbon source analysis of samples from the W9-C-1: Thai Andaman Sea.** Mineral Fuels Division, Department of Mineral Resources, Ministry of Industry, Thailand. (Confidential Report).

Exxon Production Research Company. (1976d). **Hydrocarbon source analysis of samples from the W9-D-1: Thai Andaman Sea.** Mineral Fuels Division, Department of Mineral Resources, Ministry of Industry, Thailand. (Confidential Report).

Exxon Production Research Company. (1976e). **Hydrocarbon source analysis of samples from the W9-E-1: Thai Andaman Sea.** Mineral Fuels Division, Department of Mineral Resources, Ministry of Industry, Thailand. (Confidential Report).

Geoservices Eastern Inc. (1996). **Kathu-1 Final well report: Thai Andaman Sea.** Mineral Fuels Division, Department of Mineral Resources, Ministry of Industry, Thailand. (Confidential Report).

Geoservices Eastern Inc. (1996). **Kra Buri-1 Final well report: Thai Andaman Sea.**

Mineral Fuels Division, Department of Mineral Resources, Ministry of Industry, Thailand. (Confidential Report).

Geoservices Eastern Inc. (1996). **Thalang-1 Final well report: Thai Andaman Sea.**

Mineral Fuels Division, Department of Mineral Resources, Ministry of Industry, Thailand. (Confidential Report)

Geoservices Eastern Inc. (1996). **Sikao-1 Final well report: Thai Andaman Sea.**

Mineral Fuels Division, Department of Mineral Resources, Ministry of Industry, Thailand. (Confidential Report)

Hao, F., Zou, H. and Gong, Z. (2010). **Preferential petroleum migration pathways**

and prediction of petroleum occurrence in sedimentary basins: A review.

China University of petroleum, China. (7): 2-9.

Hantschel T. and Kauerauf A. (2009). **Fundamentals of Basin and Petroleum**

Systems Modeling. Aachen, Germany: Springer-Verlag.

Harding, T.P. (1985). **Seismic characteristics and identification of negative flower structures, positive flower structures, and positive structure inversion.**

AAPG Bull. 69: 582-600.

Hunt J.M., Jamieson G.W. (1956). **Oil and Organic Matter in Source Rocks of**

Petroleum. AAPG Bull. 40(3): 477-488.

Kansas Ground Water. (2012). **Characteristics of porosity in other rocks.** [On-line].

Available <http://www.kgs.ku.edu/Publications/Bulletins/ED10/gifs/fig2.jpg>.

Katz, B.J. (1980). **Total generation potential - a preliminary analysis.** EPBL

Technical Memorandum.

- Khursida, P. (2002). **Subsurface geology of the southern part of tertiary, Mergui Basin, Andaman Sea**. Master Thesis, Chulalongkorn University, Thailand.
- Leeper, R.H., and Sassen, R. (1977). **Organic geochemical data file organic carbon of shaly rocks, preliminary analysis**. EPBL Technical Memorandum.
- Mahattanachai. T. (2007). New Petroleum Opportunities in Ranong Trough and Shallow-Water Domain of Andaman Sea, Thailand. In **DMF Technical Forum 2007** (pp. 21-28). Bangkok, Thailand: Department of Mineral Fuels.
- Martin, D.M. **Exploring for Oil and Gas Traps: Migration of Petroleum**. AAPG Bull. 1-35.
- Morley, C.K. (2002). **A tectonic model for the Tertiary evolution of strike-slip faults and rift basins in SE Asia**. Amsterdam, Elsevier Science. 347: 189–215.
- Molnar, P. and Tapponnier, P. (1975). **Cenozoic Tectonics of Asia: effects of continental collision**. Science. 189: 419-426.
- MPG Petroleum. (2012)a. **Pores in rock**. [On-line]. Available: <http://mpgpetroleum.com/images/pores.gif>.
- MPG Petroleum. (2012)b. **Connected pores in rock**. [On-line]. Available: <http://mpgpetroleum.com/images/pores2.gif>.
- Palciauskas, V.V. (1991). Primary migration of petroleum, in Merrill, R.K. **Source and migration processes and evaluation techniques**. AAPG Bull, Handbook of Petroleum Geology, 13–22.
- Peters, K.E., M.R. Cassa. (1994), Applied source rock geochemistry. In: **The petroleum system- from source to trap**, L.B. Magoon and W.G. Dows (eds.), AAPG. Bull. 60: 93-117.

- Peters, K.E., (1986). **Guideline for evaluating petroleum source rock using programmed pyrolysis**. AAPG. Bull. 70: 318-329.
- Peter, G., Weeks, L.A., and Burns, R.E., (1966). A reconnaissance geophysical survey in the Andaman Sea and across the Andaman-Nicobar Island Arc. **Journal of Geophysical Research**. 11: 495-509.
- Placid Oil Company of Thailand. (1988). **Well completion report Ranot-1: Thai Andaman Sea**. Mineral Fuels Division, Department of Mineral Resources, Ministry of Industry, Thailand. (Confidential Report).
- Placid Oil Company of Thailand. (1987). **Well completion report Yala-1: Thai Andaman Sea**. Mineral Fuels Division, Department of Mineral Resources, Ministry of Industry, Thailand. (Confidential Report).
- Placid Oil Company of Thailand. (1987). **A geochemical evaluation Ranot-1: Thai Andaman Sea**. Mineral Fuels Division, Department of Mineral Resources, Ministry of Industry, Thailand. (Confidential Report).
- Placid Oil Company of Thailand. (1987). **A geochemical evaluation Yala-1: Thai Andaman Sea**. Mineral Fuels Division, Department of Mineral Resources, Ministry of Industry, Thailand. (Confidential Report).
- Polachan, S. (1988). **The geological evolution of the Mergui Basin, SE Andaman Sea, Thailand**. Doctoral Thesis. University of London.
- Polachan, S. and Racey, A. (1993). Lower Miocene larger foraminifera and petroleum potential of the Tai Formation, Mergui Group, Andaman Sea. **Journal of Southeast Asian Earth Sciences**. 8(1): 487-496.

- Polachan, S. and Racey, A. (1994). Stratigraphy of the Mergui basin, Andaman Sea: implications for petroleum exploration. **Journal of Petroleum Geology**. 17(4): 373-406.
- Prasit, C. (2001). **Andaman Sea Exploration Summary Report 2nd Obligation Period**. Mineral Fuels Division, Department of Mineral Resources, Ministry of Industry, Thailand. (Confidential Report).
- Ridd, M.F. (1971). **Southeast Asia as part of Gondwanaland**. Nature. 234, 531-533.
- Rodolfo, K.S. (1969). **Bathymetry and marine geology of the Andaman Sea Basin, and tectonic implications for SE Asia**. Bull. Geol. Soc. Am. 80 1,203-1,230.
- Schlumberger. (2010). **Petromod 1D Tutorial Software Version 11**. Ritterstraße Aachen, Germany 52072: Schlumberger.
- Shouls, M.M. (1973). **Seismicity and plate tectonics in the Thailand-Burma-Andaman Sea area**: CCOP Newsletter. 1: 17-19.
- Srikulwong, S. (1986). **Structural evolution and sedimentation during the Oligocene, in the vicinity of the W9-E-1 Well, Mergui Basin, Andaman Sea, Thailand**. Master Thesis. University of Aberdeen (UK).
- Sweeney J. Jerry and Burham K. Alan. (1990). **Evaluation of a simple Model of Vitrinite Reflectance Based on Chemical Kinetics**. AAPG Bull. 1559-1570.
- Tapponnier, P., Peltzer, G., Le Dain, A.Y. and Armijo, R. (1982). **Propagating extrusion tectonics in Asia: New insights from simple experiments with plasticine**. Geology. 10: 611-616.
- Tissot B.P., Durand B, Espitalie J., and Combaz A. (1974). **Influence of nature and diagenesis of organic Matter in Formation of Petroleum**. AAPG Bull., 499-506.

- Tissot, B.P. and Welte, D.H. (1984). **Petroleum Formation and Occurrence (2nd Edition)**. Berlin, Germany: Springer-Verlag.
- Tissot B.P., Pelet R., and Ungerer H.P. (1987). **Thermal History of sedimentary Basins, Maturity Indices, and Kinetics of oil and Gas generation**. AAPG Bull. 1445-1466.
- Unocal Geochemistry. (1988a). **Interpretation of organic geochemical data from Kantang-1: Thai Andaman Sea**. Mineral Fuels Division, Department of Mineral Resources, Ministry of Industry, Thailand. (Confidential Report).
- Unocal Geochemistry. (1988b). **Interpretation of organic geochemical data from Kathu-1: Thai Andaman Sea**. Mineral Fuels Division, Department of Mineral Resources, Ministry of Industry, Thailand. (Confidential Report).
- Unocal Geochemistry. (1988c). **Interpretation of organic geochemical data from Kra Buri-1: Thai Andaman Sea**. Mineral Fuels Division, Department of Mineral Resources, Ministry of Industry, Thailand. (Confidential Report).
- Unocal Geochemistry. (1988d). **Interpretation of organic geochemical data from Thalang-1: Thai Andaman Sea**. Mineral Fuels Division, Department of Mineral Resources, Ministry of Industry, Thailand. (Confidential Report).
- Unocal Geochemistry. (1997). **Sedimentology and Petrography of Core and Cuttings Wells in Mergui and North Sumatra Basins, Andaman Sea Blocks W8/38 and W9/38, Offshore Thailand**. Mineral Fuels Division, Department of Mineral Resources, Ministry of Industry, Thailand. (Confidential Report).

- Unocal Geochemistry. (1988e). **Interpretation of organic geochemical data from Sikao-1: Thai Andaman Sea.** Mineral Fuels Division, Department of Mineral Resources, Ministry of Industry, Thailand. (Confidential Report).
- Union Oil Company of Thailand. (1976b). **Well completion report Trang-1: Thai Andaman Sea.** Mineral Fuels Division, Department of Mineral Resources, Ministry of Industry, Thailand. (Confidential Report).
- Union Oil Company of Thailand. (1976c). **Well completion report Mergui-1: Thai Andaman Sea.** Mineral Fuels Division, Department of Mineral Resources, Ministry of Industry, Thailand. (Confidential Report).
- Union Oil Company of Thailand. (1976d). **Well completion report Tai-1: Thai Andaman Sea.** Mineral Fuels Division, Department of Mineral Resources, Ministry of Industry, Thailand. (Confidential Report).
- Union Oil Company of Thailand. (1976e). **Well completion report Payang-1: Thai Andaman Sea.** Mineral Fuels Division, Department of Mineral Resources, Ministry of Industry, Thailand. (Confidential Report).
- University of Wisconsin. 2012. **Relationship of porosity and permeability in other rocks.** [On-line]. Available:<http://www.co.pedin.wi.us/Groundwater%20website/New%20Folder/Slide4.gif>.
- Waples W. Douglas and Marzi W. Roger. (1998). **The Universality of the relationship between vitrinite reflectance and transformation ratio.** Amsterdam, Elsevier Science. 383-388.
- Waples W., Kamata H., and Suizu M. (1992). **The Art of Maturity Modeling.** AAPG Bull. 31-46.

Waples, D. (1980). **Time and Temperature in Petroleum Formation: Application of Lopatin Method to Petroleum Exploration.** AAPG Bull. 916-926.

Weeks, L.A., Harbison, R.N. and Peter, G. (1967). **Island arc system in the Andaman Sea.** AAPG Bull. 51: 1803-1815.



BIOGRAPHY

Miss Nattaya Chaina was born on July 20, 1986 in KhonKaen province, Thailand. She received her Bachelor's Degree in Department of Materials Science and Engineering, Faculty of Engineering and Industrial Technology at Silpakorn University, majoring in Petrochemical and Polymeric Materials in 2010. And he studied for her Master's Degree in Petroleum Engineering at School of Geotechnology, Institute of Engineering at Suranaree University of Technology (SUT). During graduate study, she was teaching assistant at SUT and got good knowledge in petroleum geology and petroleum prospect assessment.

